AGH UNIVERSITY OF SCIENCE AND TECHNOLOGY

FIELD OF SCIENCE NATURAL SCIENCES

SCIENTIFIC DISCIPLINE PHYSICAL SCIENCES

DOCTORAL DISSERTATION

Dynamics of Quantum State in One-Dimensional Open Systems with Random Perturbation: Phase-Space Approach

Author: Dariusz Woźniak

Supervisor: Dr hab. inż. Bartłomiej Spisak, Prof. AGH

Completed at: AGH University of Krakow,
Faculty of Physics and Applied Computer Science

Kraków, 2025

Pragnę serdecznie podziękować promotorowi, dr. hab. inż. Bartłomiejowi Spisakowi, za opiekę naukową, poświęcony czas oraz wyrozumiałość przez cały okres studiów doktoranckich.
Pragnę również podziękować zespołowi z Katedry Fizyki Matematycznej UMK, w szczególności prof. dr. hab. Dariuszowi Chruścińskiemu, za ciepłe i merytoryczne przyjęcie w Toruniu.
Dziękuję również moim kolegom: dr. inż. Damianowi Kołaczkowi, mgr. inż. Mateuszowi Gali, mgr. inż. Maciejowi Kalce oraz mgr. inż. Piotrowi Pigoniowi, za dyskusje, pomoc oraz atmosferę, która sprzyjała prowadzeniu badań.
Na koniec pragnę podziękować Rodzinie i Przyjaciołom za cierpliwość i wsparcie - bez nich ukończenie tej pracy nie byłoby możliwe.

Oświadczenie autora rozprawy:
Oświadczam, świadomy odpowiedzialności karnej za poświadczenie nieprawdy, że niniejszą pracę doktorską wykonałem osobiście i samodzielnie i że nie korzystałem ze źródeł innych niż wymienione w pracy.

data, *podpis*

Oświadczenie promotora rozprawy:
Niniejsza rozprawa jest gotowa do oceny przez recenzentów.

data, *podpis*

Abstract

The subject of this doctoral dissertation is the dynamical analysis of open quantum system in the presence of random potential perturbations using the phase-space formalism. Using the Stratonovich-Weyl quantisation scheme for a one-dimensional system interacting with an N-dimensional environment, the equation of motion for the Wigner function was derived from a microscopic perspective. Due to the adopted assumptions, the results obtained refer to weakly interacting memoryless systems. The resulting equation of motion, after assuming a linear expression for the Lindblad symbol $L(x,p) = ax + bp$, $a, b \in \mathbb{C}$, was expressed in operator form, and subsequently, the second-order split-operator method was applied. The time evolution generator was expressed as the sum of four operators, for which a commutation table was prepared. As a result of the calculations, it was observed that the part of the generator not containing the potential term can be separated exactly, thereby reducing the number of applied Fourier transforms. Next, the equation of motion for the approximated averaged Wigner function of the statistical ensemble was derived, yielding an equation with a diffusion coefficient that is linearly dependent on time, the perturbation strength, and the second derivative of the potential. As model systems, a single Gaussian barrier and a chain of such barriers were considered, and each of these systems was then perturbed by a random vector whose components were independent random variables. For such prepared potentials, the equation of motion for the Wigner function was solved numerically using the split-operator method, with a common Gaussian initial condition. In the C++ implementation of the algorithm, the Fast Fourier Transform (FFTW3) was employed. The dynamical analysis of the studied cases was based on the following measures: statistical - averages, standard deviations, and covariance; phase-space - nonclassicality parameter and Wigner-Shannon entropy; state - purity and Loschmidt echo; distance - the $L^2(\mathbb{R}^2)$-normalised distance between the solution for the unperturbed potential and the approximate solution. These measures were used to study the influence of the environment on the dynamics of the open system. Additionally, the existence of stationary states for the studied cases was analysed.

Streszczenie

Tematem rozprawy doktorskiej jest analiza dynamiczna otwartych układów kwantowych w obecności losowego zaburzenia potencjału przy użyciu formalizmu przestrzenno-fazowego. Wykorzystując schemat kwantyzacji Stratonovicha-Weyla dla jednowymiarowego układu oddziaływującego z N-wymiarowym otoczeniem wyprowadzono, w ujęciu mikroskopowym, równanie ruchu dla funkcji Wignera. Ze względu na przyjęte założenia, uzyskane wyniki odnoszą się do słabo oddziaływujących układów bez pamięci. Otrzymane równanie ruchu, po przyjęciu liniowego wyrażenia na symbol Lindblada $L(x,p) = ax + bp$, $a, b \in \mathbb{C}$, zapisano w języku operatorowym, aby następnie przystąpiono do zastosowania metody split-operator drugiego rzędu. Generator ewolucji czasowej został wyrażony przez sumę 4 operatorów, dla których przygotowano tabelę komutacji. W wyniku przeprowadzonych obliczeń zauważono, że część generatora niezawierająca części potencjalnej może zostać odseparowana w sposób dokładny, obniżając tym samym liczbę zastosowanych transformacji Fouriera. Następnie wyprowadzono równanie ruchu dla przybliżonej uśrednionej funkcji Wignera zespołu statystycznego, otrzymując tym samym równanie ze współczynnikiem dyfuzji zależnym: liniowo od czasu, rzędu zaburzenia oraz drugiej pochodnej potencjału. Za modelowe układy przyjęto pojedynczą barierę gaussowską oraz łańcuch takich barier, a następnie każdy z tych układów zaburzono o wektor losowy, którego współrzędne były niezależnymi zmiennymi losowymi. Dla tak przygotowanych potencjałów rozwiązano numerycznie, metodą split-operator, równanie ruchu dla funkcji Wignera, przy wspólnym warunku początkowym w postaci funkcji Gaussa. Przy implementacji algorytmu w języku C++ zastosowano Szybką Transformatę Fouriera (FFTW3). Analizę dynamiczną badanych przypadków oparto o miary: statystyczne - średnie oraz odchylenia standardowe i kowariancję; przestrzenno-fazowe - parametr nieklasyczności oraz entropię Wignera-Shannona; stanu - czystość oraz echo Loschmidta; odległościowe - znormalizowana do jedności odległość w przestrzeni $L^2(\mathbb{R}^2)$ między rozwiązaniem potencjału niezaburzonego oraz między rozwiązaniem przybliżonym. Przy ich pomocy zbadano wpływ otoczenia na dynamikę układu otwartego. Dodatkowo, podjęto się analizy istnienia stanu stacjonarnego dla badanych przypadków.

Contents

Introduction

Throughout history, we have been taking part in the constant, unending race between experimental methods and theoretical models in physics, where at different periods one took over the other to pave the way for scientific research. Focusing on events after 1900, when Max Planck revolutionised physics by solving the problem of black-body radiation, we have seen massive growth in the research and scientific community, a renaissance of physics, where new ideas were born on the spot while others died nearly as quickly. A great overview by Styer et. al. [164], shows the diverse formulations of the quanta theory since Planck's discovery. We shall focus on one particular formulation of quantum theory, namely, the phase-space approach. It is built on the quasi-probability distribution function known as the Wigner function, in which the position x and momentum p variables are treated on equal footing. This formulation lays the groundwork for a similarity to statistical mechanics, however, the algebra between x and p is non-commutative [43] in this formulation. Moreover, the emphasis shifts from the probability amplitude to a new statistically proper measure, the Wigner distribution function (WDF), defined on the phase space. Its equation of motion is known as the Moyal equation, which, when written in differential form, can be treated as a quantum analogy to the classical Liouville equation but with additional terms resulting from quantumness of the system [29]. Those are represented by the power series of the Planck constant multiplied by the higher-order derivatives of the potential, and the momentum derivative of the WDF. The beginnings of this formulation can be traced to the work of H. Weyl [181], J. von Neumann [176], E. Wigner [182], and H. Groenewold [76]. Their results were synthesised by J. Moyal [126], who, from a statistical perspective, demonstrated the similarity between this new framework and fundamental quantum theory. In particular, Moyal calculated expectation values of observables, connected them to the Heisenberg uncertainty relation, and revealed that the underlying structure is generated equivalent to the deformed Poisson bracket, which in turn led to the evolution equation for the WDF. However, it should be noted that the agenda behind von Neumann's work was not concerned with the phase-space approach but rather with the Stone-von Neumann theorem. Nevertheless, the von Neumann's results were closely related to and, in fact, identical with those later obtained by Moyal [85]. In the end, the phase-space approach was elevated to the status of a statistical theory, equivalent to Schrödinger or path-integral formulation of quantum mechanics. Controversial for some and even unsettling for others [86], it nevertheless offers the best of two worlds, classical and quantum, and continues to direct research toward semiclassical analysis [27], non-commutative geometry [36], pseudodifferential operators theory [121], quantum trajectories [18], and Bohmian mechanics [84].

With current technological advances, we can experimentally verify posed theories or build new ones that explain the results. This progress has led to device dimensions so small that quantum effects can-

not be ignored, nor can devices be treated as isolated systems. For example, environmental effects in nanoscale systems can cause decoherence, which influences the dynamical properties of these systems [191, 190, 67, 189, 192]. The moral of this observation is that quantum effects, such as tunnelling or the superposition of states, can no longer be considered solely in terms of isolated or closed systems, they must be treated as open systems interacting with their environment. The first attempts to describe such systems were made by Wangsness and Bloch [178, 20] and later extended by Redfield [137]. In their work, Wangsness and Bloch derived a general Boltzmann equation for the density matrix. Redfield, inspired by their results, proposed a systematic procedure for deriving a suitable master equation describing a spin system coupled to a thermal bath. The equation introduced is known today as the Redfield equation, and remains the standard starting point for the microscopic derivation of the Gorini-Kossakowski-Sudarshan-Lindblad (GKSL) equation. The GKSL equation, independently discovered by Lindblad and Gorini, Kossakowski, and Sudarshan, represented a breakthrough in the theory of open quantum systems [112, 72]. It was derived on the basis of rigorous mathematical assumptions about the density operator of an open quantum system. The key result of these works was the general characterisation of the generator of open-system dynamics, which guarantees complete positivity, trace preservation, and hermiticity, ensuring that the time evolution maps quantum states to valid quantum states. Today, the GKSL equation is regarded as the natural generalisation of the von Neumann equation, extending the description of time evolution from isolated or closed quantum systems to the open ones. Naturally, the GKSL equation is not the *equation of everything* for open systems as it has important limitations. In particular, it does not include memory effects in the system. Subsequent research has therefore developed alternative approaches, such as the Nakajima-Zwanzig equation, which incorporates memory kernel explicitly [127, 193], and the time-convolutionless (TCL) approach introduced by Shibata [156, 155], which instead encodes the memory effects of the system in a time-dependent operator rather than an integration kernel. In addition, stochastic methods have also been developed and play an important role in the theory of open quantum systems. For a broader overview of these and other approaches, see Ref. [25].

The thesis consists of four chapters followed by a summary, where we also outline perspectives for further research. Its structure is as follows. In Chapter 1, we introduce the standard formalism of quantum mechanics. We begin with the notion of the abstract state vector and extend it to the density operator, motivated by the distinction between pure and mixed states. We discuss its key properties, the evolution equation, and the solution for a given initial condition in the case of isolated and closed systems. The chapter proceeds with an introduction to the tensor product Hilbert spaces, preparing the ground for the description of open-system dynamics via the GKSL equation. Finally, we briefly present the Nakajima-Zwanzig equation, which extends the GKSL framework to non-Markovian cases. In Chapter 2, we present the central tool of this thesis: the phase-space formulation of quantum mechanics. We begin with a comparison between classical and quantum phase spaces and the probability functions defined on them. Next, we provide the necessary analytical background, including the definitions of the Weyl transform, the Wigner function, and the Moyal product. We further introduce the Stratonovich-Weyl correspondence and apply it to the case of a flat total phase space describing two coupled systems. In Chapter 3, we provide the theoretical background for the split-operator method. We start from evolutionary-type equations and their solutions within operator

theory. Then, we recall three basic schemes for approximating the exponential of a sum of operators, and extend the method to explicitly time-dependent operators. In Chapter 4, we derive the equation of motion for the Wigner distribution function (WDF) of an open quantum system. Later, we consider linear quantum jump operators and formulate a split-operator algorithm for numerical implementation. The commutation relations between the relevant operators are analysed, leading to explicit second- and fourth-order schemes, including the case of a time-dependent potential $V(x,t)$. To complement these results, we also discuss isolated and open systems in the light of previously published work. Subsequently, we consider a randomly perturbed potential $V(x;\boldsymbol{\lambda})$, parameterised by a random vector $\boldsymbol{\lambda}$, and derive the approximate equation of motion for the ensemble-averaged WDF. Finally, we analyse the system using the split-operator method and compute its dynamical parameters.

The main motivation behind this work was to derive the GKSL equation in terms of phase-space quantisation and implement it numerically. Additionally, in the spirit of the research conducted during the studies, we aimed to analyse the measures used to characterise the quasi-probability distribution in the case of an open quantum system. The derivation used the microscopic approach to the dynamics of the open system, as described in [24], while the numerical implementation was based on the split operator algorithm for the linear type of quantum jump operators. Due to the differential nature of the equation of motion, the Fourier transform was used to convert partial differential operators into matrix multiplication. The author's contributions presented in this dissertation are directly based on the achievement of specific objectives, including the following:

1. Microscopic derivation of an equation of motion for the Wigner function of an open system, based entirely on the phase-space approach. These calculations were based on the derivation performed for the density operator and were presented in the Chapter 4, Section 4.1.

2. Derivation of the equation of motion for the Wigner function of an open system with a linear quantum jump operator, along with a numerical algorithm for calculating its evolution. This result is present in Chapter 4, Section 4.2.

3. Calculation of an exact splitting of the exponential operator into the kinetic and dissipative parts of the Wigner-Gorini-Kossakowski-Sudarshan-Lindblad equation with at most quadratic dissipators presented in Chapter 4, Section 4.2.

4. Implementation of the algorithm in C++. The initial results obtained with its help are presented in works [185, 186, 97], available in the Appendix F. The algorithm and some issues regarding its implementation are presented in chapter 4, section 4.2, and also in the Appendices E and C.

5. Proposition of an approximate equation of motion for the ensemble-averaged Wigner distribution function.

6. Analysis of single- and multi-barrier systems with random perturbations, including the study of phase-space parameters and their comparison across the systems. These are presented in Chapter 4, Sections 4.5.2, 4.5.3, 4.5.4.

During the education at AGH Doctoral School, the author contributed to and was involved in the following projects, which resulted in publications:

1. **D. Woźniak**, M. Kalka, P. Pigoń, and B.J. Spisak. Phase-space analysis of spinning particle dynamics in two-dimensional Weyl systems: Stratonovich–Weyl approach. *New Journal of Physics* [Accepted Manuscript online 17 September 2025, (DOI 10.1088/1367-2630/ae081f)]

2. **D. Woźniak**, M. Kalka, D. Kołaczek, M. Wołoszyn, and B.J. Spisak. Wignerian symplectic covariance approach to the interaction-time problem. *Scientific Reports* 14:31294 (2024);

3. **D. Woźniak**, D. Woźniak, B. J. Spisak, M. Kalka, M. Wołoszyn, M. Wleklińska, P. Pigoń, and D. Kołaczek. Interaction time of Schrödinger cat states with a periodically driven quantum system: Symplectic covariance approach. *Physical Review A* 110:022416 (2024);

4. M. Kalka, B. J. Spisak, **D. Woźniak**, M. Wołoszyn, and D. Kołaczek. Dynamical entropic measure of nonclassicality of phase-dependent family of Schrödinger cat states. *Scientific Reports* 13:16266 (2023);

5. B. J. Spisak, D. Kołaczek, and **D. Woźniak**. Dynamics of the τ-Wigner distribution function. *Journal of Physics A: Mathematical and Theoretical* 55:504003 (2023).

Chapter 1

Beyond the wave function - quantum mechanics of density matrix

1.1 Density matrix quantum mechanics

According to the fundamentals of quantum theory, every physical quantum system has an associated separable complex Hilbert space $\mathcal{H}(\mathbb{C})$ over the complex number field, with a dimension specified by its nature [177, 54]. The normalised elements of $\mathcal{H}$, called state vectors, represent possible states of the system [74, 169]. This mathematical construct is a fundamental concept that allows for a proper, and most importantly validated by experiment, description of quantum physics. The simplified description of quantum theory can be narrowed to considerations of statistically certain states that can be described in terms of a single state vector. Equivalently, these states contain maximal information about the system. Statistical certainty implies that, whenever an experiment is conducted with the same setup and the state of the system is measured, the outcome is well defined and certain [62].

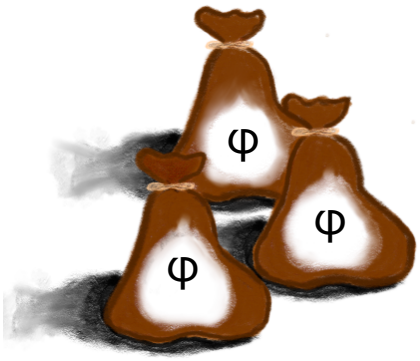

Figure 1.1: A representation of a pure system. The bag represents a single realisation of the system being, with some probability, in a state $|\varphi\rangle$. If such setups are repeated infinitely many times, and then each one is measured independently, then for a pure quantum state with 100% certainty, the state of the system will be $|\varphi\rangle$.

This property does not encompass cases where there is a mixture of different quantum states. To consider such states in quantum mechanics, one should extend the idea of a pure state, meaning the state describable by a state vector, to include a statistical mixture of states. These are mixed states, which means that they cannot be described by such a vector [15] or, equivalently, by conducting multiple copies of the same experiment, the resulting state after measurement is different, but statistically describable in terms of probability of occurrence. In this picture, a pure state is represented as a simple projection operator $\hat{P} := |\psi\rangle\langle\psi|$ with the property $\hat{P}^2 = \hat{P}$ [138]. To introduce a concept of mixed state, let us assume that a quantum state consists of different quantum states $|\psi_i\rangle$, each contributing with a weight $w_i > 0$, which plays a role of probability, such that $\sum_i w_i = 1$. Then an object that contains all the information about the system is the density operator given by [79]

$$\hat{\rho} = \sum_i w_i \, |\psi_i\rangle\langle\psi_i| \, . \tag{1.1}$$

According to this formula, the density operator can be regarded as a convex combination of projection operators on a given state $|\psi_i\rangle$ with associated projectors in the form $\hat{P}_{\psi_i} = |\psi_i\rangle\langle\psi_i|$. With this reasoning, a pure quantum state is an element of the convex set that lies on its boundary. [9] This is equivalent to describing the system as an ensemble of pure states, where w_i are the probabilistic weights associated with a given projection operator.

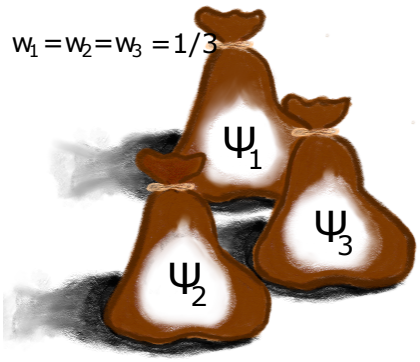

Figure 1.2: An analogous to Fig. 1.1 representation of a mixed system with equiprobable states. Each of the bags is equivalent to a single realisation of the system in a quantum state $|\psi_1\rangle$, $|\psi_2\rangle$, or $|\psi_3\rangle$. If such setups are repeated infinitely many times and measured, then the probability of occurrence of the selected state can be obtained.

The properties of a density operator are inherited from its contributing projectors. Thus, the density operator is a self-adjoint operator $\hat{\rho}^* = \hat{\rho}$, semi-positive defined: $\hat{\rho} \geq 0$, with a trace equal to identity $\mathrm{Tr}\,\hat{\rho} = 1$ [80]. To complete this natural extension of pure state quantum mechanics, we notice that the time dependence of the density operator is inherited directly from the time dependence of state vectors whose evolution is subjected to the Schrödinger equation of evolution. Let us recall that at any time, for isolated quantum systems, a state vector $|\psi(t)\rangle$ satisfies the evolution equation [177]

$$i\hbar \frac{\mathrm{d}}{\mathrm{d}t} |\psi(t)\rangle = \hat{H} \, |\psi(t)\rangle \, , \tag{1.2}$$

where $\hat{H}$ is a Hamiltonian. Thus, for each time instance $t \in \mathbb{R}_+$, the state vector $|\psi(t)\rangle$ belongs to the considered Hilbert space and describes the state of the system. Furthermore, the deterministic evolution of the state vector from initial state $|\psi(0)\rangle = |\psi_0\rangle$ is given by a strongly continuous one-parameter group [11]

$$\hat{U}(t) := e^{-\frac{i}{\hbar}\hat{H}t}, \tag{1.3}$$

where the Hamiltonian $\hat{H}$ plays the role of generator of the dynamics. Let us now extend the concept of time-dependence over the density operators. As previously stated, the properties of the density operator are direct consequences of the characteristics of projection operators $\hat{P}_{\psi_i}$. This allows for a natural extension of the time evolution, namely $\hat{\rho}(t) = \sum_i w_i \, |\psi_i(t)\rangle\langle\psi_i(t)|$, where for each $t \in \mathbb{R}_+$ the expression $\hat{\rho}(t)$ is a valid density operator. As a result, the time evolution equation of the density operator, known as the von Neumann equation, emerges

$$\frac{\mathrm{d}}{\mathrm{d}t}\hat{\rho}(t) = -\frac{i}{\hbar}\left[\hat{H}, \hat{\rho}(t)\right], \tag{1.4}$$

which is used to describe isolated quantum systems. At this point, let us clarify that for closed quantum systems, where the Hamiltonian is explicitly time-dependent, $\partial_t \hat{H}(t) \neq 0$, the time evolution operator $\hat{U}(t)$ has a similar but enhanced via the Dyson time-ordering operator for or, equivalently, is expressed through the Dyson series [179], namely

$$\hat{U}(t) = \hat{\mathcal{T}} e^{-\frac{i}{\hbar}\int_0^t \hat{H}(s)ds}, \tag{1.5}$$

where the time-ordering operator $\hat{\mathcal{T}}$ is defined as [115]

$$\hat{\mathcal{T}}[\hat{A}(t_1)\hat{B}(t_2)] = \begin{cases} \hat{A}(t_1)\hat{B}(t_2), & t_1 > t_2 \\ \hat{B}(t_2)\hat{A}(t_1), & t_2 > t_1. \end{cases} \tag{1.6}$$

For further counterparts, we focus on the statistical properties of observables, which can be deduced from this formulation [128]. Assume that $\hat{A}$ is a self-adjoint operator acting on a system's Hilbert space with spectral decomposition $\hat{A} = \sum_k a_k \hat{P}_k$. Then, the average of this operator, understood as the average result over many ensembles, is given by the following formula

$$\langle A \rangle := \mathrm{Tr}\left[\hat{\rho}\hat{A}\right], \tag{1.7}$$

in counterpart to

$$\langle A \rangle := \sum_n |c_n|^2 \left\langle \psi_n \middle| \hat{A}\psi_n \right\rangle = \sum_{k,n} |c_n|^2 |a_k|^2 \delta_{nk} = \sum_k |c_k|^2 |a_k|^2, \tag{1.8}$$

and the state of the system, after the projective measurement of the eigenvalue a_j, is given by the following density operator

$$\hat{\rho} \to \hat{\rho}_j = \frac{\hat{P}_j \hat{\rho} \hat{P}_j}{\mathrm{Tr}\left[\hat{\rho}\hat{P}_j\right]}, \tag{1.9}$$

in contrary to

$$|\psi\rangle \to |\psi'\rangle = \frac{\hat{P}_j |\psi\rangle}{\sqrt{\langle\psi|\psi\rangle}}. \tag{1.10}$$

Of course, we could consider a much more general measurement like positive operator valued measurement (POVM), nevertheless the generalisation of the results from state vectors to density operators is natural.

Under the system's time evolution or after measuring the system, a question might arise whether the state still behaves as a mixture or was purified to a single projector operator. To determine the purity of the state, a simple theorem can be used [136]:

Theorem 1.1. Let $\hat{\rho}$ be the density operator of the quantum system. Then the following statements are equivalent:

a) The state of the system is pure;

b) $\hat{\rho}^2 = \hat{\rho}$;

c) $\mathrm{Tr}\left[\hat{\rho}^2\right] = 1$.

Simultaneously, this property defines a parameter that can monitor the behaviour of the quantum system under the time-evolution, notably the purity of the system, defined as the trace of the square of the density operator. Most importantly, the purity of the system is preserved under the time evolution of the isolated or closed quantum system, as it is given by

$$\hat{\rho}(t) = \hat{U}(t)\hat{\rho}(0)\hat{U}^{\dagger}(t), \tag{1.11}$$

where $\hat{U}(t)$ is the previously defined unitary evolution operator for an isolated quantum system. Then, by the cyclicity property of the trace operation and the fact that $\hat{U}(t)\hat{U}^{\dagger}(t) = \hat{1}$, the purity is conserved. We can restate the evolution formula for the density operator in terms of a superoperator $\Phi(t)$ which has a form [93]:

$$\hat{\rho}(t) = \hat{\Phi}(t)\hat{\rho}(0) := \hat{U}(t)\hat{\rho}(0)\hat{U}^{\dagger}(t), \quad t \geq 0. \tag{1.12}$$

This superoperator satisfies a composition law $\hat{\Phi}(t)\hat{\Phi}(s) = \hat{\Phi}(t+s)$ for $t, s \geq 0$, preserves positivity, hermicity and trace of the density operators [105], constituting to a semigroup of operators. In the case of isolated or closed quantum systems, using the properties of the operator $\hat{U}(t)$, this semigroup $\{\hat{\Phi}(t), t \geq 0\}$ can be extended to a group by introducing an inverse operator $\hat{\Phi}^{-1}(t) = \hat{\Phi}(-t)$. Such systems, where the family of superoperators $\hat{\Phi}(t)$ form a group, are called Hamiltonian systems [129].

1.2 Open quantum systems

The idea behind the construction of open quantum systems comes directly from the formulation of closed systems. Through an open quantum system we shall understand a subsystem S of a total isolated system T, with a complementary system B, being the bath or the environment [122].

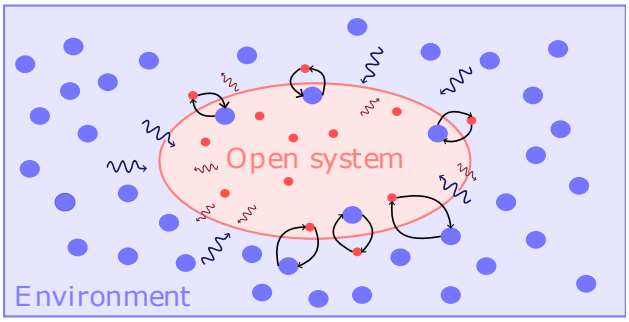

Figure 1.3: The diagram of an open quantum system. An open system interaction picture involves the interaction between the environment and the open system, which is based on either mass exchange (curved arrow between two different circles) or energy exchange (wave arrows). This interaction should be included in the form of an interaction Hamiltonian that acts upon the tensor product space of both systems' spaces.

The total quantum system is treated as isolated; thus, its time evolution can be considered unitary. However, the complexity of the total system resulting from the number of degrees of freedom greatly incapacitates the precise analysis possibilities, as the degrees of freedom of the environment are usually significantly greater than 1 or even infinite. To address this problem, a sequence of approximations must be performed to simplify the dynamics. In general, common justification, when investigating open quantum systems, is the termination of memory effects, i.e. asking if the historical states (past) of the system should influence the present state (future). Still, the Markovianity property of the system cannot be directly translated from classical to quantum theory, as it violates the Kolmogorov condition and is rather connected to the direction of the flow of information, as stated in [23]. Let us start generally by considering a tensor product Hilbert space of the total system

$$\mathcal{H}_T = \mathcal{H}_S \otimes \mathcal{H}_B \tag{1.13}$$

where $\mathcal{H}_S$ represents the Hilbert space of the considered system and $\mathcal{H}_B$ represents the Hilbert space of the states of the environment. The density matrix associated with the state of the total system must then satisfy the von Neumann equation. We shall assume that the system is isolated. This leads to the equation of motion in the form

$$\frac{\mathrm{d}}{\mathrm{d}t}\hat{\rho}_T(t) = -\frac{i}{\hbar}\left[\hat{H}_T, \hat{\rho}_T(t)\right], \tag{1.14}$$

where further, we will hold the following assumption on the form of the Hamiltonian

$$\hat{H}_T = \hat{H}_S \otimes \hat{1} + \hat{1} \otimes \hat{H}_B + g\hat{H}_I, \tag{1.15}$$

with $\hat{H}_S, \hat{H}_B$ governing the dynamics of the subsystems, and $\hat{H}_I$ being the interaction term with coupling constant g, and $\hat{1}$ being the identity operator in respective spaces. To extract the open system dynamics from the total density matrix, a partial trace is required, that is trace operation taken over the environment, incorporating information about its influence [24], namely

$$\hat{\rho}_S(t) = \mathrm{Tr}_B\, \hat{\rho}_T(t). \tag{1.16}$$

Importantly, there is no a priori assumption that $\hat{\rho}_T(t)$ can be decomposed as a tensor product of two density operators, as this would imply a lack of correlations between two systems. As by our assumption on the

unitarity of the dynamics, the density operator of the total system evolves according to the formula

$$\hat{\rho}_T(t) = \hat{U}(t)\hat{\rho}_T(0)\hat{U}^\dagger(t) \tag{1.17}$$

consequently giving a recipe for calculating the density operator of an open quantum system as follows

$$\hat{\rho}_S(t) = \mathrm{Tr}_B\left[\hat{U}(t)\hat{\rho}_T(0)\hat{U}^\dagger(t)\right] \tag{1.18}$$

that can be displayed on the simple diagram presented in Fig. 1.4

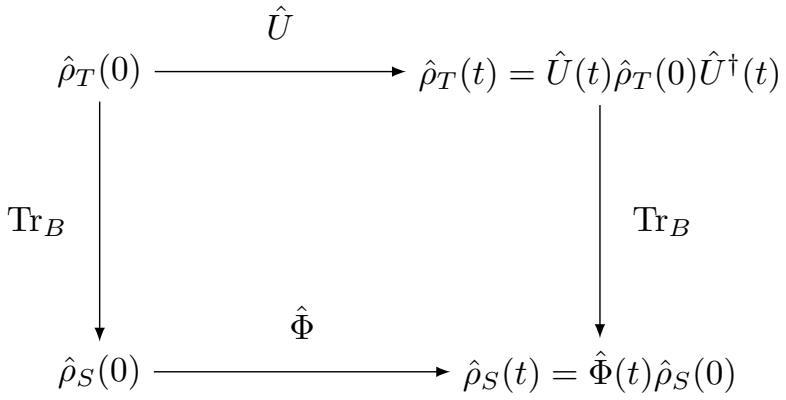

Figure 1.4: The diagram describing two approaches to evolution dynamics of open system's density operator $\hat{\rho}_S$. The top path describes the straightforward calculation of the total density matrix at time t, then *projecting* it, by tracing over the environment. The bottom path is more complying but the question of the existence of such transformation must be posed.

Similarly to the discussion presented for isolated quantum systems, we are interested in the form and general properties of the map $\hat{\Phi}(t)$ for all $t \geq 0$, that transfers the initial state of the open system ,$\hat{\rho}_S(0)$, to the state at time instant $t \geq 0$. We expect that they originate from the physical restrictions imposed on the mathematical apparatus to maintain the interpretation. As previously stated, the density operators are self-adjoint, positive, and trace-class operators and so the map $\hat{\Phi}(t)$ must preserve all those features at all times $t \geq 0$. It turns out that, apart from the semigroup property, that is $\hat{\Phi}(t)\hat{\Phi}(s) = \hat{\Phi}(t+s)$ for $t, s \geq 0$, the map $\hat{\Phi}(t)$ must be completely positive [154]. Additionaly, the characteristics of the dynamics of the open quantum system are expected to strongly depend on the type of interaction with the environment, which, in some cases, introduces memory effects. To exclude complex physical effects that might introduce past dependency of the system, we assume that the Markovianity property is preserved, and thus, by [45] we expect the interaction to be in the weak-coupling regime between the open system and the environment. All these assumptions lead to the Gorini-Kossakowski-Saudarshan-Lindblad (GKSL or Lindblad) equation of evolution for an open quantum system [72, 112]. The greatest achievement of these works is that the form of the generator of the dynamical semigroup for the weakly coupled open quantum system derives directly from

imposed mathematical restrictions. This, however, would not be possible if not for a celebrated Choi-Kraus theorem on the decomposition of completely positive dynamical maps that preserve the trace of density operator [107, 35], namely

$$\hat{\Phi}\hat{\rho} = \sum_i \hat{V}_i \hat{\rho} \hat{V}_i^\dagger, \tag{1.19}$$

where $\hat{V}_i \in B(\mathcal{H})$ are the bounded operators [cf. Appendix A], called Kraus operators, acting in the Hilbert space $\mathcal{H}$ and satisfying the completeness relation $\sum_i \hat{V}_i \hat{V}_i^\dagger = \hat{1}$[1]. In the context of quantum computation or information theory, the superoperator $\hat{\Phi}$ is called a quantum channel [128]. Then, by scrupulous reasoning, the equation of motion for the density operator of an open quantum system is given in the form [25]

$$\frac{\mathrm{d}}{\mathrm{d}t}\hat{\rho}_S(t) = \frac{1}{i}\left[\hat{H}_S, \hat{\rho}_S(t)\right] + \frac{1}{2}\sum_k \gamma_k \left(\left[\hat{L}_k \hat{\rho}_S(t), \hat{L}_k^\dagger\right] + \left[\hat{L}_k, \hat{\rho}_S(t)\hat{L}_k^\dagger\right]\right) \tag{1.20}$$

which is the GKSL master equation. The operators $\hat{L}_k$ are known as quantum jump operators or Lindblad operators. The operator $\hat{\mathcal{L}}$ generates the semigroup of dynamical operators $\{\hat{\Phi}(t) : t \geq 0\}$ by the formal exponentiation formula [157, 59]

$$\hat{\Phi}(t) = e^{t\hat{\mathcal{L}}} \tag{1.21}$$

or equivalently

$$\hat{\mathcal{L}} := \lim_{t\to 0^+} \frac{\hat{\Phi}(t) - \hat{1}}{t}. \tag{1.22}$$

We shall call $\hat{\mathcal{L}}$ the Liouvillian operator in Lindblad form [3]. This operator might not be by itself a self-adjoint operator, but it generates a dynamics that is consistent with physical expectations. As an example, we may see that by the form of the Liouvillian operator in Lindblad form (1.20) the trace of the density operator is preserved under its action.

At this point, it is worth noting that other superoperator techniques were developed to describe the evolution of a given quantum system. If we relax the Markovianity condition, then the most general evolution is given by the Nakajima-Zwanzig equation [193, 127, 143, 31] which describes the evolution of the relevant, and complementary irrelevant, part of the quantum system. The relevant part of the total system provides information about the dynamics of the open system. It is defined using a projection operator as follows:

$$\hat{\mathcal{P}}\hat{\rho}_T := (\mathrm{Tr}_B\, \hat{\rho}_T) \otimes \hat{\rho}_B, \tag{1.23}$$

and complementary, the irrelevant part defined in terms of $\hat{\mathcal{Q}}$-operator, as follows

$$\hat{\mathcal{Q}}\hat{\rho}_T := (\hat{1} - \hat{\mathcal{P}})\hat{\rho}_T, \tag{1.24}$$

where $\hat{\rho}_B$ represents an initial state of the environment, which we will assume is normalised. Differentiating both equations with respect to time t, changing to the interaction picture, and then performing some manipulations [143] one arrives at the equation for the relevant part of the total system

$$\frac{\mathrm{d}}{\mathrm{d}t}\hat{\mathcal{P}}\hat{\rho}_T(t) = \int_0^t \mathcal{K}(t,s)\hat{\mathcal{P}}\hat{\rho}_T(s)ds, \tag{1.25}$$

[1] There are two legacy approaches to the derivation of the GKSL equation, one for finite-dimensional Hilbert spaces and the other for infinite-dimensional Hilbert spaces but with bounded generator [39].

where $\mathcal{K}$ is the memory kernel of the Nakajima-Zwanzig equation. Due to dependency of the state $\hat{\mathcal{P}}\hat{\tilde{\rho}}_T$ at time t on previous states via integral kernel, the equation describes the non-Markovian evolution, that is with memory effects [63, 145]. Of course, this equation given certain assumptions, leads to the GKSL equation.

Chapter 2

Quantum theory in phase-space formalism

2.1 Phase-space quantum theory- general information

A phase-space approach to quantum theory is one of many equivalent formulations of quanta [164]. It was founded on key developments introduced gradually by H. Weyl, E. Wigner, H. Groenewold, and J. Moyal. Their work initiated a new paradigm, in which the operator-based framework in the Hilbert space was replaced by a noncommutative algebra of real-valued functions defined in phase space. The origins of this formulation trace back to 1927 and then to 1932. It was in 1927 that H. Weyl discovered the correspondence between dynamical quantities and linear Hermitian operators, formulated through a transformation that preserves the probabilistic structure of quantum mechanics [181]. Five years later, E. Wigner introduced a special type of function that changed the common view associated with the positivity of probability distribution functions. By considering quantum corrections for thermodynamic equilibrium states Wigner discovered a density function, which was notable for allowing negative values [182]. Subsequently, H. Groenewold and J. Moyal independently made significant contributions to this framework, recognising the relationship between the WDF, the density operator, and the Weyl transform. Their mutual work resulted in the construction of the noncommutative algebra of real functions that were strictly connected to the well-known quantum mechanics [76, 126].

Before we consider a rigorous description of the quantum phase space let us, by a simple example, dwell on the idea of a probabilistic description of classical particles. Let us consider a classical particle moving along a trajectory $(x(t), p(t)) \in \mathbb{R}^2$, with the initial position and momentum given by (x_0, p_0). In this case, the probability density function (PDF) of finding this particle in phase space can be expressed as [102]:

$$P(x, p) \propto \delta(x - x(t; x_0, p_0)) \otimes \delta(p - p(t; x_0, p_0)),$$

which means that the particle is moving along a trajectory generated by the solution of the classical Hamilton equations with a specific initial condition (x_0, p_0). Equivalently, the probability of finding a particle in the strip that contains its trajectory is equal 1, whereas apart from it it is 0. This can be seen as a motion of a point-centred probability distribution function along the phase-space trajectory of the system. On the other hand, consider a scenario in which the particle might have a 50% chance of starting at a different point, (x_{01}, p_{01}) or (x_{02}, p_{02}), in the phase space[1]. In this case, after repeating the setup infinitely many times and

[1] Assuming that it is not a point lying on the same trajectory as the previously chosen point

measuring the particle's trajectory, we can express the probability density function as follows:

$$P(x,p) \propto \frac{1}{2}\delta(x-x_1(t;x_{01},p_{01}))\otimes\delta(p-p_1(t;x_{01},p_{01}))+\frac{1}{2}\delta(x-x_2(t;x_{02},p_{02}))\otimes\delta(p-p_2(t;x_{02},p_{02})).$$

It is crucial to note that it does not imply the co-existence of a particle on two non-intersecting trajectories. Rather, it encapsulates the randomness of a possible state of the system. We have already discussed such cases in the previous chapter, where, instead of considering a pure quantum state, we extended the idea of statistical certainty to allow for the coexistence of multiple constituent states in a single quantum system, resulting in the density operator approach. Equipped with this idea, let us consider a quantum equivalent of classical phase space. According to the axioms of quantum mechanics and the properties of canonical operators, it is established that the canonical operators $\hat{x}_k = x_k$ and $\hat{p}_l = -i\hbar\partial_{x_l}$ are not commensurable, that is, they satisfy the canonical commutation relation in the form

$$[\hat{x}_k, \hat{p}_l] = i\hbar\delta_{kl}\hat{1}. \tag{2.1}$$

This relationship is governed by the Heisenberg uncertainty principle, which introduces a minimal volume $\Delta x_k \Delta p_k$ for $k = 1, \ldots, n$ that cannot be surpassed by any measurement. Thus, we expect that this should resemble the structure of the quantum phase space and the probability distributions defined on it. As the Heisenberg uncertainty principle forbids the simultaneous characterisation of position and momentum, rather than considering points, one should consider minimal cells obeying Heisenberg's principle.

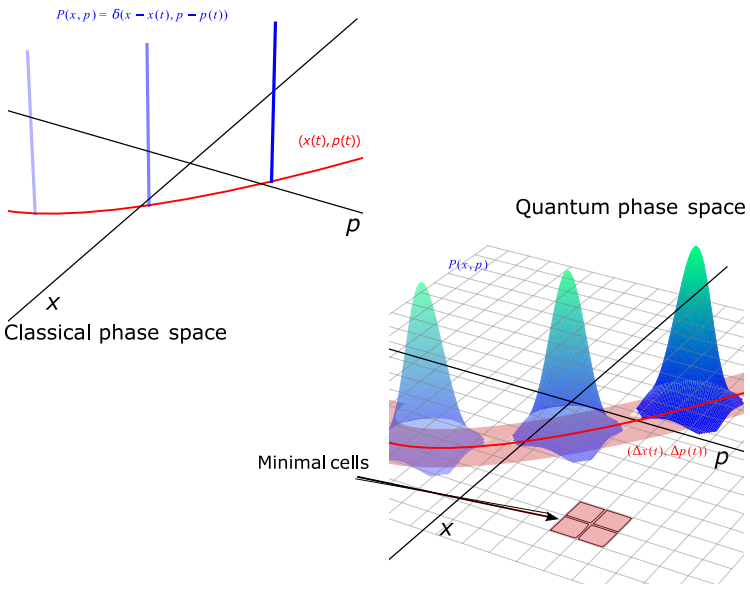

Figure 2.1: Pictorial difference between classical and quantum phase spaces. In classical space, the evolution of a particle can be regarded as a movement of a 0-width probability distribution function along the particle's trajectory. In the quantum phase space, the probability function with non-zero standard deviation evolves over the minimal cells given by Heisenberg's uncertainty principle, and rather than trajectories, we are presented with a statistical average.

The simplest flaw of this approach is the choice of centres of such minimal cells, which implies some privilege among points in the phase space. Also, this would require a transition from a continuous description of a quantum system to a countable one, since $\mathbb{R}^2$ phase space can be covered by a countable union

of squares. Additionally, as pointed out in Ref. [49], the minimal geometrical objects that simultaneously satisfy the uncertainty relationship and have the symplectic group as their symmetry group are the quantum blobs. These are ellipsoids strictly related to squeezed coherent states that can be obtained from the phase-space ball through an affine symplectic transformation. Nevertheless, the phase-space approach gives the closest description of quantum mechanics that simultaneously resembles a classical structure. The general characteristics of the quantum phase space (or p$\hbar$ase space) were based on the idea that the quantum structure, in the classical limit, has to become classical [104]. Let us recall that a complete description of a classical system in terms of Hamiltonian mechanics requires 3 elements: a phase space $\mathcal{M} = \mathbb{R}^{2n}$ given by a smooth manifold, an energy function $H : \mathcal{M} \to \mathbb{R}$ and a symplectic 2-form ω [124, 125]. For the scope of this work, we will assume that $\mathcal{M} = \mathbb{R}^2$, then the classical phase space of the system with Hamiltonian $H(x, p, t)$ is equipped with Poisson bracket [168]

$$\{f(x,p), g(x,p)\} := \frac{\partial f}{\partial x}(x,p)\frac{\partial g}{\partial p}(x,p) - \frac{\partial g}{\partial x}(x,p)\frac{\partial f}{\partial p}(x,p). \tag{2.2}$$

This allows for the description of the trajectories of the classical system via Hamilton equations

$$\begin{aligned} \tfrac{\mathrm{d}}{\mathrm{d}t}x(t) &= \{x, H(x,p,t)\}, \\ \tfrac{\mathrm{d}}{\mathrm{d}t}p(t) &= \{p, H(x,p,t)\}. \end{aligned} \tag{2.3}$$

Complementarily, let us turn our attention to the system described by some probability distribution function (PDF), $P(x, p, t)$, defined on the phase space. The Liouville theorem says that along the trajectories of the system, the PDF $P(x, p, t)$ is constant [6]. Consequently, the function $P(x, p, t)$ satisfies the Liouville equation

$$\frac{\partial}{\partial t}P(x,p,t) = \{H(x,p,t), P(x,p,t)\}\,. \tag{2.4}$$

The Liouville equation exemplifies the conservation law of the PDF $P(x, p, t)$ during time evolution. These elements constitute the statistical description of classical mechanics. To extend this structure suitably for quantum mechanical theory in such a way that there exists a *smooth* transition, from quantum to classical mechanics, one introduces the star product [88, 104]:

Definition 2.1. Let $(\mathcal{M}, \{\cdot,\cdot\})$ be a Poisson manifold. A star product $\star : C^\infty(\mathcal{M}) \times C^\infty(\mathcal{M}) \to C^\infty(\mathcal{M})$ is defined as

$$f \star g := \sum_{k=0}^{\infty} \left(\frac{i\hbar}{2}\right)^n C_n(f,g), \tag{2.5}$$

where C_n are bidifferential operators of order n with $C_0(f, g) = f \cdot g$, $C_1(f, g) = \{f, g\}$, satisfying

$$\sum_{j+k=n} C_j(C_k(f,g),h) = \sum_{j+k=n} C_j(f, C_k(g,h)). \tag{2.6}$$

The main advantage of this approach is that knowledge of classical mechanics allows for direct analysis in quantum mechanics, thus there is no need to rephrase the interpretation of canonical variables. One of many star products is the Moyal star product, or simply the Moyal product, defined over canonical phase space, where $\mathcal{M} = \mathbb{R}^2$ as follows

Definition 2.2 (Moyal product [61, 7])**.** Let $f, g \in C^\infty(\mathbb{R}^2)$. The Moyal product $\star : C^\infty(\mathbb{R}^2) \times C^\infty(\mathbb{R}^2) \to C^\infty(\mathbb{R}^2)$ is given by

$$f(x,p) \star g(x,p) := f(x,p) e^{\frac{i\hbar}{2}\left(\overleftarrow{\partial_x}\overrightarrow{\partial_p} - \overleftarrow{\partial_p}\overrightarrow{\partial_x}\right)} g(x,p), \tag{2.7}$$

where arrows over the derivative sign are understood as the direction in which it is acting.

This definition can be used interchangeably, depending on the complexity of calculations, with the following equivalent forms

$$\begin{aligned} f(x,p) \star g(x,p) &:= f\left(x + \frac{i\hbar}{2}\partial_p, p - \frac{i\hbar}{2}\partial_x\right) g(x,p) \\ &= f\,(x,p)\, g\left(x - \frac{i\hbar}{2}\partial_p, p + \frac{i\hbar}{2}\partial_x\right) \\ &= \frac{1}{(\pi\hbar)^2}\int_{\mathbb{R}^4} e^{\frac{2i}{\hbar}S(x,x',x'',p,p',p'')} f(x',p') g(x'',p'') dx' dx'' dp' dp'', \end{aligned} \tag{2.8}$$

where function $S(x, x', x'', p, p', p'')$ is the signed area of a parallelogram in a phase space spanned by 3 vectors: (x, p), (x', p'), (x'', p''), namely

$$S(x,x',x'',p,p',p'') = \det \begin{vmatrix} 1 & 1 & 1 \\ x & x' & x'' \\ p & p' & p'' \end{vmatrix}. \tag{2.9}$$

The most important property of such a defined product is its limit as $\hbar \to 0^+$. Let us notice that for any two symbols f, g one has

Proposition 2.1. For any two functions $f, g \in C^\infty(\mathbb{R}^2)$ such that their $\star$-product is well-defined, the following limits, as $\hbar \to 0^+$, hold

$$(f \star g)(x,p) \to (f \cdot g)(x,p), \tag{2.10}$$

and

$$\{f,g\}_\star := \frac{1}{i\hbar}\left[f \star g - g \star f\right](x,p) \to \{f,g\}, \tag{2.11}$$

where $\{f, g\}$ stands for the Poisson bracket of the functions f and g.

These are direct consequences of the definition of the $\star-$product. Additionally, the phase-space approach enables an operator-free description of quantum theory, which requires the use of classical functions to characterise the quantum systems. However, there is an elegant way to connect these two descriptions through the Weyl transformation [50, 64]

Definition 2.3. Let $a \in S(\mathbb{R}^2)$, and $\hat{A} : S(\mathbb{R}) \to S(\mathbb{R})$, where $S(\mathbb{R}^n)$ is the Schwartz space of rapidly vanishing functions [cf. Appendix A]. The Weyl transform between a and $\hat{A}$ is the correspondence defined as

$$\hat{A}(x,y) = \frac{1}{2\pi\hbar}\int_{\mathbb{R}} e^{\frac{i}{\hbar}p(x-y)} a\left(\frac{1}{2}(x+y), p\right) dp, \tag{2.12}$$

$$a(x,p) = \int_{\mathbb{R}} e^{-\frac{i}{\hbar}py} \left\langle x + \frac{1}{2}y \middle| \hat{A} \middle| x - \frac{1}{2}y \right\rangle dy. \tag{2.13}$$

We will denote that relationship as $\mathcal{W}[\hat{A}](x,p) = a(x,p)$. Both definitions (2.2 and 2.3) constitute the foundation of the deformation quantisation [17, 19].

2.2 Weyl transform and Wigner function

As previously mentioned, the Weyl transform serves as a correspondence tool between operator-formulated quantum mechanics and the phase-space approach. Let us provide some basic properties of the Weyl symbol of the given operators $\hat{A}$ and $\hat{B}$ [42]

Corollary 2.1. Some commonly used properties of Weyl transform $\mathcal{W}$:

1. Linearity: $\mathcal{W}[\alpha\hat{A}+\beta\hat{B}](x,p)=\alpha\mathcal{W}[\hat{A}](x,p)+\beta\mathcal{W}[\hat{B}](\boldsymbol{x},\boldsymbol{p})$;
2. If $\hat{A}^{\dagger}=\hat{A}$ then $\mathcal{W}[\hat{A}](x,p)\in\mathbb{R}$;
3. Product rule: $\mathcal{W}[\hat{A}\hat{B}](x,p)=(\mathcal{W}[\hat{A}]\star\mathcal{W}[\hat{B}])(x,p)$;
4. Commutator representation: $\mathcal{W}\left[\frac{1}{i\hbar}[\hat{A},\hat{B}]\right]=\left\{\mathcal{W}[\hat{A}](x,p),\mathcal{W}[\hat{B}](x,p)\right\}_{\star}$.

These properties give a helpful correspondence relationship between phase-space observables (symbols) and operator observables defined on the Hilbert space associated with our system. Finally, we can provide the phase-space equivalent of the carrier of the information, the density operator [50, 180] :

Definition 2.4 (Wigner function)**.** A Wigner function of the quantum system is a real-valued quasi-probability distribution function defined over the quantum phase space, with well-defined marginal distributions, and is given by the rescaled Weyl transform of the density operator, namely

$$\varrho(x,p,t):=\frac{1}{2\pi\hbar}\int_{\mathbb{R}}\left\langle x+\frac{1}{2}y\right|\hat{\rho}(t)\left|x-\frac{1}{2}y\right\rangle e^{-\frac{i}{\hbar}py}dy. \tag{2.14}$$

It is worth mentioning that there are definitions of the Wigner function for any underlying deformed geometry that can be introduced by a group-theoretical approach [4, 50].

Corollary 2.2. The equation of motion for an isolated or closed quantum system in a phase-space representation is given by the equation in the form [37]

$$\partial_t\varrho(x,p,t)+\frac{1}{m}p\partial_x\varrho(x,p,t)-\{U(x,t),\varrho(x,p,t)\}_{\star}=0. \tag{2.15}$$

Applying the property (2.10) of the star product to the equation of motion, we arrive at the so-called *classical limit* of the equation[2]. That is, at $\hbar\to 0^{+}$, the equation resembles the Liouville equation for the classical PDFs defined over the phase space, namely

$$\partial_t P(x,p,t)+\frac{1}{m}p\partial_x P(x,p,t)-\partial_x[U(x,t)]\partial_p P(x,p,t)=0, \tag{2.16}$$

and can be solved using the method of characteristics [60]. The overall volume of the phase-space PDF remains invariant during the time evolution. In other words, the PDF is constant along the trajectories of the classical system. Generally, when considering such a limit, one should not forget about the $\hbar-$dependency

[2]There are some different understandings behind the term classical limit. In this context, we will use the similarity of the mathematical formalism between quantum and classical phase space as $\hbar\to 0^{+}$.

of the WDF. Näively, the limit $\varrho(x,p,t) \to \delta(p)|\psi(x,t)|^2$ is maintained as $\hbar \to 0^+$, unless the implicit dependence of the wave function ψ on $\hbar$ is considered. Otherwise, the final form of this expression is an asymptotic exponential function multiplied by an energy-limiting Dirac delta distribution, as thoroughly derived in [151]. Last but not least, we would like to revisit the eigenproblem posed in wave function quantum theory in terms of the phase-space approach, leading to full equivalence between them. Recall that an eigenproblem for the Hamiltonian $\hat{H} = \hat{p}^2/(2m) + U(\hat{x})$ is posed as

$$\hat{H}\,|\psi\rangle = E\,|\psi\rangle\,, \tag{2.17}$$

which in position representation takes the form of the second-order partial differential equation [15]

$$-\frac{\hbar^2}{2m}\frac{\mathrm{d}^2}{\mathrm{d}x^2}\psi(x) + U(x)\psi(x) = E\psi(x), \tag{2.18}$$

where $\psi(x) = \langle x|\psi\rangle$ is the wave function of the system, E is interpreted as the energy of the system. On the basic level, it appears as a result of the application of separation of variables to the time-dependent problem, with the assumption that the time-dependent wave function is a product of the spatial function $\psi(x)$ and some time-dependent function $\phi(t)$. Similar methods can be used in phase-space quantum mechanics to deduce the phase-space eigenproblem. The Wigner eigenfunction to the eigenvalue E has to be the solution to the following pair of equations [70, 69, 37]

$$\begin{cases} H(x,p) \star \varrho(x,p) = \mathcal{E}\varrho(x,p), \\ \varrho(x,p) \star H(x,p) = \mathcal{E}\varrho(x,p), \end{cases} \tag{2.19}$$

where $H(x,p)$ is the Weyl symbol of the Hamiltonian $\hat{H}$. For the purpose of the discussion, let us assume that the eigenvalues of the Hamiltonian $\hat{H}$ form a discrete set $\sigma(\hat{H}) = \{E_n\}_{n\in\mathbb{N}}$ and are nondegenerate. Then, according to the definition 2.4, the solution to Eq. (2.19) is given by [70]

$$\varrho_{nm}(x,p) = \frac{1}{2\pi\hbar}\int_{\mathbb{R}} \psi_n\left(x + \frac{1}{2}y\right)\psi_m^*\left(x - \frac{1}{2}y\right)e^{-\frac{i}{\hbar}py}dy, \tag{2.20}$$

called the cross-Wigner function [50], to the eigenvalue $\mathcal{E}_{nm} = E_n - E_m$. It implies that a general, time-dependent WDF can be expanded into coherent and incoherent part [70]

$$\varrho(x,p,t) = \sum_n c_{nn}\varrho_{nn}(x,p) + \sum_{\substack{n,m \\ n\neq m}} c_{nm}e^{-\frac{i}{\hbar}(E_n - E_m)t}\varrho_{nm}(x,p). \tag{2.21}$$

where off-diagonal terms are withholding the information about energy exchange between the modes of the evolving system. Additionally, applying the secular approximation [116], we may conclude that in the limit $t \to +\infty$ the incoherent terms average out to zero, thus

$$\lim_{t\to+\infty}\varrho(x,p,t) = \sum_n c_{nn}\varrho_{nn}(x,p). \tag{2.22}$$

meaning that the system decohered to the stationary state.

2.3 Phase-space approach to open quantum systems

As discussed in the previous chapter, the evolution of an open quantum system is modeled by simplifying the dynamics of the total system through various approximations. So far, the phase-space quasiprobability distribution function formalism has been developed for a single, isolated, or closed system, where the independent variables relate only to that closed system. In this chapter, we will explore the properties of the Weyl transform in product spaces, which will allow us to derive the GKSL equation based on the assumptions made previously. Starting with the general properties of the WDF resulting from its definition, we can state that it is a real, bounded function with correctly defined marginal distributions, which provides an equivalent to the density operator quantum mechanics statistical description of the quantum system. The Stratonovich-Weyl (S-W) correspondence provides a powerful generalisation of the Weyl transform, offering a more meaningful connection between quantum operators and the phase-space functions [175]. At its core, this approach defines a quantisation operator that elegantly captures the geometric structure of the system, making it a versatile tool for various applications. We shall now define the Stratonovich-Weyl correspondence, according to Refs [163, 147, 170]

Definition 2.5. Let $\hat{A}, \hat{A}_1, \hat{A}_2$ be operators acting on Hilbert space $\mathcal{H}$. A 3-tuple $(\mathcal{H}, \mathcal{M}, \hat{\Omega})$ constitutes Stratonovich-Weyl (S-W) correspondence, where $\hat{\Omega} : \mathcal{M} \ni M \to \hat{\Omega}(M) \in B(\mathcal{H})$ is the S-W kernel and $\mathcal{M}$ is the phase space of the considered system with a phase-space vector given by M, if the following conditions are satisfied

1. The mapping defined as
$$\mathcal{W}[\hat{A}](M) := \mathrm{Tr}\Big[\hat{A}\hat{\Omega}(M)\Big] \tag{2.23}$$
exists, is linear and invertible;

2. If $\hat{A}$ is hermitian then the function $\mathcal{W}[\hat{A}](M)$ is real valued;

3. The trace of an operator $\hat{A}$ is equal to the integral of the function $\mathcal{W}[\hat{A}](M)$ in the phase space
$$\int_{\mathcal{M}} \mathcal{W}[\hat{A}](M)dM = \mathrm{Tr}\,\hat{A}, \tag{2.24}$$
and $\int_{\mathcal{M}} \hat{\Omega}(M)dM = \hat{1}$;

4. The following product rule holds
$$\int_{\mathcal{M}} \mathcal{W}[\hat{A}_1](M)\mathcal{W}[\hat{A}_2](M)dM = \mathrm{Tr}\Big[\hat{A}_1\hat{A}_2\Big]; \tag{2.25}$$

5. The covariance condition holds
$$\mathcal{W}[\hat{U}^\dagger\hat{A}\hat{U}](M) = \mathcal{W}[\hat{A}](T(M)), \tag{2.26}$$
where $\hat{U}$ is a unitary transformation and $T : \mathcal{M} \ni M \to T(M) \in \mathcal{M}$ is a transformation associated with $\hat{U}$, acting on the phase space.

Thus, the S-W correspondence is a one-to-one correspondence between operators and functions defined over a space with classical meaning. These conditions generate the WDF of the quantum system with any underlying geometry and allow for equivalent statistical interpretation. It should be noted that there is no mention of a $\star$-product. However, the 4th condition gives a basis for the uniqueness of an algebra of functions defined over phase space [26]. We can define a $\star-$product through the following integral relation [66]

$$(f \star g)(M) = \iint_{\mathcal{M}} \mathrm{Tr}\left[\hat{\Omega}(M)\hat{\Omega}(M_1)\hat{\Omega}(M_2)\right] f(M_1)g(M_2)dM_1dM_2, \tag{2.27}$$

which, in general, is non-commutative, and reduces to a common product of two functions when considered under the integral sign

$$\int_{\mathcal{M}} (f \star g)(M)dM = \int_{\mathcal{M}} (f \cdot g)(M)dM. \tag{2.28}$$

An observant reader will notice that we have reached the same formalism as previously introduced: the non-commutative calculus of real functions, represented as appropriate symbols of operators. This generalisation of the Weyl correspondence requires us to find an operator $\hat{\Omega}(M)$ whose form depends on the underlying Lie symmetry group [66]. As a skimmed example, we may consider a flat space $\mathcal{M} = \mathbb{R}^2$ representing a phase space with position and momentum coordinates, $M = (x, p)$, where the Lie symmetry group is given by the Heisenberg-Weyl group and is associated with standard commutation rules for position and momentum [183, 64]. By the detailed calculations that can be found i.e. in [174, 28], the $\hat{\Omega}(M)$ has the form given by a displaced parity operator [48, 144, 71], leading to the original definition of the WDF [4].

We have now obtained a powerful tool for building a WDF for any quantum system, regarding the underlying geometry of the system. Turning our attention to open quantum systems, an open system is, by general definition, a subsystem of a total system that includes the environment (or a bath) and the system in question, as explained in Sec. 1.2. Let us assume that the phase space of the total system is the flat space $\mathbb{R}^{2+2N}$, where the constituent phase spaces, $\mathbb{R}^2$ and $\mathbb{R}^{2N}$, correspond to the phase space of the one-dimensional open system and the phase space of the N-dimensional environment, respectively. This setup is equivalent to considering a tensor product Hilbert space composed of two L^2-spaces over $\mathbb{R}$ and $\mathbb{R}^N$, by (1.13). We can now apply the S-W correspondence for such systems by treating a WDF of the total system ϱ_T as a starting point. Let us define a WDF of the total system as

$$\varrho_T(\boldsymbol{Q}, \boldsymbol{K}, t) := \mathrm{Tr}\left[\hat{\rho}(t)\hat{\Omega}(\boldsymbol{Q}, \boldsymbol{K})\right], \tag{2.29}$$

where $(\boldsymbol{Q}, \boldsymbol{K}) = (x, \boldsymbol{X}, p, \boldsymbol{P}) \in \mathbb{R}^{2+2N}$ are position and momentum coordinates of the total system. These consist of the coordinates $(x, p) \in \mathbb{R}^2$ corresponding to the open system, and $(\boldsymbol{X}, \boldsymbol{P}) \in \mathbb{R}^{2N}$ corresponding to the environment. We will treat the total system T as an isolated system and thus it obeys the equation of motion

$$\partial_t \varrho_T(\boldsymbol{Q}, \boldsymbol{K}) = \{H_T(\boldsymbol{Q}, \boldsymbol{K}), \varrho_T(\boldsymbol{Q}, \boldsymbol{K})\}_{\star_T}, \tag{2.30}$$

where $H_T(\boldsymbol{Q},\boldsymbol{K})$ is the symbol of total the Hamiltonian. The form of the star product $\star_T$ in total, flat space, for two smooth functions $A, B : \mathbb{R}^{2+2N} \to \mathbb{C}$, is given by

$$\begin{aligned} A(\boldsymbol{Q},\boldsymbol{K}) \star_T B(\boldsymbol{Q},\boldsymbol{P}) &= \lim_{N\to\infty} \sum_{n=0}^{N} \left(\frac{i\hbar}{2}\right)^n \frac{1}{n!} \sum_{k=0}^{n} \left(\nabla_{\boldsymbol{Q}}^{n-k} A\right) \left(\nabla_{\boldsymbol{K}}^{n-k} B\right) (-1)^k \left(\nabla_{\boldsymbol{K}}^{k} A\right) \left(\nabla_{\boldsymbol{Q}}^{k} B\right) \\ &= A(\boldsymbol{Q},\boldsymbol{K}) e^{\frac{i\hbar}{2}\left(\overleftarrow{\nabla_{\boldsymbol{Q}}}\overrightarrow{\nabla_{\boldsymbol{K}}} - \overleftarrow{\nabla_{\boldsymbol{K}}}\overrightarrow{\nabla_{\boldsymbol{Q}}}\right)} B(\boldsymbol{Q},\boldsymbol{K}). \end{aligned} \tag{2.31}$$

We also define the star product for constituent subsystems: the open system S and the bath B, in the following way

$$A_S(x,p) \star_S B_S(x,p) := A_S(x,p) e^{\frac{i\hbar}{2}\left(\overleftarrow{\partial_x}\overrightarrow{\partial_p} - \overleftarrow{\partial_p}\overrightarrow{\partial_x}\right)} B_S(x,p), \tag{2.32}$$

$$A_B(\boldsymbol{X},\boldsymbol{P}) \star_B B_B(\boldsymbol{X},\boldsymbol{P}) := A_B(\boldsymbol{X},\boldsymbol{P}) e^{\frac{i\hbar}{2}\left(\overleftarrow{\nabla_{\boldsymbol{X}}}\overrightarrow{\nabla_{\boldsymbol{P}}} - \overleftarrow{\nabla_{\boldsymbol{P}}}\overrightarrow{\nabla_{\boldsymbol{X}}}\right)} B_B(\boldsymbol{X},\boldsymbol{P}), \tag{2.33}$$

where A_S, B_S, A_B, B_B are smooth functions defined over associated subsystems.
We are strictly interested in the evolution of the open system S. To extract valuable information from the total WDF $\varrho_T(\cdot,\cdot,t)$, we calculate its marginal distribution taken with respect to the environment variables, that is

$$\varrho_S(\boldsymbol{x},\boldsymbol{p},t) := \int_B \varrho_T(\boldsymbol{Q},\boldsymbol{K},t) d\boldsymbol{X} d\boldsymbol{P} = \int_B \varrho_T(x,\boldsymbol{X},p,\boldsymbol{P},t) d\boldsymbol{X} d\boldsymbol{P}. \tag{2.34}$$

This has been proven to be a valid approach for defining an information medium for any open quantum system [51]. To further simplify the equation of motion for the open system, let us consider a total system's Hamiltonian symbol given as a sum of three elements: the Hamiltonians of the open system, of the bath, and the interaction term, which is precisely a symbol of (1.15), namely,

$$H_T(\boldsymbol{Q},\boldsymbol{K}) = H_S(x,p) + H_B(\boldsymbol{X},\boldsymbol{P}) + \sum_k \alpha_k g_S^k(x,p) \star_T g_B^k(\boldsymbol{X},\boldsymbol{P}), \tag{2.35}$$

then the evolution of the open system is governed by the following Master equation

$$\partial_t \varrho_S(\boldsymbol{x},\boldsymbol{p},t) = \{H_S(x,p), \varrho_S(x,p,t)\}_{\star_S} + \sum_k \alpha_k \left\{ g_S^k(x,p), \mathbb{E}\left[g_B^k | x,p,t\right] \varrho_S(x,p,t) \right\}_{\star_S}, \tag{2.36}$$

where $\mathbb{E}\left[g_B^k|x,p,t\right]$ is the conditional expected value of the k-th bath interaction term, namely

$$\mathbb{E}\left[g_B^k|\boldsymbol{x},\boldsymbol{p},t\right] = \frac{1}{\varrho_S(x,p,t)} \int_B g_B(\boldsymbol{X},\boldsymbol{P}) \varrho_T(x,\boldsymbol{X},p,\boldsymbol{P},t) d\boldsymbol{X} d\boldsymbol{P}. \tag{2.37}$$

stripped of its physical meaning due to the possibility of a negative value of the total WDF. Apart from dubious interpretation, the Eq. (2.36) gives no less and no more information than the initial problem, keeping further analysis at undesirably high complexity. To simplify the dynamics of the open quantum system, a Born-Markov approximation is usually invoked, leading to GKSL equation [cf. Chapter 4]. In Wigner formalism it is read as

$$\partial_t \varrho_S(t) = \{H_S, \varrho_S(t)\} + \frac{i}{2} \sum_k \gamma_k \left(\{L_k \star \varrho_S(t), L_k^*\}_\star + \{L_k, \varrho_S(t) \star L_k^*\}_\star \right). \tag{2.38}$$

Variable dependency was omitted to keep the equation graphically appealing.

Chapter 3

Split operator approach to numerical solution of evolution equations

3.1 Evolution type PDE

Undoubtedly, physicists thrive to describe reality in terms of mathematical structures and equations. Throughout history, many phenomena have been described meticulously, and humanity has been provided with mathematical tools to predict the behaviour of many complex systems. Examples of such systems can be seen in every scientific area: a heat equation that encapsulates the behaviour of heat distribution within the medium; or the Navier-Stokes equation that provides insights within the fluid dynamics; Schrödinger equation providing us with a description of the evolution of the amplitude of probability in quantum mechanics. What all these equations have in common is their dependence on time t.

Definition 3.1. We say that a partial differential equation for function $u \in C^n(\mathbb{R}^{k+1})$ is of the evolution type if it can be written in the form [22, 113]

$$\partial_t^n u = F(t, \boldsymbol{x}, D_{\boldsymbol{x},t} u, D^2_{\boldsymbol{x},t} u, \dots, D^{n-1}_{\boldsymbol{x},t} u, D^n_{\boldsymbol{x}} u), \tag{3.1}$$

where F is some function, and $D^m_{\boldsymbol{x},t}$ is the multi-index notation for a partial derivative of the order $m \in \mathbb{N}$ of variables $\boldsymbol{x}$ and t.

This definition is comprehensive, as it encapsulates nearly all time-dependent equations of classical and quantum physics and is difficult to work with if one is interested in peculiar properties of such systems. Simultaneously, in the literature, one may find that the definition of evolution equation contains only first-order time derivative, thus we would say that

Definition 3.2. A partial differential equation for function $u \in C^n(\mathbb{R}^{k+1})$ is of the evolution type [131, 130] if it can be written as

$$\partial_t u = F(t, x, D_{\boldsymbol{x}} u, D^2_{\boldsymbol{x}} u, \dots, D^{n-1}_{\boldsymbol{x}} u, D^n_{\boldsymbol{x}} u), \tag{3.2}$$

for some function F, and $D^m_{\boldsymbol{x}}$ is the $m-$th order multi-index derivative with respect to the spatial variable $\boldsymbol{x}$.

The latter definition of the evolution equation will be the focus of our attention. More importantly, we will also consider cases where $F(.)$ is not explicitly time dependent, $\partial_t F = 0$, which we will call the time-autonomous partial differential evolution equation [82]. With suitable assumptions, we shall now rewrite (3.2) in the following operator form

$$\partial_t u = \hat{\mathcal{L}} u, \tag{3.3}$$

where $\hat{\mathcal{L}}$ is an operator which, under certain assumptions [87] can be treated as a generator of a dynamical semigroup, namely [46]

$$\hat{\mathcal{L}} u = \lim_{t \to 0^+} \frac{\hat{\Phi}(t)u - u}{t}, \tag{3.4}$$

with u taken so that the limit on the right-hand side exists and $\hat{\Phi}(t)$ being the aforementioned dynamical semigroup associated with $\hat{\mathcal{L}}$, as this is one-to-one correspondence [152, 99]. With this setup, any solution to the Cauchy problem with the initial condition $u(x,0) = u_0(x)$, can be written as [100, 83, 171]

$$u(x,t) = \hat{\Phi}(t)u_0(x) = e^{\hat{\mathcal{L}}t} u_0(x). \tag{3.5}$$

Complementarily, if the initial problem was posed as a non-homogeneous, that is

$$\partial_t u = \hat{\mathcal{L}} u + f, \tag{3.6}$$

then $u(\cdot, t)$ can be expressed via the formula [99]

$$u(x,t) = e^{\hat{\mathcal{L}}t} u_0(x) + \int_0^t e^{(s-t)\hat{\mathcal{L}}} f(x,s) ds. \tag{3.7}$$

The exponential function, $\exp\left(\hat{\mathcal{L}}t\right)$, is understood as the series expansion of the exponent, in the case of a bounded $\hat{\mathcal{L}}$. However, if $\hat{\mathcal{L}}$ is unbounded, then the exponential operator should be treated carefully via resolvent techniques (see [98, 87]). Many equations of mathematical physics, including quantum as well as classical ones, can be written in forms given by Eqs. (3.3) and (3.6). Nonetheless, we are interested in linear equations, that is, for any two functions u_1, u_2 and constants α, β we have the following property

$$\hat{\mathcal{L}}[\alpha u_1 + \beta u_2] = \alpha \hat{\mathcal{L}} u_1 + \beta \hat{\mathcal{L}} u_2. \tag{3.8}$$

As a formal solution, the expression given by Eqn. (3.3) is direct and compact in its form. However, there are only a few cases where such an expression can be calculated analytically, unproportionally less than the number of interesting cases where the solution is desirable. In particular in quantum mechanics, when $\hat{\mathcal{L}}$ is given by the sum of two operators: the kinetic energy operator $\hat{T}(\hat{p})$ and the potential energy operator $\hat{V}(\hat{x})$, the formula for time evolution might be too complicated to write down explicitly. An even more complicated case arises when $\partial_t \hat{\mathcal{L}} \neq \hat{0}$ or, equivalently, $\hat{\mathcal{L}} = \hat{\mathcal{L}}(t)$ is a time-dependent generator, leading to non-autonomous problem. Physically, in quantum mechanics, those can be associated in with oscillatory potentials [160, 89, 96] or moving barriers [32, 34] in particular cases laying the foundation of computational tools [150].

Recall an integral representation of Eq. (3.3)

$$u(x,t) = u_0(x) + \int_0^t \hat{\mathcal{L}}(s) u(x,s) ds. \tag{3.9}$$

By repetitive substitution, we arrive at the time-ordered expression

$$u(x,t) = \hat{\mathcal{T}} e^{\int_0^t \hat{\mathcal{L}}(s)ds} u_0(x), \tag{3.10}$$

where $\hat{\mathcal{T}}$ is Dyson's time-ordering operator [57]. Yet again, we obtained a formal expression for a solution to the Cauchy problem; still, no explicit formula can be written down to provide us with the information about the solution to the equation of motion. In the upcoming section, we will discuss the idea of finding the approximate expression for the solution of the Cauchy problem where the dynamics is given by the exponential operator, as in (3.5) or (3.10).

3.2 Splitting method

In the previous section, we discussed the notion of the evolution equation. Their main advantage lies in the compact form of the formal solution to the Cauchy initial problem. In physics, many problems are concentrated around the dynamics generated by the sum of two operators $\hat{A}$, $\hat{B}$. As previously mentioned, in quantum mechanics, in the Schrödinger equation, the total Hamiltonian $\hat{H}$ is given by the sum of two operators: the kinetic part $\hat{A} = \hat{p}^2/(2m)$, and the potential part associated with the potential energy $\hat{B} = \hat{U}(\hat{x})$. With no explicit time dependence in the Hamiltonian, i.e. $\partial_t \hat{H} = 0$, the näive solution to the evolution initial value problem can be given by

$$u(x,t) = e^{t(\hat{A}+\hat{B})} u_0(x) = e^{t\hat{A}} e^{t\hat{B}} u_0(x). \tag{3.11}$$

However, the last equality does not hold for kinetic and potential operators, and more importantly for general operators $\hat{A}$, $\hat{B}$, and is only true provided that $[\hat{A}, \hat{B}] = \hat{0}$. This idea of direct splitting of the exponent of the sum to the product of two exponents is known as Lie-Trotter splitting [132, 166]. It treats $\hat{A}$, $\hat{B}$ as two independent dynamic generators, at all times $t > 0$. It allows us to reconstruct the dynamics of the system by sequential composition of the dynamics generated by $\hat{A}$ and $\hat{B}$ independently, as exponential operators (see graphics below).

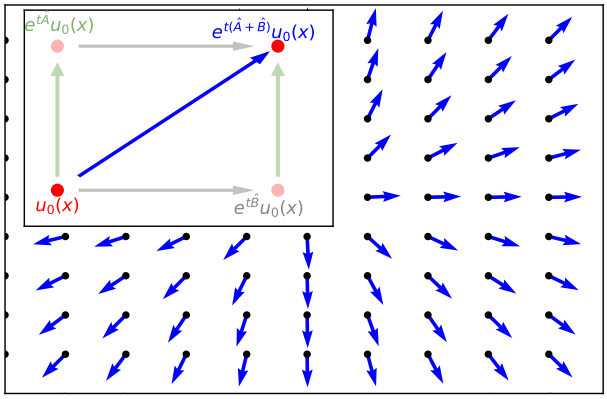

Figure 3.1: A visual explanation of Lie-Trotter approximation. The vector field can be associated with a generator of the dynamics $\hat{A} + \hat{B}$ whereas its action on the given function $u_0(x)$ is depicted in the inset. In the Lie-Trotter approximation, the dynamics can be decomposed as a product of two shifts, one along the vertical and the other along the horizontal axis, associated with operators $\hat{A}$ and $\hat{B}$ respectively.

The order of error we conduct under such a transformation is of the second power of the time step, namely [52]

$$e^{t(\hat{A}+\hat{B})}u_0(x) = e^{t\hat{A}}e^{t\hat{B}}u_0(x) + \mathcal{O}(t^2), \tag{3.12}$$

where $\mathcal{O}(t^2)$ means that the error is no greater than the 2-nd power of t. For higher accuracy of the solution, we might apply Strang approximation that reads [132, 162]

$$u(x,t) = e^{\frac{t}{2}\hat{A}}e^{t\hat{B}}e^{\frac{t}{2}\hat{A}}u_0(x) + \mathcal{O}(t^3). \tag{3.13}$$

Whether such a formula exists for any order of accuracy we desire is a valid question, which fortunately has already been answered. The first, and most reasonable answer to this question can be given by undermining the usefulness of such approximation. For numerical computations, exponentiation is a costly transformation that will ultimately prevail over the solution's accuracy. The second and formal answer is given by the non-existence theorem [166]

Theorem 3.1. (Suzuki nonexistence theorem) For noncommutative operators $\hat{A}, \hat{B}$ there is no decomposition of the form

$$e^{t(\hat{A}+\hat{B})} = e^{t_1\hat{A}}e^{t_2\hat{B}}\dots e^{t_M\hat{A}} + O(t^{m+1}), \tag{3.14}$$

with all positive t_j and finite M for $m \geq 3$.

For proof see Ref. [166].
An example of a decomposition that achieves a higher order of accuracy and is compliant with the Suzuki theorem is the Chin approximation. It is the fourth order approximation given by the following formula [33]

$$u(x,t) = e^{\frac{t}{6}\hat{A}}e^{\frac{t}{2}\hat{B}}e^{\frac{2}{3}\hat{W}}e^{\frac{t}{2}\hat{B}}e^{\frac{t}{6}\hat{A}}u_0(x) + \mathcal{O}(t^5), \tag{3.15}$$

where $\hat{W} = \hat{A} + t^2/(48)[\hat{A},[\hat{B},\hat{A}]]$. Noticeable is the fact that this decomposition is not given purely by exponential operators of $\hat{A}$ and $\hat{B}$, but includes the nested commutator expression $\hat{W}$. Generally, the splitting coefficients are determined by applying the Baker-Campbell-Hausdorff (BCH) formula [7] and its inverse, the Zassenhaus formula [114], along with a Taylor expansion to match the expansion coefficients up to the desired precision[1]. For the error analysis of the approximations presented here see Ref. [44].

Within the first sections of this work, we will assume that the generator $\hat{\mathcal{L}}$ of the dynamics of the system in interest is, first and foremost, time-independent $\partial_t\hat{\mathcal{L}} = 0$, and given as the sum of a function of only variable x, here $V(x)$, and a polynomial expression $W(x,p,\partial_x,\partial_p)$

$$\hat{\mathcal{L}} = W(x,p,\partial_x,\partial_p) + V(x), \tag{3.16}$$

where $W \in \mathbb{C}[x_1,x_2,x_3,x_4]$ is the polynomial of four variables with complex coefficients. In such cases, the unitary equivalence relation between the position and momentum operators enables us, numerically, to implement the split-operator scheme without the need to approximate the derivative operator with a difference scheme. To see this, let us first recall the definition of the unitary equivalence [134]

[1] BCH and Zassenahus formula will be provided further within the thesis.

Definition 3.3. Let $\hat{A}$, $\hat{B}$, be two operators. We say that $\hat{B}$ is unitarily equivalent to $\hat{A}$ if there exists a unitary transformation $\hat{U}$ such that

$$\hat{B} = \hat{U}\hat{A}\hat{U}^{\dagger}, \tag{3.17}$$

where $\hat{U}^{\dagger}$ is the adjoint of operator $\hat{U}$, and the equality sign is understood in the operator sense.

Then, in the sense of the previous definition, the multiplication and derivation operators are unitarily equivalent via the Fourier transform. We shall use the following convention for Fourier transform [153, 139]

$$\mathcal{F}_{1,x\to\lambda}\varrho(x,p,t) = \frac{1}{\sqrt{2\pi\hbar}}\int_{\mathbb{R}} e^{-\frac{i}{\hbar}\lambda x}\varrho(x,p,t)dx, \tag{3.18}$$

$$\mathcal{F}^{-1}_{1,\lambda\to x}\tilde{\varrho}(\lambda,p,t) = \frac{1}{\sqrt{2\pi\hbar}}\int_{\mathbb{R}} e^{\frac{i}{\hbar}\lambda x}\tilde{\varrho}(\lambda,p,t)d\lambda, \tag{3.19}$$

$$\mathcal{F}_{2,p\to y}\varrho(x,p,t) = \frac{1}{\sqrt{2\pi\hbar}}\int_{\mathbb{R}} e^{-\frac{i}{\hbar}py}\varrho(x,p,t)dp, \tag{3.20}$$

$$\mathcal{F}^{-1}_{2,y\to p}\tilde{\varrho}(x,y,t) = \frac{1}{\sqrt{2\pi\hbar}}\int_{\mathbb{R}} e^{\frac{i}{\hbar}py}\tilde{\varrho}(x,y,t)dy. \tag{3.21}$$

Then, the unitary equivalence can be read as follows [138, 149]

$$\mathcal{F}^{-1}_{1,\lambda\to x}\lambda\mathcal{F}_{1,x\to\lambda} = \frac{i}{\hbar}\partial_x, \qquad \mathcal{F}^{-1}_{2,y\to p}y\mathcal{F}_{2,p\to y} = \frac{i}{\hbar}\partial_p, \tag{3.22}$$

mostly known as a property of the Fourier transform. This implies a natural association between variables: x, λ and p, y hereafter referred to as Fourier conjugated or simply conjugated variables. Thus, by (3.22), we can substitute every occurrence of the derivative operator with the conjugated variable and vice versa, provided that we transform the total expression through this equivalence, namely for any polynomial $K(x_1, x_2)$ the following equality holds

$$K(\partial_x, \partial_p) = \mathcal{F}^{-1}_{2,y\to p}\mathcal{F}^{-1}_{1,\lambda\to x}K(\lambda, y)\mathcal{F}_{1,x\to\lambda}\mathcal{F}_{2,p\to y}. \tag{3.23}$$

Now, the expression "sandwiched" between Fourier transform is simply a polynomial expression of two variables λ, y, instead of a polynomial of derivatives, allowing for further numerical manipulations and calculations.

Further within the work we will obtain the time-dependent generator as a result of algebraic manipulations performed. If we want to extend the splitting algorithm on time-dependent operators, as desired, we shall recall the following key result by Suzuki [167]: a time-ordered exponential operator (3.10) can be reformulated in terms of the ordinary exponential operator as follows

$$\hat{\mathcal{T}}\exp\left[-i\int_0^t \hat{\mathcal{L}}(s)ds\right] = \exp\left[\left(\hat{\mathcal{L}}(t) + \hat{D}\right)t\right], \tag{3.24}$$

where the operator $\exp\left(\hat{D}\eta\right)$ is defined via the formulae

$$\hat{A}(t)e^{\hat{D}\eta}\hat{B}(t) = \hat{A}(t+\eta)\hat{B}(t). \tag{3.25}$$

In simple terms, $\hat{D}$ is equivalent to the time-derivative operator acting on the left expression $\hat{D} = \overleftarrow{\partial}_t$, leading to the time-shift operator definition for the exponential of $\hat{D}$. This equivalence between the time-ordered exponential and the time-derivative formulation significantly simplifies the numerical algorithm, particularly when the analytic form of the potential $V(x,t)$ is known. Further, within this work, we show the application of this identity in the case of a time-dependent potential.

Chapter 4

Results

4.1 Microscopic derivation of the GKSL equation in the phase space

The result presented here can be achieved via W-S correspondence used in the context of the microscopic derivation of the GKSL equation for the density operator [24]. Let us consider a total system T consisting of an open system S and an environment B, just as stated in Sec. 2.3 with the same Hamiltonian symbol (2.35). We already know that the WDF for the total system $\varrho_T(\boldsymbol{Q}, \boldsymbol{K}, t)$ obeys the Moyal equation (2.30) and the open system's WDF is related to the total system WDF via the integration over the bath coordinates (2.34). To unveil the real form of open system dynamics, we start with the initial equation of an isolated total system, but written in the interaction picture, that is, any symbol F defined over quantum phase space is transformed to the interaction representation via the interaction picture

$$F(\boldsymbol{Q}, \boldsymbol{K}, t) \to F^I(\boldsymbol{Q}, \boldsymbol{K}, t) = e^{\frac{i}{\hbar}(H_S+H_B)t} \star F(\boldsymbol{Q}, \boldsymbol{K}, t) \star e^{-\frac{i}{\hbar}(H_S+H_B)t}. \tag{4.1}$$

Then, the dynamics of the total quantum system can be rewritten as

$$\partial_t \varrho_T^I(\boldsymbol{Q}, \boldsymbol{K}, t) = \left\{ H_I^I(\boldsymbol{Q}, \boldsymbol{K}, t), \varrho_T^I(\boldsymbol{Q}, \boldsymbol{K}, t) \right\}_\star, \tag{4.2}$$

from now on the upper I index, standing for interaction picture, will be omitted.
Integrating the Eq. (4.2) once, with respect to time t, then inserting it back into the initial equation (4.2) and lastly integrating the result with respect to the bath variables $(\boldsymbol{X}, \boldsymbol{P})$, we arrive at the equation of motion for the open system

$$\begin{aligned} \partial_t \varrho_S(x, p, t) = &\int_B \{H_I(\boldsymbol{Q}, \boldsymbol{K}, t), \varrho_T(\boldsymbol{Q}, \boldsymbol{K}, 0)\}_\star \, d\boldsymbol{X} d\boldsymbol{P} \\ &+ \int_B \int_0^t \{H_I(\boldsymbol{Q}, \boldsymbol{K}, t), \{H_I(\boldsymbol{Q}, \boldsymbol{K}, s), \varrho_T(\boldsymbol{Q}, \boldsymbol{K}, s)\}_\star\}_\star \, ds \, d\boldsymbol{X} d\boldsymbol{P}, \end{aligned} \tag{4.3}$$

but still containing the dependence on the state of the total system. From now on, some assumptions must be introduced to simplify the equation of evolution. Firstly, without an in-depth explanation, which we will provide later, we shall assume that

$$\int_B \{H_I(\boldsymbol{Q}, \boldsymbol{K}, t), \varrho_T(\boldsymbol{Q}, \boldsymbol{K}, 0)\}_\star \, d\boldsymbol{X} d\boldsymbol{P} = 0. \tag{4.4}$$

This yields the new equation

$$\partial_t \varrho(x,p,t) = \int_B \int_0^t \{H_I(\boldsymbol{Q},\boldsymbol{K},t), \{H_I(\boldsymbol{Q},\boldsymbol{K},s), \varrho_T(\boldsymbol{Q},\boldsymbol{K},s)\}_\star\}_\star \, ds \, d\boldsymbol{X} d\boldsymbol{P}. \tag{4.5}$$

To exclude the dependency on the state of the total system we introduce Born approximation [24] $\varrho_T(\boldsymbol{Q},\boldsymbol{K},t) \approx \varrho_S(x,p,t) \cdot \varrho_B(\boldsymbol{X},\boldsymbol{P})$, where the state of the environment ϱ_B is stationary. Now, the equation in question can be summarised as

$$\partial_t \varrho(\boldsymbol{x},\boldsymbol{p},t) = \int_B \int_0^t \{H_I(\boldsymbol{Q},\boldsymbol{K},t), \{H_I(\boldsymbol{Q},\boldsymbol{K},s), \varrho_S(x,p,s) \cdot \varrho_B(\boldsymbol{X},\boldsymbol{P})\}_\star\}_\star \, ds \, d\boldsymbol{X} d\boldsymbol{P}, \tag{4.6}$$

whereas the previous assumption (4.4), after recalling the form of the interaction Hamiltonian (2.35) and substituting the separated WDF for the total system, now reads

$$\sum_k \alpha_k \langle g_B^k(t)\rangle \{g_S^k(x,p,t), \varrho_S(x,p,t)\} = 0, \tag{4.7}$$

implying that the average environmental disturbance that comes from the interaction with the open system $\langle B_k(t)\rangle$ is nullified. To finish this part of algebraic manipulations, we impose the Markov approximation [24, 122], that is, we assume that the Wigner function at time t is independent of its previous states, at times $0 \leq \tau < t$, which gives

$$\partial_t \varrho_S(x,p,t) = \int_B \int_0^t \{H_I(\boldsymbol{Q},\boldsymbol{K},t), \{H_I(\boldsymbol{Q},\boldsymbol{K},s), \varrho_S(x,p,t) \cdot \varrho_B(\boldsymbol{X},\boldsymbol{P})\}_\star\}_\star \, ds \, d\boldsymbol{X} d\boldsymbol{P}. \tag{4.8}$$

Simultaneously, we assume the vanishing of the integrand in long-time scales, allowing us to substitute, after the change of variables $s = t - u$, the integration limit to infinity, that is, $t \to +\infty$, leading to

$$\partial_t \varrho_S(x,p,t) = \int_B \int_0^\infty \{H_I(\boldsymbol{Q},\boldsymbol{K},t), \{H_I(\boldsymbol{Q},\boldsymbol{K},t-u), \varrho_S(x,p,t) \cdot \varrho_B(\boldsymbol{X},\boldsymbol{P})\}_\star\}_\star \, ds \, d\boldsymbol{X} d\boldsymbol{P}. \tag{4.9}$$

For next steps, we introduce a new family of operators $\{q_S^k(x,p;\omega)\}_\omega$ defined via projectors of the Hamiltonian H_S, with the assumption of a discrete spectrum, namely

$$q_S^k(x,p;\omega) = \sum_{\varepsilon_n - \varepsilon_m = \omega} \Pi(x,p;\varepsilon_m) \star g_S^k(x,p) \star \Pi(x,p;\varepsilon_n). \tag{4.10}$$

The operators $\Pi(x,p;\varepsilon_k)$ can be seen as the Weyl symbols of the projection operator $\hat{P}_{\varepsilon_k}$ onto the eigenspace associated with the ε_k eigenvalue of the Hamiltonian $\hat{H}_S$. To see it, we shall notice that $\hat{1} = \sum_k \hat{P}_{\varepsilon_k}$ is the identity operator given by the completeness relation, which allows us to rewrite each operator $\hat{A}$ as

$$\hat{A} = \sum_{n,m} \hat{P}_{\varepsilon_m} \hat{A} \hat{P}_{\varepsilon_n}. \tag{4.11}$$

As we are working with double summation, we shall conduct it over all possible differences between the eigenvalues $\varepsilon_n - \varepsilon_m = \hbar\omega$, the angular frequencies, leading to

$$\hat{A} = \sum_\omega \sum_{\varepsilon_n - \varepsilon_m = \omega} \hat{P}_{\varepsilon_m} \hat{A} \hat{P}_{\varepsilon_n}. \tag{4.12}$$

This trick allows us to rephrase the $g_S^k(x,p)$ interaction term as follows

$$g_S^k(x,p) = \sum_\omega q_S^k(x,p;\omega) = \sum_\omega \sum_{\varepsilon_n - \varepsilon_m = \omega} \Pi(x,p;\varepsilon_m) \star g_S^k(x,p) \star \Pi(x,p;\varepsilon_n). \tag{4.13}$$

The operators $q_S^k(x,p;\omega)$ satisfy the following relations:

- they are the eigenoperators[1] of superoperator $\{H_S, \cdot\}$:

$$\{H_S, S_k(\omega)\} = -\frac{\omega}{i\hbar} q_S^k(\omega), \tag{4.14}$$

$$\{H_S, S_k^*(\omega)\} = \frac{\omega}{i\hbar} q_S^{k\,*}(\omega), \tag{4.15}$$

- they are preserved, up to a phase factor, by a unitary evolution of system S:

$$e^{\frac{i}{\hbar}H_S t} \star q_S^k(\omega) \star e^{-\frac{i}{\hbar}H_S t} = e^{-\frac{i}{\hbar}\omega t} q_S^k(\omega), \tag{4.16}$$

$$e^{\frac{i}{\hbar}H_S t} \star q_S^{k\,*}(\omega) \star e^{-\frac{i}{\hbar}H_S t} = e^{\frac{i}{\hbar}\omega t} q_S^{k\,*}(\omega), \tag{4.17}$$

- they are parity-reversal symmetric with respect to the frequency ω:

$$q_S^{k\,*}(-\omega) = q_S^k(\omega). \tag{4.18}$$

One can now rephrase the time-dependent interaction Hamiltonian symbol with the help of the properties above

$$\begin{aligned} H_I(t) &= e^{\frac{i}{\hbar}(H_S+H_B)t} \star \sum_{k,\omega} \alpha_k q_S^k(\omega) g_B^k \star e^{-\frac{i}{\hbar}(H_S+H_B)t} = \sum_{k,\omega} \alpha_k e^{-\frac{i}{\hbar}\omega t} q_S^k(\omega) g_B^k(t) \\ &= \sum_{k,\omega} \alpha_k e^{\frac{i}{\hbar}\omega t} q_S^{k\,*}(\omega) g_B^{k\,*}(t). \end{aligned} \tag{4.19}$$

To keep the equations more transparent, we omit the dependency upon variables connected to the degrees of freedom, both for open systems and baths. Introducing new operators allows us to rewrite the equation for the Wigner function in the following manner

$$\begin{aligned} \partial_t \varrho_S(x,p,t) &= \sum_{k,\omega}\sum_{j,\delta} \int_B \int_0^\infty \Big(\alpha_k \alpha_j e^{\frac{i}{\hbar}\omega t} e^{-\frac{i}{\hbar}\delta(t-u)} \\ &\times \Big\{ q_S^{k\,*}(\omega) g_B^{k\,*}(t), \Big\{ q_S^j(\delta) g_B^j(t-u), \varrho_S(x,p,t)\varrho_B(\boldsymbol{X},\boldsymbol{P}) \Big\}_\star \Big\}_\star \Big)\, du\, d\boldsymbol{X} d\boldsymbol{P} \\ &= \sum_{k,\omega}\sum_{j,\delta} \alpha_k \alpha_j e^{\frac{i}{\hbar}t(\omega-\delta)} \\ &\times \int_0^\infty \int_B \Big(e^{\frac{i}{\hbar}\delta u} \Big\{ q_S^{k\,*}(\omega) g_B^{k\,*}(t), \Big\{ q_S^j(\delta) g_B^j(t-u), \varrho_S(x,p,t)\varrho_B(\boldsymbol{X},\boldsymbol{P}) \Big\}_\star \Big\}_\star \Big) d\boldsymbol{X} d\boldsymbol{P} du. \end{aligned} \tag{4.20}$$

Furthermore, conducting necessary manipulations of the integrated expression is required to simplify the form of the equation. We start with the expansion of the inner and outer Moyal brackets, leading to

$$\begin{aligned} I = {} & q_S^{k\,*}(\omega) \star q_S^j(\delta) \star \varrho_S(x,p,t) g_B^{k\,*}(t) \star g_B^j(t-u) \star \varrho_B(\boldsymbol{X},\boldsymbol{P}) \\ & - q_S^{k\,*}(\omega) \star \varrho_S(x,p,t) \star q_S^j(\delta) g_B^{k\,*}(t) \star \varrho_B(\boldsymbol{X},\boldsymbol{P}) \star g_B^j(t-u) \\ & - q_S^j(\delta) \star \varrho_S(x,p,t) \star q_S^{k\,*}(\omega) g_B^j(t-u) \star \varrho_B(\boldsymbol{X},\boldsymbol{P}) \star g_B^{k\,*}(t) \\ & + \varrho_S(x,p,t) \star q_S^j(\delta) \star q_S^{k\,*}(\omega) \varrho_B(\boldsymbol{X},\boldsymbol{P}) \star g_B^j(t-u) \star g_B^{k\,*}(t). \end{aligned} \tag{4.21}$$

[1] The term eigenoperator was used e.g. in Ref. [68], as a natural generalisation of eigenfunction to the language of superoperators.

Now integrating this expression with respect to bath degrees of freedom $(\boldsymbol{X}, \boldsymbol{P})$ gives

$$\begin{aligned} I' = &\left\langle g_B^{k\,*}(t) \star g_B^j(t-u) \right\rangle \left[q_S^{k*}(\omega) \star q_S^j(\delta) \star \varrho_S(x,p,t) - q_S^j(\delta) \star \varrho_S(x,p,t) \star q_S^{k*}(\omega) \right] \\ &+ \left\langle g_B^j(t-u) \star g_B^{k\,*}(t) \right\rangle \left[\varrho_S(x,p,t) \star q_S^j(\delta) \star q_S^{k*}(\omega) - q_S^{k*}(\omega) \star \varrho_S(x,p,t) \star q_S^j(\delta) \right]. \end{aligned} \tag{4.22}$$

Including the integration with respect to u, and preceding the exponential expression one gets

$$\begin{aligned} I'' = &\Gamma_{kj}(\delta) \left[q_S^{k*}(\omega) \star q_S^j(\delta) \star \varrho(x,p,t) - q_S^j(\delta) \star \varrho(x,p,t) \star q_S^{k*}(\omega) \right] \\ &+ \Gamma_{kj}^*(\delta) \left[\varrho(x,p,t) \star q_S^j(\delta) \star q_S^{k*}(\omega) - q_S^{k*}(\omega) \star \varrho(x,p,t) \star q_S^j(\delta) \right]. \end{aligned} \tag{4.23}$$

resulting in

$$\begin{aligned} \partial_t \varrho(\boldsymbol{x}, \boldsymbol{p}, t) = \sum_{k,\omega} \sum_{j,\delta} \alpha_k \alpha_j e^{\frac{i}{\hbar} t(\omega - \delta)} \Big(&\Gamma_{kj}(\delta) \left\{ q_S^{k*}(\omega), q_S^j(\delta) \star \varrho_S(x,p,t) \right\} \\ &+ \Gamma_{kj}^*(\delta) \left\{ \varrho_S(x,p,t) \star q_S^j(\delta), q_S^{k*}(\omega) \right\} \Big), \end{aligned} \tag{4.24}$$

where

$$\Gamma_{kj}(\delta) = \int_0^\infty e^{\frac{i}{\hbar}\delta u} \left\langle g_B^{k\,*}(t) \star g_B^j(t-u) \right\rangle du, \tag{4.25}$$

is the one-sided Fourier transform of the autocorrelation function. Assuming that only resonant terms $\omega = \delta$ contribute to the dynamics, as they average out, known as secular approximation [24, 116], leads to

$$\begin{aligned} \partial_t \varrho_S(x,p,t) = \sum_{\omega} \sum_{k,j} \alpha_k \alpha_j \Big(&\Gamma_{kj}(\omega) \left\{ q_S^{k*}(\omega), q_S^j(\omega) \star \varrho_S(x,p,t) \right\} \\ &+ \Gamma_{kj}^*(\omega) \left\{ \varrho_S(x,p,t) \star q_S^j(\omega), q_S^{k*}(\omega) \right\} \Big). \end{aligned} \tag{4.26}$$

Lastly, to excavate the final form of the equation of motion, the following decomposition of $\Gamma_{kj}(\delta)$ must be imposed: $\Gamma_{kj}(\omega) = \gamma_{kj}(\omega)/2 + i s_{kj}(\omega)$. This, after long, nontrivial, tedious manipulations, led to

$$\partial_t \varrho_S(x,p,t) = \left\{ \tilde{H}(x,p), \varrho_S(x,p,t) \right\}_S + \mathcal{D}(\varrho_S(x,p,t)), \tag{4.27}$$

where

$$\tilde{H}(x,p) = \sum_{\omega} \sum_{k,j} \alpha_k \alpha_j s_{kj}(\omega) q_S^{k*}(\omega) \star q_S^j(\omega), \tag{4.28}$$

and

$$\begin{aligned} \mathcal{D}(\cdot) &= \frac{i}{2} \sum_{\omega} \sum_{k,j} \alpha_k \alpha_j \gamma_{kj}(\omega) \left\{ q_S^{k*}(\omega), \left\{ q_S^j(\omega), \cdot \right\}_\star^{(+)} \right\}_\star \\ &= -\frac{i}{\hbar^2} \sum_{\omega} \sum_{k,j} \gamma_{kj}(\omega) \left(q_S^j(\omega) \star (\cdot) \star q_S^{k*}(\omega) - \frac{1}{2} \{ q_S^{k*}(\omega) \star q_S^j(\omega), \cdot \}_\star^{(+)} \right). \end{aligned} \tag{4.29}$$

As a result, we obtained the GKSL equation in the phase space by microscopic derivation. However, as mostly stated in the literature, an algebraically appealing form of the equation was provided in Eq. (2.38).

4.2 Splitting of the exponential expression describing the model

The results of the presented thesis are anchored by the Wigner-Lindblad equation for a Weyl symbol of a single linear Lindblad operator $L_k = L(x,p)$, given by

$$L(x,p) = ax + bp, \quad a,b \in \mathbb{C}. \tag{4.30}$$

This form leads to the following equation of motion for the WDF for an open quantum system, with an initial condition at time $t = 0$

$$\begin{cases} \partial_t \varrho & = -\frac{p}{m}\partial_x \varrho + \{V(x), \varrho\}_\star + \Gamma\left[\partial_x(x\varrho) + \partial_p(p\varrho)\right] + \frac{1}{2}D_{xx}\partial^2_{pp}\varrho + \frac{1}{2}D_{pp}\partial^2_{xx}\varrho - D_{xp}\partial^2_{xp}\varrho, \\ \varrho(t=0) & = \varrho_0, \end{cases} \tag{4.31}$$

where coefficients present within the equation are related to initial quantities a, b by the following relation:

$$\begin{array}{rclcrcl} D_{xx} & = & |a|^2, & & D_{pp} & = & |b|^2, \\ D_{xp} & = & \mathrm{Re}(a^*b), & & \Gamma & = & \mathrm{Im}(a^*b). \end{array} \tag{4.32}$$

This Liouvillian operator, with Lindblad operators taken as the linear combination of position and momentum operators, leads to the dynamics of the system subjected to the decoherence and dissipation effects. However, this approach does not embed the simplest example of an open quantum system, that is, Brownian particle dynamics, because its dynamics is not completely positive [24, 119, 95]. To include it in our approach, we would like to reduce some of the requirements posed on the coefficients of the Eq. (4.31), so that a Brownian motion for high temperatures can be reconstructed from our model [109, 94]. Consider the following dynamics generator

$$\hat{\mathcal{L}}_B = \{H(x,p), \cdot\}_\star + \gamma\partial_p(p(\cdot)) + D\partial^2_{pp}, \tag{4.33}$$

which generates the motion of a quantum Brownian particle. Our model (4.31) does not allow for manipulation of constants $\Gamma, D_{xx}, D_{xp}, D_{pp}$ which keeps the complete positivity of the evolution and simultaneously reproduces the case of Brownian particle for certain values of the parameters given. With that in mind, we focus our attention to the scaling part, namely:

$$\hat{S} = \Gamma\left[\partial_x(x(\cdot)) + \partial_p(p(\cdot))\right] = \Gamma\partial_x(x(\cdot)) + \Gamma\partial_p(p(\cdot)),$$

and assume that constants connected to the x-rescaling and p-rescaling are independent of each other allowing us to rewrite this expression as

$$\hat{S} = \Gamma_x\partial_x(x(\cdot)) + \Gamma_p\partial_p(p(\cdot)), \tag{4.34}$$

where we have introduced new constants Γ_x and Γ_p. Separating the influences of spatial and momentum scaling allows for broader analysis of the dynamics. This introduction of the modified operator gives the following dynamics generator

$$\hat{\mathcal{L}} = -\frac{p}{m}\partial_x + \{V(x), \cdot\}_\star + \Gamma_x\partial_x(x(\cdot)) + \Gamma_p\partial_p(p(\cdot)) + \frac{1}{2}D_{xx}\partial^2_{pp} + \frac{1}{2}D_{pp}\partial^2_{xx} - D_{xp}\partial^2_{xp}. \tag{4.35}$$

The dynamics given by such operator cannot be solved analytically unless $U(x)$ is polynomial of at most 2nd order. To prepare for the numerical analysis of this equation we define the following set of operators: the closed dynamics operators

$$\hat{V} = \{V(x), \cdot\}_\star, \quad \hat{T} = -\tfrac{p}{m}\partial_x, \tag{4.36}$$

the scaling operators

$$\hat{S}_1 = \Gamma_x + \Gamma_p, \quad \hat{S}_2 = \Gamma_x x\partial_x, \quad \hat{S}_3 = \Gamma_p p\partial_p, \tag{4.37}$$

and the second-order operators

$$\hat{G}_1 = \tfrac{1}{2}D_{xx}\partial^2_{pp}, \quad \hat{G}_2 = \tfrac{1}{2}D_{pp}\partial^2_{xx} \quad \hat{G}_3 = -D_{xp}\partial^2_{xp}, \tag{4.38}$$

where $\hat{G}_1$ can be seen as a decoherence operator [191, 190], $\hat{G}_2$ is a diffusion operator [60, 142] whereas the mixed derivative operator $\hat{G}_3$ can be seen as a measure of correlation between (x, p) or inseparability. The operator $\hat{\mathcal{L}}$, for the potential in the form of a polynomial of at most 2nd order, has the following properties:

- the initial value problem with initial condition $\varrho(x, p, 0) = \varrho_0(x, p)$ is exactly solvable,
- if $\varrho_0(x, p)$ is a Gaussian function, then $\varrho(x, p, t)$ is Gaussian for $t \geq 0$,

for both results see Appendix B.

The commutation relations between the previously defined operators are the clue to derive, in some cases exact, formulas which allow to calculate the exponential of the operator $\hat{\mathcal{L}}$. Thus, for the set of operators $\{\hat{T}, \hat{G}_1, \hat{G}_2, \hat{G}_3, \hat{S}_1, \hat{S}_2, \hat{S}_3\}$ the commutation relation between them is presented in the Tab. 4.1.

Table 4.1: Commutation relation table for set of operators considered. The potential energy operator $\hat{V}$ was omitted due to its general form.

$[\downarrow, \rightarrow]$	$\hat{T}$	$\hat{G}_1$	$\hat{G}_2$	$\hat{G}_3$	$\hat{S}_1$	$\hat{S}_2$	$\hat{S}_3$
$\hat{T}$	0	$-\frac{1}{m}\frac{D_{xx}}{D_{xp}}\hat{G}_3$	0	$-\frac{2}{m}\frac{D_{xp}}{D_{pp}}\hat{G}_2$	0	$\Gamma_x\hat{T}$	$-\Gamma_p\hat{T}$
$\hat{G}_1$	$-$	0	0	0	0	0	$2\Gamma_p\hat{G}_1$
$\hat{G}_2$	$-$	$-$	0	0	0	$2\Gamma_x\hat{G}_2$	0
$\hat{G}_3$	$-$	$-$	$-$	0	0	$\Gamma_x\hat{G}_3$	$\Gamma_p\hat{G}_3$
$\hat{S}_1$	$-$	$-$	$-$	$-$	0	0	0
$\hat{S}_2$	$-$	$-$	$-$	$-$	$-$	0	0
$\hat{S}_3$	$-$	$-$	$-$	$-$	$-$	$-$	0

Due to the property of a commutator: $[\hat{A}, \hat{B}] = -[\hat{B}, \hat{A}]$, it is sufficient to fill only the overdiagonal (or underdiagonal) part of the table. For further analysis, we introduce the following notation

$$\begin{aligned} \hat{G} &= \hat{G}_1 + \hat{G}_2 + \hat{G}_3, \\ \hat{S} &= \hat{S}_2 + \hat{S}_3, \\ \hat{\Pi} &= \hat{T} + \hat{S}. \end{aligned} \tag{4.39}$$

Substituting just-introduced operators to the dynamics generator yields the following operator

$$\hat{\mathcal{L}} = \hat{V} + \hat{\Pi} + \hat{G}, \tag{4.40}$$

and with that we can write a formal solution to the Wigner-Lindblad equation, for given initial condition $\varrho_0(x,p)$, namely

$$\varrho(x,p,t) = e^{t\hat{\mathcal{L}}}\varrho_0(x,p) = e^{t(\hat{V}+\hat{\Pi}+\hat{G})}\varrho_0(x,p). \tag{4.41}$$

As mentioned in the previous chapter, the exponential operator of a sum does not factorise to independent exponentials, unless the underlying operators commute. We will show that there exists a direct factorisation for the term $\hat{\Pi} + \hat{G}$. Beforehand, we shall recall the definition of the *adjoint* action operator

Definition 4.1. [81] Let $\hat{A}$, $\hat{B}$ be two operators. We define the adjoint operator of $\hat{A}$, acting on $\hat{B}$ as

$$Ad_{\hat{A}}(\hat{B}) = [\hat{A}, \hat{B}]. \tag{4.42}$$

Naturally, we define the k-th adjoint by recursive relation

$$Ad^k_{\hat{A}} = Ad^{k-1}_{\hat{A}} Ad_{\hat{A}}, \quad Ad^0_{\hat{A}} = \hat{1}. \tag{4.43}$$

Continuing, let us point out some relevant properties of operators $\hat{\Pi}$, and $\hat{G}$

1. Operators $\hat{G}$ and $\hat{G}_i$ for $i = 1,2,3$ commute pairwise;
2. The k–th adjoint operator with respect to $\hat{G}$ acting on operators $\hat{G}_i$ for $i = 1,2,3$ gives zero operator

   $$Ad^k_{\hat{G}}\left(\{\hat{G}_1, \hat{G}_2, \hat{G}_3\}\right) = \{\hat{0}\}, \tag{4.44}$$

   for $k \in \mathbb{N}$;
3. The k–th adjoint operator with respect to $\hat{\Pi}$ acting on operators $\hat{G}_i$ for $i = 1,2,3$ is a subset of set spanned by these operators

   $$Ad^k_{\hat{\Pi}}\left(\{\hat{G}_1, \hat{G}_2, \hat{G}_3\}\right) \subset \text{span}\{\hat{G}_1, \hat{G}_2, \hat{G}_3\}, \tag{4.45}$$

   for $k \in \mathbb{N}$.

These properties are a direct result of the commutation relation between operators collected in Table 4.1. Furthermore, we define a function Ψ by the following relation

$$\Psi(\hat{G}_1) = (1,0,0)^T, \quad \Psi(\hat{G}_2) = (0,1,0)^T, \quad \Psi(\hat{G}_3) = (0,0,1)^T, \tag{4.46}$$

then each element of the set spanned by $\hat{G}_1$, $\hat{G}_2$, $\hat{G}_3$ can be associated with a three-dimensional vector, whereas adjoint operations such that with $Ad_{\hat{\Pi}}\hat{G}_j = \sum_{i=1}^3 \alpha_{ij}\hat{G}_i$ are given by matrices

$$\Psi(Ad_{\hat{\Pi}}) = \begin{bmatrix} \alpha_{11} & \alpha_{12} & \alpha_{13} \\ \alpha_{21} & \alpha_{22} & \alpha_{23} \\ \alpha_{31} & \alpha_{32} & \alpha_{33} \end{bmatrix} = \mathbb{A}_{\hat{\Pi}}. \tag{4.47}$$

As this is common practice, we will omit the function Ψ when performing calculations.
To find the exact splitting for the exponent of the sum $\hat{\Pi}+\hat{G}$, first the identity for non-commuting operators must be used [56, 165]

$$\begin{aligned}\exp\left[t(\hat{X}+\hat{Y})\right] &= \exp\left[t\hat{X}\right]\exp\left[t\hat{Y}\right]\exp\left[\int_0^t e^{-sAd_{\hat{Y}}}\left(e^{-sAd_{\hat{X}}}-\hat{1}\right)\hat{Y}ds\right]\\ &= \exp\left[t\hat{Y}\right]\exp\left[t\hat{X}\right]\exp\left[\int_0^t e^{-sAd_{\hat{X}}}\left(e^{-sAd_{\hat{Y}}}-\hat{1}\right)\hat{X}ds\right].\end{aligned} \tag{4.48}$$

Associating $\hat{X}=\hat{G}$, $\hat{Y}=\hat{\Pi}$ and using previously defined function Φ one gets

$$\begin{aligned}\exp\left[\Delta t(\hat{G}+\hat{\Pi})\right] &= \exp\left[\Delta t\hat{\Pi}\right]\exp\left[\Delta t\hat{G}\right]\exp\left[\int_0^{\Delta t} e^{-sAd_{\hat{G}}}\left(e^{-sAd_{\hat{\Pi}}}-\hat{1}\right)\hat{G}\,ds\right]\\ &= \exp\left[\Delta t\hat{\Pi}\right]\exp\left[\Delta t\hat{G}\right]\exp\left[\int_0^{\Delta t} e^{-s\mathbb{A}_{\hat{G}}}\left(e^{-s\mathbb{A}_{\hat{\Pi}}}-\mathbb{1}\right)(1,1,1)^T\,ds\right].\end{aligned} \tag{4.49}$$

The restriction of the adjoint with respect to $\hat{G}$ to the set spanned by operators $\hat{G}_i$ for $i=1,2,3$ yields a zero operator, that is

$$Ad_{\hat{G}}|_{\text{span}\{\hat{G}_1,\hat{G}_2,\hat{G}_3\}}=\hat{0},$$

and thus

$$\mathbb{A}_{\hat{G}}=0\ \wedge\ e^{-s\mathbb{A}_{\hat{G}}}=\mathbb{1}.$$

This is great simplification for further manipulations by 3rd property [cf. Eq. (4.45)], as the integral expression simplifies to

$$\int_0^{\Delta t} e^{-s\mathbb{A}_{\hat{G}}}\left(e^{-s\mathbb{A}_{\hat{\Pi}}}-\mathbb{1}\right)(1,1,1)^T\,ds=\int_0^{\Delta t}\left(e^{-s\mathbb{A}_{\hat{\Pi}}}-\mathbb{1}\right)(1,1,1)^T\,ds. \tag{4.50}$$

Furthermore

$$\begin{aligned}Ad_{\hat{\Pi}}\hat{G}_1 &= -2\Gamma_p\hat{G}_1+0\cdot\hat{G}_2-\frac{1}{m}\frac{D_{xx}}{D_{xp}}\hat{G}_3,\\ Ad_{\hat{\Pi}}\hat{G}_2 &= 0\cdot\hat{G}_1-2\Gamma_x\hat{G}_2+0\cdot\hat{G}_3,\\ Ad_{\hat{\Pi}}\hat{G}_3 &= 0\cdot\hat{G}_1+-\frac{2}{m}\frac{D_{xp}}{D_{pp}}\hat{G}_2-(\Gamma_x+\Gamma_p)\hat{G}_3,\end{aligned} \tag{4.51}$$

and thus

$$\mathbb{A}_{\hat{\Pi}}=\begin{bmatrix}-2\Gamma_p & 0 & 0\\ 0 & -2\Gamma_x & -\frac{2}{m}\frac{D_{xp}}{D_{pp}}\\ -\frac{1}{m}\frac{D_{xx}}{D_{xp}} & 0 & -(\Gamma_x+\Gamma_p)\end{bmatrix}. \tag{4.52}$$

Secondly, the exponential under the integral containing adjoint action generated by operator $\hat{\Pi}$ is given by

$$e^{-s\mathbb{A}_{\hat{\Pi}}}-\mathbb{1}=\sum_{n=1}^{\infty}\frac{\left(-s\mathbb{A}_{\hat{\Pi}}\right)^n}{n!}=\begin{bmatrix}e^{2\Gamma_p s}-1 & 0 & 0\\ \frac{1}{m^2}\frac{D_{xx}}{D_{pp}}\frac{\left(e^{s\Gamma_p}-e^{s\Gamma_x}\right)^2}{(\Gamma_p-\Gamma_x)^2} & e^{2\Gamma_x s}-1 & \frac{2}{m}\frac{D_{xp}}{D_{pp}}\frac{e^{s(\Gamma_p+\Gamma_x)}-e^{2\Gamma_x s}}{\Gamma\text{p}-\Gamma\text{x}}\\ \frac{1}{m}\frac{D_{xx}}{D_{xp}}\frac{e^{2\Gamma_p s}-e^{s(\Gamma_p+\Gamma_x)}}{\Gamma_p-\Gamma_x} & 0 & e^{s(\Gamma_p+\Gamma_x)}-1\end{bmatrix}. \tag{4.53}$$

Integrating, in the limits 0 to Δt, the action of this operator on vector $(1,1,1)^T$ yields the following expression

$$\int_0^{\Delta t} ds e^{-sL_{\hat{G}}}\left(e^{-sL_{\hat{\Pi}}}-\hat{1}\right)\hat{G}=c_1(\Delta t)\hat{G}_1+c_2(\Delta t)\hat{G}_2+c_3(\Delta t)\hat{G}_3, \tag{4.54}$$

where the coefficients $c_i(\Delta t)$ for $i = 1, 2, 3$ are equal to

$$c_1(\Delta t) = -\Delta t + \frac{e^{2\Gamma_p \Delta t} - 1}{2\Gamma_p}, \tag{4.55a}$$

$$\begin{aligned} c_2(\Delta t) = {} & \frac{1}{2D_{pp}m^2\Gamma_x\Gamma_p(\Gamma_p - \Gamma_x)^2(\Gamma_p + \Gamma_x)} \\ & \times \Big[D_{xx}\left(\Gamma_p^2\left(e^{2\Delta t\Gamma_x} - 1\right) + \Gamma_x^2\left(e^{2\Delta t\Gamma_p} - 1\right) + 2\Gamma_x\Gamma_p\left(1 - e^{\Delta t(\Gamma_x+\Gamma_p)}\right) + \Gamma_x\Gamma_p\left(e^{\Delta t\Gamma_x} - e^{\Delta t\Gamma_p}\right)^2\right) \\ & + m\Gamma_p(\Gamma_p - \Gamma_x)\left(-2D_{xp}\left(\Gamma_p(e^{2\Delta t\Gamma_x} - 1) + \Gamma_x\left(1 + e^{2\Delta t\Gamma_x} - 2e^{\Delta t(\Gamma_x+\Gamma_p)}\right)\right)\right. \\ & \left. + \; D_{pp}m\left(\Gamma_p^2 - \Gamma_x^2\right)\left(-2\Gamma_x\Delta t + e^{2\Gamma_x\Delta t} - 1\right)\right)\Big], \end{aligned} \tag{4.55b}$$

$$\begin{aligned} c_3(\Delta t) = {} & -\Delta t + \frac{e^{\Delta t(\Gamma_x+\Gamma_p)} - 1}{\Gamma_x + \Gamma_p} - \frac{D_{xx}}{2mD_{xp}\Gamma_p(\Gamma_p - \Gamma_x)}\left(1 - e^{2\Delta t\Gamma_p}\right) \\ & + \frac{D_{xx}}{D_{xp}m(\Gamma_p^2 - \Gamma_x^2)}\left(1 - e^{\Delta t(\Gamma_x+\Gamma_p)}\right). \end{aligned} \tag{4.55c}$$

Following performed calculations with the fact that $\hat{G}$ commutes with a linear combination of $\hat{G}_i$, we are allowed to write the final splitting in the form

$$\begin{aligned} e^{\Delta t(\hat{\Pi}+\hat{G})} &= e^{\Delta t\hat{\Pi}}e^{\Delta t\hat{G}}e^{c_1(\Delta t)\hat{G}_1 + c_2(\Delta t)\hat{G}_2 + c_3(\Delta t)\hat{G}_3} \\ &= e^{\Delta t\hat{\Pi}}e^{(\Delta t + A_1(\Delta t))\hat{G}_1 + (\Delta t + A_2(\Delta t))\hat{G}_2 + (\Delta t + A_3(\Delta t))\hat{G}_3} \\ &= e^{\Delta t\hat{\Pi}}e^{F_1(\Delta t)\hat{G}_1 + F_2(\Delta t)\hat{G}_2 + F_3(\Delta t)\hat{G}_3}, \end{aligned} \tag{4.56}$$

where $F_i(\Delta t) = c_i(\Delta t) + \Delta t$, for $i = 1, 2, 3$. It should be borne in mind that operators $\hat{G}_1$, $\hat{G}_2$, $\hat{G}_3$ must be held under a common exponential expression, as their Fourier transform is of the form $-D_{xx}\lambda^2 - D_{pp}y^2 + 2D_{xp}\lambda y$ which can introduce divergent evolution traits if $D_{xx}D_{pp} \leq D_{xp}^2$ The complementary splitting for the operator $\exp\left(\Delta t\hat{\Pi}\right)$ is done according to properties presented in [56]. Recall $\hat{\Pi} = \hat{T} + \hat{S}$ where the commutator of its components is equal to

$$[\hat{T}, \hat{S}_2 + \hat{S}_3] = u\hat{T} + v(\hat{S}_2 + \hat{S}_3) + c\hat{1}, \tag{4.57}$$

where $u = \Gamma_x - \Gamma_p$, $v = 0$, $c = 0$. According to [56] operators that satisfy the commutation relation

$$[\hat{X}, \hat{Y}] = u\hat{X} + v\hat{Y} + c\hat{1},$$

for some constants $u, v, c \in \mathbb{R}$ undergo exact splitting

$$e^{\hat{X}+\hat{Y}} = e^{g_l(u,v)[\hat{X},\hat{Y}]}e^{\hat{X}}e^{\hat{Y}},$$

where $g_l(u, v)$ is given by the expression

$$g_l(u, v) = \frac{(e^{v-u} - e^v) + u\,(e^v - 1)}{uv(v - u)}. \tag{4.58}$$

Using it, we get the following equality for exact splitting

$$\begin{aligned} e^{\Delta t(\hat{T}+\hat{S}_2+\hat{S}_3)} &= e^{g_l(\Delta t(\Gamma_x-\Gamma_p),0)(\Gamma_x-\Gamma_p)(\Delta t)^2\hat{T}}e^{\Delta t\hat{T}}e^{\Delta t(\hat{S}_2+\hat{S}_3)} \\ &= e^{\left(\Delta t - \frac{e^{-\Delta t(\Gamma_x-\Gamma_p)} - 1 + \Delta t(\Gamma_x-\Gamma_p)}{\Gamma_x-\Gamma_p}\right)\hat{T}}e^{\Delta t(\hat{S}_2+\hat{S}_3)}. \end{aligned} \tag{4.59}$$

Combining previous results, the following exact splitting for the exponential of the sum of two operators $\hat{\Pi}+\hat{G}$ might be presented, as follows

$$e^{\Delta t(\hat{T}+\hat{S}+\hat{G})} = e^{\left(\Delta t-\frac{e^{-\Delta t(\Gamma_x-\Gamma_p)}-1+\Delta t(\Gamma_x-\Gamma_p)}{\Gamma_x-\Gamma_p}\right)\hat{T}} e^{\Delta t(\hat{S}_2+\hat{S}_3)} \times e^{F_1(\Delta t)\hat{G}_1+F_2(\Delta t)\hat{G}_2+F_3(\Delta t)\hat{G}_3}.$$

To sufficiently calculate expressions containing derivatives as exponential, we use the Fourier transform, and the equivalence between multiplication and derivative operators. For scaling operators $\hat{S}_i$ for $i=2,3$ this procedure leads nowhere, as both operators are in the form

$$\hat{S}_i = e^{\lambda x_i \partial_{x_i}}, \tag{4.60}$$

and the Fourier transform preserves the form of these operators, marking our method futile. However, they can be implemented as four consecutive Fourier transforms with suitable exponentials. Namely, given the transformation of scaling of x_i variable, by the factor $\eta>0$, that is

$$\hat{S}_i f(x_i) := f(\eta x_i) = e^{\ln(\eta)x_i\partial_{x_i}} f(x_i), \tag{4.61}$$

it can be expressed as [12]

$$f(\eta x) = \eta^{-1/2} e^{-i\epsilon\alpha_\eta\partial_x^2} e^{-i\beta_\eta x^2} e^{i\epsilon\beta_\eta\partial_x^2} e^{i\alpha_\eta x^2} f(x), \tag{4.62}$$

where $\epsilon=-1$, if $\eta>1$ or $\epsilon=1$, if $0<\eta\leq 1$ and

$$\alpha_\eta = \frac{1}{2}\sqrt{|\eta^{-1}-1|\eta^{-1}}, \qquad \beta_\eta = \frac{1}{2}\sqrt{|1-\eta|}. \tag{4.63}$$

For operators $\hat{S}_i$ where $i=2,3$ the scaling parameter is equal to $\eta=\exp[\Gamma_{x_i}\Delta t]$ with $x_2=x$ and $x_3=p$. With this in mind, we can introduce the full split-operator method for the considered evolution generator: the second-order (Strang splitting) (3.13)

$$\begin{aligned}\varrho(x,p,\Delta t) \approx{}& e^{\frac{\Delta t}{2}\hat{V}} e^{\Delta t(\hat{T}+\hat{S}+\hat{G})} e^{\frac{\Delta t}{2}\hat{V}} \varrho_0(x,p,0) = e^{\Delta t\hat{S}_1} e^{\frac{\Delta t}{2}\hat{V}} e^{\left(\Delta t-\frac{e^{-\Delta t(\Gamma_x-\Gamma_p)}-1+\Delta t(\Gamma_x-\Gamma_p)}{\Gamma_x-\Gamma_p}\right)\hat{T}} \\ &\times \eta_x^{-1/2} e^{-i\epsilon\alpha_{\eta_x}\partial_x^2} e^{-i\beta_{\eta_x}x^2} e^{i\epsilon\beta_{\eta_x}\partial_x^2} e^{i\alpha_{\eta_x}x^2} \\ &\times \eta_p^{-1/2} e^{-i\epsilon\alpha_{\eta_p}\partial_p^2} e^{-i\beta_{\eta_p}p^2} e^{i\epsilon\beta_{\eta_p}\partial_p^2} e^{i\alpha_{\eta_p}p^2} \\ &\times e^{F_1(\Delta t)\hat{G}_1+F_2(\Delta t)\hat{G}_2+F_3(\Delta t)\hat{G}_3} e^{\frac{\Delta t}{2}\hat{V}} \varrho_0(x,p,0),\end{aligned} \tag{4.64}$$

and the fourth-order (3.15):

$$\varrho(x,p,\Delta t) \approx e^{\frac{\Delta t}{6}\hat{V}} e^{\frac{\Delta t}{2}(\hat{T}+\hat{S}+\hat{G})} e^{\frac{2}{3}\hat{W}} e^{\frac{\Delta t}{2}(\hat{T}+\hat{S}+\hat{G})} e^{\frac{\Delta t}{6}\hat{V}}, \tag{4.65}$$

where $\eta_x,\eta_p,\alpha,\beta,\epsilon$ are constants associated with the scaling operator presented earlier, and

$$\hat{W} = \hat{V} + \frac{(\Delta t)^2}{48}\left[\hat{V},\left[\hat{T}+\hat{S}+\hat{G},\hat{V}\right]\right]. \tag{4.66}$$

For time-dependent potentials, there is no need to repeat the process, even though the formal solution to the evolutionary type equation with time-dependent generator is given by the Dyson series

$$\partial_t\varrho(x,p,t) = \hat{\mathcal{L}}(t)\varrho(x,p,t) \implies \varrho(x,p,t) = \hat{\mathcal{T}} e^{\int_0^t \hat{\mathcal{L}}(s)ds}\varrho_0(x,p). \tag{4.67}$$

Using the aforementioned Suzuki's relation (3.24) and the fact that the time-shift operator commutes with the kinetic operator $\hat{T}$, we arrive at the splitting formula for time-dependent potentials with splitting of the second order:

$$\begin{aligned}\varrho(x,p,t_0+\Delta t) &\approx e^{\frac{\Delta t}{2}\hat{V}(t_0)}e^{\Delta t(\hat{T}+\hat{S}+\hat{G}+\hat{D})}e^{\frac{\Delta t}{2}\hat{V}(t_0)}\varrho_0(x,p,t_0)\\ &= e^{\frac{\Delta t}{2}\hat{V}(t_0+\Delta t)}e^{\Delta t(\hat{T}+\hat{S}+\hat{G})}e^{\frac{\Delta t}{2}\hat{V}(t_0)}\varrho_0(x,p,t_0),\end{aligned} \tag{4.68}$$

and fourth order

$$\begin{aligned}\varrho(x,p,t_0+\Delta t) &\approx e^{\frac{\Delta t}{6}\hat{V}(t_0)}e^{\frac{\Delta t}{2}(\hat{T}+\hat{S}+\hat{G})}e^{\frac{2}{3}\hat{W}(t_0)}e^{\frac{\Delta t}{2}(\hat{T}+\hat{S}+\hat{G})}e^{\frac{\Delta t}{6}\hat{V}(t_0)}\varrho(x,p,t_0)\\ &= e^{\frac{\Delta t}{6}\hat{V}(t_0+\Delta t)}e^{\frac{\Delta t}{2}(\hat{T}+\hat{S}+\hat{G})}e^{\frac{2}{3}\hat{W}(t_0+\frac{\Delta t}{2})}e^{\frac{\Delta t}{2}(\hat{T}+\hat{S}+\hat{G})}e^{\frac{\Delta t}{6}\hat{V}(t_0)}\varrho(x,p,t_0).\end{aligned} \tag{4.69}$$

Thus, we have introduced iterative methods to generate a WDF in instances of time that are multiples of the time step Δt. The direct splitting for the exponential function of $\hat{T}+\hat{S}+\hat{G}$ reduces the number of Fourier transforms required to calculate the next iteration of the WDF, as per each partial derivative operator, we should include 2 Fourier transforms: forward and backward. Certainly, there are possible reductions of the number of Fourier transforms, depending on the form of preceding and subsequent exponentials. In addition to the results provided, we have found that in the case of the 4th order approximation, the operator $\hat{W}$ can be calculated using only operators $\hat{T}$, and $\hat{V}$, namely

$$\hat{W} = \hat{V} + \frac{(\Delta t)^2}{48}[\hat{V},[\hat{T},\hat{V}]]. \tag{4.70}$$

Consequently, no dissipative or decoherence terms affect this operator. The algorithms presented were implemented in C++, with the help of the Fast Fourier Transform [65].

4.3 A short comment on closed quantum systems

For the sake of the authors' sense of fulfilment, a brief comment on the dynamics of closed quantum systems is in order. Although distant from the main topic of the thesis, the results obtained, by the authors' standards, contribute to the broader sense of PhD research process. These results emerged as a byproduct of tests, calculations, and creative exploration during which the algorithm was developed, tested, and used to generate nontrivial findings. The main topic of the calculations mentioned in this short section refers to the dynamics of Schrödinger Cat States and the behaviour of some descriptive parameters of quantum states like nonclassicality parameter and Rényi entropies.

4.3.1 Dynamical entropic measure of nonclassicality of phase-dependent family of Schrödinger cat states [185]

Within this work, we have tried to unify the concept of interaction time between the quantum state and an absolutely integrable potential. Building purely on the phase-space approach to quantum mechanics, we used the symplectic covariance property to define the interaction time. This new quantity is associated with dynamical properties of a quantum system. In this case, two representatives of the family of Rènyi's entropies were selected, namely entropies of order one-half and one. The first one is associated with the measure of nonclassicality, as we displayed in [97], whereas the latter is equivalent to the continuous Shannon entropy. To lay the foundation for this novel measure, we can start with a simple academic example of a scattering of a free particle. Its evolution, before and after the interaction with the scatterer, can be described as a movement within the constant potential - which is a simple model. On the contrary, the interaction with the potential might be difficult to describe in terms of formulas, leading to an unsolvable equation of evolution. It is crucial to notice that free particle evolution is assumed in the infinite distance from the potential as a result of its absolute integrability over the real line. In terms of the WDF, the evolution of a free particle is equivalent to the shearing transformation of the WDF, which is given by the symplectic matrix acting on the (x, p) variables. With the assumption that the support of the Wigner function is compact in $\mathbb{R}^2$, we can say that before and after the interaction any WDF-dependent functional doesn't change in value, as the Jacobian of the symplectic transformation is equal to 1, and no WDF is present close to the scatterer.

We start by adjusting the definition of the Wigner function as an integral transformation of a wave function

$$\varrho(x,p) = \hat{W}[\psi](x,p) := \frac{1}{2\pi\hbar}\int_{\mathbb{R}} \psi\left(x+\frac{X}{2}\right)\psi^*\left(x-\frac{X}{2}\right)\exp\left(-\frac{i}{\hbar}pX\right)dX. \tag{4.71}$$

This definition highlights the symplectic covariance property of the WDF, that is, for a metaplectic transformation $\hat{K}_{\hat{S}}$, associated with a symplectic matrix $\hat{S}$, acting on the wave function, we have the following identity [47]

$$\hat{W}[\hat{K}_{\hat{S}}\psi](x,p) = \hat{W}[\psi](\hat{S}^{-1}(x,p)). \tag{4.72}$$

It can be interpreted as statemenet that transforming a wave function through a particular transformation is equivalent to symplectic change of variables of the Wigner function of pre-transformed wave function.

Throught this identity, one can define the symplecitcally invariant measures as

$$\xi := \int_{\mathbb{R}^2} f\left(\hat{W}[\psi](x,p)\right) dxdp, \tag{4.73}$$

where $f : [-1/(\pi\hbar), 1/(\pi\hbar)] \to \mathbb{R}$ is chosen so that the integral exists and is finite. Currently, it is unclear how to associate defined expressions with the time evolution of the quantum system. However, it is true that for Hamiltonians of type $\hat{H} = \hat{p}^2/(2m) + \alpha\hat{x}^2$, where $\alpha \in \{0, 2\}$, the evolution can be associated with a metaplectic transformation $\hat{K}_{\hat{S}}(t)$ given by the time-evolution operator $\hat{U}(t;\alpha)$ for all $t \geq 0$. We will focus our attention on the case $\alpha = 0$ which stands for the free-particle evolution. Our previous explanation implies that

$$\hat{W}[\psi(t)](x,p) = \hat{W}[\hat{K}_{\hat{S}}(t)\psi](x,p) = \hat{W}[\psi](\hat{S}^{-1}(t)(x,p)), \tag{4.74}$$

where we have used the fact, that $\hat{K}_{\hat{S}}(t)$ is given by the time evolution operator, yielding $\psi(t)$ for ψ. Furthermore

$$\xi(t) = \int_{\mathbb{R}^2} f\left(\hat{W}[\psi(t)](x,p)\right) dxdp \tag{4.75}$$

defines the natural generalisation of symplectically invariant measures for time-dependent wave functions. Then, by a simple change of variables, we have

$$\begin{aligned} \xi(t) &= \int_{\mathbb{R}^2} f\left(\hat{W}[\psi(t)](x,p)\right) dxdp = \int_{\mathbb{R}^2} f\left(\hat{W}[\hat{K}_{\hat{S}}(t)\psi](x,p)\right) dxdp \\ &= \int_{\mathbb{R}^2} f\left(\hat{W}[\psi](\hat{S}^{-1}(t)(x,p))\right) dxdp = \int_{\mathbb{R}^2} f\left(\hat{W}[\psi](x,p)\right) dxdp, \end{aligned} \tag{4.76}$$

where the last equality holds by the fact that $\left|\det \hat{S}(t)\right| = 1$. This, by the previous considerations, implies that $\xi(t) = const.$ where evolution is governed equivalently by symplectic matrix. This can be easily visualised as follows

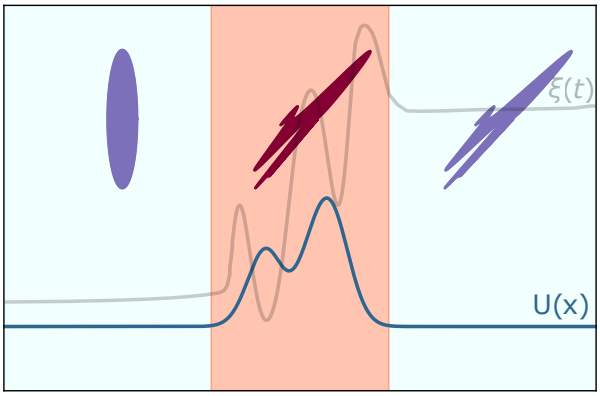

Figure 4.1: An idealised picture of the time evolution of the WDF subjected to the $L^1(\mathbb{R})$ potential $U(x)$. The blob on the LHS depicts the area occupied by the initial WDF. It evolves freely until it reaches a certain area (middle segment, orange color) where evolution is no longer describable by the metaplectic transformation. This reflects on the time evolution of the symplectic measure $\xi(t)$ (background curve) where prior to rapid evolvution within segment it behaved nearly constantly. After the interaction with the potential, the symplectically invariant measure stabilizes again.

Such setup allowed us to define the interaction time τ, up to a certain tolerance ϵ, in the following manner:

Proposition 4.1. For a symplectically invariant measure $\xi(t)$, the interaction time τ, between state represented by the Wigner distribution function and potential energy belonging to the class of absolutely integrable functions, can be defined as

$$\begin{aligned}\tau &= \min\{t\in\mathbb{R}_+ : |\xi(t)-\xi(\infty)|>\epsilon\} - \max\{t\in\mathbb{R}_+ : |\xi(t)-\xi(0)|>\epsilon\}\\ &= t_f - t_i,\end{aligned} \tag{4.77}$$

where $\xi(0)$ is the value of the symplectically invariant measure at the beginning of the evolution, whereas $\xi(\infty)$ is the value at the end of the evolution. $M=\max_{t\in\mathbb{R}_+}\xi(t)$ is the maximum of Wigner–Rényi entropic measure, $m=\min_{t\in\mathbb{R}_+}\xi(t)$ is its minimum, and $0<\varepsilon\ll 1$ is a dimensionless threshold parameter that can be understood as the precision of the measuring device.

The threshold parameter present in the proposition might seem to be chosen arbitrary small. However, it should be small relative to the values of the symplectically invariant measure. Within our research, we treated it as a percentile of the difference between maximal and minimal value of the symplectically invariant measure. Moreover, we narrowed the class of symplectically invariant measures $\xi(t)$ to the following measures: the Wigner-Rényi entropy of order one-half and one. Those metrics can be derived directly from the formula [97]

$$S_\alpha(t)=\frac{1}{1-\alpha}\ln\left[(2\pi\hbar)^{2\alpha-1}\int_{\mathbb{R}^2}dxdp\,|\varrho(x,p,t)|^{2\alpha}\right], \tag{4.78}$$

where α is the order of the entropy. The main goal of our research was to propose a phase-space method to estimate an interaction time of the quantum state subjected to the integrable potential, which shifts the importance from the analysis of the dynamics of the system to the evolution of the symplectically invariant measure. To visualise our findings we conducted a numerical calculation of Schrödinger cat state evolution in the Gaussian barrier system, with time-dependent amplitude, in the form [185]

$$V(x,t;\alpha)=V_0\exp\left[-\frac{(x-x_B)^2}{2w^2}\right][1-\alpha\,\theta(t-t_{\rm s})], \tag{4.79}$$

where $\alpha\in\{0.5,2\}$. This greatly highlighted the advantages and limitations of our method, providing results comparable with other interaction time measures, such as tunnelling time.

4.3.2 Interaction time of Schrödinger cat states with a periodically driven quantum system: Symplectic covariance approach [186]

The idea of symplectic covariance of the Wigner distribution function was used to estimate the interaction time between an oscillating Gaussian barrier, where the time dependence was included within the amplitude of the potential, leading to frequent swaps between the barrier and a well; and a Schrödinger Cat State Wigner distribution function (SC-WDF). We have numerically solved the equation of evolution, using the split-operator method for time-dependent potentials, with initial state given by SC-WDF subjected to the Gaussian potential with oscillating amplitude. Within this research, we investigated the behaviour of the family of Wigner-Rényi entropies with emphasis on the hierarchy of interaction time based on those symplectically invariant measures. The potential we considered is given by the following formula [186]

$$U(x,t;T)=U_0\exp\left[-\frac{(x-x_B)^2}{2w^2}\right]\left(\theta(t_b-t)+\operatorname{sgn}\left[\sin\frac{2\pi(t-t_b)}{T}\right]\theta(t-t_b)\right), \tag{4.80}$$

where U_0 is the maximum of the amplitude, x_B is the position of the centre of the barrier, w is the width of the barrier, T is the period of potential changes and t_b is the delay time before the periodicity of the potential is switched on. We distinguished three cases for system considered, based upon the timescale the period of oscillations between barrier and well state of the potential: short, intermediate, and long. This setup was ideal for previously defined interaction time, as we have time-dependent potential and initial state in the backscattering regime for which the casual tunnelling is ill-defined. We have shown that the family of Wigner-Rényi entropies is nonincreasing with respect to $\alpha \geq 1/2$, that is

$$S_\alpha(t) \leq S_\beta(t) \iff \alpha \geq \beta, \tag{4.81}$$

for functions belonging to $f \in L^1(\mathbb{R}, dxdp) \cap L^\alpha(\mathbb{R}^2, dxdp)$. A natural question arises if the interaction time satisfies similar property, namely, if $\tau_\alpha \; ? \; \tau_\beta \iff \alpha \geq \beta$ for different periods T of the oscillatory potential.

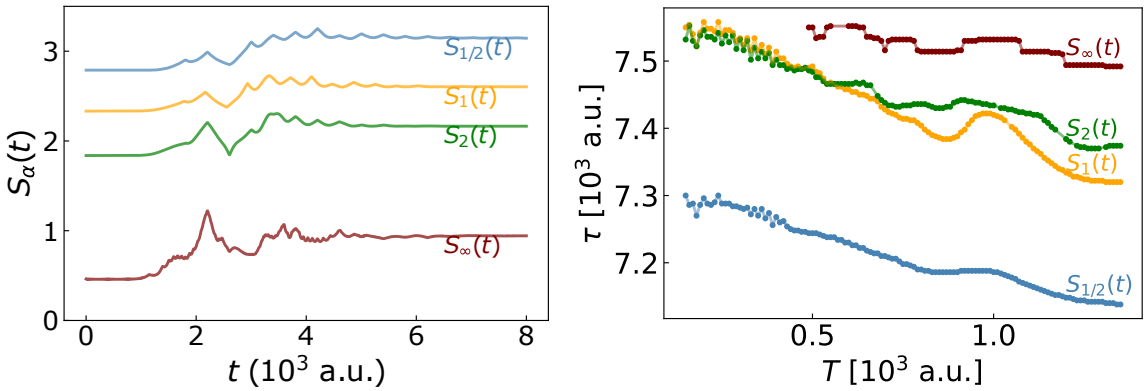

Figure 4.2: An example of the family of Wigner-Rényi entropies for $\alpha \in \{1/2, 1, 2, +\infty\}$, and the interaction time τ based upon them, as a function of potential's period T, for the system in question. We can notice the monotonicity of entropies but can not conclude that interaction time exhibits the same pattern although it appears to be ordered reversely, i.e. monotonicly increasing as α increases.

We have noticed that after a certain value of period T, the interaction time exhibits monotone ordering where $\tau_\alpha \leq \tau_\beta \iff \alpha \leq \beta$ but this issue requires further in-depth analysis to prove it rigorously. Moreover, a question of how to construct a measurement such that this method of calculating the interaction time is valid and in the frame of physical theory, is also crucial to answer and will be investigated in the future.

4.4 Averaged system dynamics

Convention: the averages with respect to position and momentum variables are noted via the angular brackets, whereas statistical functions $\mathrm{E}[\cdot]$, $\mathrm{Var}[\cdot]$ are calculated with respect to the vector parameter $\boldsymbol{\lambda}$.
Let us consider two general initial value problems with a common initial condition $\varrho_0(x,p)$

$$\begin{cases} \bar{\varrho}_t(x,p,t) = \hat{\bar{\mathcal{L}}}\bar{\varrho}(x,p,t) + g(x,p,t), \\ \bar{\varrho}(x,p,0) = \varrho_0(x,p), \end{cases} , \quad \begin{cases} \varrho_t(x,p,t;\boldsymbol{\lambda}) = \hat{\mathcal{L}}(\boldsymbol{\lambda})\varrho(x,p,t;\boldsymbol{\lambda}), \\ \varrho(x,p,0;\boldsymbol{\lambda}) = \varrho_0(x,p), \end{cases} \tag{4.82}$$

where $\boldsymbol{\lambda}$ is a random vector of independent and identically distributed variables (IID) λ_i from PDF $f(\lambda_i)$, which implies that $P(\boldsymbol{\lambda}) = \Pi_i f(\lambda_i)$; $\bar{\varrho} = \mathrm{E}[\varrho]$ is the ensemble averaged solution function, $\hat{\bar{\mathcal{L}}} = \mathrm{E}[\hat{\mathcal{L}}]$ is the ensemble averaged dynamics generator. To find the correction to this dynamic, let us assume that the function g can be expressed as a power series in time t with operator coefficients $\hat{B}_n$, namely

$$g(x,p,t) = \sum_{n=0} t^n \hat{B}_n \bar{\varrho}(x,p,t). \tag{4.83}$$

By the theory of abstract evolutionary equations, the formal general solutions can be written consecutively as: for the first, non-homogenous Cauchy problem [133]

$$\bar{\varrho}(t) = e^{t\hat{\bar{\mathcal{L}}}}u_0 + \int_0^t e^{(t-s)\hat{\bar{\mathcal{L}}}} g(s)ds, \tag{4.84}$$

whereas the second solution is given by

$$\varrho(x,p,t;\boldsymbol{\lambda}) = e^{t(\hat{\bar{\mathcal{L}}}+\hat{\Delta}(\boldsymbol{\lambda}))}\varrho_0(x,p). \tag{4.85}$$

where $\hat{\Delta}(\boldsymbol{\lambda}) = \hat{\mathcal{L}}(\boldsymbol{\lambda}) - \hat{\bar{\mathcal{L}}}$. To make a convincing comparison between these two solutions, we express their functions through power series in time t. We are particularly interested in short periods of time, so we keep terms that are at most of the 2nd order of t. As a result, from Eq. (4.84) one gets

$$\bar{\varrho}(x,p,t) \approx \varrho_0(x,p) + t\left[\hat{\bar{\mathcal{L}}} + \hat{B}_0\right]\varrho_0(x,p) + \frac{t^2}{2}\left[\hat{\bar{\mathcal{L}}}^2 + \hat{B}_1 + \{\hat{\bar{\mathcal{L}}}, \hat{B}_0\}\right]\varrho_0(x,p), \tag{4.86}$$

where we have used the following identity [75]

$$\int_0^t (t-s)^n s^m ds = \frac{n!m!}{(n+m+1)!}t^{n+m+1}, \quad n,m \in \mathbb{Z}_+, \tag{4.87}$$

and, after integrating both sides of equation (4.85) w.r.t $\boldsymbol{\lambda}$, we get complementary

$$\begin{aligned} \bar{\varrho}(x,p,t) &\approx \int P(\boldsymbol{\lambda})\left[\hat{1} + \left(\hat{\bar{\mathcal{L}}} + \hat{\Delta}(\boldsymbol{\lambda})\right)t + \frac{1}{2}\left(\hat{\bar{\mathcal{L}}} + \hat{\Delta}(\boldsymbol{\lambda})\right)^2 t^2\right] d\boldsymbol{\lambda}\ \varrho_0(x,p) \\ &= \varrho_0(x,p) + t\hat{\bar{\mathcal{L}}}\varrho_0(x,p) + \frac{t^2}{2}\left[\hat{\bar{\mathcal{L}}}^2 + \mathrm{Var}[\hat{\Delta}(\boldsymbol{\lambda})]\right]\varrho_0(x,p). \end{aligned} \tag{4.88}$$

Comparing both expressions we arrive at the lowest correction to the averaged system dynamics

$$\bar{\varrho}_t(x,p,t) = \hat{\bar{\mathcal{L}}}\bar{\varrho}(x,p,t) + t\mathrm{Var}[\hat{\Delta}(\boldsymbol{\lambda})]\bar{\varrho}(x,p,t), \tag{4.89}$$

with

$$\mathrm{Var}[\hat{\Delta}(\boldsymbol{\lambda})] = \int P(\boldsymbol{\lambda})\left(\hat{\mathcal{L}}(\boldsymbol{\lambda}) - \hat{\bar{\mathcal{L}}}\right)^2 d\boldsymbol{\lambda}. \tag{4.90}$$

Still keeping the undefined character of operators above, one may notice that assuming that there exists a real symbol $G(x,p,t)$ such that $\Delta(\boldsymbol{\lambda})$ can be written in the star-product adjoint form, namely $\Delta(\boldsymbol{\lambda}) = \{G(x,p,t;\boldsymbol{\lambda}),\cdot\}_\star$, then

$$\mathrm{Var}[\hat{\Delta}(\boldsymbol{\lambda})] \sim \int P(\boldsymbol{\lambda})\{G(x,p,t;\boldsymbol{\lambda}),\{G(x,p,t;\boldsymbol{\lambda},\cdot\}_\star\}_\star d\boldsymbol{\lambda}, \tag{4.91}$$

is the continuous sum of quantum jump operators with positive coefficients, present in the Lindblad equation. Leading to the conclusion, that the average of solutions of evolutionary equations with random parameters, in short times, introduces a Lindbladian corrections to the dynamics. In the case of quantum mechanics, $\hat{\mathcal{L}}(\boldsymbol{\lambda})$ can be understood as the Moyal bracket for an isolated/closed system or Wigner-Lindblad generator for an open system dynamics. In presented case, we will consider an open quantum system, where random perturbation of the potential is present, namely $V = V(x,t;\boldsymbol{\lambda})$. Such case lead to following averaged Lindblad operator

$$\hat{\bar{\mathcal{L}}} = -\frac{p}{m}\partial_x + \int P(\boldsymbol{\lambda})\{V(x,t;\boldsymbol{\lambda}),\cdot\}_\star d\boldsymbol{\lambda} + \Gamma_x\partial_x(x(\cdot)) + \Gamma_p\partial_p(p(\cdot)) + \frac{1}{2}D_{xx}\partial^2_{pp} + \frac{1}{2}D_{pp}\partial^2_{xx} - D_{xp}\partial^2_{xp}, \tag{4.92}$$

and complementary

$$\Delta(\boldsymbol{\lambda}) = \hat{\mathcal{L}}(\boldsymbol{\lambda}) - \hat{\bar{\mathcal{L}}} = \{V(x,t;\boldsymbol{\lambda}) - \bar{V}(x,t),\cdot\}_\star = \{\delta V(x,t;\boldsymbol{\lambda}),\cdot\}_\star \tag{4.93}$$

giving

$$\left\langle \Delta^2(x,t,\boldsymbol{\lambda})\right\rangle_{\boldsymbol{\lambda}} = \int P(\boldsymbol{\lambda})\{\delta V(x,t;\boldsymbol{\lambda}),\{\delta V(x,t;\boldsymbol{\lambda}),\cdot\}_\star\}_\star d\boldsymbol{\lambda}. \tag{4.94}$$

To better visualise the operator $\mathrm{Var}[\hat{\Delta}(\boldsymbol{\lambda})]$ we use the different representation of the Moyal bracket, leading to

$$\mathrm{Var}[\hat{\Delta}(\boldsymbol{\lambda})] = -\frac{1}{\hbar^2}\left[\delta V\left(\boldsymbol{x} + \frac{i\hbar}{2}\nabla_{\boldsymbol{p}},t;\boldsymbol{\lambda}\right) - \delta V\left(\boldsymbol{x} - \frac{i\hbar}{2}\nabla_{\boldsymbol{p}},t;\boldsymbol{\lambda}\right)\right]^2, \tag{4.95}$$

so total approximated equation of motion for averaged system is

$$\begin{aligned}\partial_t\bar{\varrho} = &-\frac{p}{m}\partial_x\bar{\varrho} + \int P(\boldsymbol{\lambda})\{V(x,t;\boldsymbol{\lambda}),\bar{\varrho}\}d\boldsymbol{\lambda} + \Gamma_x\partial_x(x\bar{\varrho}) + \Gamma_p\partial_p(p\bar{\varrho})\\ &+ \frac{1}{2}D_{xx}\partial^2_{pp}\bar{\varrho} + \frac{1}{2}D_{pp}\partial^2_{xx}\bar{\varrho} - D_{xp}\partial^2_{xp}\bar{\varrho}\\ &- \frac{t}{\hbar^2}\int P(\boldsymbol{\lambda})\left[\delta V\left(\boldsymbol{x} + \frac{i\hbar}{2}\nabla_{\boldsymbol{p}},t;\boldsymbol{\lambda}\right) - \delta V\left(\boldsymbol{x} - \frac{i\hbar}{2}\nabla_{\boldsymbol{p}},t;\boldsymbol{\lambda}\right)\right]^2\bar{\varrho}\, d\boldsymbol{\lambda}.\end{aligned} \tag{4.96}$$

Since the equation of motion for the WDF for the averaged system is not explicitly available in an analytical or calculable form, we instead focus on the law of large numbers, which gives us the following expression [110]:

$$E[\varrho](x,p,t) = \frac{1}{N}\sum_{k=1}^{N}\varrho(x,p,t;\boldsymbol{\lambda}_k), \quad \text{as } N\to\infty, \tag{4.97}$$

which will be used to calculate the averaged WDF for open system. As a model for simulations a time-independent potential is considered in the form of the sequence of nearly periodic Gaussian barriers

$$V(x;\boldsymbol{\lambda}) = \sum_k V_0\frac{1}{\sqrt{2\pi}\sigma}e^{-\frac{(x-k\mu-\lambda_k)^2}{2\sigma^2}}, \tag{4.98}$$

where it is assumed that all barriers are initially, without introducing the random vector $\boldsymbol{\lambda}$, equidistant, with equal amplitudes and standard deviations. We will consider two probability distributions from which components of the vector $\boldsymbol{\lambda}$ are drawn:

1. A uniform distribution over a symmetric interval:
$$P(\lambda_k) = \frac{1}{2\alpha\sigma}\theta(|\lambda_k| \leq \alpha\sigma);$$
2. A Gaussian distribution centred around 0 with standard deviation $w > 0$:
$$P(\lambda_k) = \frac{1}{\sqrt{2\pi}w} e^{-\frac{1}{2w^2}\lambda_k^2}, \quad \lambda_k \in \mathbb{R}.$$

Generally, it will be assumed that parameters presented in the probability distributions are of the order of single Gaussian barrier of the potential, so the influence of the λ_k is treated as a perturbation from periodicity of the system rather than the complete anihilation of these characteristics. Then the following averaged value of the potential holds

1. For the uniform distribution
$$\bar{V}_1(x) = \frac{V_0}{4\alpha\sigma}\sum_k \left[\mathrm{erf}\left(\frac{\alpha\sigma - x + k\mu}{\sqrt{2}\sigma}\right) + \mathrm{erf}\left(\frac{\alpha\sigma + x - k\mu}{\sqrt{2}\sigma}\right)\right]; \tag{4.99}$$
2. For the normal distribution of λ
$$\bar{V}_2(x) = \frac{V_0}{\sqrt{2\pi(\sigma^2 + w^2)}}\sum_k e^{-\frac{(x-k\mu)^2}{2(\sigma^2+w^2)}}. \tag{4.100}$$

With averaged potentials, we can re-express the Eq.(4.95) in terms of $\bar{V}_i(x)$ and the value of $\left\langle V^2(x;\boldsymbol{\lambda})\right\rangle_{\boldsymbol{\lambda}}$ as shown in the Appendix E.2. However, using standard statistical measures and their properties, we can gain insight into the equation (4.96), holding as an assumption that the potential $V(x)$ is smooth. Firstly, let us rewrite the potential as a sum of potentials where each component depends only on one coordinate of random vector $\boldsymbol{\lambda}$, that is:
$$V(x;\boldsymbol{\lambda}) = \sum_k v_k(x;\lambda_k). \tag{4.101}$$
Here we do not specify the form of the function $v_k(x,\lambda_k)$, to keep the result as general as possible. Nevertheless, we make the assumption that it is a smooth function and that the integrals
$$\mathrm{E}[v_k(x;\lambda_k)] := \int P(\lambda_k)v_k(x;\lambda_k)d\lambda_k, \tag{4.102}$$
and
$$\mathrm{Var}[v_k(x;\lambda_k)] := \int P(\lambda_k)(v_k(x;\lambda_k) - \mathrm{E}[v_k](x))^2 d\lambda_k, \tag{4.103}$$
are finite for any k. The integral expression in (4.96) can be rewritten as
$$\begin{aligned}-\hbar^2\int P(\boldsymbol{\lambda})\{\delta V(x,t;\boldsymbol{\lambda}),\{\delta V(x,t;\boldsymbol{\lambda}),\cdot\}\}d\boldsymbol{\lambda} = \mathrm{Var}\left[V\left(x+\frac{i\hbar}{2}\partial_p;\boldsymbol{\lambda}\right)\right] + \mathrm{Var}\left[V\left(x-\frac{i\hbar}{2}\partial_p;\boldsymbol{\lambda}\right)\right] \\ - 2\mathrm{cov}\left[V\left(x+\frac{i\hbar}{2}\partial_p;\boldsymbol{\lambda}\right), V\left(x-\frac{i\hbar}{2}\partial_p;\boldsymbol{\lambda}\right)\right].\end{aligned} \tag{4.104}$$

With the form of the potential $V(x;\boldsymbol{\lambda})$ provided previously we can simplify this expression, using the properties of the variance and covariance, namely

$$\begin{aligned}\mathrm{Var}\left[V\left(z;\boldsymbol{\lambda}\right)\right] &= \mathrm{Var}\left[\sum_k v_k(z;\lambda_k)\right] = \sum_{k,l}\mathrm{cov}\left[v_k(z;\lambda_k), v_l(z;\lambda_l)\right] \\ &= \sum_k \mathrm{Var}\left[v_k(z;\lambda_k)\right],\end{aligned} \tag{4.105}$$

where $\mathrm{cov}\left[v_k(z;\lambda_k), v_l(z;\lambda_l)\right] = 0$ for $k \neq l$ as λ_k, λ_l are independent random variables. Complementarily, the covariance present in the initial expression can be rewritten using the bilinearity property, i.e

$$\begin{aligned}\mathrm{cov}\left[V\left(y;\boldsymbol{\lambda}\right), V\left(z;\boldsymbol{\lambda}\right)\right] &= \mathrm{cov}\left[\sum_k v_k(y;\lambda_k), \sum_l v_l(z;\lambda_l)\right] = \sum_{k,l}\mathrm{cov}\left[v_k(y;\lambda_k), v_l(z;\lambda_l)\right] \\ &= \sum_k \mathrm{cov}\left[v_k(y;\lambda_k), v_k(z;\lambda_k)\right],\end{aligned} \tag{4.106}$$

where mixed-terms covariances are equal to 0, same as before. In conclusion, the correction to the dynamics resulting from the randomness of the system can be expressed as

$$\begin{aligned}\int P(\boldsymbol{\lambda})\{\delta V(x,t;\boldsymbol{\lambda}), \{\delta V(x,t;\boldsymbol{\lambda}),\cdot\}\}d\boldsymbol{\lambda} &= -\frac{1}{\hbar^2}\sum_k \left(\mathrm{Var}\left[v_k(y;\lambda_k)\right] + \mathrm{Var}\left[v_k(z;\lambda_k)\right]\right. \\ &\quad \left. - 2\mathrm{cov}\left[v_k(y;\lambda_k), v_k(z;\lambda_k)\right]\right)\Big|_{\substack{y=x+\frac{i\hbar}{2}\partial_p \\ z=x-\frac{i\hbar}{2}\partial_p}} \\ &= -\frac{1}{\hbar^2}\sum_k \mathrm{Var}\left[v_k\left(x+\frac{i\hbar}{2}\partial_p;\lambda_k\right) - v_k\left(x-\frac{i\hbar}{2}\partial_p;\lambda_k\right)\right].\end{aligned} \tag{4.107}$$

Using now the assumption about the smoothness of the constituent functions $u_k(x;\lambda_k)$, we expand each in Taylor series, leading to

$$v_k\left(x+\frac{i\hbar}{2}\partial_p;\lambda_k\right) - v_k\left(x-\frac{i\hbar}{2}\partial_p;\lambda_k\right) = i\hbar\sum_{n/0}^{+\infty}\frac{(-1)^n}{(2n+1)!}\left(\frac{\hbar}{2}\right)^{2n}\partial_x^{2n+1}[v_k(x;\lambda_k)]\partial_p^{2n+1}, \tag{4.108}$$

and consequently, the variance of the difference can be written as

$$\begin{aligned}&\mathrm{Var}\left[v_k\left(x+\frac{i\hbar}{2}\partial_p;\lambda_k\right) - v_k\left(x-\frac{i\hbar}{2}\partial_p;\lambda_k\right)\right] = \\ &-\hbar^2\sum_{\substack{m=0\\l=0}}^{+\infty}\frac{(-1)^{m+l}}{(2m+1)!(2l+1)!}\left(\frac{\hbar}{2}\right)^{2(m+l)}\mathrm{cov}\left[\partial_x^{2m+1}v_k(x;\lambda_k), \partial_x^{2l+1}v_k(x;\lambda_k)\right]\partial_p^{2(m+l)+2}.\end{aligned} \tag{4.109}$$

The lowest order correction to the dynamics can be achieved by taking $m = l = 0$, then

$$\mathrm{Var}\left[v_k\left(x+\frac{i\hbar}{2}\partial_p;\lambda_k\right) - v_k\left(x-\frac{i\hbar}{2}\partial_p;\lambda_k\right)\right] = -\hbar^2\mathrm{Var}[v_k'(x;\lambda_k)]\partial_{pp}, \tag{4.110}$$

or in the context of the equation of motion

$$\begin{aligned}\partial_t\bar{\varrho} &= -\frac{p}{m}\partial_x\bar{\varrho} + \{\bar{V}(x,t),\bar{\varrho}\} + \Gamma_x\partial_x(x\bar{\varrho}) + \Gamma_p\partial_p(p\bar{\varrho}) \\ &\quad + \frac{1}{2}D_{xx}\partial_{pp}^2\bar{\varrho} + \frac{1}{2}D_{pp}\partial_{xx}^2\bar{\varrho} - D_{xp}\partial_{xp}^2\bar{\varrho} + t\left(\sum_k \mathrm{Var}[v_k'(x;\lambda_k)]\right)\partial_{pp}\bar{\varrho}.\end{aligned} \tag{4.111}$$

As a result, the derived correction can be treated in the lowest order as a position-dependent decoherence term, and its strength is coupled to the variance of the potential components' derivative. Moreover, it displays the emergence of decoherence in averaged systems. Even further simplification of the problem is possible, allowing us to bound the decoherence to the spread of the random parameter. Let us recall that for a function $f(x;\lambda)$ parameterised by a random variable λ, with mean $E[\lambda] = 0$, we can approximate its variance via the following relation

$$\mathrm{Var}[f(x;\lambda)] \approx \sigma_\lambda^2 \left(\frac{\partial f}{\partial \lambda}\right)^2 \Bigg|_{\lambda=E[\lambda]=0}, \tag{4.112}$$

which is known as the delta method [30], which reduces to applying the Taylor expansion with respect to λ for function $f(x;\cdot)$. In our case, this approximation leads to

$$\mathrm{Var}[v_k'(x;\lambda_k)] \approx \sigma_\lambda^2 \left(\frac{\partial^2 v_k}{\partial x \partial \lambda_k}\right)^2 \Bigg|_{\lambda_k=E[\lambda_k]=0}. \tag{4.113}$$

Within this work, we will consider constituent potentials, v_k, dependent on the difference between position x, and random variable λ_k, $v_k(x;\lambda_k) = v_k(x-\lambda_k)$ allowing for further simplifications, where the derivative with respect to λ can be substituted with the derivative with respect to position, taken with a negative sign, $-\partial_x$, giving us the following equation:

$$\begin{aligned}\partial_t \bar{\varrho} = &-\frac{p}{m}\partial_x \bar{\varrho} + \{\bar{V}(x,t), \bar{\varrho}\} + \Gamma_x \partial_x (x\bar{\varrho}) + \Gamma_p \partial_p (p\bar{\varrho}) \\ &+ \frac{1}{2} D_{xx}\partial_{pp}^2 \bar{\varrho} + \frac{1}{2} D_{pp}\partial_{xx}^2 \bar{\varrho} - D_{xp}\partial_{xp}^2 \bar{\varrho} + t\sigma_\lambda^2 \sum_k (\partial_{xx}^2 v_k(x;0))^2 \partial_{pp}^2 \bar{\varrho}.\end{aligned} \tag{4.114}$$

For a better understanding of the derived dynamics, an example was considered for the linear potential $V(x;\boldsymbol{\lambda}) = V(x;E) = Ex$, in Appendix D.

4.5 Numerical results

Within this section, we have used the algorithm developed in Sec. 4.2 to investigate the dynamics of the system described by equation (4.114). The numerical calculations were performed on a symmetric $N_x \times N_p = 1024 \times 1024$ (x, p) grid with the initial WDF state taken as a Gaussian function with uncorrelated position and momentum.

$$\varrho(x, p, 0) = \varrho_0(x, p) = \frac{1}{2\pi\sigma_x\sigma_p} e^{-\frac{1}{2}\left(\frac{x-x_0}{\sigma_x}\right)^2 - \frac{1}{2}\left(\frac{p-p_0}{\sigma_p}\right)^2}, \tag{4.115}$$

with the following parameters: $x_0 = -300$ [a.u.], $p_0 = 0.15$ [a.u.], $\sigma_x = \sqrt{500}$ [a.u.], $\sigma_p = 1/(2 \cdot \sqrt{500})$ [a.u.]. This gives the mean energy of the initial state at the value $\langle E \rangle \approx 0.0113$ [a.u.]. The maximum position value on the grid was set to $x_{max} = 1500$ [a.u.] while for the momentum $p_{max} = 1.5$ [a.u.] which gives the grid steps $\Delta x = 2.93$ [a.u.] and $\Delta p = 0.00293$ [a.u.], as the grid is rectangular $[-x_{max}, x_{max}] \times [-p_{max}, p_{max}]$. The time step for the closed single barrier and chain of barriers systems was set as $\Delta t = 10$ [a.u.]. For the single-barrier system, it overlaps with the parameters used in our publications [185, 186, 97]. The parameters of the environment were chosen so that the whole evolution resembles Brownian evolution, with $\Gamma_x = D_{pp} = D_{xp} = 0$ while $\Gamma_p = 10^{-5}$, $D_{xx} = 10^{-6}$. The values of the parameters were guided by the stability of the algorithm. As for the perturbation vector $\boldsymbol{\lambda}$ of the potential, we considered 50 cases, each having either 1 (single barrier) or 20 (chain of barriers) coordinates, which together constitute a statistical ensemble.

4.5.1 Dynamical parameters of the system

To characterise the dynamical properties of the system, we considered a group of parameters which can be classified as follows:

1. **The statistical parameters**
   Measures which stem directly from the definition and properties of the WDF and have physical and statistical interpretation. Those include: mean values of position and momentum and centralised second moments. We define those as follows: the mean position and momentum

$$\langle x \rangle (t, \boldsymbol{\lambda}) = \int_{\mathbb{R}^2} x \varrho(x, p, t; \boldsymbol{\lambda}) dx dp, \tag{4.116}$$

   and

$$\langle p \rangle (t, \boldsymbol{\lambda}) = \int_{\mathbb{R}^2} p \varrho(x, p, t; \boldsymbol{\lambda}) dx dp, \tag{4.117}$$

   complementarly, the second centralised moments:

$$\begin{aligned} \sigma_x^2(t, \boldsymbol{\lambda}) &= \left\langle x^2 \right\rangle (t, \boldsymbol{\lambda}) - \langle x \rangle^2 (t, \boldsymbol{\lambda}), \\ \sigma_p^2(t, \boldsymbol{\lambda}) &= \left\langle p^2 \right\rangle (t, \boldsymbol{\lambda}) - \langle p \rangle^2 (t, \boldsymbol{\lambda}), \\ \mathrm{cov}[x, p](t, \boldsymbol{\lambda}) &= \langle xp \rangle (t, \boldsymbol{\lambda}) - \langle x \rangle \langle p \rangle (t, \boldsymbol{\lambda}). \end{aligned} \tag{4.118}$$

   The pair $(\langle x \rangle (t, \boldsymbol{\lambda}), \langle p \rangle (t, \boldsymbol{\lambda}))$ will be understood as quantum phase-space trajectories, and are in close relation with classical ones. They are the main concern of Ehrenfest theorem [149], drawing

similarities between classical and quantum mechanics. Additionally, we recieve the trajectory for each realisation of the system. Using the linearity of mean value, with respect to the (quasi-)probability density function, we expect that average Wigner function $\bar{\varrho}$ moves along the average of phase-space trajectories. Complementarly, the second moments allow us to characterize the deviation from the mean trajectory and also the correlation between both variables considered. The evolution equation for mentioned moments is given by the following system of coupled ordinary differential equations: the first moments (means)

$$\begin{cases} \partial_t \langle x \rangle = \dfrac{1}{m} \langle p \rangle - \Gamma_x \langle x \rangle , \\ \partial_t \langle p \rangle = - \langle \partial_x V(x; \boldsymbol{\lambda}) \rangle - \Gamma_p \langle p \rangle . \end{cases} \tag{4.119}$$

and second centralised moments (variations and covariance)

$$\begin{cases} \partial_t \sigma_x^2 = \dfrac{2}{m} \mathrm{cov}(x,p) - 2\Gamma_x \sigma_x^2 + D_{pp}, \\ \partial_t \sigma_p^2 = -2\mathrm{cov}(p, \partial_x V(x;\boldsymbol{\lambda})) - 2\Gamma_p \sigma_p^2 + D_{xx}, \\ \partial_t \mathrm{cov}(x,p) = \dfrac{1}{m}\sigma_p^2 - \mathrm{cov}(x, \partial_x V(x;\boldsymbol{\lambda})) - (\Gamma_x + \Gamma_p)\mathrm{cov}(x,p) - D_{xp}. \end{cases} \tag{4.120}$$

Yet again, we see that Gaussian states are preserved in the case of potentials of the polynomial type of at most second order, as the system of presented equations is then closed, and gives full evolution of the parameters of the Gaussian state.

This can also be debated in the case of the averaged dynamics. Then the system of ODEs describing the moments is given by

$$\begin{cases} \partial_t \langle \bar{x} \rangle = \dfrac{1}{m} \langle p \rangle - \Gamma_x \langle x \rangle , \\ \partial_t \langle \bar{p} \rangle = - \left\langle \partial_x \bar{V}(x) \right\rangle - \Gamma_p \langle p \rangle . \end{cases} \tag{4.121}$$

and complementarily

$$\begin{cases} \partial_t \bar{\sigma}_x^2 = \dfrac{2}{m} \bar{\mathrm{cov}}(x,p) - 2\Gamma_x \bar{\sigma}_x^2 + D_{pp}, \\ \partial_t \bar{\sigma}_p^2 = -2\mathrm{cov}(p, \partial_x \bar{V}(x)) - 2\Gamma_p \bar{\sigma}_p^2 + D_{xx} + t\sigma_\lambda^2 \sum\limits_k (\partial_{xx} v_k(x;\mathbf{0}))^2, \\ \partial_t \bar{\mathrm{cov}}(x,p) = \dfrac{1}{m}\sigma_p^2 - \mathrm{cov}(x, \partial_x \bar{V}(x)) - (\Gamma_x + \Gamma_p)\bar{\mathrm{cov}}(x,p) - D_{xp}. \end{cases} \tag{4.122}$$

which especially changes in the evolution of the momentum-variance of the average solution.

2. **The phase-space characteristics**

   Measures that are a functionals of the WDF. Between all possibilities, the most recognizable is the nonclassicality parameter [101]. It classifies the negativity of the WDF, simultaneously quantifying the quantum effects [148]. According to Ref. [91], the WDF is classified as real probability distribution function, thus is non-negative, only when the underlying wave function of the quantum system is Gaussian exponential. This yields yet another interpretation of the nonclassicality parameter - as the measure of deviation from Gaussian distribution function. Moreover, it was shown that negativity of the WDF is required to witness the tunneling effects in quantum systems [111]. nonclassicality parameter found its applications in the Resource Theory [161], as logarithmic nonclassicality which

is a computable resource measure, capturing the negativity of the WDF and behaving monotonically under Gaussian free operations [2].

In the case of mixed quantum states, however, there exist postivie WDFs that are simultanously non-Gaussian [117]. The nonclassicality parameter is defined as [101]

$$\delta := \int_{\mathbb{R}^2} (|\varrho(x,p)| - \varrho(x,p))dxdp = \int_{\mathbb{R}^2} |\varrho(x,p)|dxdp - 1, \tag{4.123}$$

and it satisfies the following bound $\delta \in [0, +\infty)$. The time and $\boldsymbol{\lambda}$ dependence is naturally transfered from the WDF to $\delta(t;\boldsymbol{\lambda})$.

The second measure, quantifying the amount of information the WDF possesses, is the Wigner-Shannon entropy. It is associated with a deformation of the area occupied in the phase space, that was caused by quantum position-momentum correlations [186]. It is a special case of a family of Wigner-Rényi entropy [172, 97]

$$S_\alpha(t;\boldsymbol{\lambda}) = \frac{1}{1-\alpha} \ln \left[(2\pi\hbar)^{\alpha-1} \int_{\mathbb{R}^2} dxdp \ \left(|\widetilde{\varrho}(x,p,t;\boldsymbol{\lambda})|^2 \right)^\alpha \right], \tag{4.124}$$

which for $\alpha \to 1$ has the form

$$S_1(t;\boldsymbol{\lambda}) = -2 \int_{\mathbb{R}^2} dxdp \ |\widetilde{\varrho}(x,p,t;\boldsymbol{\lambda})|^2 \ln \left(|\widetilde{\varrho}(x,p,t;\boldsymbol{\lambda})|^2 \right), \tag{4.125}$$

where $\tilde{\varrho} = \varrho / \|\varrho\|_{L^2(\mathbb{R}^2)}$. Additionally, according to [1], the rate of change of the Shannon entropy can be associated with the rate of diffusion of the quasiprobability function over the phase space. It should be noted, that the topic of quantum entropy for quasiprobability distributions is quite vast, and many definitions and directions were considered that resemble the standard differential Shannon entropy [172, 53, 173, 118]. However, the definition provided in Eq. (4.125) uses the interpretation of the Wigner function as the probability amplitude function [21, 38]. In our work [97], we have shown the relationship between the nonclassicality parameter, and the Wigner-Rényi entropy of order $\alpha = 1/2$.

3. **State characteristics**

We shall recall one of the previously mentioned parameters. By theorem 1.1 the purity of the state can be used to determine whether the state of the system is pure or mixed. In terms of Wigner function, the purity is defined as

$$D(t;\boldsymbol{\lambda}) = 2\pi\hbar \int_{\mathbb{R}^2} \varrho^2(x,p,t;\boldsymbol{\lambda})dxdp, \tag{4.126}$$

and can be used to track the characteristic trait of the quantum state. However, as underlying Hilbert space of the system is infinite-dimensional, the crucial property is missed, namely we are not able to state which state of the system is maximally mixed. This is especially interesting, as the maximally mixed state has the maximal Shannon entropy, equal to $\ln d$ [128], where d is the dimension of the Hilbert space, providing connection between two measures and their physical interpretations. Moreover, under Liouvillian dynamics (2.38), the purity of the system is non-increasing function of time, namely $\dot{D}(t) \leq 0$. This is proven as great criterion for correctness of the dynamics of the system, as increasing purity would suggest that the motion of the system is no longer governed by the GKSL equation.

Another measure, associated mostly with the investigation of the influence of the perturbation of the system on its dynamics, is the Lochschmidt Echo, introduced by A. Peres [135]. It can be defined as a overlap measure between unperturbed system Wigner function $\varrho(x,p,t;\mathbf{0}) = \varrho(x,p,t)$ and perturbed one $\varrho(x,p,t;\boldsymbol{\lambda})$ [73, 41]

$$M(t;\boldsymbol{\lambda}) := 2\pi\hbar \int_{\mathbb{R}^2} \varrho(x,p,t)\varrho(x,p,t;\boldsymbol{\lambda})dxdp. \tag{4.127}$$

Its interpretation, based on the mathematical formula, is straight forward: it measures the overlap between the two types of the dynamics with similar initial condition $\varrho_0(x,p)$ allowing for quantitative describtion of the *divergence* from unperturbed evolution. However, the main physicall question standing behind this measure is the reversibility of the dynamics. Due to its simplicity, it especially found applications in chaos theory for quantum mechanical systems [135, 187] as a tool for analysis of reversibility of the evolution but it can also be interpreted as sensivity of the quantum system to perturbations.

4. **The distances between states**

The distance between two density operators, $\hat{\rho}_1$, $\hat{\rho}_2$ is given by the trace distance defined as follows [128, 108]

$$d(\hat{\rho}_1,\hat{\rho}_2) := \frac{1}{2}\,\mathrm{Tr}(|\hat{\rho}_1 - \hat{\rho}_2|), \tag{4.128}$$

which can not be easily transferred to the quantum phase space, as by the Weyl quantisation procedure we get

$$d(\varrho_1,\varrho_2) := \frac{1}{2}\int_{\mathbb{R}^2} |\varrho_1(x,p,t) - \varrho_2(x,p,t)|_\star dxdp, \tag{4.129}$$

where modulus function presented in the integrand expression is understood as $\star$-modulus. Its definition is rather complicated and can be given in terms of a limit, instead of an analytic formula

$$|\varrho(x,p,t)|_\star := \lim_{k\to+\infty} \tanh_\star(k\varrho(x,p,t)) \star \varrho(x,p,t). \tag{4.130}$$

which is one of many ways to define a *standard* modulus within the scope of commutative product. Thus, a different distance measure should be considered, where an explicit formula can be written down and then calculated - even numerically. Fortunately, the Hilbert-Schmidt distance is one of such measures, that can be directly translated in terms of Weyl transform, namely

$$\tilde{d}_1(\varrho_1,\varrho_2) := \sqrt{\int [\varrho_1(x,p,t) - \varrho_2(x,p,t)]^2 dxdp}, \tag{4.131}$$

where ϱ_1, ϱ_2 are the WDFs of density operators $\hat{\rho}_1$, $\hat{\rho}_2$. By the triangle inequality $\|\varrho_1 - \varrho_2\|_2 \leq \|\varrho_1\|_2 + \|\varrho_2\|_2$ we can normalize this expression to identity, namely

$$d_1(\varrho_1,\varrho_2) := \frac{\sqrt{\int [\varrho_1(x,p,t) - \varrho_2(x,p,t)]^2 dxdp}}{\sqrt{\int \varrho_1^2(x,p,t)dxdp} + \sqrt{\int \varrho_2^2(x,p,t)dxdp}}. \tag{4.132}$$

The integral of the square of the WDF, as previously stated, is proportional to the purity of the state, hence, the distance considered allows for measuring what fraction of the sum of purities of two states,

calculated independently, is covered by the difference between these states. For the sake of this work, we are interested in two distances: the one between the average of the solution and the approximated average solution, and the other between states and the unperturbed system. This approach should quantify the discrepancies between the approximation and the amount of deviation from the dynamics without the vector of random parameters $\boldsymbol{\lambda}$.

4.5.2 Single barrier with perturbed centre

For the first case of the system, we considered a closed quantum system with a potential of the form

$$V(x;\lambda) = V_0 \frac{1}{\sqrt{2\pi}\sigma} e^{-\frac{(x-\lambda)^2}{2\sigma^2}}, \tag{4.133}$$

where for each λ, being a random variable. In this setting, the perturbation λ corresponds to shifting of the barrier towards or away from the initial state WDF, as it is centralised at point (x_0, p_0) in the phase space, according to Eq. (4.115). Therefore, for each value of λ, the evolution is either delayed or advanced: $\lambda > 0$ gives a delay, while $\lambda < 0$ gives an advance. This repulsive Gaussian potential model can be related to nanowire defects models [184, 103], to studies of interacting Bose-Einstein condensate through a barrier [120, 92], or considered for a tunnelling model for estimation of tunnelling time [55] and semiclassical analysis [13]. In this first simulation, we did not include the environmental effects to see if our intuition behind the isolated model is right. As noted earlier, both the averaged system and its approximation should be influenced by the effective environmental effects introduced through averaging, rather than by a physical coupling to an external system. Classically, this system corresponds to a simple $\boldsymbol{\lambda}$-shifted barrier, which exhibits two types of dynamics: reflection from the barrier or free evolution above it.

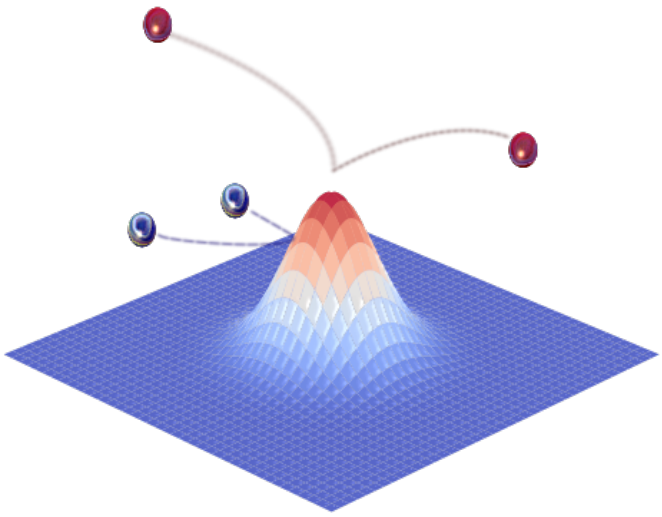

Figure 4.3: An artistic visualisation of the types of dynamics in the presented system. The classical particle (blue-bottom or red-top ball) can either back-scatter from the potential or transfer right above the barrier, depending on the initial energy it has. The curves represent a phase-space trajectories associated with those dynamics.

Isolated system

Convention: In all subsequent figures, the results for Gaussian disorder are shown in the left panel (or column), and the results for uniform disorder are shown in the right panel (or column). The grey band represents the ensemble of realisations of the parameters for the disordered system, while the green line is associated with the parameters of the unperturbed system. The red and blue lines indicate the parameters of the ensemble average WDF and of our approximation, respectively.

The phase-space trajectories of this system, as expected, form a family of shifted curves on the x, p-plane, as visible in Fig. 4.4

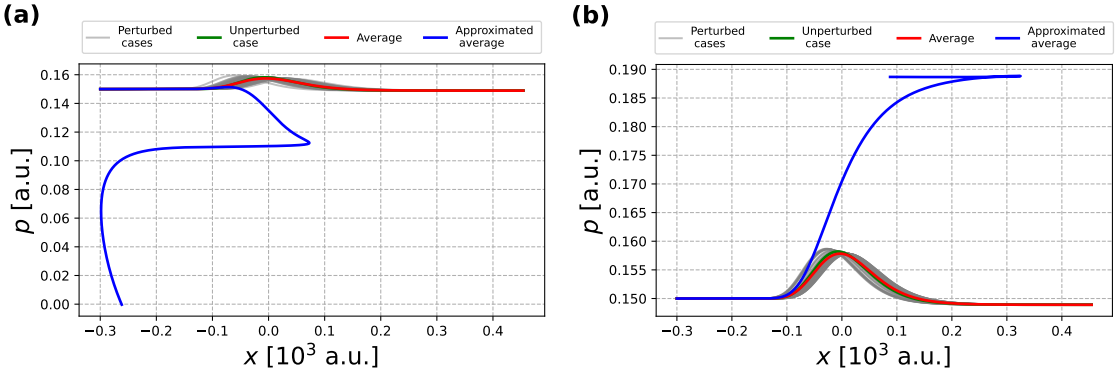

Figure 4.4: The phase-space trajectories of the WDFs for the isolated system.

One can immediately notice that the grey curves are not only shifted, but also their extrema are lower for each $\boldsymbol{\lambda}$ vector considered. This behaviour results from the evolution associated with a free particle. When the potential energy vanishes $V(x;\boldsymbol{\lambda}) = 0$ or when there are unbounded regions where $V(x;\boldsymbol{\lambda}) \approx 0$ within some tolerance, the evolution follows (or is close to) a transformation known as shearing [47]. In particular, for the free particle potential, the general solution to the Moyal equation, with the initial condition ϱ_0, is given by

$$\varrho(x,p,t) = \varrho_0(x - pt, p), \tag{4.134}$$

which means that the solution is constant along the characteristics $x - pt = c_1$ and $p = c_2$. Although the momentum p does not change, it still governs the behaviour of the position through its amplitude and sign. As a result, parts of the Wigner function, lying below the x axis ($p < 0$), move to the left, while those above move to the right, and the shift increases over time $t > 0$. The closer the barrier is to the initial state, the less sheared the Wigner function becomes before reaching it. This creates a shifted and lowered maximum on the (x, p)-plane. It is also noticeable that all phase-space trajectories, except the one given by the approximate average solution, have a final momentum smaller than the initial value. Looking at the second moments of the WDF, they exhibit the following evolution patterns, displayed in Fig. 4.5

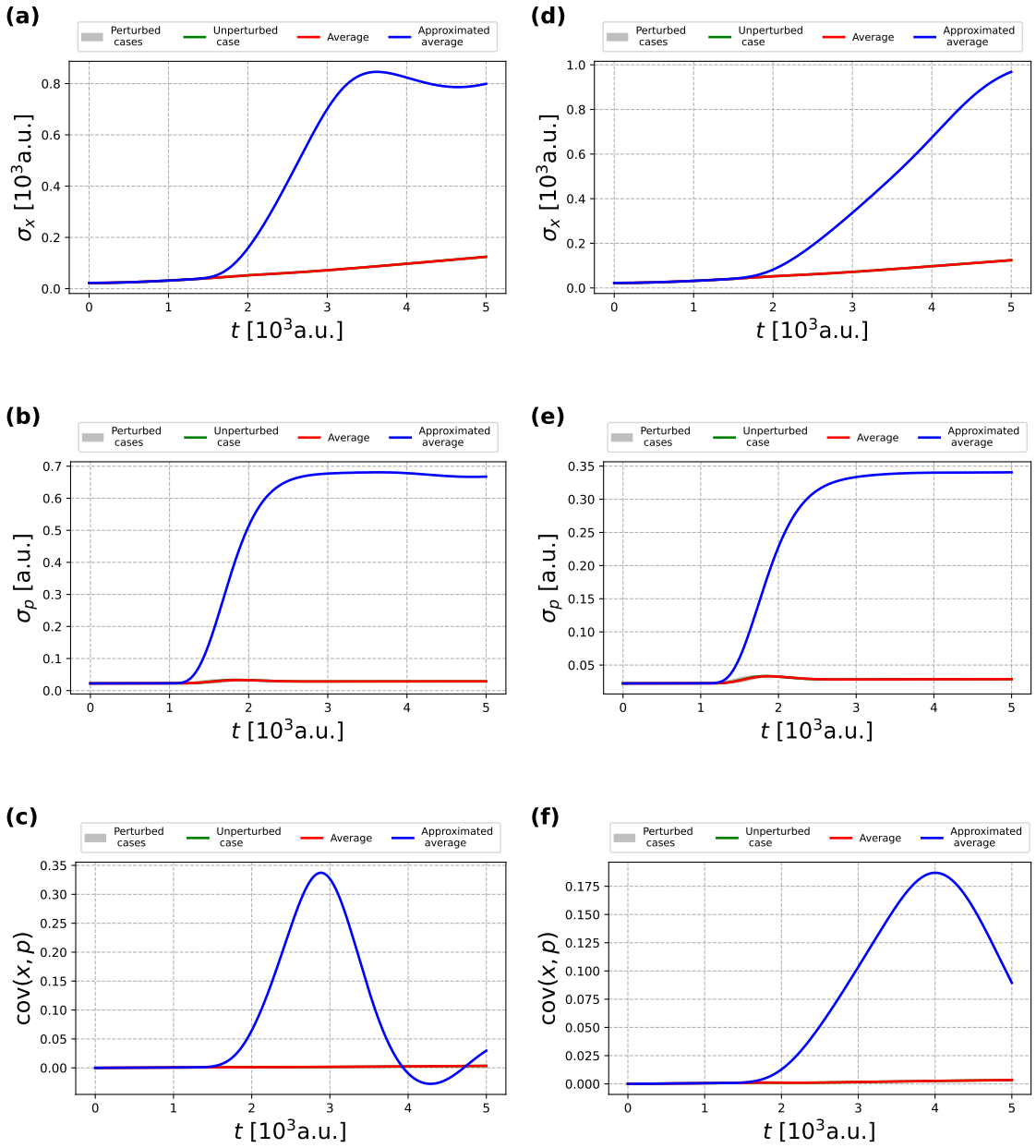

Figure 4.5: The standard deviation and covariance of momentum and position of the WDF for the isolated single barrier system. In this particular case, the grey band associated with the second centralised moments of the perturbed systems is not visible in the figure (covered by the red line), which suggests that the random location of the potential does not influence these parameters.

We can see that for both cases of random location distributions $P(\boldsymbol{\lambda})$, the behaviour of second moments of the WDF is similar. In particular, the standard deviation and the covariance of the average WDF seem to be kept within the bounds of the evolution, and more importantly, the shift of the potential does not exhibit crucial changes to its moments. Therefore, we can state that the structural change of a barrier does not influence the spreading of the WDF. In contrast, the blue line in Fig. 4.5, which represents the approximated average solution parameters, is visibly different from its previous counterparts. The sigmoid-like structure for both σ_x and σ_p is inconsistent with the ensemble average and should be treated rather as a worst-case scenario. This leads to the appearance of the maximum covariance between position and momentum, which is delayed in the case of a uniform distribution.

Since the initial state is given by a Gaussian function, which is a proper classical PDF, it is natural to investigate how the nonclassicality parameter changes during evolution together with the Wigner-Shannon entropy, as seen in Fig. 4.6 From the evolution of $\delta(t;\boldsymbol{\lambda})$, it is visible that before the interaction with the

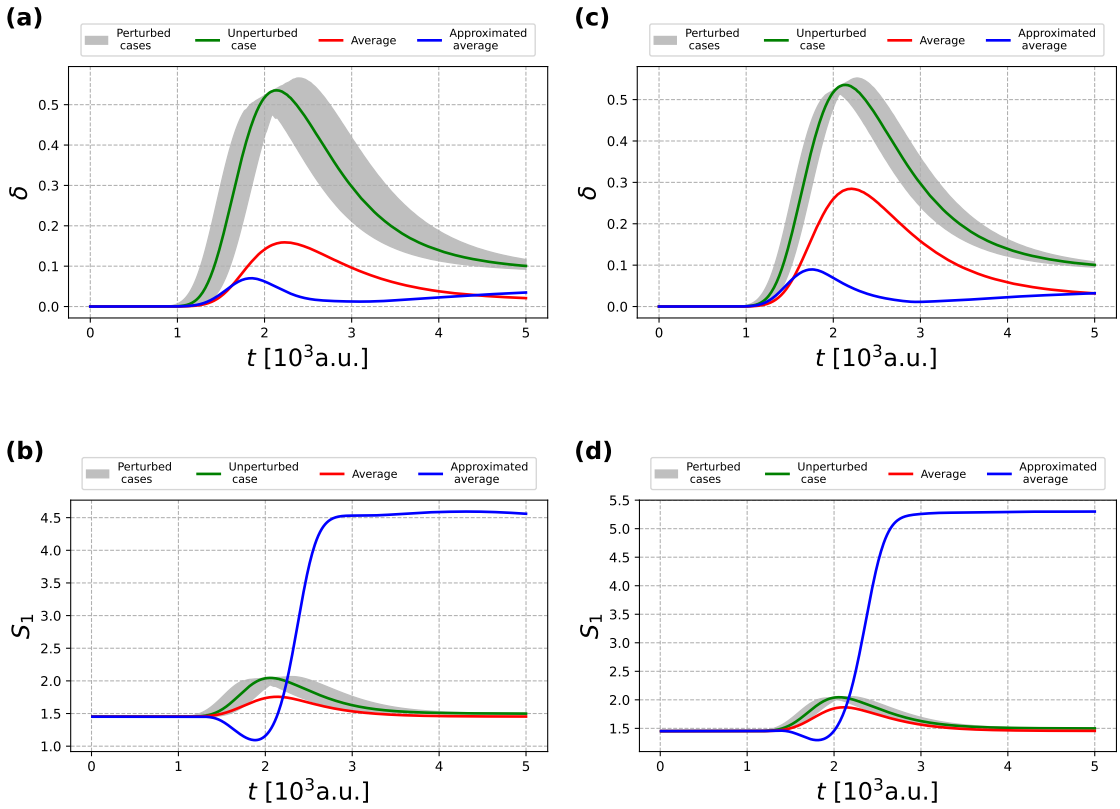

Figure 4.6: The nonclassicality parameter and Wigner-Shannon entropy of the isolated single barrier system.

centre of the barrier, the Wigner function stays positive and Gaussian. As discussed earlier, away from the barrier, the potential resembles that of a free particle, and the evolution is governed by the shearing transformation. This preserves the form of a function, which implies that $\delta(t;\boldsymbol{\lambda}) = 0$ or, more precisely, $\delta(t;\boldsymbol{\lambda}) \approx 0$ since some interaction between the Gaussian tail and the barrier is still expected. Once the barrier is reached, the value of $\delta(t;\boldsymbol{\lambda})$ increases, indicating an enlargement of the area where the WDF is negative, and suggesting the appearance of quantum effects, such as quantum interference. After the interaction,

$\delta(t;\boldsymbol{\lambda})$ slowly approaches a fixed nonzero value. For the ensemble's average WDF, however, $\delta(t;\boldsymbol{\lambda})$ tends towards zero, while for the approximated solution, the nonclassicality parameter begins to increase again. To examine whether the nonclassicality parameter continues to change under further evolution, we can analyse the Wigner-Shannon entropy shown in the Figs 4.6b, 4.6d. After approximately $t = 3 \times 10^3$ [a.u.], the entropy remains nearly constant, which means that the system no longer interacts with the potential. Therefore, the nonclassicality reaches asymptotically a fixed value. Additionally, the spread of the WDF for the ensemble and its average, after the interaction with the potential, slows down as $dS(t;\boldsymbol{\lambda})/dt \approx 0$, which is consistent with the expected behaviour.

For the analysis of the type of dynamics of the system, we shall consider the purity and Loschmidt echo, displayed in Fig. 4.7 The purity of each realisation of the system is constant and equal to unity, which

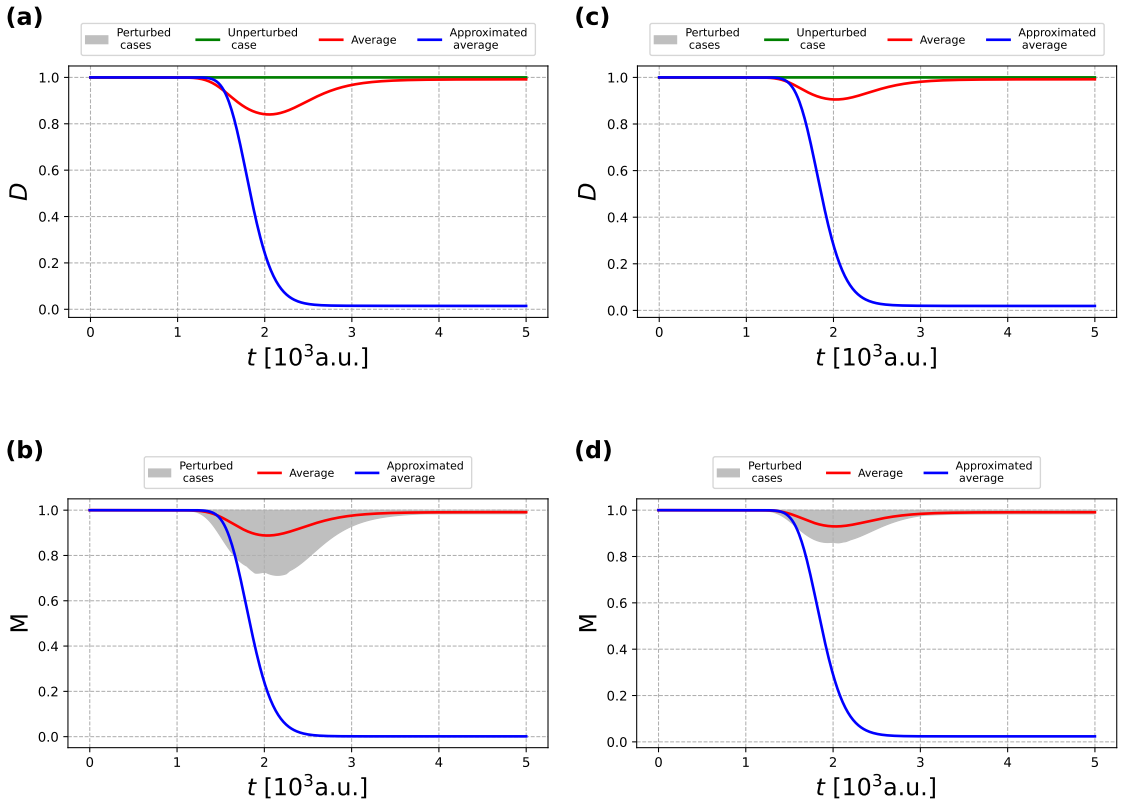

Figure 4.7: The purity and Loschmidt echo for the isolated single barrier system. For the purity, the grey band is perfectly tracing the green line of the unperturbed system, as the evolution is unitary.

confirms that the evolution of the system is isolated. In contrast, the purity of the averaged case shows unusual behaviour. It initially decreases and later returns to unity. This rules out interpreting the dynamics of the average as isolated, or even as Lindbladian, since in that case the value of purity should be nonincreasing. On the other hand, the approximated average purity decreases monotonically, which is consistent with the evolution guided by Eq. (4.114). Furthermore, as shown in the Figs 4.7b, 4.7d, the system itself exhibits reversible dynamics, whereas the approximated average solution's echo suggests the complete loss of the information within the system, with simultaneous overdamping of the ensemble's dynamics. On the other

hand, the system's reversibility is largely insensitive to spatial perturbations of the potential. Apart from a single extremum in the Loschmidt echo, its value tends to unity for each realisation within the ensemble, apart from the proposed average approximation, where the reversibility is lost.

To gain a deeper understanding of the relationship between constituent realisation of the system, we analysed the distance between each WDF, including the average WDF and its approximation, and the unperturbed system WDF in the Fig. 4.8 With an additional analysis of the distance between the averaged

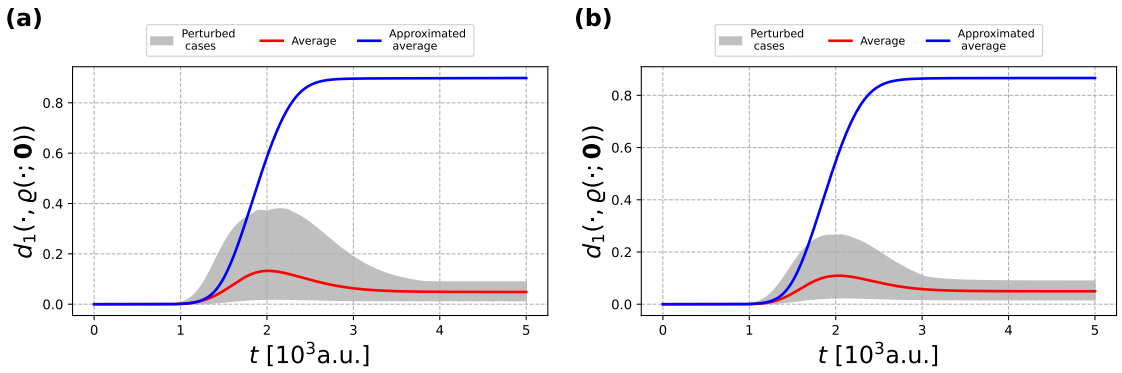

Figure 4.8: The distance between the WDF for the unperturbed potential and each of the following for the isolated single barrier system: the perturbed WDF, the ensemble average, and the proposed approximation of the average.

WDF and the proposed approximation, in Fig. 4.9 The distance between the unperturbed WDF and the

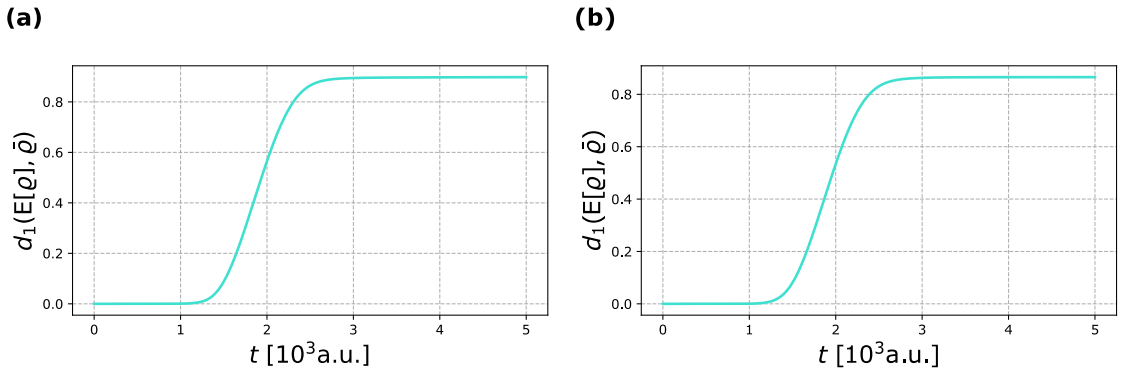

Figure 4.9: The distance between the ensemble average $E[\varrho]$ and proposed approximation $\bar{\varrho}$ in the case of the isolated single barrier system.

perturbed cases and averages starts from zero, then changes upon reaching the centre of the potential, and eventually stabilises at a nonzero constant value. Since the initial evolution resembles that of a free particle, it is expected that the perturbed solution initially overlaps with the unperturbed one. The same behaviour is observed for the ensemble average and its approximation. It suggests that states, after the interaction, stay in constant separation from each other. The averaged WDF does not fully resemble the unperturbed WDF, as their distance stabilises at a value greater than 0. The same reasoning can be applied for the distance between

the suggested approximation and the average WDF, seen in Figs 4.9a, 4.9b, and thus it poorly approximates the evolution, especially when interaction with the potential starts and after it.

Open system

As a next step, we *open* the system by introducing the environmental effects, which are included by keeping the coefficients Γ_p and D_{xx} non-zero in Eq. (4.35). This leads to the following dynamics of the WDFs considered, seen in Figs 4.10 Compared to the isolated system, the phase-space trajectories of the open

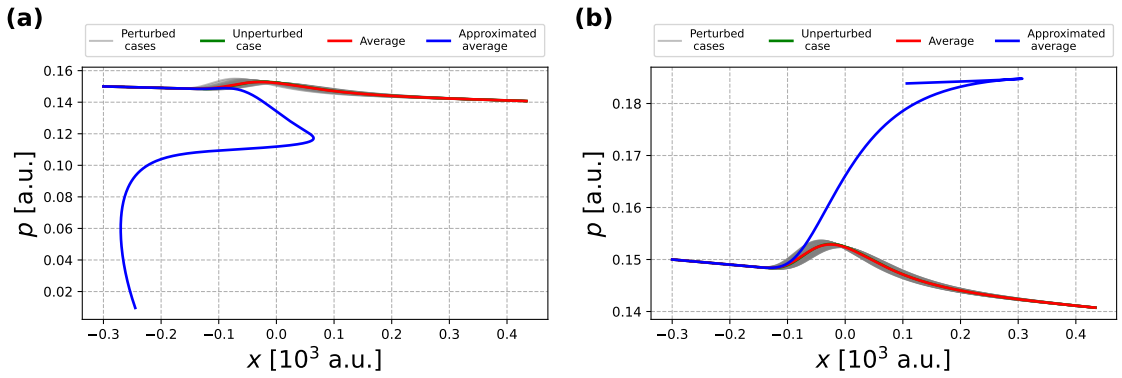

Figure 4.10: The phase-space trajectories of the WDFs for the open system.

system do not appear to differ significantly. However, there is a visible constant loss of momentum for all cases after interaction with the barrier, due to the loss of energy. The same conclusions can be applied to the phase-space trajectories of the ensemble average. This result is not surprising, as the constants present in the evolution equation are taken small, so that the decoherence and dissipation effects are prolonged through evolution. However, the small amplitude of those coefficients does not significantly influence the decoherence constant present in the approximated equation for the ensemble average WDF, and thus its trajectory remains similar to that of the isolated dynamics. As a next set of parameters, we consider the second moments of the WDFs, seen in Fig. 4.11

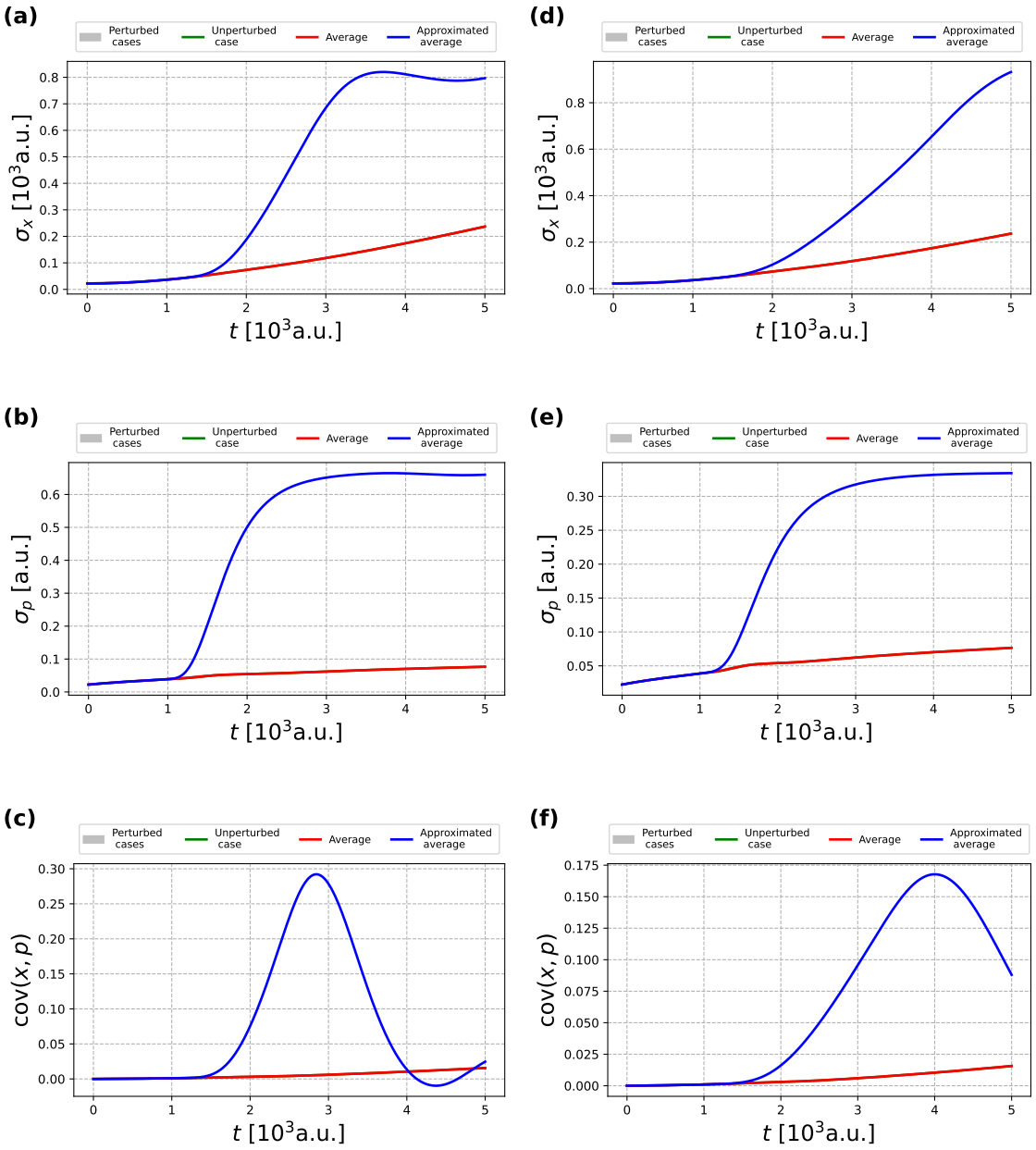

Figure 4.11: The standard deviation and covariance of momentum and position of the WDF for the isolated single barrier system. As is the case with the isolated system, there is no grey band present in the figures.

The second moments of the WDFs considered align almost perfectly with the case of the isolated system. This would imply that environmental effects do not affect their behaviour. However, the standard deviation of the momentum increases in the case of the open system, while it was almost constant for the isolated one. Consequently, we try to notice differences between the systems using the phase-space and state measures, displayed in Figs 4.12, 4.13 Although the phase-space trajectories of the WDFs do not differ significantly

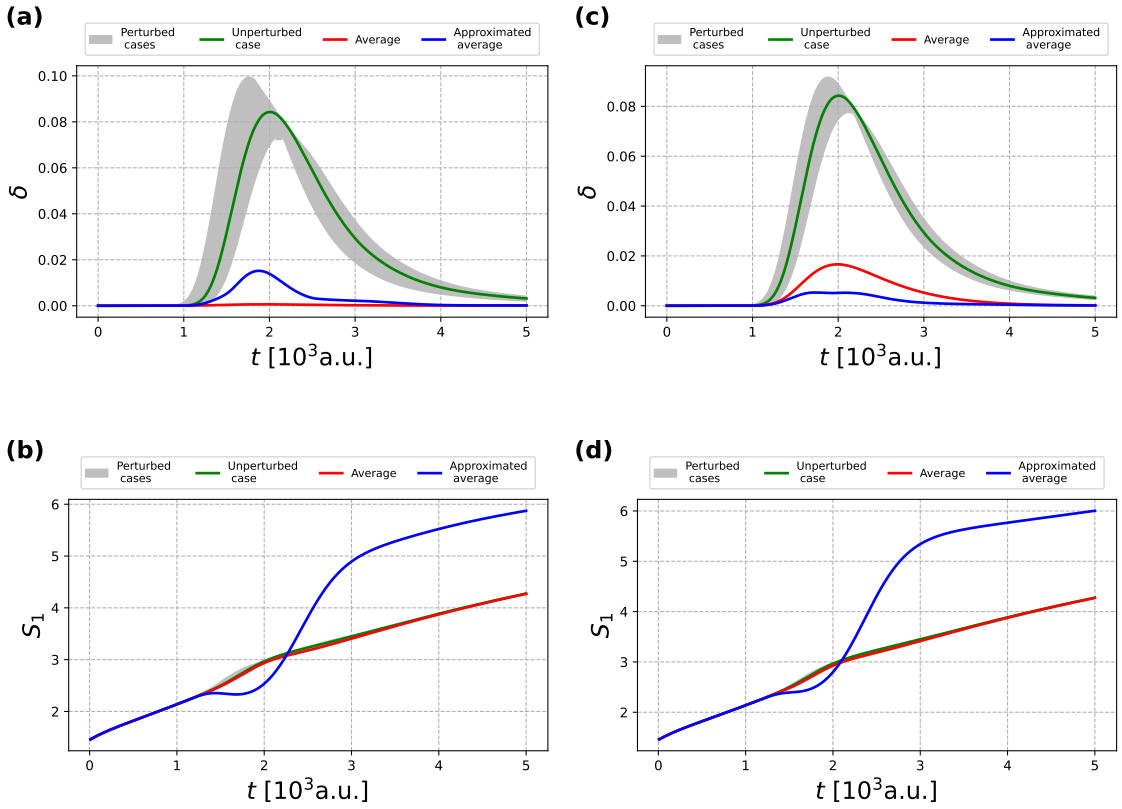

Figure 4.12: The nonclassicality parameter and Wigner-Shannon entropy of the open single barrier system.

between isolated and open systems, the nonclassicality parameter and entropy exhibit completely different behaviour. In the long-time limit, the nonclassicality parameter for all WDFs considered approaches zero. As a consequence, the asymptotic state of the system is represented by a positive WDF for all random vectors $\boldsymbol{\lambda}$, which implies that the final state of the system is a Gaussian or a positive mixed quantum state. The Wigner-Shannon entropy increases monotonically, with a small "bump" around the time instant $t \approx 2 \times 10^3$ [a.u.]. This result suggests a further spread of the distribution as time increases. The rate of spreading is similar for the perturbed WDF and the ensemble average, while the approximated average initially diffuses faster but eventually stabilises at a constant rate. However, the presence of the environment reduces the spread of the Wigner-Shannon entropy across the contributing realisations of the system. It acts as a *barrier* to information spreading, limiting the possible dispersion of the WDF among ensemble elements, and controlling the rate at which entropy increases.

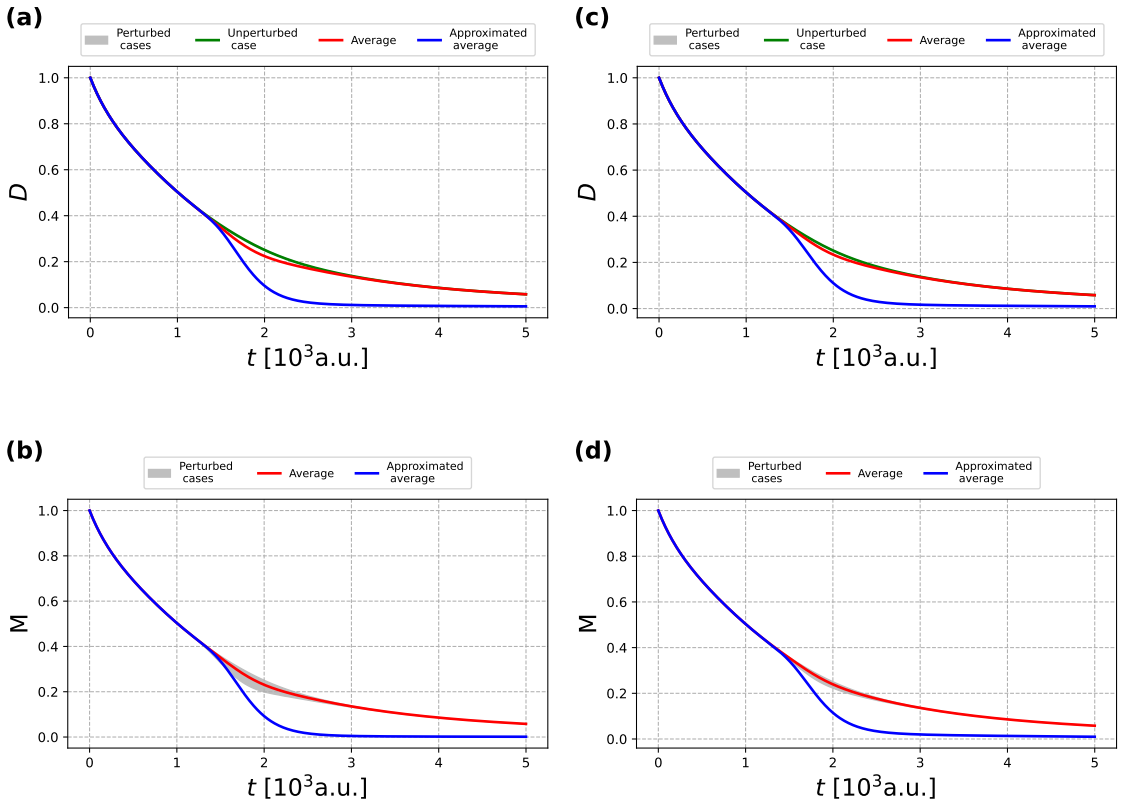

Figure 4.13: The purity and Loschmidt echo for the open single barrier system. Yet again, the randomised location of the barrier does not significantly influence the measures considered.

Both the purity and the Loschmidt echo, shown in Fig. 4.13, are monotonic functions that tend to zero as $t \to +\infty$. This shows that the system, in addition to becoming a strong mixture of quantum states, also loses reversibility during evolution. This tendency is precisely depicted by the echo of the approximated average WDF, where, after the time $t \approx 2 \times 10^3$ [a.u.], the approximation is overdamped, leading to a much faster loss of purity and information. Thus, opening the initially isolated system, the interaction with the environment decreases the purity of the state, simultaneously disallowing for any reversibility within the ensemble, as the grey band narrows for the Loschmidt echo in Figs 4.13b, 4.13d.

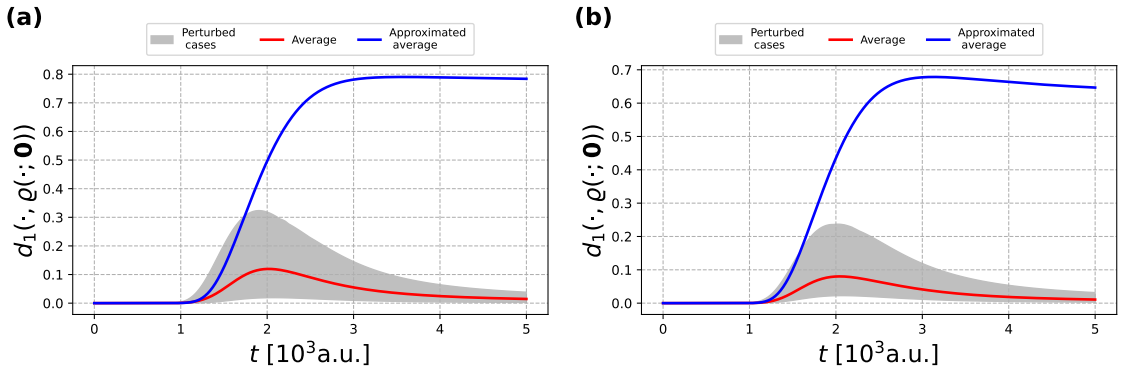

Figure 4.14: The distance between the WDF for the unperturbed potential and each of the following for the open single barrier system: the perturbed WDF, the ensemble average, and the proposed approximation of the average.

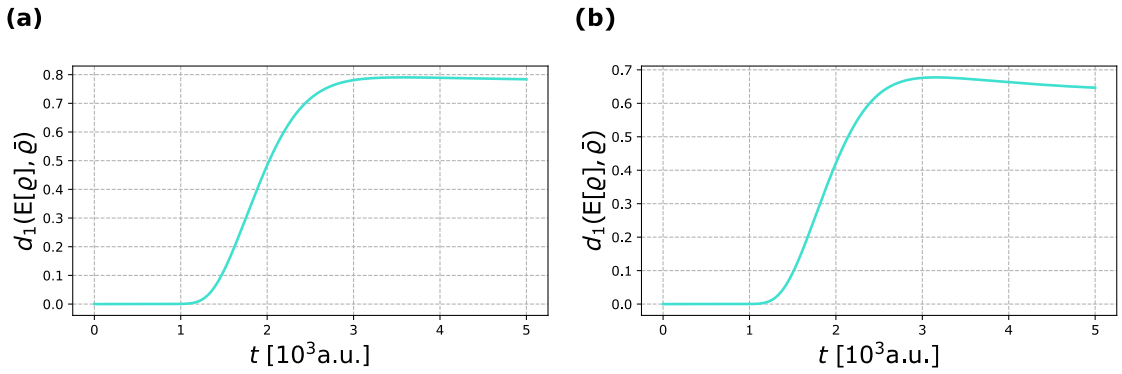

Figure 4.15: The distance between the ensemble average $E[\varrho]$ and proposed approximation $\bar{\varrho}$ in the case of the open single barrier system.

A notable property that occurs after the introduction of environmental effects is the asymptotic behaviour of the distance between the considered WDFs and unperturbed dynamics. From the Fig. 4.14a, we can deduce that this measure also tends to zero, suggesting that in the long time $t \to +\infty$, the final state of the system is similar regardless of the scale of the barrier perturbation and their mean averages to the stationary state. This last implication is straightforward, since the mean of identical states is the same state. However, the same does not apply to the approximation in Fig. 4.15, which converges to some distribution, but one that differs from that of the perturbed system.

4.5.3 Chain of Gaussian barriers with perturbed centres

In this case, the potential has the form

$$V(x;\boldsymbol{\lambda}) = \sum_k V_0 \frac{1}{\sqrt{2\pi}\sigma} e^{-\frac{(x-k\mu-\lambda_k)^2}{2\sigma^2}}, \tag{4.135}$$

where the index k is restricted by the length of the calculation box and μ is the distance between the centres of the barriers. Due to the presence of random perturbations in the positions of the barrier centres, the system loses its displacement symmetry. In other words, the Hamiltonian of the system no longer commutes with the spatial translation operator $\hat{T}_\mu = \exp((-i/\hbar)\mu\hat{p})$, where a is the period of the potentnial, deeming the Bloch approach inapplicable. We shall refer to this system as a structurally disordered system [159, 106, 58]. The natural point of comparison for such systems is the non-perturbed structurally periodic potential $V(x;\mathbf{0})$ that represents a chain of Gaussian barriers. Unlike the previous case, this system cannot be simply interpreted in classical terms, even when $\boldsymbol{\lambda} = \mathbf{0}$, unless the position variable covers the whole real line $x \in \mathbb{R}$. To illustrate where the classical interpretation fails, let us consider the unperturbed potential $V(x;\mathbf{0})$. In this case, the system can indeed be interpreted as a periodic potential, namely a Gaussian chain of barriers, each separated by distance μ. Let x_j denote the position of the j-th barrier centre, that is, $x_j = j\mu$. From the formula above, we compute the derivative with respect to x in order to locate the extrema:

$$\partial_x V(x;\mathbf{0}) = -\frac{V_0}{\sqrt{2\pi}\sigma^3} \sum_k (x-k\mu) e^{-\frac{(x-k\mu)^2}{2\sigma^2}}. \tag{4.136}$$

Substituting $x = x_j = j\mu$, we obtain a nonzero remainder term:

$$\partial_x V(x_j;\mathbf{0}) = -\frac{V_0\mu}{\sqrt{2\pi}\sigma^3} \sum_{k\neq j} (j-k) e^{-\frac{\mu^2(j-k)^2}{2\sigma^2}}, \tag{4.137}$$

where the summand is antisymmetric in j, k and vanishes only for $k \in \mathbb{Z}$. However, in numerical calculations, especially in the perturbed case, the system is restricted to a finite grid, allowing only for a finite number of centres. As a result, antisymmetry is broken, and a nonzero contribution remains. Furthermore, additional extrema may emerge at positions other than integer multiples of μ, depending on the width of the Gaussian barriers. The classical dynamics of this system is therefore more involved, but can still be described qualitatively. It is a combination of bounded motion around fixed points, unbounded motion over the barriers, and semi-bounded motion over smaller barriers up to a higher-energy barrier where reflection occurs. Nevertheless, as the number of barriers increases and the width of each Gaussian increases, this classical description becomes progressively less traceable.

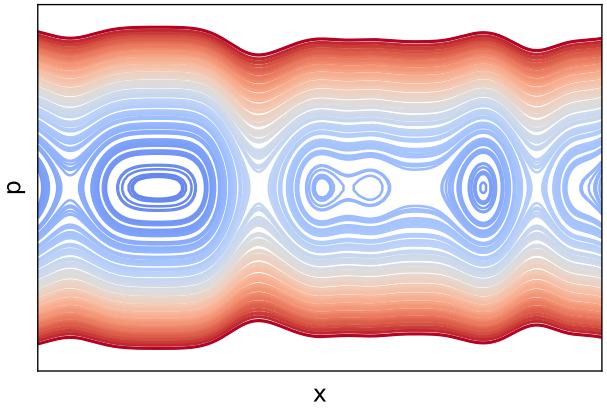

Figure 4.16: An example of a classical flow of a perturbed Gaussian chain. The variety of the types of dynamics is diverse: from bounded motion in local wells (blue-colored closed curves) to unbounded evolution of the classical system (red curves going from far left to far right), existing without any regularity.

Isolated system

For the simulations, we considered an isolated system with the potential defined in Eq. (4.135), using the parameters $V_0 = 0.015$ [a.u.] for the barrier amplitude, $\sigma = \sqrt{50}$ [a.u.] for the barrier width and $\mu = 50 \cdot \Delta x$ [a.u.] for the mean separation. For these parameters, the mean phase-space trajectories of the system and the corresponding averages are shown in Fig. 4.17

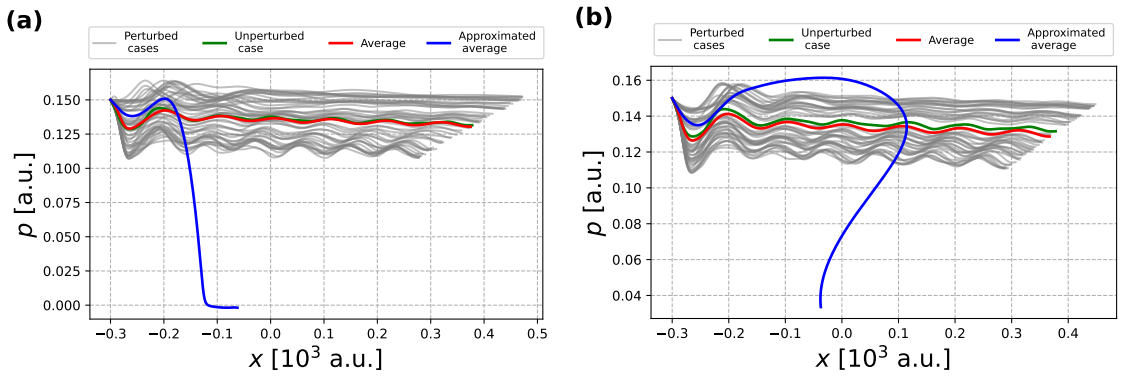

Figure 4.17: The phase-space trajectories of the WDFs for the open system.

We can notice that no closed phase-space trajectories form under time evolution for all the considered cases, where for some cases of $\boldsymbol{\lambda}$, a trajectory is a straight line, regardless of the underlying probability distribution. Additionally, the ensemble average almost precisely follows the dynamics of the unperturbed system. The approximated average of the ensemble is strongly damped, where shortly after the start of the simulation, it loses all of the momentum, jittering around $p \approx 0^{-}$ [a.u.]. To complement this picture, we investigated the statistical parameters of the WDF and their change, which leads to the behaviour displayed in Fig. 4.18.

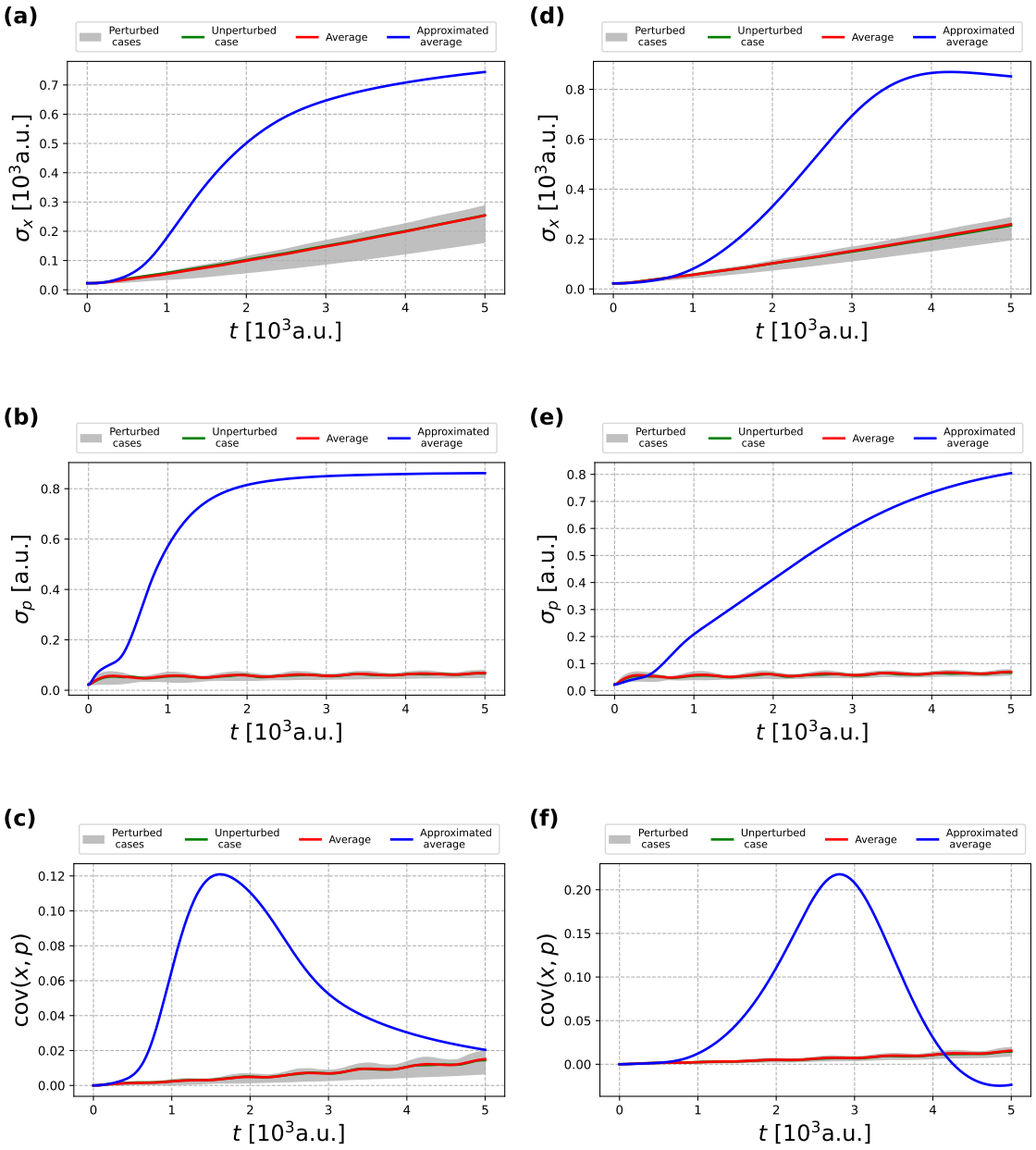

Figure 4.18: The standard deviation and covariance of momentum and position of the WDF for the isolated multiple barrier system.

At first glance, the second centralised moments for the perturbed system and the ensemble average follow almost identical behaviour, with the average resembling the dynamics of the unperturbed system. The grey band is narrow, suggesting that, yet again, the structural disorder of the system does not impact the spread of the WDFs drastically. In contrast, the approximation predicts excessive growth of the moments, which is inconsistent with the isolated ensemble. The structure of the potential can be noticed in the oscillatory character of the ensemble average and in the grey band that represents the elements of the ensemble.

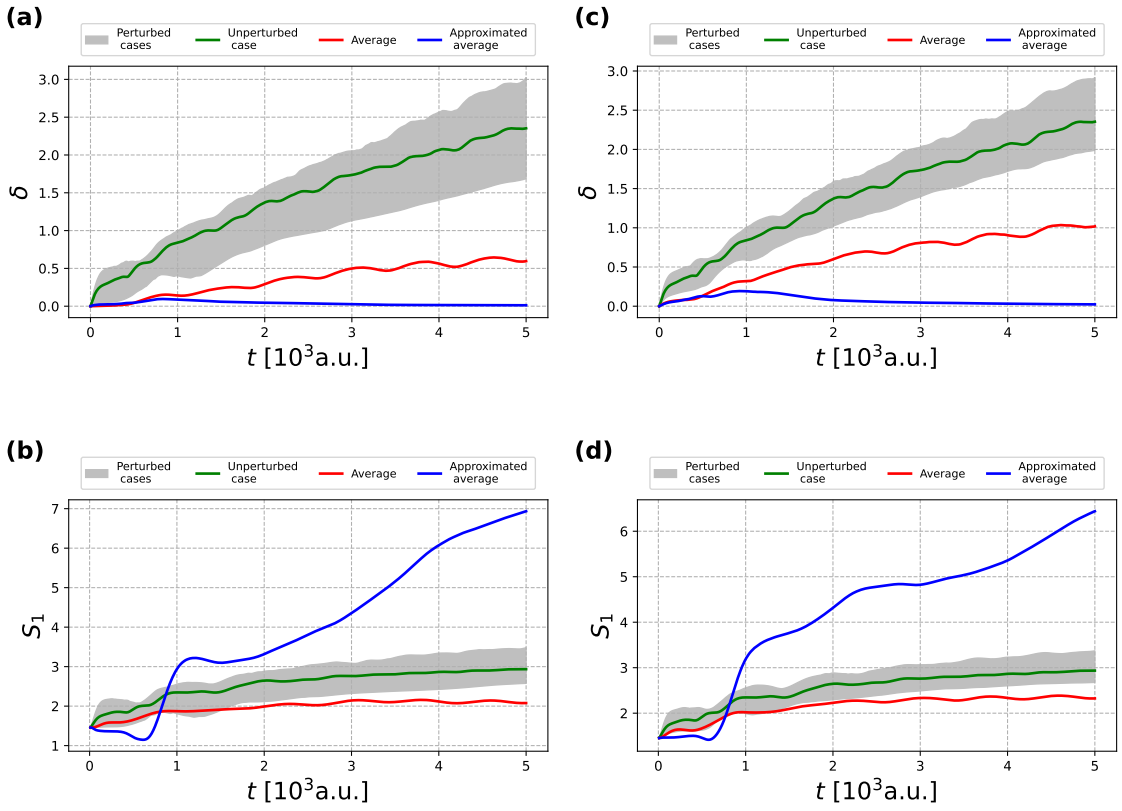

Figure 4.19: The nonclassicality parameter and the Wigner-Shannon entropy of the isolated multiple barrier system.

In the isolated case, the nonclassicality parameter increases with time, while the Wigner-Shannon entropy increases modestly, as seen in Fig. 4.19. This reflects the persistence of the interference patterns within the system when there are no environmental effects present. The values of the parameters for each perturbed system stay relatively close to those for the WDF of the unperturbed system. However, the introduction of multiple barriers reduces the effectiveness of ensemble averaging, as the parameters for the averaged WDF lie below the values for the unperturbed case, indicating that more samples should be considered for such systems. Although the parameters for the ensemble average display a similar but weaker behaviour, the approximated average overshoots the entropy values and overdamps the interference within the system. This is especially visible in the nonclassicality parameter, Figs 4.19a, 4.19c, where shortly after the beginning of the evolution, the system ends up in a positive state with nonclassicality equal to 0. Of course, this

is unsurprising, as the decoherence term appears in the evolution equation for the approximated Wigner function.

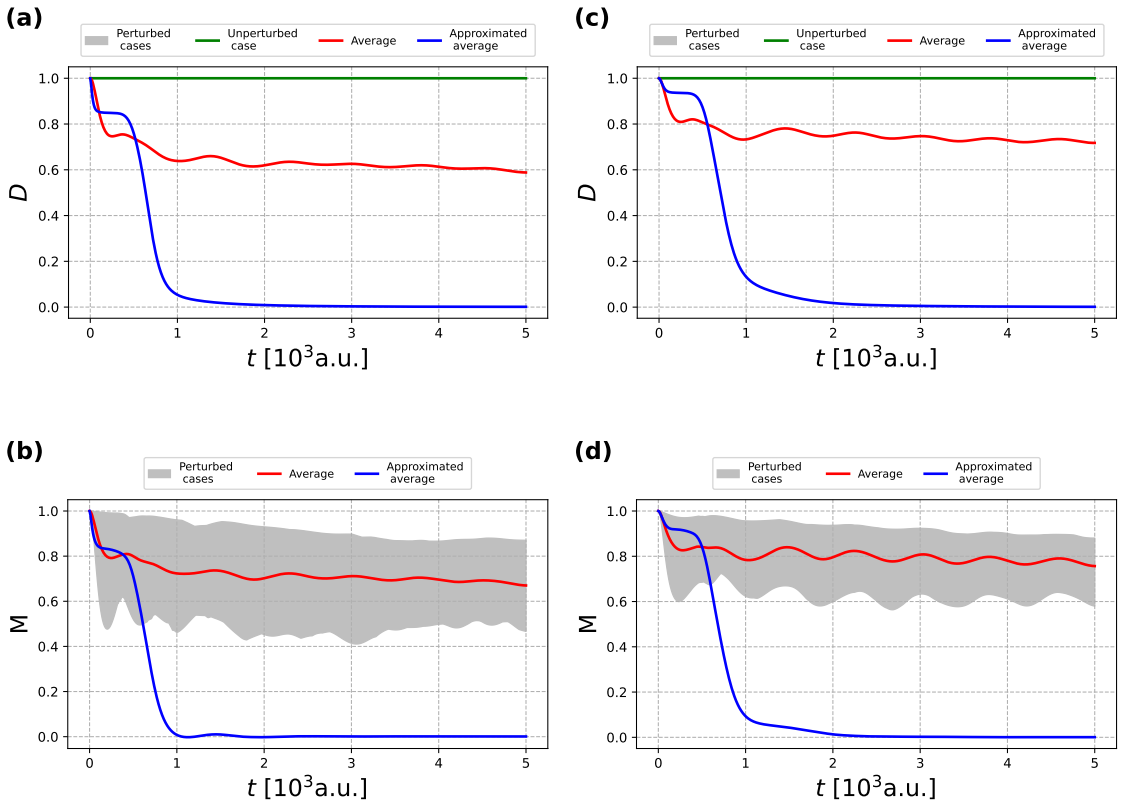

Figure 4.20: The purity and the Loschmidt echo for the isolated multiple barrier system.

The purity of the system remains the same for both perturbed and unperturbed evolutions, in Figs 4.20a, 4.20c, confirming that static disorder alone does not induce mixing. Due to the dephasing between each realisation, the purity of the ensemble average is lower than 1. However, it appears to tend to a constant in a long time limit with vanishing oscillations around it, which suggests a consistent mixture throughout the rest of the evolution. In contrast, the approximation overestimates the drop in purity, leading to a perfect mixture in a finite time. Moreover, we are unable to notice the narrow grey band in the case of the Loschmidt echo, in Figs. 4.20b, 4.20d, as was present in the single-barrier systems. It suggests a strong susceptibility of the system to perturbation. Based on the dual interpretation of the Loschmidt echo, we can also say that the system loses the dynamical invertibility property, but only to some extent, as it does not tend to 0. However, as it also measures the overlap between each realisation and the unperturbed WDF, we can say that the disorder within the initially periodic potential greatly influences the state of the system, which will be emphasised in the subsequent figures. To further investigate the system, we now consider the distance measures in Figs 4.21 and 4.22.

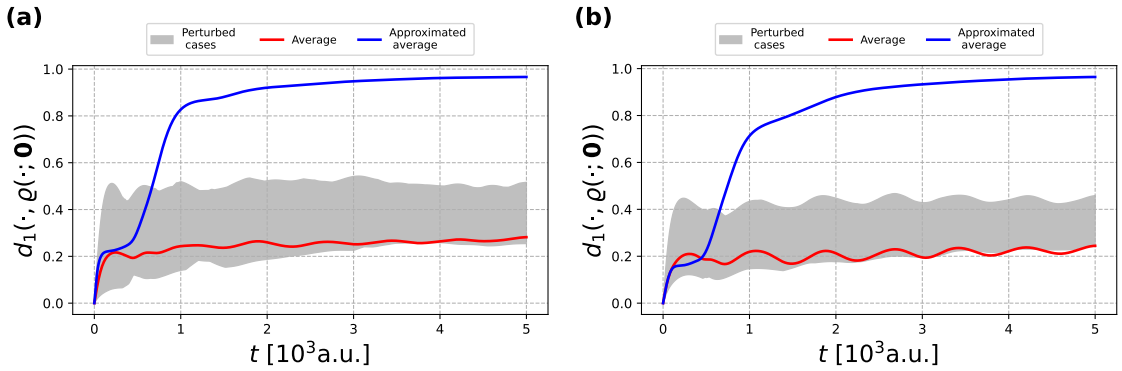

Figure 4.21: The distance between the WDF for the unperturbed potential and each of the following for the isolated multiple barrier system: the perturbed WDF, the ensemble average, and the proposed approximation of the average.

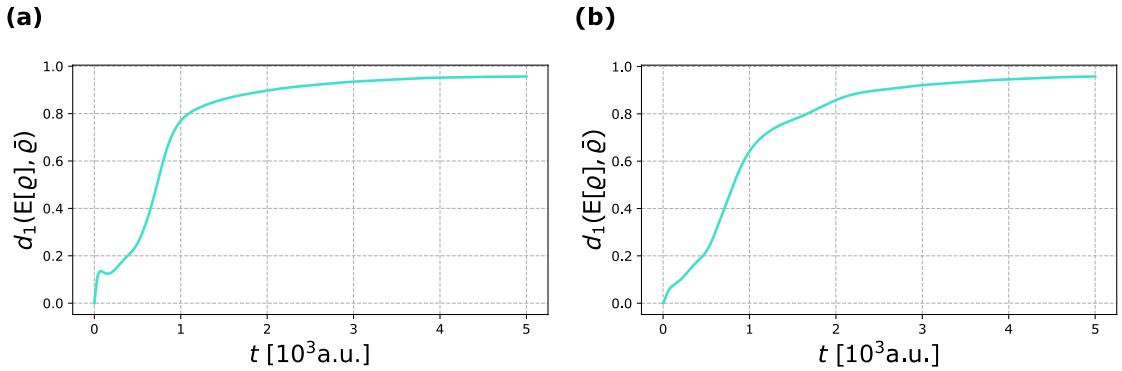

Figure 4.22: The distance between the ensemble average $E[\varrho]$ and proposed approximation $\bar{\varrho}$ in the case of the isolated multiple barrier system.

In the barrier chain case, the distance measure from the unperturbed case forms a nearly constant-width band from perturbed realisations. Each realisation of the system stays within a certain distance from the unperturbed WDF throughout the evolution period and does not tend, as $t \to +\infty$, to a common final state. Disorder alone does not diverge trajectories in the phase space of initially structurally symmetric systems. The ensemble average is confined within this band, however, in all cases, the distance remains strictly positive $d_1 > 0$. This indicates that, in terms of the L^2-norm, both functions differ regardless of the underlying probability distribution of the random vector $\boldsymbol{\lambda}$. However, the ensemble average stays closest to the unperturbed WDF. By contrast, the blue line representing the distance between the approximated average and the unperturbed WDF rapidly increases towards unity, meaning that it is nearly orthogonal to the unperturbed WDF. This contradictory divergence is clearly visible in Fig. 4.22. Therefore, the approximation does not track the ensemble but instead provides a bound on possible decoherence effects.

Open system

Like in previous cases, we start with the phase-space trajectories of the system, displayed in Fig. 4.23.

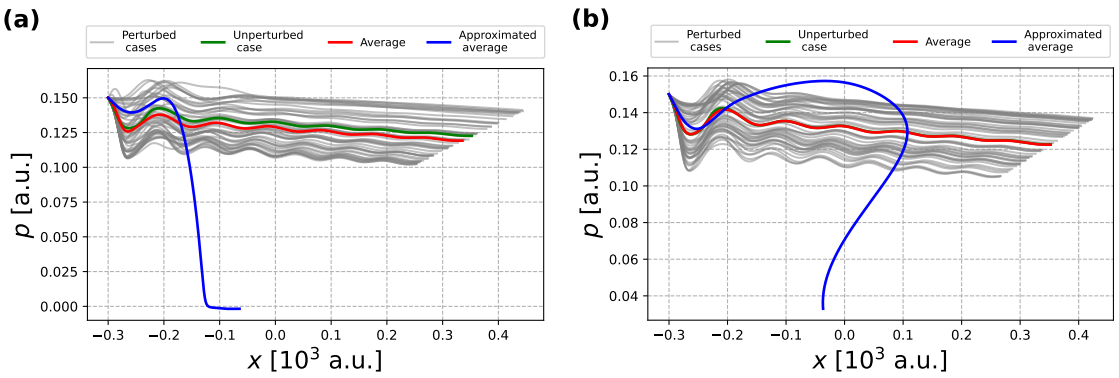

Figure 4.23: The phase-space trajectories of the WDFs for the open system.

Judging by the type of phase-space trajectories, we can state that there are no premises for the closed trajectory within the system. By including the environmental effects, we can notice the gradual decrease of the average momentum value for all functions considered, which was also present in the case of the open single-barrier system 4.10. Moreover, there is a visible decrease in the oscillatory character of the phase-space trajectory compared to the isolated system 4.17. The phase-space trajectory for the average of the ensemble WDF traces the unperturbed dynamics, while its approximation also depicts the worst-case scenario of the damping of the system. We complement the discussion of the statistical parameters for the WDF by considering the centralised second moments, as done previously. Those are shown in the Fig. 4.24.

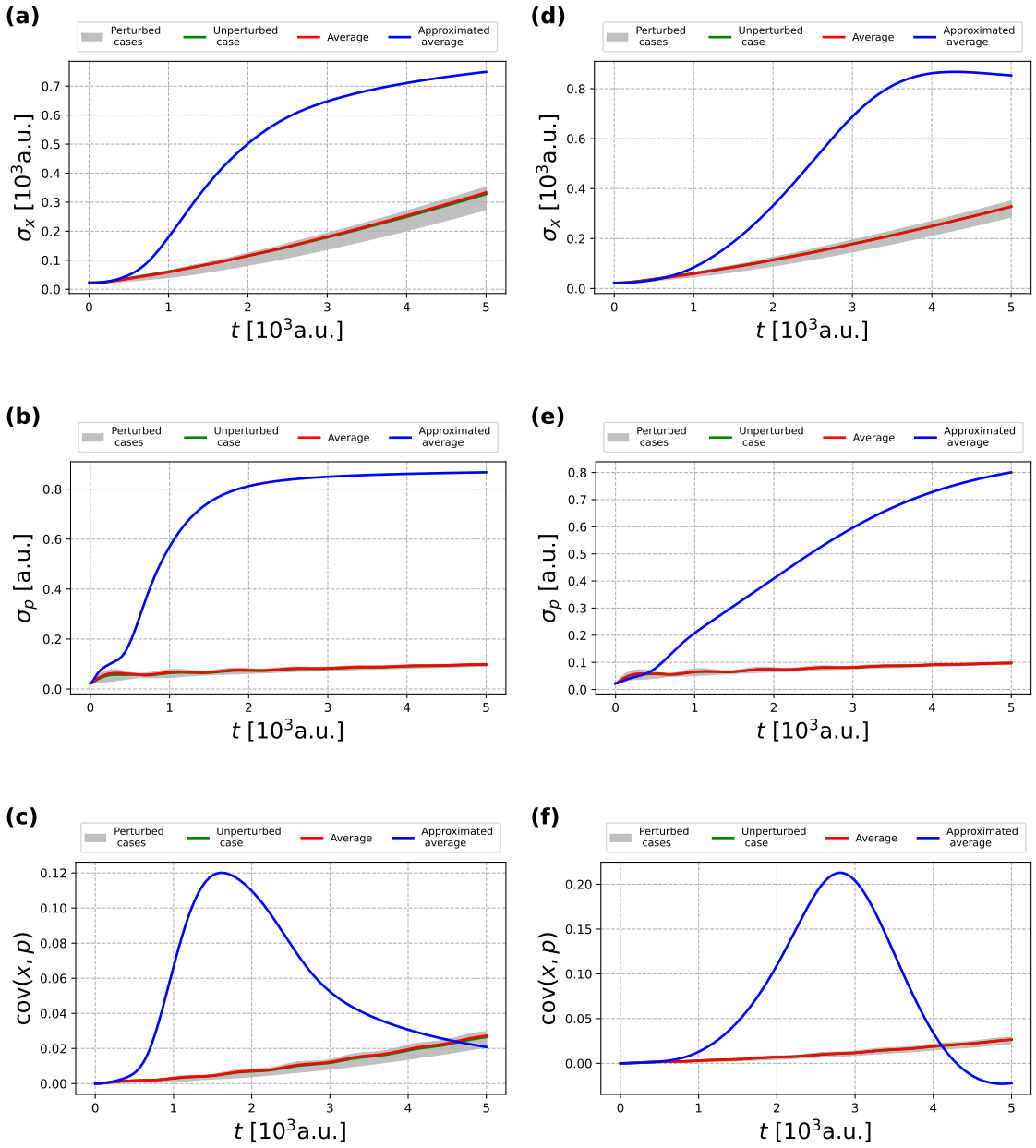

Figure 4.24: The standard deviation and covariance of momentum and position of the WDF for the open multiple barrier system.

In addition to the prior discussion, the bandwidth depicting the influence of the disorder of the system is greatly reduced, suggesting that no significant spreading of the position and momentum between the realisations takes place. This narrowing of the grey band results from the interaction with the environment and was not visible in the case of the single-barrier system. However, this effect might result from the choice of the potential rather than the interaction with the environment. Moreover, the σ_p is nearly constant. Additionally, the average Wigner distribution's statistical parameters are closer to the unperturbed dynamics, whilst the approximation does not resemble the behaviour of the real system, but still is held within the system's bounds.

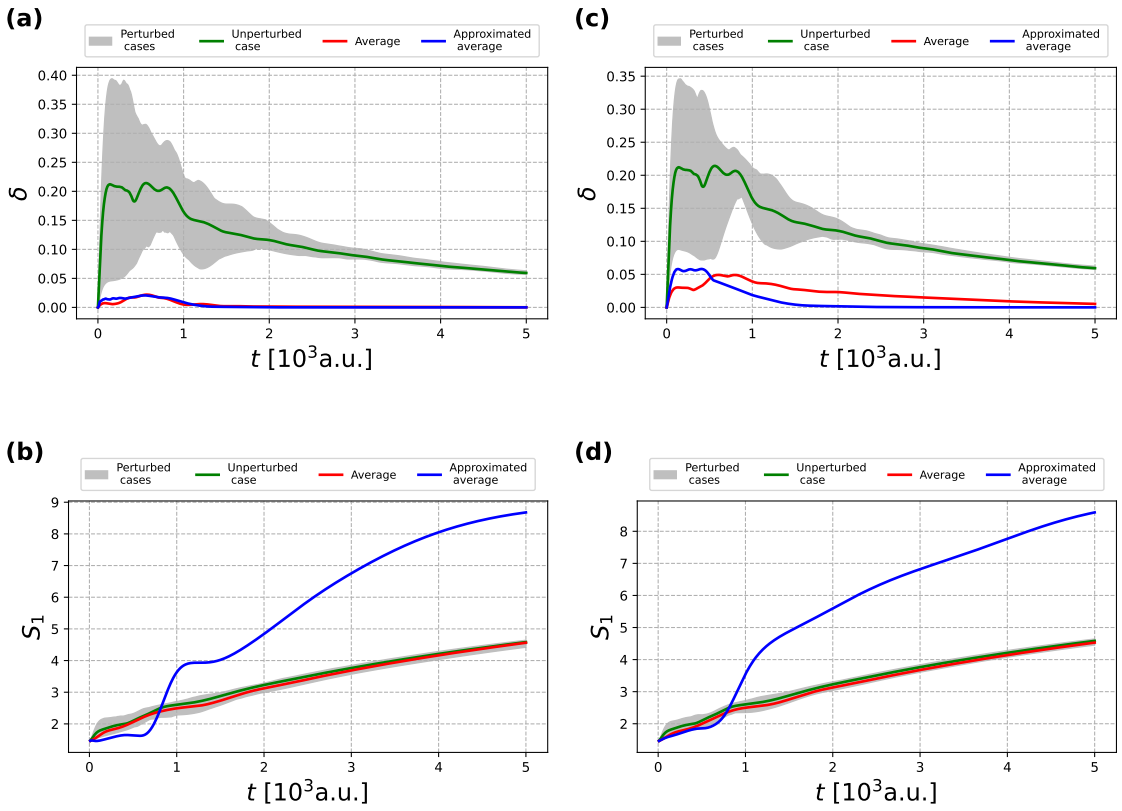

Figure 4.25: The nonclassicality parameter and the Wigner-Shannon entropy of the open multiple barrier system.

The introduction of environmental effects drastically changes the behaviour of nonclassicality parameter and Wigner-Shannon entropy. Let us start by noticing that the grey band formed by the values of the nonclassicality and Wigner-Shannon entropy from all considered realisations is becoming narrower during the time evolution. Both measures are monotone after the initial evolution: the nonclassicality is strictly decreasing towards some unknown constant while the Wigner-Shannon entropy increases. Moreover, the nonclassicality of the ensemble-averaged WDF is drastically lower than the nonclassicality of each realisation of the system. In contrast, the Wigner–Shannon entropy of the averaged WDF closely follows the values for the unperturbed case. This behaviour is clearly different from that observed in the isolated system, where both measures underperformed. Yet again, it confirms that the environment influences the spread of informa-

tion between the realisations of the system, as in the case of the single-barrier open system 4.12b, 4.12d. Surprisingly, the nonclassicality parameter of the approximated ensemble average is strictly closer to the ensemble average value but still overdamps the value. However, the entropy production is still higher in the approximated case, especially in the long-time limit.

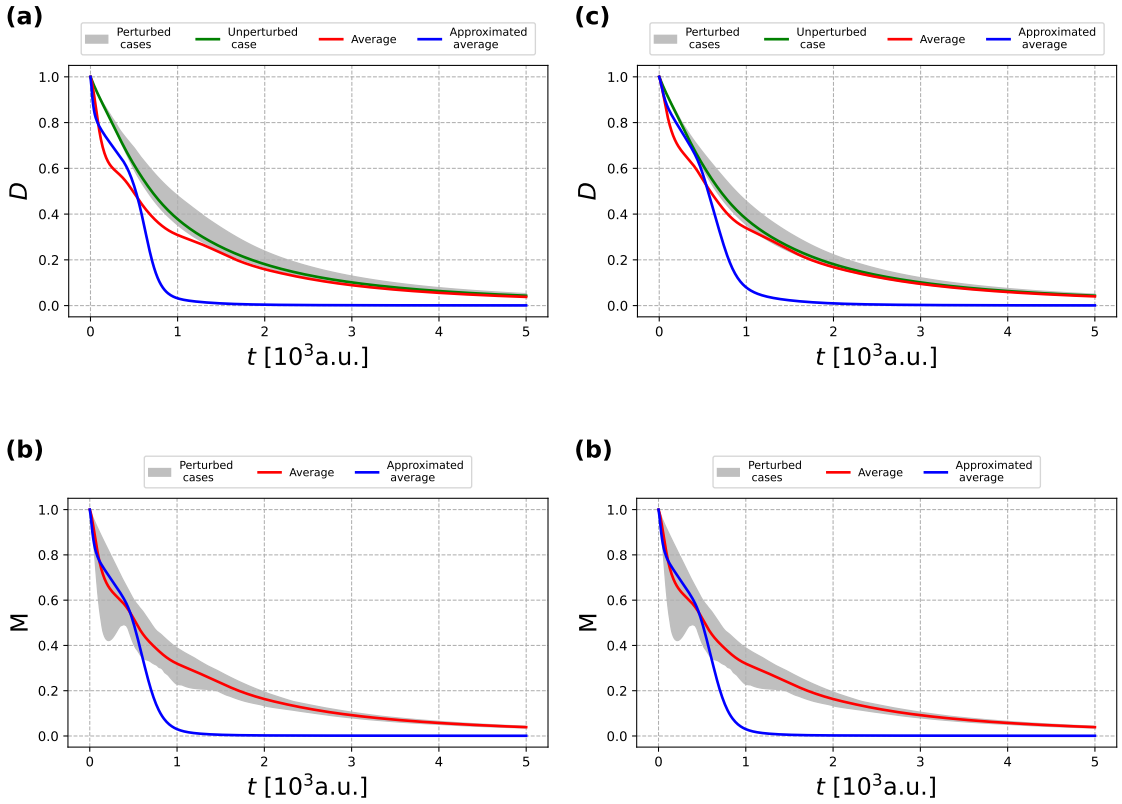

Figure 4.26: The purity and the Loschmidt echo for the open multiple barrier system.

Both the purity and the Loschmidt echo decrease, reflecting the expected loss of coherence, tending to 0 for both measures. Thus, as time progresses, the system becomes a perfect mixture of states. The echo of the ensemble average WDF is kept within the grey band of the realisations of the ensemble. However, for purity, it underestimates the initial values, so that later during the evolution, it aligns with the green line. The approximation yields a significantly faster decay, consistently underestimating both quantities. In contrast to the isolated case, the purity of the system does not form a narrow band. Instead, a dependence on the realisation of the system is observed. Complementarily, the echo of the system forms a narrower band in the case of the open system. This behaviour confirms that static disorder and decoherence perturb the purity and reversibility of the dynamics, while the lack of environmental effects preserves purity and allows for some degree of reversibility within the system. However, as evolution progresses, the interaction with the environment results in a decreased spread between each component of the ensemble.

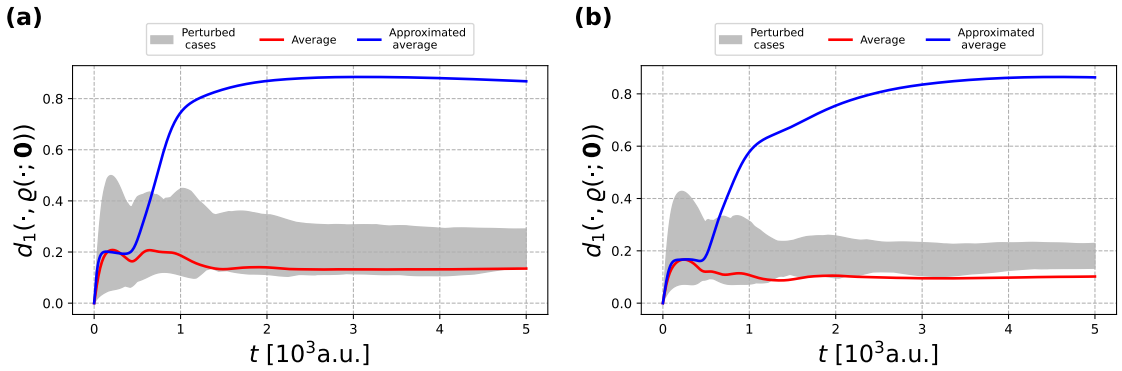

Figure 4.27: The distance between the WDF for the unperturbed potential and each of the following for the open multiple barrier system: the perturbed WDF, the ensemble average, and the proposed approximation of the average.

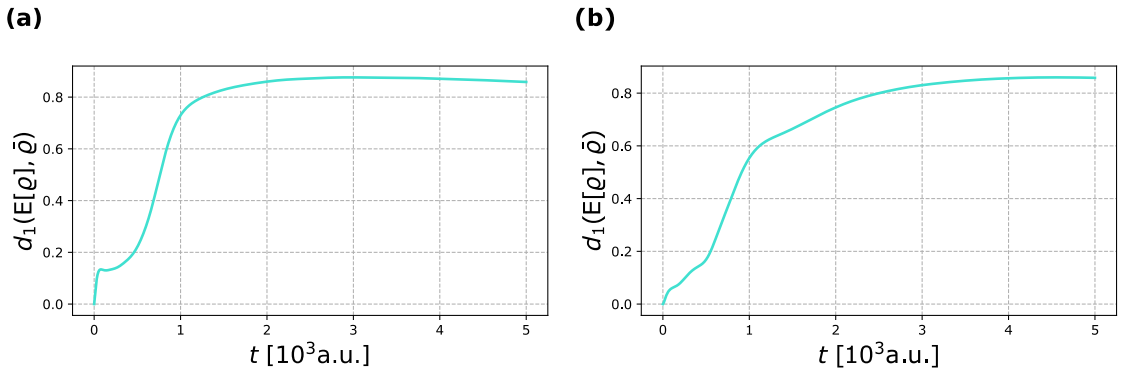

Figure 4.28: The distance between the ensemble average $E[\varrho]$ and proposed approximation $\bar{\varrho}$ in the case of the open multiple barrier system.

Ensemble averages remain close to the unperturbed state, while the approximation diverges. The growth and saturation of distances involving the approximation confirm that it overestimates the effect of disorder, irrespective of its distribution. The small separations among realisations and the ensemble average highlight the limited role of disorder in modifying the dynamics.

4.5.4 Discussion of numerical results

Comparisons of considered measures across Gaussian and uniform disorder reveal qualitatively similar behaviour for isolated and open quantum systems. Starting with the single-barrier system, we noticed that the phase-space trajectories, as well as the second moments, do not differ between the isolated and the open system for a weakly interacting environment. By Eq. (4.119), the difference in the phase-space trajectories is visible in the asymptotic region, where away from the potential barrier we can assume $\langle \partial_x V(x;\boldsymbol{\lambda})\rangle \approx 0$. Then, the solutions to the respective ODEs can be presented as follows: for the isolated system

$$\begin{aligned} \langle x\rangle(t) &= \frac{p_{as}}{m}t + x_{as}, \\ \langle p\rangle(t) &= p_{as}, \end{aligned} \tag{4.138}$$

and the open system

$$\begin{aligned} \langle x\rangle(t) &= e^{-\Gamma_x t}x_{as} + \frac{p_{as}}{m(\Gamma_x-\Gamma_p)}e^{(\Gamma_x-\Gamma_p)t}, \\ \langle p\rangle(t) &= p_{as}e^{-\Gamma_p t}. \end{aligned} \tag{4.139}$$

This leads to the conclusion that if $\Gamma_p > 0$ then $p(t) \to 0$, as $t \to +\infty$. This decreasing tendency of $p(t)$ is already visible in Fig. 4.10 for the evolution of an open system, due to the scale of Γ_p chosen for the simulations. Most importantly, however, the average momentum should be constant as time approaches infinity, while in the case of the open system, it should decrease towards 0, unless $\Gamma_p = 0$.

In the case of second moments, the asymptotic equations of Eq. (4.120) yield

$$\begin{aligned} \sigma_x^2(t) &= \frac{1}{m^2}\sigma_{p_{as}}^2 t^2 + \frac{2}{m}\mathrm{cov}_{as}(x,p)t + \sigma_{x_{as}}^2 \\ \sigma_p^2(t) &= \sigma_{p_{as}}^2, \\ \mathrm{cov}(x,p)(t) &= \frac{1}{m}\sigma_{p_{as}}^2 + \mathrm{cov}_{as}(x,p). \end{aligned} \tag{4.140}$$

while the solution to the system for the open system is given by

$$\begin{bmatrix} \sigma_x^2(t) \\ \sigma_p^2(t) \\ \mathrm{cov}(x,p)(t) \end{bmatrix} = e^{t\mathbb{M}} \begin{bmatrix} \sigma_{x_{as}}^2 \\ \sigma_{p_{as}}^2 \\ \mathrm{cov}_{as}(x,p) \end{bmatrix} + \int_0^t e^{(t-s)\mathbb{M}} \begin{bmatrix} D_{pp} \\ D_{xx} \\ -D_{xp} \end{bmatrix} ds, \tag{4.141}$$

where

$$\mathbb{M} = \begin{bmatrix} e^{-2t\Gamma_x} & \frac{1}{m^2(\Gamma_p-\Gamma_x)^2}\left(e^{-\Gamma_x t}-e^{-\Gamma_p t}\right)^2 & \frac{2e^{-\Gamma_x t}}{m(\Gamma_p-\Gamma_x)}\left(e^{-\Gamma_x t}-e^{\Gamma_p t}\right) \\ 0 & e^{-2\Gamma_p t} & 0 \\ 0 & \frac{e^{-t\Gamma_p}}{m(\Gamma_p-\Gamma_x)}\left(e^{-t\Gamma_x}-e^{-t\Gamma_p}\right) & e^{-t(\Gamma_x+\Gamma_p)} \end{bmatrix}, \tag{4.142}$$

where the matrix form was used for convenience. Taking the limit $t \to +\infty$ we see that the isolated system's x-standard deviation and covariance tend to infinity while σ_p^2 is constant. On the contrary, the same limit applied to the parameters of the open system gives

$$\begin{bmatrix} \sigma_{x_{as}}^2 \\ \sigma_{p_{as}}^2 \\ \mathrm{cov}_{as}(x,p) \end{bmatrix} = \begin{bmatrix} \frac{1}{2\Gamma_x} & \frac{1}{2m^2\Gamma_x\Gamma_p(\Gamma_x+\Gamma_p)} & \frac{1}{m(\Gamma_x+\Gamma_p)\Gamma_x} \\ 0 & \frac{1}{2\Gamma_p} & 0 \\ 0 & \frac{1}{2m(\Gamma_x+\Gamma_p)\Gamma_p} & \frac{1}{\Gamma_x+\Gamma_p} \end{bmatrix} \begin{bmatrix} D_{pp} \\ D_{xx} \\ -D_{xp} \end{bmatrix}, \tag{4.143}$$

keeping the asymptotic values of the second moments finite.

Unfortunately, similar asymptotic approximations cannot be applied to the case of the chain of Gaussian barriers because the potential is no longer vanishing at infinity. This would imply that $\langle \partial_x V(x;\boldsymbol{\lambda})\rangle \neq 0$. We shall, however, approximate the function in the following manner: let $\partial_x V(x) = F(x)$ and define $\delta = x - \langle x\rangle$. Assuming F is smooth, we can expand it in the Taylor series around the mean $\langle x\rangle$

$$F(x) = F(\delta + \langle x\rangle) \approx F(\langle x\rangle) + \frac{\mathrm{d}}{\mathrm{d}x}F(\langle x\rangle)\delta + \frac{1}{2!}\frac{\mathrm{d}^2}{\mathrm{d}x^2}F(\langle x\rangle)\delta^2 + O(\delta^3), \tag{4.144}$$

assuming $\langle\delta\rangle = 0$. Averaging this equality gives

$$\langle F(x)\rangle = \langle V(x)\rangle \approx F(\langle x\rangle) + \frac{1}{2!}\frac{\mathrm{d}^2}{\mathrm{d}x^2}F(\langle x\rangle)\left\langle (x-\langle x\rangle)^2\right\rangle. \tag{4.145}$$

Omitting further terms, we see that the last term is the square of the standard deviation of position, and thus the average momentum is coupled with second moments. The total system of equations reads

$$\begin{cases} \partial_t \langle x\rangle = \dfrac{1}{m}\langle p\rangle - \Gamma_x \langle x\rangle, \\ \partial_t \langle p\rangle = -\partial_x V(\langle x\rangle;\boldsymbol{\lambda}) - \dfrac{1}{2!}\partial^3_{xxx}V(\langle x\rangle;\boldsymbol{\lambda})\sigma_x^2 - \Gamma_p\langle p\rangle, \\ \partial_t\sigma_x^2 = \dfrac{2}{m}\mathrm{cov}(x,p) - 2\Gamma_x\sigma_x^2 + D_{pp}, \\ \partial_t\sigma_p^2 = -2\mathrm{cov}(p,\partial_x V(x;\boldsymbol{\lambda})) - 2\Gamma_p\sigma_p^2 + D_{xx}, \\ \partial_t\mathrm{cov}(x,p) = \dfrac{1}{m}\sigma_p^2 - \mathrm{cov}(x,\partial_x V(x;\boldsymbol{\lambda})) - (\Gamma_x+\Gamma_p)\mathrm{cov}(x,p) - D_{xp}. \end{cases} \tag{4.146}$$

We shall do the same approximation in the case of terms: $\mathrm{cov}(x,\partial_x V(x;\boldsymbol{\lambda}))$, $\mathrm{cov}(p,\partial_x V(x;\boldsymbol{\lambda}))$. Applying previous calculations to the first expression yields $\mathrm{cov}(x,\partial_x V(x;\boldsymbol{\lambda})) \approx \partial^2_{xx}V(\langle x\rangle;\boldsymbol{\lambda})\sigma_x^2$ and $\mathrm{cov}(p,\partial_x V(x;\boldsymbol{\lambda})) \approx \partial_{xx}V(\langle x\rangle;\boldsymbol{\lambda})\mathrm{cov}(x,p)$. Substituting those expressions into the system of ODEs, we arrive at the following system of coupled equations

$$\begin{cases} \partial_t \langle x\rangle = \dfrac{1}{m}\langle p\rangle - \Gamma_x \langle x\rangle, \\ \partial_t \langle p\rangle = -\partial_x V(\langle x\rangle;\boldsymbol{\lambda}) - \dfrac{1}{2!}\partial^3_{xxx}V(\langle x\rangle;\boldsymbol{\lambda})\sigma_x^2 - \Gamma_p\langle p\rangle, \\ \partial_t\sigma_x^2 = \dfrac{2}{m}\mathrm{cov}(x,p) - 2\Gamma_x\sigma_x^2 + D_{pp}, \\ \partial_t\sigma_p^2 = -2\partial^2_{xx}V(\langle x\rangle;\boldsymbol{\lambda})\sigma_p^2 - 2\Gamma_p\sigma_p^2 + D_{xx}, \\ \partial_t\mathrm{cov}(x,p) = \dfrac{1}{m}\sigma_p^2 - \partial^2_{xx}V(\langle x\rangle;\boldsymbol{\lambda})\sigma_x^2 - (\Gamma_x+\Gamma_p)\mathrm{cov}(x,p) - D_{xp}. \end{cases} \tag{4.147}$$

For further simplification, the values of parameters Γ_x, D_{pp} and D_{xp} are fixed corresponding to the simulations performed, leading to the following equations

$$\begin{cases} \partial_t \langle x\rangle = \dfrac{1}{m}\langle p\rangle, \\ \partial_t \langle p\rangle = -\partial_x V(\langle x\rangle;\boldsymbol{\lambda}) - \dfrac{1}{2!}\partial^3_{xxx}V(\langle x\rangle;\boldsymbol{\lambda})\sigma_x^2 - \Gamma_p\langle p\rangle, \\ \partial_t\sigma_x^2 = \dfrac{2}{m}\mathrm{cov}(x,p), \\ \partial_t\sigma_p^2 = -2\partial^2_{xx}V(\langle x\rangle;\boldsymbol{\lambda})\sigma_p^2 - 2\Gamma_p\sigma_p^2 + D_{xx}, \\ \partial_t\mathrm{cov}(x,p) = \dfrac{1}{m}\sigma_p^2 - \partial^2_{xx}V(\langle x\rangle;\boldsymbol{\lambda})\sigma_x^2 - \Gamma_p\mathrm{cov}(x,p). \end{cases} \tag{4.148}$$

We notice that in the lowest order of approximation, the system strongly depends on the form of the potential $V(x;\boldsymbol{\lambda})$. The most standard approach, assuming that V can be treated locally as a harmonic potential drops the information about the coupling between the momentum average and standard deviation of position. From this system, we can identify the stationary points of the phase-space trajectories, that is, by assuming that the LHS is equal to zero. The solution to the stationary problem is given by the following 5-tuple

$$(\langle x\rangle, \langle p\rangle, \sigma_x^2, \sigma_p^2, \mathrm{cov}(x,p))_{stationary} = (\langle x\rangle_0, 0, \sigma_{x_0}^2, \sigma_{p_0}^2, 0), \tag{4.149}$$

where $\langle x\rangle_0$, $\sigma_{x_0}^2$, $\sigma_{p_0}^2$ are solutions, provided they exist, to the following algebraic equations

$$\begin{aligned}
&\langle x\rangle_0 : \partial_x(\partial_x V)^2(\langle x\rangle_0;\boldsymbol{\lambda}))(\partial_{xx}^2 V(\langle x\rangle_0;\boldsymbol{\lambda}) + \Gamma_p) = \frac{D_{xx}}{2m}\partial_{xxx}^3 V(\langle x\rangle_0;\boldsymbol{\lambda}),\\
&\sigma_{x_0}^2 : \sigma_{x_0}^2 = 2\frac{\partial_x V(\langle x\rangle_0;\boldsymbol{\lambda})}{\partial_{xxx}^3 V(\langle x\rangle_0;\boldsymbol{\lambda})},\\
&\sigma_{p_0}^2 : \sigma_{p_0}^2 = m\frac{\partial_x(\partial_x V)^2(\langle x\rangle_0;\boldsymbol{\lambda}))}{\partial_{xxx}^3 V(\langle x\rangle_0;\boldsymbol{\lambda})}.
\end{aligned} \tag{4.150}$$

First of all, we shall start with the fact that it is not necessary to consider the case of the isolated system separately, since substituting $\Gamma_p = D_{xx} = 0$ leads to the equivalent system of equations. The existence of the solution to the first equation gives us qualitative insight into the dynamics of the system around the stationary point. It is especially important due to the Grobman-Hartman theorem [8], which states that the dynamics of the linearised system around a stationary point is the same as that of the original system. Knowing that $\langle p\rangle_0 = 0$ is the coordinate of the stationary point, it would imply that the system might be approaching the average momentum equal to 0 or diverge from it. In the case of the isolated system, we see that the first or second derivative of the potential vanishes at the stationary mean position, which means that $\langle x\rangle_0$ is simply an extremum or an inflection point. In this case, $\sigma_{p_0}^2 = 0$ and $\sigma_{x_0}^2 < +\infty$. However, the existence of the stationary point does not mean that the whole dynamics of the system is dependent upon it, as the Grobman-Hartman theorem works only locally. As can be seen in the phase-space trajectories of the system of chain of barriers 4.17, the isolated system's average momentum is not approaching 0, and neither its average position approaches a finite value. The dynamic is visibly unbounded. However, in the case of the open system, where $\Gamma_p, D_{xx} > 0$, the first of the equations (4.150) may produce the stationary point, depending on the parameters of the potential and the environment. By Fig. 4.23, we suspect that this system has a unique solution, associated with the parameters of the stationary state of the equation of motion, as by the remark that the nonclassicality, in Figs. 4.25a, 4.25c, tends to 0 as $t \to +\infty$, and by Hudson's theorem [91] we expect the final state to be of the type of Gaussian distribution or a positive mixed state with parameters given by the stationary points.

Continuing with the evolution of the state, let us answer the question of how the introduction of the environment changes the positivity of the WDF. By the definition of the nonclassicality parameter, we can investigate its time derivative

$$\frac{\mathrm{d}}{\mathrm{d}t}\delta(t) = \int_{\mathbb{R}^2} \partial_t \left|\varrho(x,p,t;\boldsymbol{\lambda})\right| dxdp. \tag{4.151}$$

Using the fact that, in the distributional sense, $\partial_t|\varrho| = \mathrm{sgn}(\varrho)\partial_t\varrho$, we can write

$$\frac{\mathrm{d}}{\mathrm{d}t}\delta(t) = \int_{\mathbb{R}^2} \delta(\varrho(x,p,t;\boldsymbol{\lambda}))\partial_t\varrho(x,p,t;\boldsymbol{\lambda})dxdp, \tag{4.152}$$

where the delta under the integral is the Dirac delta composed with a Wigner function. For the next step, we substituted for the time derivative the form of the equation of motion (4.31), and used the Dirac delta, interpreted as the simple layer integral [153]

$$\int_{\mathbb{R}^2} \delta(u(x,p))\varphi(x,p)dxdp := \int_{\Sigma} \frac{\varphi(x,p)}{|\nabla u(x,p)|} d\Sigma, \tag{4.153}$$

together with its derivative with respect to the composed function, that is

$$\begin{aligned}\int_{\mathbb{R}^2} \frac{\mathrm{d}}{\mathrm{d}u}[\delta(u(x,p))]\varphi(x,p)dxdp = -\int_{\mathbb{R}^2} \delta(u(x,p)) \Bigg[\frac{\nabla\varphi(x,p)\circ\nabla u(x,p)}{|\nabla u(x,p)|^2} \\ -\varphi(x,p)\frac{\nabla|\nabla u(x,p)|\circ\nabla u(x,p)}{|\nabla u(x,p)|^3}\Bigg] dxdp,\end{aligned} \tag{4.154}$$

where $\Sigma = \{(x,p):\ u(x,p)=0\}$ is the level set of the function $u(x,p)$, and $\varphi \in C_0^\infty(\mathbb{R}^2)$. Performing a few cumbersome manipulations, we arrive at the following expression

$$\begin{aligned}\frac{\mathrm{d}}{\mathrm{d}t}\delta(t) = 2\int_{\mathbb{R}^2} \delta(\varrho(x,p,t;\boldsymbol{\lambda})) \sum_{k=0}^{+\infty} \frac{(-1)^k}{(2k+1)!}\left(\frac{\hbar}{2}\right)^{2k} \partial_x^{2k+1}[V(x;\boldsymbol{\lambda})]\partial_p^{2k}[\varrho(x,p,t;\boldsymbol{\lambda})]\partial_p\varrho(x,p,t;\boldsymbol{\lambda})dxdp \\ -\int_{\mathbb{R}^2} \delta(\varrho(x,p,t;\boldsymbol{\lambda}))\nabla\varrho(x,p,t;\boldsymbol{\lambda})^T\mathbb{D}\nabla\varrho(x,p,t;\boldsymbol{\lambda})dxdp,\end{aligned} \tag{4.155}$$

where

$$\mathbb{D} = \begin{bmatrix} D_{pp} & -D_{xp} \\ -D_{xp} & D_{xx}\end{bmatrix}. \tag{4.156}$$

As we can observe, the time evolution of the nonclassicality parameter is strictly linked to the appearance of negative regions of the Wigner function. The first term on the right-hand side of Eq. (4.155) corresponds to isolated dynamics and arises solely from the potential. In particular, if the potential $V(x;\boldsymbol{\lambda})$ is a polynomial of at most second order, the nonclassicality parameter in isolated systems remains constant. This is consistent with the results we have presented in [185]. Furthermore, the first derivative of the potential does not affect the time evolution of the nonclassicality parameter. In general, the only difference between the evolution of the nonclassicality parameter of isolated and open quantum systems lies in the presence of the matrix $\mathbb{D}$ and the form of $\varrho(x,p,t;\boldsymbol{\lambda})$. Considering a single-barrier system away from the potential, we may assume $V(x;\boldsymbol{\lambda}) \approx 0$. This leaves the only nonvanishing contribution associated with the environment, while the dynamical term originating from the potential vanishes. In our scenario with $D_{pp} = D_{xp} = 0$, we have

$$\frac{\mathrm{d}}{\mathrm{d}t}\delta(t) = -D_{xx}\int_{\mathbb{R}^2} \delta(\varrho(x,p,t;\boldsymbol{\lambda}))(\partial_x\varrho(x,p,t;\boldsymbol{\lambda}))^2 dxdp = -D_{xx}\int_{\Sigma} \frac{(\partial_x\varrho(x,p,t;\boldsymbol{\lambda}))^2}{|\nabla\varrho(x,p,t;\boldsymbol{\lambda})|} d\Sigma \leq 0, \tag{4.157}$$

and since nonclassicality parameter is bounded from below by 0, we conclude that $\delta(t) \to 0^+$ as $t \to +\infty$. This argument remains valid for nonzero D_{pp} and D_{xp}, since Lindbladian dynamics require that the matrix $\mathbb{D}$ be positive.

Turning our attention to the case of the system of a sequence of Gaussian barriers, we notice in Fig. 4.19a, 4.19c that the nonclassicality of the unperturbed and disordered system in the isolated case increases with time. Simultaneously, for the open system 4.25a, 4.25c , it initially increases and then inflects. We can associate it with the possible increase of the negative area of the WDF, which contributes to

the second term of the right-hand side of the Eq. (4.155), surpassing the contribution from isolated dynamics. A particularly interesting phenomenon arises in the case of a single barrier, where disorder leads to a grey bandwidth of allowed nonclassicality values, regardless of whether the system is isolated 4.6a, 4.6c or open 4.12a, 4.12c. In contrast, for a chain of Gaussian barriers, the grey band exhibits a different geometric structure in the open system. The environment gradually filters the disordered system toward a specific final state, as the initially broad grey band shrinks with increasing time. This implies that the nonclassicality parameter in this scenario is becoming disorder-insensitive.

For further analysis, we shall consider together the purity of the state and the Wigner-Shannon entropy. According to the provided definition, the Wigner-Shannon entropy is coupled with the purity of the state. This is the result of the normalisation used. Namely, during our previous [97, 185, 186], we investigated the interpretation of the Wigner function as a probability amplitude, rather than the quasi-probability distribution, leading to the refined Wigner-Shannon entropy for the Wigner function (4.125). From the fact that $\|\varrho\|^2_{L_2(\mathbb{R}^2)} = D(t;\boldsymbol{\lambda})/(2\pi\hbar)$, where $D(t;\boldsymbol{\lambda})$ is the purity of the state, we have the following equality

$$S_1(t;\boldsymbol{\lambda}) = 2\ln\frac{D(t;\boldsymbol{\lambda})}{2\pi\hbar} - 2\frac{2\pi\hbar}{D(t;\boldsymbol{\lambda})}\int_{\mathbb{R}^2}\varrho^2(x,p,t;\boldsymbol{\lambda})\ln\big(\varrho^2(x,p,t;\boldsymbol{\lambda})\big)dxdp. \tag{4.158}$$

For all considered cases, we observe that the entropy increases over time. Consequently, the square of WDF divided by the purity gradually occupies an increasingly larger area in the phase space. In the case of the isolated single-barrier system, however, entropy increases only over a finite time interval, due to the interaction with the potential barrier, as the purity is equal to the identity. Further evolution, driven by shearing transformation, does not influence the area occupied. Since entropy is associated with a rate of diffusivity of the distribution, we also conclude that interaction with the potential induces spreading of the distribution over the phase space. On the other hand, in the case of the open system, the spreading of the distribution is simultaneously driven by the interaction with both the potential and the environment. This continuous interaction with the environment prevents the appearance of visible plateau intervals in Figs 4.12b, 4.12d, which were observed in Figs 4.6b, 4.6d. However, in the entropy of the open system, the moment of interaction with the potential barrier is visible as a small inflection of the entropy curve, around $t \approx 2\times10^3$ [a.u.], not as severe as in the case of the isolated system. Nonetheless, just like in the case of the nonclassicality parameter, the grey band of the Wigner-Shannon entropy created from different realisations of the system tightens consequently. The entropy is strictly constrained, and no $\boldsymbol{\lambda}$-dependent deviations occur in the evolution.

The width of the band can be estimated in terms of the standard deviation of a given measure with respect to the probability distribution $P(\boldsymbol{\lambda})$. Let us define a function $\nu(x,p,t;\boldsymbol{\lambda})$ as

$$\nu(x,p,t;\boldsymbol{\lambda}) := \nabla_{\boldsymbol{\lambda}}\varrho(x,p,t;\boldsymbol{\lambda}), \tag{4.159}$$

that is, a $\boldsymbol{\lambda}$ derivative or a gradient of a WDF. This rate of change of the WDF with respect to the vector $\boldsymbol{\lambda}$ satisfies the modified equation of motion

$$\begin{aligned}\partial_t\nu = &-p\partial_x\nu + \{V(x;\boldsymbol{\lambda}),\nu\}\\ &+\Gamma_x\partial_x(x\nu) + \Gamma_p\partial_p(p\nu) + \frac{1}{2}D_{pp}\partial^2_{xx}\nu + \frac{1}{2}D_{xx}\partial^2_{pp}\nu - D_{xp}\partial^2_{xp}\nu\\ &+\{\nabla_{\boldsymbol{\lambda}}V(x;\boldsymbol{\lambda}),\varrho(x,p,t;\boldsymbol{\lambda})\}_\star.\end{aligned} \tag{4.160}$$

The only difference in the form of the equation of motion for $\nu(x,p,t;\boldsymbol{\lambda})$ and $\varrho(x,p,t;\boldsymbol{\lambda})$ is the appearance of the driving term associated with the sensitivity of the potential to the random parameter. By the fact that the initial condition for the equation of motion of the WDF is independent of $\boldsymbol{\lambda}$, $\nu(x,p,0;\boldsymbol{\lambda}) = \mathbf{0}$, we can write a solution in the form

$$\nu(x,p,t;\boldsymbol{\lambda}) = \int_0^t e^{(t-s)\hat{\mathcal{L}}(\boldsymbol{\lambda})}\{\nabla_{\boldsymbol{\lambda}} V(x;\boldsymbol{\lambda}), \varrho(x,p,s;\boldsymbol{\lambda})\}_\star \, ds. \tag{4.161}$$

Simultaneously, let us consider any functional of the WDF. Namely, let $f : [-1/(\pi\hbar), 1/(\pi\hbar)] \to \mathbb{R}$ be a function such that the following integral

$$F[\varrho](t;\boldsymbol{\lambda}) := \int_{\mathbb{R}^2} f(\varrho(x,p,t;\boldsymbol{\lambda}))dxdp, \tag{4.162}$$

is well-defined for any $t \geq 0$. This functional encapsulates the most of the phase-space measures used to quantify the WDF, namely for $f(u) = |u| - u$, we regain the nonclassicality parameter, while for $f(u) = u^2$ we reclaim the rescaled purity.

Let us re-express the WDF in terms of the Taylor series with respect to the random parameter $\boldsymbol{\lambda}$

$$\varrho(x,p,t;\boldsymbol{\lambda}) \approx \varrho(x,p,t;\mathbf{0}) + \nabla_{\boldsymbol{\lambda}}\varrho(x,p,t;\boldsymbol{\lambda})\Big|_{\boldsymbol{\lambda}=\mathbf{0}} \circ \boldsymbol{\lambda}, \tag{4.163}$$

then expanding the function f in the Taylor series yields

$$\begin{aligned} f(\varrho(x,p,t;\boldsymbol{\lambda})) &\approx f\left(\varrho(x,p,t;\mathbf{0}) + \nabla_{\boldsymbol{\lambda}}\varrho(x,p,t;\boldsymbol{\lambda})\Big|_{\boldsymbol{\lambda}=\mathbf{0}} \circ \boldsymbol{\lambda}\right) \\ &\approx f(\varrho(x,p,t;\mathbf{0})) + f'(\varrho(x,p,t;\mathbf{0}))\nabla_{\boldsymbol{\lambda}}\varrho(x,p,t;\boldsymbol{\lambda})\Big|_{\boldsymbol{\lambda}=\mathbf{0}} \circ \boldsymbol{\lambda}. \end{aligned} \tag{4.164}$$

Integrating the expression above over $dxdp$ gives the following equality

$$F[\varrho](t;\boldsymbol{\lambda}) = F[\varrho](t;\mathbf{0}) + \int_{\mathbb{R}^2} f'(\varrho(x,p,t;\mathbf{0}))\nabla_{\boldsymbol{\lambda}}\varrho(x,p,t;\boldsymbol{\lambda})\Big|_{\boldsymbol{\lambda}=\mathbf{0}} dxdp \circ \boldsymbol{\lambda}. \tag{4.165}$$

Notice that $F[\varrho](t;\mathbf{0})$ is nothing different but the measure of the unperturbed WDF. Then, the variance of the functional F is given by

$$\begin{aligned} \sigma^2(F[\varrho]) &= E\left[(F[u] - E[F[u]])^2\right] \\ &= E\left[\left(\int_{\mathbb{R}^2} f'(\varrho(x,p,t;\mathbf{0}))\nabla_{\boldsymbol{\lambda}}\varrho(x,p,t;\boldsymbol{\lambda})\Big|_{\boldsymbol{\lambda}=\mathbf{0}} dxdp \circ \boldsymbol{\lambda}\right)^2\right] \\ &= \sigma_{\boldsymbol{\lambda}}^2\left\|\int_{\mathbb{R}^2} f'(\varrho(x,p,t;\mathbf{0}))\nabla_{\boldsymbol{\lambda}}\varrho(x,p,t;\boldsymbol{\lambda})\Big|_{\boldsymbol{\lambda}=\mathbf{0}} dxdp\right\|^2, \end{aligned} \tag{4.166}$$

where the last expression was obtained due to the statistical independence of the coordinates of the vector $\boldsymbol{\lambda}$. Using now the formula (4.161) we obtain the following

$$\sigma^2(F[\varrho]) \approx \sigma_{\boldsymbol{\lambda}}^2\left\|\int_{\mathbb{R}^2} f'(\varrho(x,p,t;\mathbf{0}))\int_0^t e^{(t-s)\hat{\mathcal{L}}(\mathbf{0})}\{\nabla_{\boldsymbol{\lambda}} V(x;\mathbf{0}), \varrho(x,p,s;\mathbf{0})\}_\star \, dsdxdp\right\|^2. \tag{4.167}$$

We conclude that the width of the band of the realisations in this setup is only associated with the sensitivity of the potential to the perturbations. To emphasise this dependence even further, we assume that the time instance is so short that $\exp\Big\{((t-s)\hat{\mathcal{L}}(\mathbf{0}))\Big\} \approx \hat{1}$, then

$$\sigma^2(F[\varrho]) \approx \sigma_{\boldsymbol{\lambda}}^2\left\|\int_{\mathbb{R}^2} f'(\varrho(x,p,t;\mathbf{0}))\{\nabla_{\boldsymbol{\lambda}} V(x;\mathbf{0}), \varrho_0(x,p)\}_\star \, dxdp\right\|, \tag{4.168}$$

which depends only on the sensitivity of the underlying measure function f to changes in the values of the unperturbed WDF, and the potential sensitivity to the disorder.

The previous formula can be applied to any measure, however, we would like to focus on the following pair: the purity and the Loschmidt echo. Both of those measures evolve according to the following equations, for the purity

$$\frac{\mathrm{d}}{\mathrm{d}t}D(t;\boldsymbol{\lambda}) = (\Gamma_x+\Gamma_p)D(t;\boldsymbol{\lambda}) - \int_{\mathbb{R}^2} \nabla\varrho(x,p,t;\boldsymbol{\lambda})^T\mathbb{D}\nabla\varrho(x,p,t;\boldsymbol{\lambda})\,dxdp, \tag{4.169}$$

and for the Loschmidt echo

$$\begin{aligned}\frac{\mathrm{d}}{\mathrm{d}t}M(t;\boldsymbol{\lambda}) &= (\Gamma_x+\Gamma_p)M(t;\boldsymbol{\lambda})\\ &\quad + 2\pi\hbar\int_{\mathbb{R}^2}\left[\{V(x;\mathbf{0})-V(x;\boldsymbol{\lambda}),\varrho(x,p,t;\mathbf{0})\} - \nabla\varrho(x,p,t;\mathbf{0})^T\mathbb{D}\nabla\varrho(x,p,t;\boldsymbol{\lambda})\right]dxdp.\end{aligned} \tag{4.170}$$

Both satisfy similar evolution equations, yet the Loschmidt echo evolution depends on one additional term, namely the difference of the unperturbed and perturbed potentials. Unlike purity for the isolated system, which does not vary in time, the Loschmidt echo might still exhibit changes, as the potential difference term influences its time derivative, as visible in Figs 4.20b 4.20d and especially in Figs 4.26b 4.26d. The latter figure distinctively shows the irreversibility of the dynamics, as, unlike in the single barrier case, the Loschmidt echo does not return to the initial value. This highlights its power, as purity in the case of isolated systems does not exhibit any change, while qualitative properties of the system drastically change. Opening both systems leads to natural decreas in their purities as seen in both equations. There is a possibility to estimate the bound on the rate of decrease of purity, however it requires a bounded domain. Let us assume that instead of an unbounded domain $\mathbb{R}^2$ we are considering some bounded domain $\Omega\subset\mathbb{R}^2$, and suitable class of functions $\varrho(x,p,t;\boldsymbol{\lambda})$ vanishing on the boundary, that is, $\varrho\big|_{\partial\Omega}=0$. Then by Friedrichs' inequality [140, 40, 60] we have

$$\begin{aligned}\int_{\mathbb{R}^2}\nabla\varrho(x,p,t;\boldsymbol{\lambda})^T\mathbb{D}\nabla\varrho(x,p,t;\boldsymbol{\lambda})\,dxdp &\geq \min(\sigma(\mathbb{D}))\|\nabla\varrho(x,p,t;\boldsymbol{\lambda})\|^2_{L^2(\Omega)}\\ &\geq \frac{\min(\sigma(\mathbb{D}))}{\mathrm{diam}(\Omega)}\|\varrho\|^2_{L^2(\Omega)} = \frac{\min(\sigma(\mathbb{D}))}{2\pi\hbar\mathrm{diam}(\Omega)}D(t;\boldsymbol{\lambda}).\end{aligned} \tag{4.171}$$

Thus, the rate of decrease of purity for bounded domains cannot be greater than

$$D(t;\boldsymbol{\lambda}) \geq e^{t\left(\Gamma_x+\Gamma_p-\frac{\min(\sigma(\mathbb{D}))}{2\pi\hbar\mathrm{diam}(\Omega)}\right)}, \tag{4.172}$$

where $\min(\sigma(\mathbb{D}))$ is the smallest of the eigenvalues of $\mathbb{D}$ and $\mathrm{diam}(\Omega)=\sup_{x,y\in\Omega}|x-y|$ is the diameter of the set Ω. While it holds for bounded domains, the author was not aware of the similar inequalities for unbounded ones, believing that for suitably weighted spaces, a similar inequality can be achieved.

Before concluding, we focus on the behaviour of the parameters of the proposed approximation of the ensemble average. Let us recall, that we define the approximated ensemble averaged WDF, $\bar{\varrho}(x,p,t)$, as a solution to the equation (4.114), with the initial condition in the form of the Gaussian function (4.115). In most figures, the ensemble average's parameters nearly perfectly trace behind the values obtained for the unperturbed system, whereas the WDF for the ensemble average is relatively *"close"* to the unperturbed

WDF, given the distance (4.132). Even more significantly, in the case of the single barrier, the interaction with the potential $V(x;\boldsymbol{\lambda})$ temporarily breaks this similarity, after which the system returns close to the unperturbed behaviour, as seen in Figs 4.8 4.14. This is not the case in the chain of barriers, where the distance between those distributions initially increases to a certain level, around which it stays for further evolution, by Figs 4.21 4.27. Tracing the evolution of the parameters of the approximated ensemble average, we can conclude that they do not resemble the parameters of the real ensemble average WDF. The values are generally over- or underestimated, while some similarities can be found in a very short time. However, the distance between approximation and ensemble average or the unperturbed WDF increases quickly, saturating the distance up to a nearly maximal value. This would imply that the time-proportional decoherence term in Eq. (4.114) suppresses the initial state very quickly in comparison to the decoherence associated with averaging the realisations of the system. Let us consider one more property of the system under study. In general, it is expected that, for each $\boldsymbol{\lambda}$, the initial value problem given by (4.31) possesses what is known as a stationary solution. It is defined as the limit of the solution to the initial value problem as $t \to +\infty$ [3, 77, 188]

$$\varrho_\infty(x,p;\boldsymbol{\lambda}) := \lim_{t\to+\infty} \varrho(x,p,t;\boldsymbol{\lambda}). \tag{4.173}$$

Although the existence of such solutions was proved for the Fokker-Planck equation with harmonic potential [5, 158], these results do not cover the case of a time-dependent dissipative term, as presented in our approximate solution. From the form of the equation of motion (4.114) we observe that for $t \gg 1$, the following relation holds

$$\partial_t \bar{\varrho} = \{\bar{V}(x), \bar{\varrho}\}_\star + t\sigma_\lambda^2 \sum_k (\partial_{xx}^2 v_k(x;0))^2 \partial_{pp}^2 \bar{\varrho}, \tag{4.174}$$

Introducing the effective dissipation function $D_{eff}(x) := \sigma_\lambda^2 \sum_k (\partial_{xx}^2 v_k(x;0))^2$ the solution to this equation can be expressed as

$$\bar{\varrho}(x,p,t) = \int_{\mathbb{R}} R(x,p') K(x,p,p',t) dp', \tag{4.175}$$

where $R(x,p')$ is an unspecified time-independent asymptotic function of the system, and the kernel $K(x,p,p',t)$ has the following form

$$K(x,p,p',t) = \frac{1}{2\pi\hbar} \int_{\mathbb{R}} e^{-\frac{i}{\hbar}t\left[\bar{V}\left(x+\frac{y}{2}\right)-\bar{V}\left(x-\frac{y}{2}\right)\right]-\frac{t^2}{2\hbar^2}D_{eff}(x)y^2} e^{\frac{i}{\hbar}y(p-p')} dy. \tag{4.176}$$

From this expression, it follows that

$$|\bar{\varrho}(x,p,t)| = \left| \int_{\mathbb{R}} R(x,p') K(x,p,p',t) dp' \right| \leq \frac{1}{\sqrt{2\pi D_{eff}(x)}t} \int_{\mathbb{R}} |R(x,p')| dp'. \tag{4.177}$$

Thus, as long as the integral of the RHS is finite, the solution tends pointwise to 0, as $t \to +\infty$, for all x such that $D_{eff}(x) > 0$. The bound of the function is independent of the type of potential, since the potential only contributes oscillatory terms, which vanish under the modulus. In the case of an ensemble of single-barrier systems, each perturbed by the random vector λ, the average potential $\bar{V}(x)$ is expected to be mostly confined around the mean $x = 0$. This corresponds to the regions where $D(x) > 0$ and where the dissipation occurs, as shown in Figs. 4.6 4.12. During further evolution, where $\bar{V}(x) \approx 0$ and also $D_{eff}(x) \approx 0$, the decay of a function slows down. This effect is visible in the same figure, where the nonclassicality parameter exhibits inflection around $t \approx 3 \times 10^3$ [a.u.]. In contrast, for the open system, the decoherence introduced

by the environment enhances dissipation, suppressing nonclassicality to 0, and driving $\bar{\varrho} \to 0$. Certainly, the average potential $\bar{V}(x)$ has a more exotic form, in the case of multiple Gaussian barriers, as it does not exhibit a typical asymptotic of the barrier, that is, $\bar{V}(x) \to 0^+$ as $|x| \to +\infty$. This property influences the effective dissipation term $D_{eff}(x)$ as $D_{eff}(x) > 0$ almost everywhere, leading to the rapid disappearance of the approximated solution. Those results are supported by the distance measures 4.21 4.27, as they do not decrease during the simulation period.

Nonetheless, for each realisation of the ensemble in the single barrier case, we expect that advection in the position variable x, resulting from the absence of a confining potential, dominates the dynamics. This implies that whether the system is isolated or open, long-time behaviour is governed primarily by advection, with additional momentum spreading in the open case. Consequently, no stationary state is expected. In contrast, the ensemble of chains of Gaussian barriers, the constant interaction with the potential suppresses the advection in position and momentum, allowing for the formation of the stationary state for each case. However, the form of this state is unknown and must be investigated separately.

Summary and perspectives

The phase-space approach to quantum mechanics provides well-structured and intuitive tools, closely related to the mathematical framework of classical mechanics, for analysing the dynamics of various complex quantum systems. This strong connection to the classical formalism has motivated its application across various areas of physics, typically through slight modifications of the underlying Moyal equation. Examples include the study of carrier transport in semiconductors via the Wigner-Boltzmann equation, or the evolution of relativistic plasmas described by the Wigner-Vlasov equation. Moreover, this formulation facilitates semiclassical analysis, since its classical counterpart, the Liouville equation, has already been extensively studied. However, several challenges remain, one of which is the difficulty of determining whether a given Wigner function corresponds to a physical quantum state without referring back to the density operator. More significantly, the phase-space approach inherently doubles the number of variables required to describe the system. Although this issue is not a major obstacle in theoretical analysis, it imposes substantial limitations on the numerical implementation of computational algorithms.

Throughout this work, many of these challenges have been encountered. Still, the use of phase-space methods for open quantum systems offers clear advantages, particularly in terms of interpretability. The results presented in this work can be summarised in three main steps: (1) the derivation of the equation of motion for the Wigner function of an open quantum system, (2) the development of a numerical algorithm and a split-operator scheme for subsequent calculations, (3) the derivation of the equation of motion for the approximated ensemble average Wigner function, and the analysis of numerical results for the phase-space characteristics of the quantum system. We began with the phase-space formulation of the evolution of the total system, where integration over the bath degrees of freedom was carried out, along with a series of approximations. These included the assumption of weak interaction between the system and its environment, allowing for separability of the Wigner function of the total system; the Markovian approximation, which neglects memory effects; and the secular approximation, which averages out non-resonant terms in the equation of motion. Although this approach proved successful, the author's initial aim was to obtain the equation through a derivation more directly related to phase-space quantum mechanics. The final equation of motion of the system consisted of the Hamiltonian of the isolated system in the form of either a Gaussian barrier or a chain of Gaussian barriers and a linear Lindblad operator. To solve this equation, we employed the split-operator method, rewriting the exponential of the full operator as a product of separate exponentials, up to a certain approximation error. However, we found that the kinetic and Lindbladian parts of the operator can, in fact, be separated exactly. This result improves the algorithm, as no approximation is needed to separate these contributions, which greatly simplifies the implementation.

Although this work has focused on two specific potential models, a more general analysis of phase-space parameters in quantum systems is clearly required. Given the extent of this topic, several directions for future research emerged during the preparation of this thesis. The first, currently under development, is the construction of a general splitting scheme for quadratic operators. We have found that an exact splitting method can be achieved for such operators, yielding precise solutions in terms of Fourier transforms without the need for approximation. A second direction of research concerns the analysis of the Lindblad equation for Cohen-class functions, i.e., functions expressed as the convolution of a kernel with a Wigner function. We have already demonstrated that for the family of the so-called τ-Wigner functions, the Lindblad-Wigner equation of motion introduces imaginary terms dependent on the diffusion coefficients. Finally, the study of symmetries in disordered open quantum systems, along with the conditions for the existence of steady-state solutions, represents another promising direction for further investigation.

Appendix A

Useful definitions and theorems

Definition A.1. [74] Let $\mathcal{H}$ be a vector space over field $\mathbb{C}$. We call $\mathcal{H}$ a *Hilbert space* if:

1. It is equipped with a sesquilinear inner product $\langle\cdot|\cdot\rangle : \mathcal{H} \times \mathcal{H} \to \mathbb{C}$ (inner product space);
2. It is a complete metric space with respect to the norm induced by inner product (convergence of all Cauchy sequences).

Moreover, we say that $\mathcal{H}$ is *separable* Hilbert space if there exists a dense, countable subset of $\mathcal{H}$.
An element belonging to the Hilbert space is called a *state vector*.

Definition A.2. [138, 128, 80] Let $\mathcal{H}_1 \otimes \mathcal{H}_2$ denote a set of all linear combinations of formal products of the type $\phi \otimes \psi$ for $\phi \in \mathcal{H}_1$ and $\psi \in \mathcal{H}_2$. A *tensor product* of Hilbert spaces $\mathcal{H}_1$, $\mathcal{H}_2$, is a completion of $\mathcal{H}_1 \otimes \mathcal{H}_2$ with respect to an inner product defined as

$$\langle \phi_1 \otimes \psi_1 | \phi_2 \otimes \psi_2 \rangle := \langle \phi_1 | \phi_2 \rangle_{\mathcal{H}_1} \cdot \langle \psi_1 | \psi_2 \rangle_{\mathcal{H}_2} ,$$

for $\phi_1, \phi_2 \in \mathcal{H}_1$, and $\psi_1, \psi_2 \in \mathcal{H}_2$. Moreover such defined space is valid Hilbert space.

Definition A.3. [10] Let $\hat{A}$ be a linear operator defined in a Hilbert space $D(\hat{A}) \subset \mathcal{H}_1$ with image in $\mathcal{H}_2$, $\hat{A}(D(\hat{A})) \subset \mathcal{H}_2$. Moreover, let $\|\cdot\|_{\mathcal{H}_1}, \|\cdot\|_{\mathcal{H}_2}$ be norms in respective spaces. We say that $\hat{A}$ is a *bounded* (*continuous*) *operator* if

$$\exists c > 0 \; \forall \psi \in D(\hat{A}) : \; \left\| \hat{A}\psi \right\|_{\mathcal{H}_2} \leq c \|\psi\|_{\mathcal{H}_1}. \tag{A.1}$$

The smallest such constant c is called the *norm* of the operator $\hat{A}$.
By $\mathcal{B}(\mathcal{H}_1, \mathcal{H}_2)$ we shall understand the *set of all bounded operators* from $\mathcal{H}_1$ to $\mathcal{H}_2$, and if $\mathcal{H} = \mathcal{H}_1 = \mathcal{H}_2$, then $\mathcal{B}(\mathcal{H}_1, \mathcal{H}_2) = \mathcal{B}(\mathcal{H})$.

Definition A.4. [138, 10, 16] Let $\mathcal{H}_1$ and $\mathcal{H}_2$ be two Hilbert spaces with inner products $\langle\cdot|\cdot\rangle_1$, $\langle\cdot|\cdot\rangle_2$ respectively. If there exists a linear operator $\hat{U} : \mathcal{H}_1 \to \mathcal{H}_2$ such that

$$\left\langle \hat{U}\psi \middle| \hat{U}\phi \right\rangle_{\mathcal{H}_2} = \langle \psi | \phi \rangle_{\mathcal{H}_1} \tag{A.2}$$

holds for all $\psi, \phi \in \mathcal{H}_1$ then we say that $\mathcal{H}_1$ and $\mathcal{H}_2$ are *isomorphic*. If two space coincide $\mathcal{H}_1 = \mathcal{H}_2 = \mathcal{H}$ and of the domain and range of the operator are equal to $\mathcal{H}$, namely $D(\hat{U}) = \mathrm{Ran}(\hat{U}) = \mathcal{H}$ then we say that $\hat{U}$ is a *unitary* operator.

Definition A.5. [138] Let $\mathcal{H}$ be a separable Hilbert space with inner product $\langle\cdot|\cdot\rangle$ and let $\{\varphi_n\}_{n=1}^{+\infty}$ be an orthonormal basis. For a positive operator $\hat{A}$ we define the *trace* of $\hat{A}$ as a number

$$\mathrm{Tr}\,\hat{A} = \sum_{n=1}^{+\infty} \left\langle \varphi_n \middle| \hat{A}\varphi_n \right\rangle . \tag{A.3}$$

The trace is independent of the chosen basis.

Definition A.6. [78, 24] Let $\mathcal{H}$ be a Hilbert space. By $\mathbf{L}$ we denote a set of all operators $\hat{A}$ over $\mathcal{H}$ for which the trace

$$\mathrm{Tr}\left[\hat{A}^\dagger \hat{A}\right] < \infty \tag{A.4}$$

is finite. Additionally, we define a sesquilinear form: $\langle .|.\rangle : \mathbf{L}\times\mathbf{L} \to \mathbb{C}$ given as

$$\left\langle \hat{A} \middle| \hat{B} \right\rangle := \mathrm{Tr}\left[\hat{A}^\dagger \hat{B}\right]. \tag{A.5}$$

The pair $(\mathbf{L}, \langle .|.\rangle)$ is called the *Liouville space* and it is a proper Hilbert space [138].

Definition A.7. An operator $\hat{\Phi}$ acting on elements of Liouville space $\mathbf{L}$ is called a *superoperator*.

Definition A.8. Let $u \in C^k(\mathbb{R}^n)$ be a $k-$differentiable function defined over $\mathbb{R}^n$ with coordinates $\boldsymbol{x} = (x_1, x_2, \ldots, x_n)$. We define the m-th, $0 \le m \le k$ multi-index derivative as

$$D^m_{\boldsymbol{x}} u(\boldsymbol{x}) = \frac{\partial^m u}{\partial x_1^{\alpha_1} \partial x_2^{\alpha_2} \ldots \partial x_n^{\alpha_n}} \tag{A.6}$$

where $\alpha_1 + \alpha_2 + \ldots + \alpha_n = m$.
Analogously we define the m-th multi-index power of vector variable $\boldsymbol{x}$, that is

$$\boldsymbol{x}^m = x_1^{\alpha_1} x_2^{\alpha_2} \ldots x_n^{\alpha_n}, \tag{A.7}$$

where $\alpha_1 + \alpha_2 + \ldots + \alpha_n = m$.

Definition A.9. [153, 50, 123] Let $\mathcal{S}(\mathbb{R}^n)$ denote the space of infinitely differentiable functions $\varphi(\boldsymbol{x})$ defined over $\mathbb{R}^n$ for which the following inequality holds

$$\forall \alpha \ge 0, \beta \ge 0 \ \sup_{\boldsymbol{x}\in\mathbb{R}^n} |\boldsymbol{x}^\alpha D^\beta \varphi| < +\infty \tag{A.8}$$

then we call $\mathcal{S}(\mathbb{R}^n)$ the *Schwartz space* or the space of smooth, rapidly vanishing functions.

Theorem A.1. [50] The following inclusion holds $\mathcal{S}(\mathbb{R}^n) \subset L^2(\mathbb{R}^n)$ and the Schwartz space is dense in $L^2(\mathbb{R}^n)$.

Definition A.10. [153, 60, 123] A *Fourier transform* of a $\varphi \in \mathcal{S}(\mathbb{R})^n$ is an integral transform $\mathcal{F} : \mathcal{S}(\mathbb{R}^n) \to \mathcal{S}(\mathbb{R}^n)$ defined as

$$(\mathcal{F}\varphi)(\boldsymbol{\xi}) := \frac{1}{(2\pi)^{n/2}} \int_{\mathbb{R}^n} \varphi(\boldsymbol{x}) e^{-i\boldsymbol{x}\cdot\boldsymbol{\xi}} d^n x, \tag{A.9}$$

with an inverse given by

$$(\mathcal{F}^{-1}\psi)(\boldsymbol{\xi}) := \frac{1}{(2\pi)^{n/2}} \int_{\mathbb{R}^n} \psi(\boldsymbol{x}) e^{i\boldsymbol{x}\cdot\boldsymbol{\xi}} d^n x. \tag{A.10}$$

Theorem A.2. [60] The previous definition of Fourier transform can be used for functions in $L^1(\mathbb{R}^n)$. Then $\varphi \in L^1(\mathbb{R}^2) \implies \mathcal{F}\varphi \in L^\infty(\mathbb{R}^n)$.

Definition A.11. [146] Let $\mathcal{B}$ be a normed space, that is a vector space with a defined norm $\|.\|$, then we say that $\mathcal{B}$ is a Banach space if it is a complete space, namely every Cauchy sequence is convergent to an element of this space.

Definition A.12. [141] Let $\mathcal{B}$ be a Banach space. The family of bounded linear operators $\{\hat{U}(t)\}$, $t \geq 0$ is called a *strongly continuous semigroup* if it satisfies the following conditions

- $\hat{U}(t+s) = \hat{U}(t)\hat{U}(s)$ for $t, s \geq 0$
- $\hat{U}(0) = \hat{1}$
- the mapping $[0, +\infty) \ni t \to \hat{U}(t)\boldsymbol{v}$ is continuous for every $\boldsymbol{v} \in \mathcal{B}$.

Appendix B

Exact solution for polynomial potentials of order at most 2

In this Appendix, we will consider a quadratic potential $V(x) = ax^2 + bx + c$ with $a > 0$, $b, c \in \mathbb{R}$ to seek a general solution for the evolution equation. First, let us recall a form of the Lindblad-Wigner equation for such a potential

$$\partial_t \varrho = -\frac{p}{m}\partial_x \varrho + ax\partial_p \varrho + b\partial_p \varrho + \Gamma_p \partial_p(p\varrho) + \Gamma_x \partial_x(x\varrho) + \frac{1}{2}D_{xx}\partial^2_{pp}\varrho + \frac{1}{2}D_{pp}\partial^2_{xx}\varrho - D_{xp}\partial^2_{xp}\varrho \quad \text{(B.1)}$$

Using Fourier's transform with respect to (x, p) variables we arrive at

$$\partial_t \hat{\varrho} = \frac{\lambda}{m}\partial_y \hat{\varrho} - ay\partial_\lambda \hat{\varrho} + iby\hat{\varrho} - \Gamma_x \lambda \partial_\lambda \hat{\varrho} - \Gamma_p y \partial_y \hat{\varrho} - \frac{1}{2}\left(D_{xx}y^2 + D_{pp}\lambda^2 - 2D_{xp}y\lambda\right)\hat{\varrho} \quad \text{(B.2)}$$

or equivalently

$$\partial_t \hat{\varrho} + (ay + \Gamma_x \lambda)\partial_\lambda \hat{\varrho} + \left(\Gamma_p y - \frac{1}{m}\lambda\right)\partial_y \hat{\varrho} = \left(-\frac{1}{2}D_{xx}y^2 - \frac{1}{2}D_{pp}\lambda^2 + D_{xp}\lambda y + iby\right)\hat{\varrho}, \quad \text{(B.3)}$$

that leads to the characteristic equation

$$\frac{dt}{1} = \frac{d\lambda}{ay + \Gamma_x \lambda} = \frac{dy}{\Gamma_p y - \frac{1}{m}\lambda} = \frac{d\hat{\varrho}}{\left(-\frac{1}{2}D_{xx}y^2 - \frac{1}{2}D_{pp}\lambda^2 + D_{xp}\lambda y + iby\right)\hat{\varrho}}, \quad \text{(B.4)}$$

and further, it can be written as a system of ordinary differential equations

$$\begin{cases} \frac{d\lambda}{dt} &= ay + \Gamma_x \lambda, \\ \frac{dy}{dt} &= \Gamma_p y - \frac{1}{m}\lambda, \\ \frac{d\hat{\varrho}}{dt} &= \left(-\frac{1}{2}D_{xx}y^2 - \frac{1}{2}D_{pp}\lambda^2 + D_{xp}\lambda y + iby\right)\hat{\varrho}, \end{cases} \quad \text{(B.5)}$$

where two matrices were introduced

$$\mathbf{\Gamma} = \begin{bmatrix} \Gamma_x & a \\ -\frac{1}{m} & \Gamma_p \end{bmatrix}, \quad \mathbb{D} = \begin{bmatrix} D_{pp} & -D_{xp} \\ -D_{xp} & D_{xx} \end{bmatrix}. \quad \text{(B.6)}$$

For upcoming manipulations, we decided to write this system in the following matrix-scalar form

$$\begin{cases} \frac{\mathrm{d}\boldsymbol{v}}{\mathrm{d}t} &= \mathbf{\Gamma}\boldsymbol{v} \\ \frac{d\hat{\varrho}}{dt} &= \left(-\frac{1}{2}\boldsymbol{v}^T\mathbb{D}\boldsymbol{v} + i\boldsymbol{b}^T\boldsymbol{v}\right)\hat{\varrho}, \end{cases} \quad \text{(B.7)}$$

where $\boldsymbol{v} = (\lambda, y)^T$. By the results in the theory of systems of ordinary differential equations, the first pair is solved by the following vector $\boldsymbol{v} = \exp(t\boldsymbol{\Gamma})\boldsymbol{\omega}$ where $\boldsymbol{\omega}$ is a vector of integration constants. Then, the second equation can be rephrased as

$$\frac{d\hat{\varrho}}{dt} = \left(-\frac{1}{2}\boldsymbol{\omega}^T\left(e^{t\boldsymbol{\Gamma}^T}\mathbb{D}e^{t\boldsymbol{\Gamma}}\right)\boldsymbol{\omega} + i\left(\boldsymbol{b}^T e^{t\boldsymbol{\Gamma}}\right)\boldsymbol{\omega}\right)\hat{\varrho}, \tag{B.8}$$

which can also be directly solved via the following function

$$\hat{\varrho}(\lambda, y, t) = \Phi(\boldsymbol{\omega})\exp\left[-\frac{1}{2}\boldsymbol{\omega}^T\int\left(e^{t\boldsymbol{\Gamma}^T}\mathbb{D}e^{t\boldsymbol{\Gamma}}\right)dt\,\boldsymbol{\omega} + i\left(\boldsymbol{b}^T\int e^{t\boldsymbol{\Gamma}}dt\right)\boldsymbol{\omega}\right]\Bigg|_{\boldsymbol{\omega}=e^{-t\boldsymbol{\Gamma}}\boldsymbol{v}}. \tag{B.9}$$

The integrals within the exponential can be evaluated directly if needed. However, we notice one peculiarity: the first integral in the expression on the RHS yields a symmetric matrix. To see this, we mark that such an integral is equivalent to finding a solution to the Sylvester matrix equation [14]

$$\boldsymbol{\Gamma}^T\mathbb{X} + \mathbb{X}\boldsymbol{\Gamma} = \mathbb{D}. \tag{B.10}$$

which results from the time derivative of the following expression: $\exp\big(t\boldsymbol{\Gamma}^T\big)\mathbb{X}\exp(t\boldsymbol{\Gamma})$ that might be associated with the antiderivative of the initial integrand, only if the Sylvester equation is satisfied. Moreover, assuming $\mathbb{D}$ is a symmetric matrix, $\mathbb{D}^T = \mathbb{D}$, we obtain the associated equation for the transpose of $\mathbb{X}$

$$\mathbb{X}^T\boldsymbol{\Gamma} + \boldsymbol{\Gamma}^T\mathbb{X}^T = \mathbb{D}, \tag{B.11}$$

that coincides with the initial equation. According to Sylvester theorem [90], this equation has a unique solution, for any $\mathbb{D}$, if and only if $\sigma(\Gamma^T) \cap \sigma(-\Gamma) = \emptyset$, that is, Γ^T and $-\Gamma$ do not share a common eigenvalue. By the standard result of matrix algebra, a transpose of a matrix has the same eigenvalues, and thus former condition can be rephrased as $\sigma(\Gamma) \cap \sigma(-\Gamma) = \emptyset$, meaning that there are no pairs of the type $(\lambda, -\lambda)$ within the spectrum of matrix Γ. Assume for now that $\sigma(\Gamma) = \{\lambda_1, \lambda_2\}$, then

$$\Gamma_x + \Gamma_p = \lambda_1 + \lambda_2 \tag{B.12}$$

and

$$\Gamma_x\Gamma_p + \frac{a}{m} = \lambda_1\lambda_2 \tag{B.13}$$

imposing $\lambda_2 = -\lambda_1 = -\lambda$, we have the following system of equations

$$\begin{cases} 0 & = \frac{1}{2}(\Gamma_x + \Gamma_p) \\ \lambda^2 & = -\Gamma_x\Gamma_p - \frac{a}{m}. \end{cases} \tag{B.14}$$

If no such λ can be found, then the Sylvester equation (B.10) has a unique solution and thus $\mathbb{X} = \mathbb{X}^T$, meaning $\mathbb{X}$ is symmetric. Bearing that in mind, we arrive at the following conclusion, the solution to the Lindblad-Wigner equation for the potential $U(x)$ with initial condition $\varrho_0(x, p)$ is given by a convolution of a Gaussian with the function $\varrho_0(x, p)$. Even more, if the initial state is given as a Gaussian function, then the solution, at all times $t > 0$, is still Gaussian thus, a set of Gaussian functions is invariant under the evolution generated by the Wigner-Lindblad operator for the potential associated with at most 2nd order polynomial.

Appendix C

The scaling operator implementation

Recall that the scaling operator $\hat{S}$ [12]

$$\hat{S}f(x) := f(\eta x) = e^{\ln(\eta)x\partial_x} f(x) \tag{C.1}$$

can be expressed as

$$f(\eta x) = \eta^{-1/2} e^{-i\epsilon\alpha_\eta \partial_x^2} e^{-i\beta_\eta x^2} e^{i\epsilon\beta_\eta \partial_x^2} e^{i\alpha_\eta x^2} f(x) \tag{C.2}$$

The general issue encountered in the given expression is the size of the grid of the conjugated space to the variable x. From Fast Fourier Transform implementation, we know that being given an initial grid with an amplitude X_{max} and size N

$$X = (-X_{max}, -X_{max} + \Delta X, \ldots, 0, \Delta X, \ldots, X_{max} - \Delta X), \tag{C.3}$$

the set of conjugated variables L has the amplitude equal to

$$\max L = \frac{\pi}{\Delta X}. \tag{C.4}$$

Thus, if one considers highly populated grids with small amplitude $X_{max} \ll 1$ and $N \gg 1$, then $\max L$ is a huge number. This implies that, especially near the endpoints of the conjugated interval, the $\exp\{iL^2\}$ takes values that might contribute to numerical errors. To omit this issue, we take a step back to investigate the definition of a scaling operator, precisely its exponent $x\partial_x$. We shall define it as a special case of the Weyl operator

$$x\partial_x = \hat{\mathcal{W}}\left(ix\xi - \frac{1}{2}\right). \tag{C.5}$$

By this definition, we notice that the simultaneous division of x by some constant γ, and the multiplication of ξ by the same constant, does not change the initial expression

$$x\partial_x = \hat{\mathcal{W}}\left(i\frac{x}{\gamma}(\gamma\xi) - \frac{1}{2}\right). \tag{C.6}$$

This allows us to rescale each grid considered by a constant γ, diminishing the numerical errors appearing due to the exponential function, without changing the value of the total result.

Appendix D

Example of averaged dynamics

Let us consider a simple closed system where $V(x;\lambda) = Ex$, where E is a random variable with mean $\langle E\rangle = 0$ with PDF $P(E)$. For simplicity, we set the Lindblad operator to $\hat{0}$ to see the influence of the averaging procedure upon the averaged evolution. We can approach solving the equation of motion in the case of a Gaussian state as an initial condition. This leads to the following equation for the system

$$\partial_t \varrho = -p\partial_x \varrho + E\partial_p \varrho, \tag{D.1}$$

whereas for the averaged system, the approximated equation is

$$\partial_t w = -p\partial_x w + t\nu\partial_{pp}^2 w, \tag{D.2}$$

where $\nu = \left\langle E^2\right\rangle$. Both equations can be solved in terms of the Fourier transform, leading to

$$\begin{aligned} \varrho(x,p,t;E) &= \int_{\mathbb{R}^2} \Phi_0(x',p') K_1(x',p';x,p,t;E)dx'dp', \\ w(x,p,t) &= \int_{\mathbb{R}^2} \Phi_0(x',p') K_2(x',p';x,p,t;E)dx'dp', \end{aligned} \tag{D.3}$$

where

$$\begin{aligned} K_1(x',p';x,p,t;E) &= \delta\left(x'-x+pt-\frac{Et^2}{2}\right)\delta(p'-p+Et), \\ K_2(x',p';x,p,t) &= \frac{3\sqrt{2}}{2\pi\nu t^3} e^{-\frac{9\nu}{t^4}\left[\frac{1}{6}t^2(p^2+3p'^2+2pp')+\frac{2}{3}t(2p'x'-2p'x-px)+(x-x')^2\right]}. \end{aligned} \tag{D.4}$$

Then, the averaged result for different realisations of the amplitude parameter E is simply

$$R(x,p,t) = \int_{\mathbb{R}^2} \Phi_0(x',p') \int P(E) K_1(x',p';x,p,t;E)dE\ dx'dp'. \tag{D.5}$$

The general difference between the two solutions is given by the kernels of the integration, thus, we are interested in discrepancies occurring in

$$\tilde{K}_1 = \int P(E)\delta\left(x'-x+pt-\frac{Et^2}{2}\right)\delta(p'-p+Et)dE = \frac{1}{t}P\left(\frac{p'-p}{t}\right)\delta\left(x-x'-\frac{t}{2}(p'+p)\right), \tag{D.6}$$

and

$$K_2 = \frac{3\sqrt{2}}{2\pi\nu t^3}\exp\left\{-\frac{9\nu}{t^4}\left[\frac{1}{6}t^2(p^2+3p'^2+2pp') + \frac{2}{3}t(2p'x' - 2p'x - px) + (x-x')^2\right]\right\}. \tag{D.7}$$

To visualise the discrepancies between two kernels, a common initial condition $\Phi_0(x,p)$ was considered in the form of a multivariate Gaussian function with mean $\boldsymbol{\mu} = \mathbf{0}$ and covariance matrix Σ, namely

$$\Phi_0(x,p) = \frac{1}{2\pi\sqrt{\det\Sigma}}e^{-\frac{1}{2}(x,p)\Sigma^{-1}(x,p)^T}, \tag{D.8}$$

with

$$\boldsymbol{\Sigma} = \begin{pmatrix} \sigma_{11} & \sigma_{12} \\ \sigma_{12} & \sigma_{22} \end{pmatrix}, \quad \sigma_{11},\sigma_{22} > 0 \wedge \sigma_{11}\sigma_{22} \geq \sigma_{12}^2, \tag{D.9}$$

being the covariance matrix. Then, the solution to the initial value problem (IVP) is given by

$$\begin{aligned} R(x,p,t) &= \frac{1}{2\pi\sqrt{\det\Sigma}}\int P(E)e^{-\frac{1}{2}\left(-\frac{E}{2}t^2+pt-x,p-Et\right)\boldsymbol{\Sigma}^{-1}\left(-\frac{E}{2}t^2+pt-x,p-Et\right)^T}dE \\ &= \frac{1}{2\pi\sqrt{\det\Sigma}}\int P(E)e^{-\frac{1}{2}(\boldsymbol{z}-\hat{A}^{-1}\boldsymbol{\mu})^T\hat{A}^T\boldsymbol{\Sigma}^{-1}\hat{A}(\boldsymbol{z}-\hat{A}^{-1}\boldsymbol{\mu})}dE \\ &= \int P(E)\mathcal{N}_{(x,p)}\left(\hat{A}(t)^{-1}\boldsymbol{\mu}(t,E), \hat{A}(t)^{-1}\Sigma(\hat{A}(t)^T)^{-1}\right)dE \\ &= \int P(E)\mathcal{N}_{(x,p)}\left(\hat{A}(-t)\boldsymbol{\mu}(t,E), \hat{A}(-t)\Sigma\hat{A}(-t)^T\right)dE, \end{aligned} \tag{D.10}$$

where $\boldsymbol{z} = (x,p)$,

$$\hat{A} = \hat{A}(t) = \begin{pmatrix} 1 & -t \\ 0 & 1 \end{pmatrix}, \quad \hat{A}(t)^{-1} = \hat{A}(-t) \wedge \det\hat{A} = 1, \tag{D.11}$$

and $\boldsymbol{\mu} = \boldsymbol{\mu}(t,E) = \left(\frac{E}{2}t^2, Et\right)^T$. Complementarily, the solution to the second IVP is given by

$$w(x,p,t) = \frac{3}{\pi\sqrt{\Xi}} \times e^{-\frac{3}{\Xi}(x,p)\begin{pmatrix} 6(\sigma_{22}+t^2\nu) & -2(3\sigma_{12}+3\sigma_{22}t+t^3\nu) \\ -2(3\sigma_{12}+3\sigma_{22}t+t^3\nu) & t^4\nu+6\sigma_{22}t^2+12\sigma_{12}t+6\sigma_{11}\end{pmatrix}(x,p)^T}, \tag{D.12}$$

where $\Xi = \Xi(t,\nu,\sigma_{11},\sigma_{22},\sigma_{12}) = 2\nu^2t^6 + 18\nu\sigma_{22}t^4 + 48\nu\sigma_{12}t^3 + 36\nu\sigma_{11}t^2 + 36|\Sigma|$. The state w can be rewritten in a much more appealing form

$$w(x,p,t) = \frac{1}{2\pi\sqrt{|\hat{\Sigma}^{-1}|}}e^{-\frac{1}{2}(x,p)\hat{\Sigma}(x,p)^T} = \mathcal{N}(0,\hat{\Sigma}^{-1}), \tag{D.13}$$

where

$$\hat{\Sigma} = \frac{6}{\Xi}\begin{pmatrix} 6(\sigma_{22}+t^2\nu) & -2(3\sigma_{12}+3\sigma_{22}t+t^3\nu) \\ -2(3\sigma_{12}+3\sigma_{22}t+t^3\nu) & t^4\nu+6\sigma_{22}t^2+12\sigma_{12}t+6\sigma_{11}\end{pmatrix}, \tag{D.14}$$

so w is just a Gaussian function centred around $\mathbf{0}$ with the covariance matrix given by $\hat{\Sigma}^{-1}$. As an approach to distinguish between these two states, we calculate two metrics, the normalised Hilbert-Schmidt norm

$$d_1(\varrho_1,\varrho_2) := \frac{\sqrt{\int[\varrho_1(x,p,t)-\varrho_2(x,p,t)]^2dxdp}}{\sqrt{\int\varrho_1^2(x,p,t)dxdp} + \sqrt{\int\varrho_2^2(x,p,t)dxdp}}, \tag{D.15}$$

and normalised overlap function

$$d_2(\varrho_1,\varrho_2) := 1 - \frac{\int \varrho_1(x,p,t)\varrho_2(x,p,t)dxdp}{\sqrt{\int \varrho_1^2(x,p,t)dxdp}\sqrt{\int \varrho_2^2(x,p,t)dxdp}}, \tag{D.16}$$

as these two measures can be directly translated from the density matrix approach in terms of the Weyl transform. Both functions considered are in the Gaussian form with respect to (x,p) variables, thus calculations can be conducted analytically. The distance d_1 between the approximated state w and the mean state R is equal to

$$\begin{aligned} d_1(w,R) = \Bigg(&\frac{3}{2\pi}\frac{1}{\sqrt{\Xi}} + \int\int P(E)P(E')\mathcal{N}_{\boldsymbol{\mu}(t,E)}(\boldsymbol{\mu}(t,E'),2\Sigma)dEdE' \\ &-2\int P(E)\mathcal{N}_{\hat{A}(-t)\boldsymbol{\mu}(t,E)}(\mathbf{0},\hat{A}(-t)\Sigma\hat{A}(-t)^T+\hat{\Sigma}^{-1})dE\Bigg)^{\frac{1}{2}} \\ &\times\left(\sqrt{\frac{3}{2\pi}}\Xi^{-\frac{1}{4}} + \left(\int\int P(E)P(E')\mathcal{N}_{\boldsymbol{\mu}(t,E)}(\boldsymbol{\mu}(t,E'),2\Sigma)dEdE'\right)^{\frac{1}{2}}\right)^{-1}, \end{aligned} \tag{D.17}$$

whereas d_2 is given by

$$d_2(w,R) = \frac{1}{2}\sqrt{2 - 2\frac{\int P(E)\mathcal{N}_{\hat{A}(-t)\boldsymbol{\mu}(E,t)}(\mathbf{0},\hat{A}(-t)\Sigma\hat{A}(-t)^T+\hat{\Sigma}^{-1})dE}{\sqrt{\frac{3}{2\pi}}\Xi^{-\frac{1}{4}}\left(\int\int P(E)P(E')\mathcal{N}_{\boldsymbol{\mu}(t,E)}(\boldsymbol{\mu}(t,E'),2\Sigma)dEdE'\right)^{\frac{1}{2}}}}. \tag{D.18}$$

The simplest check for the validity of the results presented is taking $P(E)=\delta(E)$, which simultaneously implies $\nu=0$, by the previous assumption $\langle E\rangle = 0$, and the dynamics resembles that of the free particle for both equations. Then

$$d_1(w,R) = d_2(w,R) = 0. \tag{D.19}$$

This equality should also hold for an arbitrary probability distribution $P(E)$, at $t=0$. For further analysis, we consider distributions $P(E)$ such that $\langle E\rangle = 0$ and $0 < \sigma(E) < +\infty$. As a first distribution, the continuous uniform distribution is considered with the domain extending over the interval $E\in[-1,1]$, thus $P(E)=1/2$. As a second case, the Gaussian distribution centred around 0 is considered. For simplicity and to reduce the number of parameters, the standard normal distribution will be used, that is, $E\sim\mathcal{N}_E(0,1)$. Last but not least, a generalised Gaussian distribution centred around $E=0$ will be considered. As depicted in the charts, the discrepancy between two WDFs increases quickly throughout the evolution, To provide the order of change of the $d_i(t)$ with respect to time t, a log-log scale was applied to the chart, and linear regression was performed. The tangent coefficient was equal to 2.89 which suggests that for $t \ll 1$ the order of increase in distance is of $d_i(t) \sim t^3$. To keep states closer to each other, one may sharpen the probability distribution around $E=0$, as by the previously mentioned property, for $P(E)=\delta(E)$ one has $d_1(t)=d_2(t)=0$.

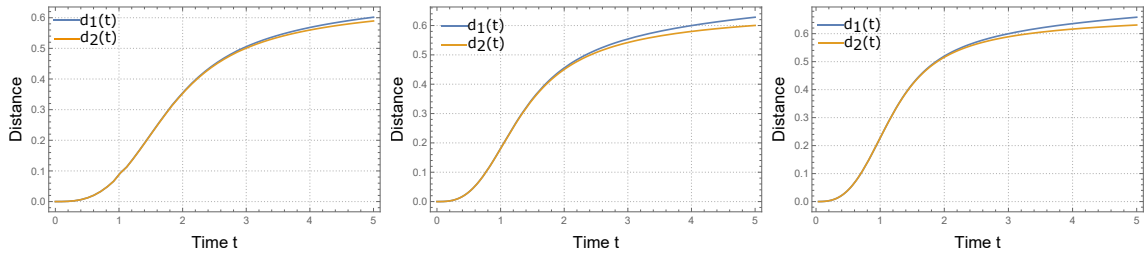

Figure D.1: Comparison of the distance functions $d_1(t), d_2(t)$ for different probability distributions $P(E)$. Starting from the left: the uniform distribution, the standard normal distribution and generalised Gaussian distribution

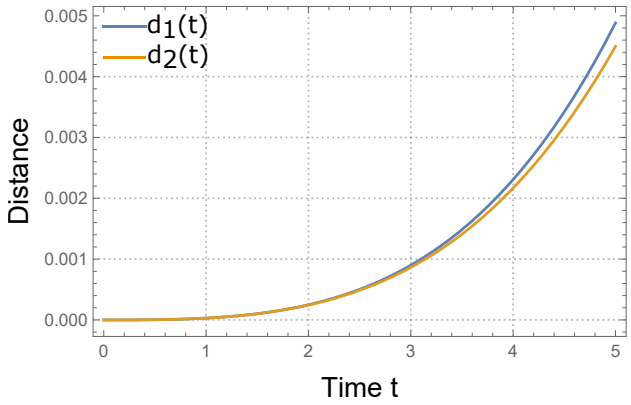

Figure D.2: The distance functions $d_1(t), d_2(t)$ for normal distribution with standard deviation $\sigma = 0.01$. The similarity of the states holds longer than in previous cases, for both measures.

This is rather a property of system considered, than the general trait of the averaged system.

Appendix E

The $\left\langle \Delta^2 \right\rangle$ formula for considered distributions.

In this appendix, we would like to show the exact form for the $\left\langle \Delta^2 \right\rangle$ operator present in the approximated equation of motion for the averaged WDF. We will consider a random $(2N+1)$ dimensional vector $\boldsymbol{\lambda}$ with uncorrelated entries. Each random variable contributing to this vector will be drawn from either a uniform or a Gaussian probability distribution. Before providing an explicit formula for probability distributions, we will simplify the $-\left\langle \Delta^2(\boldsymbol{\lambda}) \right\rangle_{\boldsymbol{\lambda}}$ expression (4.94). We keep $\hbar = 1$ throughout the calculations.

$$\begin{aligned} -\left\langle \Delta^2(\boldsymbol{\lambda}) \right\rangle_{\boldsymbol{\lambda}} &= \int P(\boldsymbol{\lambda}) \left[\delta V \left(\boldsymbol{x} + \frac{i\hbar}{2} \nabla_{\boldsymbol{p}}; \boldsymbol{\lambda} \right) - \delta V \left(\boldsymbol{x} - \frac{i\hbar}{2} \nabla_{\boldsymbol{p}}; \boldsymbol{\lambda} \right) \right]^2 d\boldsymbol{\lambda} \\ &= \int P(\boldsymbol{\lambda}) \left[\delta V^2 \left(\boldsymbol{x} + \frac{i\hbar}{2} \nabla_{\boldsymbol{p}}; \boldsymbol{\lambda} \right) + \delta V^2 \left(\boldsymbol{x} - \frac{i\hbar}{2} \nabla_{\boldsymbol{p}}; \boldsymbol{\lambda} \right) \right. \\ &\quad \left. -2\delta V \left(\boldsymbol{x} + \frac{i\hbar}{2} \nabla_{\boldsymbol{p}}, t; \boldsymbol{\lambda} \right) \delta V \left(\boldsymbol{x} - \frac{i\hbar}{2} \nabla_{\boldsymbol{p}}; \boldsymbol{\lambda} \right) \right] d\boldsymbol{\lambda}. \end{aligned} \tag{E.1}$$

Recall, that the minus sign is a result of a composition of two Moyal brackets. Let us introduce an operator $\hat{x}^{\pm} := \boldsymbol{x} \pm \frac{i}{2} \nabla_{\boldsymbol{p}}$. Then using the definition of δV (4.93) this expression can be simplified to the following

$$\begin{aligned} -\left\langle \Delta^2(\boldsymbol{\lambda}) \right\rangle_{\boldsymbol{\lambda}} &= \int P(\boldsymbol{\lambda}) \left[V^2 \left(\hat{x}^+; \boldsymbol{\lambda} \right) + V^2 \left(\hat{x}^-; \boldsymbol{\lambda} \right) - 2V \left(\hat{x}^+; \boldsymbol{\lambda} \right) V \left(\hat{x}^-; \boldsymbol{\lambda} \right) \right] d\boldsymbol{\lambda} \\ &\quad - \left[\bar{V}^2(\hat{x}^+) + \bar{V}^2(\hat{x}^-) - 2\bar{V}(\hat{x}^+)\bar{V}(\hat{x}^-) \right]. \end{aligned} \tag{E.2}$$

Consequently, to calculate the correction to the dynamics, we have to find the following quantities

$$\left\langle V^2(\hat{x}^{\pm}; \boldsymbol{\lambda}) \right\rangle_{\boldsymbol{\lambda}} = \int P(\boldsymbol{\lambda}) V^2(\hat{x}^{\pm}; \boldsymbol{\lambda}) d\boldsymbol{\lambda}, \tag{E.3}$$

and

$$\left\langle V(\hat{x}^+; \boldsymbol{\lambda}) V(\hat{x}^-; \boldsymbol{\lambda}) \right\rangle_{\boldsymbol{\lambda}} = \int P(\boldsymbol{\lambda}) V(\hat{x}^+; \boldsymbol{\lambda}) V(\hat{x}^-; \boldsymbol{\lambda}) d\boldsymbol{\lambda}. \tag{E.4}$$

We will use the following notation $\mathcal{N}(x; \mu, \sigma^2)$ for the x-dependent Gaussian distribution with mean μ and deviation σ. Now, we calculate all the expressions using the following forms of the PDF $P(\boldsymbol{\lambda})$:

E.1 The Gaussian distribution

We considered a constituent PDFs in the following form

$$f(\lambda_k) = \frac{1}{\sqrt{2\pi}w} e^{-\frac{1}{2w^2}\lambda_k^2} = \mathcal{N}(\lambda_k; 0, w^2) \quad \lambda_k \in \mathbb{R}, \tag{E.5}$$

then the full probability distribution for the random vector $\boldsymbol{\lambda}$ is

$$P(\boldsymbol{\lambda}) = \prod_{k=-N}^{N} f(\lambda_k) = \left(\frac{1}{\sqrt{2\pi}w}\right)^{2N+1} e^{-\frac{1}{2w^2}|\boldsymbol{\lambda}|^2}. \tag{E.6}$$

Recall that the mean potential field is given by the following formula (4.99)

$$\bar{V}_2(x) = \frac{V_0}{\sqrt{2\pi(\sigma^2+w^2)}} \sum_{k=-N}^{N} e^{-\frac{(x-k\mu)^2}{2(\sigma^2+w^2)}} = V_0 \sum_{k=-N}^{N} \mathcal{N}(x; k\mu, \sigma^2+w^2), \tag{E.7}$$

then we get the following expressions:

$$\begin{aligned}\left\langle V^2(\hat{x}^{\pm};\boldsymbol{\lambda})\right\rangle_{\boldsymbol{\lambda}} = V_0^2 \sum_{\substack{k_1,k_2=-N \\ k_1\neq k_2}}^{N} \mathcal{N}\left(k_1\mu; k_2\mu, 2(w^2+\sigma^2)\right) \mathcal{N}\left(\hat{x}^{\pm}; \frac{\mu}{2}(k_1+k_2), \frac{1}{2}(w^2+\sigma^2)\right) \\ + \frac{V_0^2}{2\sqrt{\pi}\sigma} \sum_{k=-N}^{N} \mathcal{N}\left(\hat{x}^{\pm}; k\mu, \frac{\sigma^2}{2}+w^2\right),\end{aligned} \tag{E.8}$$

and furthermore

$$\begin{aligned}\left\langle V(\hat{x}^{+};\boldsymbol{\lambda})V(\hat{x}^{-};\boldsymbol{\lambda})\right\rangle_{\boldsymbol{\lambda}} = V_0^2 \sum_{\substack{k_1,k_2=-N \\ k_1\neq k_2}}^{N} \mathcal{N}\left(\hat{x}^{+}; k_1\mu, w^2+\sigma^2\right) \mathcal{N}\left(\hat{x}^{-}; k_2\mu, w^2+\sigma^2\right) \\ + V_0^2 \mathcal{N}\left(\hat{x}^{+}-\hat{x}^{-}; 0, 2\sigma^2\right) \sum_{k=-N}^{N} \mathcal{N}\left(\frac{\hat{x}^{+}+\hat{x}^{-}}{2}; k\mu, \frac{\sigma^2}{2}+w^2\right).\end{aligned} \tag{E.9}$$

Then, the expression (E.2) can be rewritten with the help of the following differences

$$\begin{aligned}\left\langle V^2(\hat{x}^{\pm};\boldsymbol{\lambda})\right\rangle_{\boldsymbol{\lambda}} - \bar{V}^2(\hat{x}^{\pm}) = \frac{V_0^2}{2\sqrt{\pi}} \sum_{k=-N}^{N} \left[\frac{1}{\sigma}\mathcal{N}\left(\hat{x}^{\pm}; k\mu, \frac{\sigma^2}{2}+w^2\right)\right. \\ \left. - \frac{1}{\sqrt{\sigma^2+w^2}}\mathcal{N}\left(\hat{x}^{\pm}; k\mu, \frac{\sigma^2+w^2}{2}\right)\right],\end{aligned} \tag{E.10}$$

and

$$\begin{aligned}\left\langle V(\hat{x}^{+};\boldsymbol{\lambda})V(\hat{x}^{-};\boldsymbol{\lambda})\right\rangle_{\boldsymbol{\lambda}} - \bar{V}(\hat{x}^{+})\bar{V}(\hat{x}^{-}) = V_0^2 \sum_{k=-N}^{N} \left[\mathcal{N}(\hat{x}^{+}-\hat{x}^{-}; 0, 2\sigma^2)\mathcal{N}\left(\frac{\hat{x}^{+}+\hat{x}^{-}}{2}; k\mu, w^2+\frac{\sigma^2}{2}\right)\right. \\ \left. - \mathcal{N}(\hat{x}^{+}; k\mu, \sigma^2+w^2)\mathcal{N}(\hat{x}^{-}; k\mu, \sigma^2+w^2)\right].\end{aligned} \tag{E.11}$$

E.2 The uniform distribution

We considered a constituent PDFs in the following form

$$f(\lambda_k) = \frac{1}{2\alpha\sigma}\theta(|\lambda_k| \leq \alpha\sigma), \tag{E.12}$$

then the full probability distribution for the random vector $\boldsymbol{\lambda}$ is given by

$$P(\boldsymbol{\lambda}) = \prod_{k=-N}^{N} f(\lambda_k) = \left(\frac{1}{2\alpha\sigma}\right)^{2N+1}. \tag{E.13}$$

Recall that the mean potential field is given by the following formula (4.99)

$$\bar{V}_1(x) = \frac{V_0}{4\alpha\sigma}\sum_{k=-N}^{N}\left[\operatorname{erf}\left(\frac{\alpha\sigma - x + k\mu}{\sqrt{2}\sigma}\right) + \operatorname{erf}\left(\frac{\alpha\sigma + x - k\mu}{\sqrt{2}\sigma}\right)\right], \tag{E.14}$$

with it, we get the following expressions:

$$\begin{aligned}\left\langle V^2(\hat{x}^{\pm};\boldsymbol{\lambda})\right\rangle_{\boldsymbol{\lambda}} = \frac{V_0^2}{16\alpha^2\sigma^2}\sum_{\substack{k_1,k_2=-N\\k_1\neq k_2}}^{N}\left[\operatorname{erf}\left(\frac{u+k_1\mu-\hat{x}^{\pm}}{\sqrt{2}\sigma}\right)\right]\Bigg|_{u=-\alpha\sigma}^{u=\alpha\sigma}\left[\operatorname{erf}\left(\frac{v+k_2\mu-\hat{x}^{\pm}}{\sqrt{2}\sigma}\right)\right]\Bigg|_{v=-\alpha\sigma}^{v=\alpha\sigma}\\ + \frac{V_0^2}{8\sqrt{\pi}\alpha\sigma^2}\sum_{k=-N}^{N}\left[\operatorname{erf}\left(\frac{u+k\mu-\hat{x}^{\pm}}{\sigma}\right)\right]\Bigg|_{u=-\alpha\sigma}^{u=\alpha\sigma},\end{aligned} \tag{E.15}$$

and complementarily

$$\begin{aligned}\left\langle V(\hat{x}^{+};\boldsymbol{\lambda})V(\hat{x}^{-};\boldsymbol{\lambda})\right\rangle_{\boldsymbol{\lambda}} = \frac{V_0^2}{16\alpha^2\sigma^2}\sum_{\substack{k_1,k_2=-N\\k_1\neq k_2}}^{N}\left[\operatorname{erf}\left(\frac{u+k_1\mu-\hat{x}^{+}}{\sqrt{2}\sigma}\right)\right]\Bigg|_{u=-\alpha\sigma}^{u=\alpha\sigma}\left[\operatorname{erf}\left(\frac{v+k_2\mu-\hat{x}^{-}}{\sqrt{2}\sigma}\right)\right]\Bigg|_{v=-\alpha\sigma}^{v=\alpha\sigma}\\ + \frac{V_0^2}{4\alpha\sigma}\mathcal{N}\left(\hat{x}^{+}-\hat{x}^{-};0,2\sigma^2\right)\sum_{k=-N}^{N}\left[\operatorname{erf}\left(\frac{u-2k\mu+\hat{x}^{+}+\hat{x}^{-}}{2\sigma}\right)\right]\Bigg|_{u=-\alpha\sigma}^{u=\alpha\sigma}.\end{aligned} \tag{E.16}$$

Thus, in general, we can express the differences present in Eq. (E.2) as

$$\begin{aligned}\left\langle V^2(\hat{x}^{\pm};\boldsymbol{\lambda})\right\rangle_{\boldsymbol{\lambda}} - \bar{V}^2(\hat{x}^{\pm}) = \frac{V_0^2}{8\sqrt{\pi}\alpha\sigma^2}\sum_{k=-N}^{N}\left[\operatorname{erf}\left(\frac{\alpha\sigma+k\mu-\hat{x}^{\pm}}{\sigma}\right) + \operatorname{erf}\left(\frac{\alpha\sigma-k\mu+\hat{x}^{\pm}}{\sigma}\right)\right]\\ - \frac{V_0^2}{16\sigma^2\alpha^2}\sum_{k=-N}^{N}\left[\operatorname{erf}\left(\frac{\alpha\sigma+k\mu-\hat{x}^{\pm}}{\sqrt{2}\sigma}\right) + \operatorname{erf}\left(\frac{\alpha\sigma-k\mu+\hat{x}^{\pm}}{\sqrt{2}\sigma}\right)\right]^2\end{aligned} \tag{E.17}$$

whereas mixed terms can be written as

$$\begin{aligned}\left\langle V(\hat{x}^{+};\boldsymbol{\lambda})V(\hat{x}^{-};\boldsymbol{\lambda})\right\rangle_{\boldsymbol{\lambda}} - \bar{V}(\hat{x}^{+})\bar{V}(\hat{x}^{-}) = \frac{V_0^2}{4\alpha\sigma}\mathcal{N}(\hat{x}^{+}-\hat{x}^{-};0,2\sigma^2)\\ \times\sum_{k=-N}^{N}\left[\operatorname{erf}\left(\frac{\alpha\sigma-2k\mu+\hat{x}^{+}+\hat{x}^{-}}{2\sigma}\right) + \operatorname{erf}\left(\frac{\alpha\sigma+2k\mu-\hat{x}^{+}-\hat{x}^{-}}{2\sigma}\right)\right]\\ - \frac{V_0^2}{16\alpha^2\sigma^2}\sum_{k=-N}^{N}\left(\left[\operatorname{erf}\left(\frac{\alpha\sigma+k\mu-\hat{x}^{+}}{\sqrt{2}\sigma}\right) + \operatorname{erf}\left(\frac{\alpha\sigma-k\mu+\hat{x}^{+}}{\sqrt{2}\sigma}\right)\right]\right.\\ \left.\times\left[\operatorname{erf}\left(\frac{\alpha\sigma+k\mu-\hat{x}^{-}}{\sqrt{2}\sigma}\right) + \operatorname{erf}\left(\frac{\alpha\sigma-k\mu+\hat{x}^{-}}{\sqrt{2}\sigma}\right)\right]\right)\end{aligned} \tag{E.18}$$

Both cases lead to overcomplicated expressions, and any way of implementing them numerically seems futile, bearing in mind the possibility of encountering an infinite series of operators. However, the operators $\hat{x}^{\pm}$, under the Fourier transformation, can be re-expressed as $x \pm \frac{1}{2}y$ where y is a Fourier variable associated with momentum p. In conclusion, both expressions can be implemented, and the behaviour of the proposed equation of motion for the averaged WDF can be investigated. However, this was not the approach we used in this work, as manual rewriting of such expressions is error-prone, and thus statistical estimators of those expressions were used instead.

Appendix F

Related articles and copyright statements

- The article: **Wignerian symplectic covariance approach to the interaction-time problem [185]**. According to the Scientific Reports policy, the reprint of the manuscript within the thesis is guided by the Nature Portfolio guidelines, which state: *Authors have the right to reuse their article's Version of Record, in whole or in part, in their own thesis. Additionally, they may reproduce and make available their thesis, including Springer Nature content, as required by their awarding academic institution.*[1]

[1] Author reuse section in: https://www.nature.com/nature-portfolio/reprints-and-permissions/permissions-requests#types¸

www.nature.com/scientificreports

scientific reports

Check for updates

OPEN

Wignerian symplectic covariance approach to the interaction-time problem

D. Woźniak[1], M. Kalka[1], D. Kołaczek[2], M. Wołoszyn[1] & B. J. Spisak[1]✉

The concept of the symplectic covariance property of the Wigner distribution function and the symplectic invariance of the Wigner–Rényi entropies has been leveraged to estimate the interaction time of the moving quantum state in the presence of an absolutely integrable time-dependent potential. For this study, the considered scattering centre is represented initially by the Gaussian barrier. Two modifications of this potential energy are considered: a sudden change from barrier to barrier and from barrier to well. The scattering state is prepared in the form of a Schrödinger cat, and the Moyal equation governs its further time evolution. The whole analysis of the considered scattering problem is conducted in the above-barrier regime using the phase-space representation of quantum theory. The presented concept shifts the focus from the dynamics of the quantum state to a symplectically invariant state functions in the form of the Wigner–Rényi entropies of order one and one-half. These quantities serve as indicators of the beginning and end of the interaction of the non-Gaussian state with the sufficiently fast decaying potential representing the scattering centre. The presented approach is significant because it provides a new way to estimate the interaction time of moving quantum states with the dynamical scattering centre. Moreover, it allows for studying scattering processes in various physical systems, including atoms, molecules, and condensed matter systems.

Keywords Symplectic covariance, Traversal time, Wigner distribution function, Schrödinger cat state, Wigner–Rényi entropy

It is widely assumed that the scattering experiments provide valuable information about the quantum systems studied[1]. The elementary model of the scattering process assumes the existence of a region of space (interaction zone) where a relevant scatterer effectively interacts with an incident beam or an impulse of light or particles. As a result of this interaction, the outgoing state of the beam or impulse changes depending on the mechanism of this interaction, and analysis of this state allows one to draw conclusions regarding the scatterer. One of the most intriguing issues arising from this description concerns the traversal time, i.e. the time it takes for a particle to traverse the considered region[2,3]. Light and matter's wave nature makes this issue complex, especially when the scattering description is beyond the plane-wave approximation[4,5]. Such approximation is highly desired in real situations because the incident wave is rarely monoenergetic. This variety of energy spectrum of the state allows for simultaneous mixture of scattering and tunneling behavior leading to challenging analysis of these components of the dynamics on the experimental basis. Hence, the traversal time can be rather viewed as the time of interaction of the quantum state with the finite-range potential barrier. This problem has been arousing widespread interest for a long time, but also some controversy[6,7]. Nevertheless, due to the development of measurement techniques[8,9], it seems advisable to generalize the question[6] 'How long does it take to tunnel through a barrier?', and instead of asking about the tunnelling time, we should ask about the interaction time. This issue is now becoming particularly relevant because the results of Spierings and Steinberg's experiments[10] have paved the way for the comparison of measurements with the direct and indirect theoretical measures of barrier crossing times, see Ref.[11] and references therein. Those inspiring results create the possibility of searching methods and research tools enabling a quantitative determination of the interaction time, regardless of whether we are in the scattering or tunnelling regime. Analyzing this issue within Wigner's phase-space formalism, we discovered a universally applicable method of assessing the interaction times based on well-established physical concepts like entropy or entropic measures. This method is deeply embedded in the symplectic covariance

[1]Faculty of Physics and Applied Computer Science, AGH University of Krakow, al. Mickiewicza 30, 30-059 Kraków, Poland. [2]Department of Applied Mathematics, University of Agriculture in Kraków, ul. Balicka 253c, 30-198 Kraków, Poland. ✉email: bjs@agh.edu.pl

www.nature.com/scientificreports/

property of the Wigner distribution function (WDF)[12–14]. This function is commonly used to describe the quantum states of the system in the phase space[15–22]. Especially for pure states, the WDF is defined as follows[23,24]

$$\mathscr{W}(\psi)(x,p)=\frac{1}{2\pi\hbar}\int_{\mathbb{R}}dX\ \psi\left(x+\frac{X}{2}\right)\psi^{*}\left(x-\frac{X}{2}\right)\exp\left(-\frac{i}{\hbar}pX\right), \tag{1}$$

where $\psi(\cdot)\in L^2(\mathbb{R},dx)$ is the wave function, and the rest of the symbols have the usual meaning. Surprisingly, if one is considering only pure states, then the interpretation of WDF not only as the phase-space distribution but rather the probability amplitude function is valid, as stated in[25], allowing for wider entropic analysis[26]. It is worth noting here that the WDF, up to a multiplicative constant, is the only quasi-probability distribution function that is covariant under both translations and all symplectic transformations (including shear transformations, rotations and scalings)[27]. The fundamental characteristic of these transformations lies in their ability to maintain the area occupied by the WDF regardless of the deformations they impose. Generally the area occupied by the WDF in the phase space is invariant with respect to the group of symplectic transformations[28]

$$Sp(1,\mathbb{R})=\left\{\mathbf{S}\in\mathscr{M}_{2\times2}(\mathbb{R}):\mathbf{S}^{T}\mathbf{J}\mathbf{S}=\mathbf{J}\right\}=\left\{\mathbf{S}\in\mathscr{M}_{2\times2}(\mathbb{R}):\det\mathbf{S}=1\right\}, \tag{2}$$

where $\mathscr{M}_{2\times2}(\mathbb{R})$ is the set of 2×2 real matrices and $\mathbf{J}$ is the standard symplectic matrix ($\mathbf{J}^T=-\mathbf{J}$ and $\mathbf{J}^2=-\mathbf{I}$, where $\mathbf{I}$ is the identity matrix). On the other hand, a symplectic change of variables performed on arguments of the WDF is equivalent to calculating the WDF for the transformed wave function at previous points. This property is known as the symplectic covariance of the WDF[29], and formally it can be expressed by the following equality:

$$\mathscr{W}\left(\hat{\mathscr{K}}_{\mathbf{S}}\psi\right)(x,p)=\mathscr{W}(\psi)\left(\mathbf{S}^{-1}[x\quad p]^{T}\right), \tag{3}$$

where $\mathbf{S}\in Sp(1,\mathbb{R})$ is the aforementioned symplectic matrix and $\hat{\mathscr{K}}_{\mathbf{S}}$ is an associated operator belonging to the metaplectic group $Mp(1)$ of unitary operators[30] that act in the Hilbert space of square-integrable functions $\psi(\cdot)\in L^2(\mathbb{R},dx)$. Let us note that the relation between $\hat{\mathscr{K}}_{\mathbf{S}}$ and $\mathbf{S}$ is two-to-one, so the difference in the choice of the operator $\hat{\mathscr{K}}_{\mathbf{S}}$ is barely in its sign[31]. This issue can be omitted in the presented discussion due to the insensitivity of the WDF to phase disturbance of the wave function. The meaning of the metaplectic operators is revealed in the description of the WDF dynamics. For this purpose, we consider the time dependence of the WDF that results from the time evolution of the wave function $\psi(\cdot;t)$ generated by the Cauchy problem in the form

$$\begin{cases} i\hbar\partial_t\psi(\cdot,t)=\hat{H}(t)\psi(\cdot,t), & t>0\\ \psi(\cdot,0)=\psi_0(\cdot), \end{cases} \tag{4}$$

where the wave function $\psi_0(\cdot)$ represents the initial condition and $\hat{H}(t)$ is the time-dependent one-particle Hamiltonian defined as the sum of the kinetic and potential parts of the considered system. The formal solution of Eq. (4) can be written as follows,

$$\psi(\cdot,t)=\hat{\mathscr{U}}(t,0)\psi_0(\cdot), \tag{5}$$

where $\hat{\mathscr{U}}(t,0)$ is the unitary time evolution operator[32]. If we assume the potential energy to be in the form of a polynomial of order two with time-dependent coefficients[33], then the operator $\hat{\mathscr{U}}(t,0)$ is a product of two unitary operators. The first one translates the wave function in position and momentum and also shifts the global phase of the wave function. The second one is a product of three metaplectic operators belonging to the group $Mp(1)$ hence it is also a metaplectic operator as shown in Refs.[34,35]. In particular, this statement holds in the case of motion in the free space. This observation is a starting point of our analysis; the time-evolution operator generated by the free-particle Hamiltonian is a metaplectic operator, and according to symplectic covariance property of WDF the following formula holds:

$$\int_{\mathbb{R}^2}dxdp\ f\left(\mathscr{W}\left(e^{-\frac{i}{\hbar}\frac{\hat{p}^2}{2m}t}\psi_0\right)(x,p)\right)=\int_{\mathbb{R}^2}dxdp\ f\left(\mathscr{W}(\psi_0)(x,p)\right), \tag{6}$$

where the function $f:[-1/(\pi\hbar),1/(\pi\hbar)]\to\mathbb{R}$ and both integrals are finite. This characteristic serves as the motivation for looking beyond the scenario of free propagation through the establishment of the time-dependent symplectically invariant measure $\zeta(t)$, according to the formula

$$\zeta(t):=\int_{\mathbb{R}^2}dxdp\ f\left(\mathscr{W}\left(\psi(t)\right)(x,p)\right). \tag{7}$$

Using these two equations we can conclude that the measure in question remains unchanged until a barrier potential disrupts the free motion. Owing to this property one can find a specific time interval for which the time evolution of the WDF differs from the free-space motion.

In Fig. 1, we present a qualitative explanation of the idea used.

First, the initial state evolves in free space (F), equivalently undergoing a symplectic shearing transformation. Following that, the result of this evolution is subjected to nonsymplectic deformations through the nonzero potential region (I). After that, such a deformed state evolves again as a state in free space (F), and its further evolution is symplectically invariant. In other words, we use the symplectic invariance of the quantum state resulting from the free motion in space to determine the interaction time through the non-zero potential energy region defining the interaction zone. One might pose the question of whether this concept, as per Eq. (7), can be extended to encompass cases involving harmonic or anharmonic potentials. While the answer is affirmative, it's crucial to keep in mind that arbitrary smooth potentials primarily display anharmonic repelling or harmonic bounding behavior in localized regions, such as close neighborhood of local extrema of the potential. Considering this, and the fact that the wave function's support is rarely compact, it leads us to the conclusion that these cases cannot serve as a reliable indicator of the interaction between a quantum object and a potential. In other words, there is always a portion of the wave function that interacts with the non-harmonic part of the potential, with the exception of cases involving pure ax^2 potentials, for $a \neq 0$.

In this paper, we use the symplectically invariant measures: Wigner–Rényi one-half entropy, Wigner–Shannon entropy to estimate the interaction time of the highly nonclassical state in the form of Schrödinger Cat (SC) state[36–40] with the Gaussian potential barrier with time-modulated amplitude. It opens an engaging perspective for spectroscopic methods, especially in application to quantum-optical spectroscopy with the goal of enhancing the signal and narrow spectral lines, as presented in Ref.[41,42]. To prove the usefulness, as well as to indicate the scope of applicability of the proposed method, we considered two limiting cases of the time-dependent scattering potential, i.e. we chose the potential amplitude in two ways. The first one corresponds to a single change in the value of the potential energy amplitude without changes in its sign, while the second one concerns its sign change without changes in the value. Based on both these cases, we directly determine the time-dependent Wigner–Shannon entropy[43–45] and the time-dependent Wigner–Rényi one-half entropy, recently examined as an equivalent measure of nonclassicality of the WDF[26] as two different examples of symplectically invariant measures. The careful analysis of these dynamical quantities allows us to estimate the interaction time in one of these cases. On the contrary, the second case is treated as a counterexample, illustrating the limitations of the offered method. We support these results by analyzing the dynamical transmission and capture coefficients which allow us to reinforce presented results.

Theoretical framework

Phase-space approach

In the following sections, we denote the time-dependent WDF as $\mathscr{W}(\psi(\cdot,t))(x,p) = \varrho(x,p,t)$ if there is no need to explicitly specify what the wave function of the quantum state is. This shorter notation allows us to introduce the explicit time dependence of the WDF in a compact way. According to the general rules describing the quantum systems in the phase space, dynamical variables $A(x, p)$ characterizing the considered system are expressed by the corresponding Weyl symbols, $a_W(x,p)$, which are functions defined on the phase space. The construction of the appropriate Weyl symbol is based on the Weyl transform[22], according to which the Hermitian operator, $\hat{A}(\hat{x},\hat{p})$, acting on the Hilbert space, is assigned the real function $a_W(x,p)$ expressed by the formula[46]

$$a_W(x,p) = \int_{\mathbb{R}} dX \left\langle x + \frac{X}{2} \middle| \hat{A}(\hat{x},\hat{p}) \middle| x - \frac{X}{2} \right\rangle \exp\left(-\frac{i}{\hbar} pX\right). \tag{8}$$

In the case of the time-dependent Hamiltonian of the one-particle system, $\hat{H} = \hat{p}^2/(2m) + W(\hat{x},t)$, the corresponding Weyl symbol, $H_{\mathrm{W}}(x,p,t)$, takes the form of the following real function

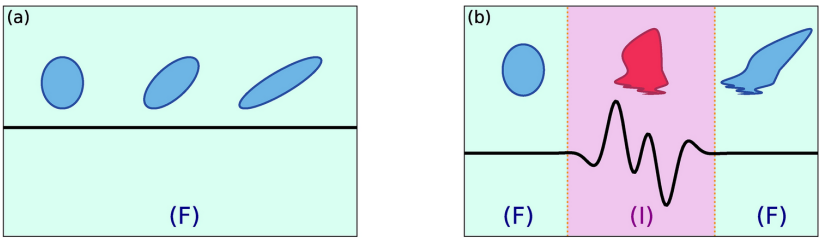

Fig. 1. The deformation of patch defined over p*ħ*ase space (x, p) under transformation generated by a free potential (a) and arbitrary potential (b) (marked with black line). For transformations generated by free particle potential (F), it is known that any patch defined on p*ħ*ase space undergoes shearing transformation, that is linear, momentum-dependent stretching. By the contrast, for area of interaction (I), transformation is no longer of this type, so no symplectic transformation can be assigned to such an operator. Thus, symplectic covariance property is violated resulting in changes in the symplectically invariant measure. This allows finding certain times t_i, t_f, for which given invariant measure respectively begins and ends to vary with time. This area of interaction is marked with purple color.

$$H_{\mathrm{W}}(x,p,t)=\frac{p^2}{2m}+W(x,t), \tag{9}$$

where $W(x, t)$ is the potential term assumed to be separable, i.e. $W(x,t)=U(x)\Sigma(t)$, wherein $U(x)$ is the short-range potential energy, i.e. it belongs to the class of absolutely integrable functions (cf. Supplementary Information for more details), and $\Sigma(t)$ is the time-dependent modulation factor of the potential amplitude. For the above-established Weyl symbol of the Hamiltonian, the time evolution of the WDF can be expressed by the Moyal equation,

$$\partial_t\varrho(x,p,t)=-\frac{p}{m}\partial_x\varrho(x,p,t)+\frac{1}{i\hbar}\left[U\left(x+\frac{i\hbar}{2}\partial_p\right)-U\left(x-\frac{i\hbar}{2}\partial_p\right)\right]\Sigma(t)\;\varrho(x,p,t). \tag{10}$$

The dynamics of the WDF generated by solving the initial value problem for the Moyal equation also requires establishing an initial condition. This initial condition is taken as the phase-space representation of the SC state for which the WDF is given by the formula

$$\begin{aligned}\varrho(x,p,0)=&A_1^2\frac{(1-\beta)}{\pi\hbar}\exp\left[-\frac{(x-x_1)^2}{2\delta_x^2}-\frac{2\delta_x^2(p-p_0)^2}{\hbar^2}\right]+A_1^2\frac{\beta}{\pi\hbar}\exp\left[-\frac{(x-x_2)^2}{2\delta_x^2}-\frac{2\delta_x^2(p-p_0)^2}{\hbar^2}\right]\\&+2A_1^2\frac{\sqrt{\beta(1-\beta)}}{\pi\hbar}\cos\left[\vartheta+\frac{p-p_0}{\hbar}(x_1-x_2)\right]\exp\left[-\frac{\left(x-\frac{x_1+x_2}{2}\right)^2}{2\delta_x^2}-\frac{2\delta_x^2(p-p_0)^2}{\hbar^2}\right],\end{aligned} \tag{11}$$

where the normalization factor A_1 has the form

$$A_1=\left[1+2\sqrt{\beta(1-\beta)}\exp\left(-\frac{(x_1-x_2)^2}{8\delta_x^2}\right)\right]^{-\frac{1}{2}}. \tag{12}$$

This state is further denoted as the SC-WDF. The first two terms of the SC-WDF correspond to the two Gaussian wave packets localized at the different phase-space points, namely (x_1,p_0) and (x_2,p_0). In turn, the last term represents the quantum interference pattern with a Gaussian envelope. This term is centered around the phase-space point $((x_1+x_2)/2,p_0)$ and rapidly oscillates along the x-axis. The set of parameters defining this SC-WDF is taken in the same form as follows: $\beta=0.5$, $\vartheta=0$, $\delta_x^2=500$ a.u., $x_1=-300$ a.u., $x_2=-500$ a.u. and $p_0=0.15$ a.u. This choice of parameters means that the initial SC-WDF is located to the left of the Gaussian barrier at a distance greater than its initial spatial dimension, and it approaches the barrier with the expected value of the kinetic energy slightly greater than the top of the barrier. It means that our computational scattering experiments are conducted in the above-barrier regime[47].

Dynamical characteristics

Due to the time-dependent character of the performed analysis, we propose the following set of dynamical quantities that characterize the system described by Eq. (9). The remaining dynamical quantities considered by us are based on the fact that the expression

$$\zeta(t)=\int_{\mathbb{R}^2}dxdp\;f\left(\varrho(x,p,t)\right) \tag{13}$$

is invariant under the time evolution governed by the Hamiltonian with the potential term in the form of a polynomial of the order less than or equal to 2, independent of the form of the function f (more details can be found in Supplementary Information). One of the quantities that can be understood in the sense of the above expression is the Wigner–Rényi entropic measure of order α which is defined for pure states as follows[26]

$$S_\alpha(t)=\frac{1}{1-\alpha}\ln\left[(2\pi\hbar)^{2\alpha-1}\int_{\mathbb{R}^2}dxdp\,|\varrho(x,p,t)|^{2\alpha}\right], \tag{14}$$

where α is the Rényi index ($\alpha\geq 0$ and $\alpha\neq 1$). However, for further analysis, we focus our attention on the special case of this entropy, namely $\alpha=1$, which corresponds to the Wigner–Shannon entropy[45]

$$S_1(t)=\lim_{\alpha\to 1}S_\alpha(t)=-\ln(2\pi\hbar)-2\pi\hbar\int_{\mathbb{R}^2}dxdp\,|\varrho(x,p,t)|^2\ln\varrho^2(x,p,t)\,, \tag{15}$$

where the coefficient $2\pi\hbar$ is a byproduct of normalization condition of the WDF in the $L^2(\mathbb{R}^2,dxdp)$ norm.

Another dynamic quantity consistent with the expression given by Eq. (7) is the time-dependent Wigner–Rényi one-half entropy which is equal to

$$S_{1/2}(t) = 2\ln\left(\int_{\mathbb{R}^2} dxdp\ |\varrho(x,p,t)|\right) + \ln(2\pi\hbar), \tag{16}$$

The Wigner–Rényi one-half entropy can be related to the nonclassicality parameter

$$\delta(t) = \int_{\mathbb{R}^2} dxdp\ |\varrho(x,p,t)| - 1, \tag{17}$$

which encapsulates information about the changes of the phase-space area occupied by the negative values of the WDF during the time evolution of this function[47–50]. According to the discussions concerning the symplectic invariance measures and the symplectic covariance of the WDF presented in earlier parts of this paper, these two dynamic quantities, i.e. the Wigner–Shannon entropy and the Wigner–Rényi one-half entropy, can be applied to determine the interaction time of the state represented by the WDF with the potential given in the form of absolutely integrable functions because these both quantities should be stabilized if the WDF leaves the interaction zone and its motion is recognized as the free movement. In other words, the end of the interaction process should be manifested by the absence of changes in the values of one of these quantities over time. Based on this observation, the time of interaction between the potential and the WDF can be calculated according to:

Proposition 1 *For a fixed Rényi index $\alpha > 0$ the interaction time τ, between state represented by the Wigner distribution function and potential energy belonging to the class of absolutely integrable functions, based upon Wigner–Rényi entropic measure, can be defined as*

$$\begin{aligned}\tau =& \min\{t \in \mathbb{R}_+ : |S_\alpha(t) - S_\alpha(\infty)| > \varepsilon(M-m)\}\\ &-\max\{t \in \mathbb{R}_+ : |S_\alpha(t) - S_\alpha(0)| > \varepsilon(M-m)\}\\ =& t_f - t_i,\end{aligned} \tag{18}$$

where $S_\alpha(t)$ is a Wigner–Rényi entropy with Rényi index α, $S_\alpha(0)$ is the value of the entropy at the beginning of the evolution, $S_\alpha(\infty)$ is the value at the end of the evolution, $M = \max_{t\in\mathbb{R}_+} S_\alpha(t)$ is the maximum of Wigner–Rényi entropic measure, $m = \min_{t\in\mathbb{R}_+} S_\alpha(t)$ is its minimum, and $0 < \varepsilon \ll 1$ is a dimensionless threshold parameter, that can be understood as the precision of the measuring device.

During the early evolution of the WDF, any $\zeta(t)$ is constant due to the lack of significant interaction between the potential and the initial condition; thus, one should expect nearly constant values of $\zeta(t)$ which implies a facilitated calculation of t_i. The problem arises when one tries to evaluate t_f because, as mentioned earlier, if the SC-WDF happens to settle in the well, then formally the interaction continues and as a result a symplectically invariant measure is nonconstant in long-time behavior. The criterion we propose to find t_f is the numerical analysis of the first derivative of the symplectically invariant measure with respect to time. The suitable choice of $\zeta(t)$ will be explained in detail within the next sections.

Results and discussion

Numerical algorithm

The following Fourier transforms,

$$\mathscr{F}_{1,x\to\lambda}\varrho(x,p,t) = \frac{1}{\sqrt{2\pi\hbar}}\int_{\mathbb{R}} dx\ e^{-\frac{i}{\hbar}\lambda x}\varrho(x,p,t) \tag{19}$$

$$\mathscr{F}^{-1}_{1,\lambda\to x}\tilde{\varrho}(\lambda,p,t) = \frac{1}{\sqrt{2\pi\hbar}}\int_{\mathbb{R}} d\lambda\ e^{\frac{i}{\hbar}\lambda x}\tilde{\varrho}(\lambda,p,t) \tag{20}$$

$$\mathscr{F}_{2,p\to y}\varrho(x,p,t) = \frac{1}{\sqrt{2\pi\hbar}}\int_{\mathbb{R}} dp\ e^{-\frac{i}{\hbar}py}\varrho(x,p,t) \tag{21}$$

$$\mathscr{F}^{-1}_{2,y\to p}\tilde{\varrho}(x,y,t) = \frac{1}{\sqrt{2\pi\hbar}}\int_{\mathbb{R}} dy\ e^{\frac{i}{\hbar}py}\tilde{\varrho}(x,y,t), \tag{22}$$

and the unitary equivalence of multiplication and derivative operators, i.e.,

$$\mathscr{F}^{-1}_{1,\lambda\to x}\lambda\mathscr{F}_{1,x\to\lambda} = \frac{i}{\hbar}\partial_x, \qquad \mathscr{F}^{-1}_{2,y\to p}y\mathscr{F}_{2,p\to y} = \frac{i}{\hbar}\partial_p, \tag{23}$$

allow us to transform Eq. (10) to the following form

$$\partial_t \varrho(x,p,t) = \left(-\frac{i}{\hbar m}\mathscr{F}^{-1}_{1,\lambda\to x} p\lambda \mathscr{F}_{1,x\to\lambda} + \frac{i}{\hbar}\Sigma(t)\mathscr{F}^{-1}_{2,y\to p} U_\Delta(x,y)\mathscr{F}_{2,p\to y}\right)\varrho(x,p,t), \tag{24}$$

where the variables λ and y are the canonically conjugate variables to x and p, respectively, as it results from the definition of the Fourier transform pairs (19)–(22), and the auxiliary function $U_\Delta(x,y)$ is defined as

$$U_\Delta(x,y) = U\left(x+\frac{y}{2}\right) - U\left(x-\frac{y}{2}\right). \tag{25}$$

In the presented case, $\Sigma(t)$ is a piecewise constant function. For this class of functions, the time evolution can be obtained by solving the dynamical problem in consecutive intervals where $\Sigma(t)$ is constant. For each of those intervals, we impose a new initial condition, taken as the state resulting from the previous stage of calculations.

Let $[t_k, t_{k+1})$ be the interval where $\Sigma(t) = u_k$, and $\{t_{k_j}\}_{j\in J}$ be a set of equidistant, by time step Δt, points within that interval for some set of indexes J. Then, the evolution within a given interval can be calculated using the Strang approximation for the exponential operator[51–54], as

$$\begin{aligned}\varrho(x,p,t_{k_{j+1}}) &= \varrho(x,p,t_{k_j}+\Delta t) = \exp\left(-\tfrac{i}{\hbar m}\mathscr{F}^{-1}_{1,\lambda\to x} p\lambda\mathscr{F}_{1,x\to\lambda} + \tfrac{i}{\hbar}u_k\mathscr{F}^{-1}_{2,y\to p}U_\Delta(x,y)\mathscr{F}_{2,p\to y}\right)\varrho(x,p,t_{k_j})\\ &\approx \mathscr{F}^{-1}_{1,\lambda\to x}\exp\left[-\frac{i\Delta t}{2m}\lambda p\right]\mathscr{F}_{1,x\to\lambda}\mathscr{F}^{-1}_{2,y\to p}\exp\left[iu_k\Delta t U_\Delta(x,y)\right]\mathscr{F}_{2,p\to y}\mathscr{F}^{-1}_{1,\lambda\to x}\exp\left[-\frac{i\Delta t}{2m}\lambda p\right]\mathscr{F}_{1,x\to\lambda}\varrho(x,p,t_{k_j}).\end{aligned} \tag{26}$$

The result of Eq. (26) gives the final state in time t_{k+1}, which becomes the initial condition for the next interval $[t_{k+1}, t_{k+2})$ with constant $\Sigma(t) = u_{k+1}$. This procedure is repeated to find the entire evolution of the WDF. The algorithm can be used for the single change in the amplitude of the potential at time t_s if one assumes that $t_0 = 0$, $t_1 = t_s$, $t_2 = t_{\mathrm{end}}$. Then, according to the formula above, the initial condition is iterated first within the interval $[0, t_s)$ preceded by iteration within $[t_s, t_{\mathrm{end}})$. Due to the fact that the Fast Fourier Transform is applicable for periodic boundary conditions, we propose a uniform grid of size $N_x \times N_p$ with right half-open intervals, where the box size is chosen so that the WDF vanishes at or near the boundaries during the whole simulation.

Simulation parameters

To construct the explicit form of the Weyl symbol of the Hamiltonian given by Eq. (9), we propose the potential energy part of $W(x, t)$ in the form of a Gaussian barrier,

$$U(x) = U_0 \exp\left[-\frac{(x-x_B)^2}{2w^2}\right], \tag{27}$$

with the following parameters: the center of the barrier localization is $x_B = 0$ a.u., the strength of this barrier is $U_0 = 0.008$ a.u., and its width is given by $w^2 = 50$ a.u. Let us note that the choice of the potential in the form of a Gaussian function guarantees that it is absolutely integrable. Moreover, this potential rapidly decays in the interval $L = [x_B - 3w, x_B + 3w]$, where w can be interpreted as the standard deviation. Hence, we conclude that at infinity the scattered state can be regarded as a free state. In turn, the time-dependent modulation factor of the potential amplitude $W(x, t)$, denoted by $\Sigma(t)$, is chosen in two ways. The first one illustrates a single change in the value of the potential energy amplitude without changes in its sign, while the second refers to its sign change without changes in the value. We discuss these two cases in consecutive subsections separately, because they clearly illustrate the presented idea, power of the method, and its limitations.

Simulations were performed on the grid with the size

- $x \in [-1500, 1500)$ a.u. with $N_x = 1024$,
- $p \in [-1, 1)$ a.u. with $N_p = 1024$,

and $t \in [0, 9000)$ a.u. with $N_t = 900$. That choice of parameters ensures that all points where the WDF is non-zero are always sufficiently far from the boundaries, so that no significant error propagates throughout the simulation.

One-time change in barrier height

As the first case, the single modulation of the amplitude is considered, resulting in lowering the barrier's height in half. To this end, for a fixed potential energy, $U(x)$, the potential term of the Moyal equation is given by the function $W(x,t) = U(x)\Sigma(t)$, where time-dependent modulation factor of the potential amplitude, $\Sigma(t)$, is assumed in the form

$$\Sigma(t) = 1 - 0.5\,\theta(t - t_s), \tag{28}$$

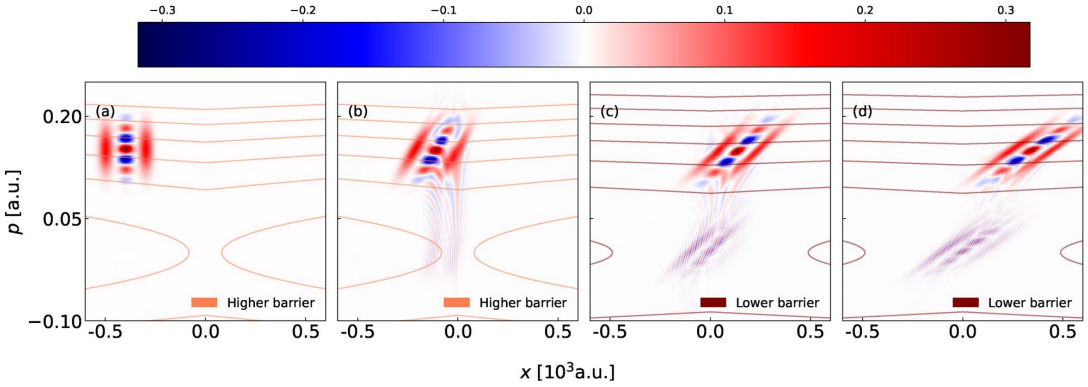

Fig. 2. The phase-space snapshot of the SC-WDF with a single potential change at $t_s = 2.1 \times 10^3$a.u. shown in snapshots taken at (**a**) $t = 0.0 \times 10^3$a.u., (**b**) 1.9×10^3a.u., (**c**) 3.6×10^3a.u. and (**d**) 5.0×10^3a.u. The red lines stand for the isolines of Hamiltonian for barrier before and after the cut down.

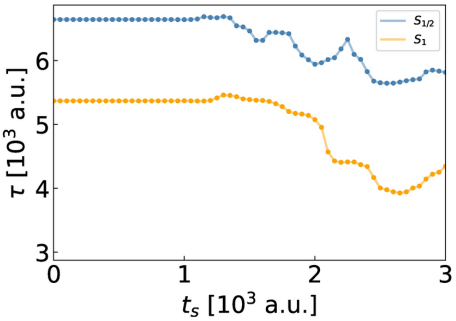

Fig. 3. The interaction time calculated as a function of switching time t_s. Results obtained are based on Wigner–Rényi one-half entropy $S_{1/2}(t)$, and Wigner–Shannon entropy $S_1(t)$.

where $\theta(\cdot)$ is the Heaviside function and t_s is the switching time corresponding to a sudden change in the amplitude of the potential by half of its initial value. This choice of the potential term allows us to find the time evolution of the WDF in the proposed model of the time-dependent potential by the numerical solution of the Moyal equation based on the previously discussed algorithm. The obtained results show that the initial state represented by the SC-WDF freely propagates towards the Gaussian barrier.

Depending on the time instant t_s, a greater or smaller part of the WDF might interact with the barrier undergoing scattering, before the sudden drop in the amplitude of the barrier. Then, the motion of the WDF continues in the region of the lowered barrier. In the long time, it is expected that the WDF will evolve freely, without any significant disruption from the scattering center. Figure 2 displays snapshots of the time evolution of the WDF in the phase space of the considered system at selected time instants. Let us note that these figures also contain several isolines of the classical Hamiltonian identical to its Weyl symbol. Most important concept of the system considered is that the potential governing the evolution of the WDF changes at t_s which disturbs the ongoing evolution of the WDF as seen in Fig. 2.

The interaction time was calculated, according to Proposition 1 with $\varepsilon = 0.01$, for different switching times t_s, as seen in Fig. 3. Apparently, one may notice some behavioral similarities between the two curves presented, especially for time $t_s < 1.4 \times 10^3$ a.u. the interaction time $\tau(t_s)$ is constant in value but the amplitudes differ in value. This is due to the fact that the Wigner–Shannon entropy stabilizes quicker, according to Fig. 4 than the Wigner–Renyi one-half entropy resulting in lower interaction time values.

Both figures depict a significant constant value of interaction time for $t_s \leq 1.5 \times 10^3$ a.u. For these times, the WDF interacts with the lower barrier of the 0.004 a.u. amplitude. As the time t_s increases, a more significant part of the WDF interacts with a high-amplitude barrier, and as a result, the disturbance from the constant value of interaction time τ occurs. The overall character of the subsequent t_s-dependence of τ is out of the scope of this work. Lastly, the overall character suggests that the appearance of a lower barrier while the

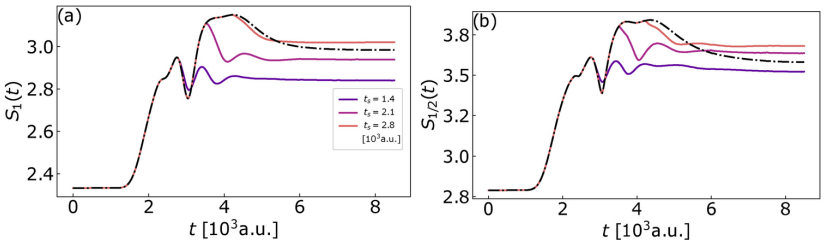

Fig. 4. The Wigner–Shannon entropy (**a**) and Wigner–Rényi one-half entropy (**b**) of the WDF state over time. Different colors stand for different potential switching times t_s and the black dash-dotted line corresponds to the case of time-independent potential barrier.

interaction is already taking place reduces the interaction time. Previously presented interaction time value can be supported by the time evolution of the symplectically invariant measures chosen for consideration, as shown in Fig. 4. The common characteristic of these two measures is that they are both a time-dependent functions that can be segmented into three different stages: before the interaction, during the interaction, and flattening after the interaction. The first part is a consequence of the rapid spatial decrease in potential energy, $U(x)$, at long distances, where it can be assumed to be nearly constant ($U(x) \approx \text{const}$). Thus, the WDF undergoes a shearing transformation, that is, a momentum-dependent translation that elongates the WDF. This evolution continues as long as the WDF is away from the potential barrier. When it reaches the interaction zone, the Wigner–Shannon entropy and the Wigner–Rényi one-half entropy start to vary over time. This is the result of breaking of the assumptions for symplectic invariance: the potential is no longer in the form of a polynomial of at most quadratic order. Last but not least, we have the flattening of these curves. The time at which any of the given symplectically invariant measures begins to vary from a constant value is assumed to be the start of the interaction t_i The time when the interaction stops, t_f, can be specified as the time when the symplectically invariant measure becomes flat (or nearly flat). This allows us to estimate the interaction time $\tau = t_f - t_i$ of the WDF with a potential $W(x, t)$, which in the presented case has the form shown in Fig. 3. The argument of the lack of the WDF interaction with the potential can be reinforced by additional analysis based on the measures quantifying overall character of the dynamics: dynamical transmission and dynamical capture coefficients. The former provides the information about the amount of the SC-WDF that passes through the interaction zone according to the formula,

$$P(t, x_P) = \int_{\mathbb{R}} \int_{x_P}^{\infty} dxdp\ \varrho(x, p, t). \tag{29}$$

For a fixed x_P we denote $P(t, x_P) = P(t)$. The position x_P is chosen in the region where the influence of the potential is negligible or, preferably, zero. Complementary to $P(t)$, we introduce the dynamical capture coefficient $C(t, \varepsilon)$, defined as

$$C(t, \varepsilon) = \int_{\mathbb{R}} \int_{L(\varepsilon)} dxdp\ \varrho(x, p, t), \tag{30}$$

which quantitatively describes the trapped part of the WDF. Analogically to $P(t)$ if ε is fixed, then $C(t, \varepsilon) = C(t)$. The interval $L(\varepsilon)$ is the region where the absolute value of the potential $U(x)$ is significantly nonzero, i.e. its values are greater than some fixed $\varepsilon > 0$. Complementary to the previously defined dynamical measures is the dynamical reflection coefficient, defined as

$$R(t, x_R) = \int_{\mathbb{R}} \int_{-\infty}^{x_R} dxdp\ \varrho(x, p, t), \tag{31}$$

where x_R is chosen sufficiently far from the initial condition so that it does not contribute to the reflected part of the WDF. It is expected that the following condition is held: $\lim_{t\to+\infty}[R(t, x_R) + C(t, \varepsilon) + P(t, x_P)] = 1$. The $P(t)$ and $C(t)$, as already mentioned, quantify the dynamics of the WDF as the amount of the quasi-probability distribution function present within given subspace of the p*ħ*ase-space of the system.

In Fig. 5a one can see the nondecreasing character of the dynamical transmission coefficient. As the switching time t_s increases, due to scattering, the lower amount of the WDF is transmitted through the interaction zone. For time instants t_s greater than the time for which purely scattering occurs, the dynamical transmission coefficient $P(t)$ will follow the same course as in the case of scattering on the static Gaussian barrier with amplitude 0.008 a.u. However, for lower values of the switching time t_s, the WDF interacts with the low-energy barrier, thus nearly the entire WDF goes above the barrier, resulting in a long-time behavior of the dynamical transmission

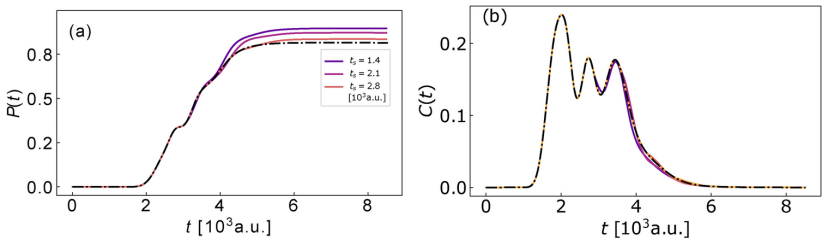

Fig. 5. (**a**) Dynamical transmission P, and (**b**) dynamical capture C coefficients as functions of time t in the case of barrier-to-barrier switching. Different colors stand for the different potential switching times t_s, and the black dash-dotted line corresponds to the case of time-independent potential barrier.

Measure	Reference	Interaction time [a.u.]	
		$t_s \in [0, 1200]$ [a.u.]	$t_s \in (1200, 3000]$ [a.u.]
$S_1(t)$ with $\varepsilon = 0.01$	This work	5368	3054–5460
$P(t)$	Tannor[4]	4550	4550–4562
$\langle \tau \rangle$	Dragoman[56]	5089	4545
$\langle t \rangle_T @ Y = 600$ a.u.	Pollak[57]	6632	6604–6833
$S_{1/2}(t)$ with $\varepsilon = 0.01$	This work	6642	4556–6688

Table 1. Comparison of interaction times based on different measures calculated in two ranges of the switching time t_s. Two ranges of the switching time t_s were selected because for $t_s < 1.2 \times 10^3$a.u., all of the presented interaction times have constant values.

coefficient that is nearly equal to one ($P(t) \approx 1.0$). The complementary measure is the capture coefficient $C(t)$, which indicates the amount of the WDF within the interaction zone with the potential. According to Fig. 5b, for long times (about $t > 6 \times 10^3$ a.u.) there is no interaction of WDF with the potential barrier. The black dash-dotted line presented in the Fig. 5 is associated with the dynamical transmission and capture coefficients in the case of the time-independent potential in the barrier state. This allows for juxtaposition of dynamical measures associated with stationary and time-varying barrier systems. Namely, one can visually track the behavior of quantum state parameters against the evolutionary properties of the same state governed by a simplified system. This curve of reference for the dynamical quantity of the simplified system is present in all figures to shed light on the behavior of considered potentials. Apart from strengthening of the arguments presented in previous figures, the dynamical capture coefficient opens a different perspective on the concept of the interaction time, which greatly differs in the physical interpretation. As $C(t)$ measures the amount of WDF that interacts with a strictly significant part of the potential, the time when $C(t)$ diverges from zero could be regarded as the start of the interaction. Similarly, the time when the dynamical capture coefficient approaches zero would be the end of the interaction between the WDF and the potential. While this insight might be correct for some classes of potentials, it tackles the problem of the interaction time from a different perspective. The interaction time defined by Proposition 1 is the distance in time space between two free propagating states. Physically means that there is no potential disturbing the evolution of the system. On the other hand, $C(t)$ measures the absence of the quantum state within the potential considered, regardless of the form of the quantum state before, and after the interaction. Let us note that the parameters of the time-dependent Gaussian barrier determine the interaction with the quantum state for the scattering process in terms of energy scale and space-time scale.

The preceding discussion demonstrates that the transmission and capture coefficients can also be employed as complementary measures to ascertain the SC-WDF's interaction time with the potential. This approach is commonly employed to characterize tunnelling and related phenomena through barriers[4,55]. It can, in particular, be utilized to estimate the interaction time straightforwardly. Let us note that these times can be read directly from Fig. 5. For this purpose, the moment when the transmission coefficient reaches one and the capture coefficient simultaneously reaches zero must be indicated with the given accuracy. The read-off results from Fig. 5 are provided in tabular form in Table 1. As is noticed, the values of these interaction times are similar in magnitude to those obtained using entropic methods based on Proposition 1. Although both methods yield comparable order of magnitude results, it is noteworthy that the transmission and capture coefficients are not symplectic invariant quantities. This is evidenced by the fact that they do not satisfy the property given by Eq. (6).

In addition to the method mentioned above, we decided to compare our results with two other approaches that enable estimating the interaction time. The first one is the method proposed by Dragoman[56]. It is a modified version of the Büttiker-Landauer semiclassical time, as presented in reference[2]. Based on this method, the interaction time can be estimated according to the formula

$$\tau(t) = \frac{d\int_0^d dx \int_{\mathbb{R}} dp\ \varrho(x,p,t)}{\int_0^d dx \int_{\mathbb{R}} dp\ (p/m)\varrho(x,p,t)}. \tag{32}$$

In our calculations we set $d = 6w$, where $w^2 = 50$ a.u. is the width of the Gaussian barrier. Direct application of Dragomon's method requires some modifications because it was initially formulated for the time-independent problem with the scatterer defined on the compact support of size d. For our purpose, we performed additional averaging of Eq. (32) over the simulation time. Hence, the time $\tau(t)$ is replaced by the averaging quantity, $\langle\tau\rangle$, by the formula

$$\langle\tau\rangle = \frac{1}{t_{end}}\int_0^{t_{end}} dt \left[\frac{6w\int_{-3w}^{3w} dx \int_{\mathbb{R}} dp\ \varrho(x,p,t)}{\int_{-3w}^{3w} dx \int_{\mathbb{R}} dp\ (p/m)\varrho(x,p,t)}\right], \tag{33}$$

where t_{end} is the time of the end of the simulation. The calculations were performed for the several switching times, t_s, and results are collected in Table 1. The estimated interaction times with this method are also comparable to those presented in this paper.

Pollak et al.[11,57,58] developed the second method of estimating the interaction time, with which we want to compare our results. This approach is referred to as the mean flight time method. According to this method, the interaction time can be determined as follows:

$$\langle t\rangle_T = \int_0^{\infty} dt\ tP(Y,t), \tag{34}$$

where $P(Y, t)$ is the flight-time distribution measured at the detector located at Y. The explicit expression for this quantity is given by the formula

$$P(Y,t) = \frac{|n(Y,t)|^2}{\int_0^{\infty} dt\ |n(Y,t)|^2}, \tag{35}$$

in which $n(Y, t)$ is the marginal distribution of the WDF with respect to the position Y. Its form is following

$$n(x = Y,t) = \int_{\mathbb{R}} dp\ \varrho(x = Y,p,t). \tag{36}$$

As recommended by the authors of the research mentioned above, the detector distance from the scattering centre should be at least as far as the initial location of the incident wavepacket. In the simulations that were carried out, the initial SC-WDF is located at a distance of $d = 500$ a.u. from the scattering centre. Thus, we have decided to evaluate mean flight time given by Eq. (34) for the detector, which is positioned at a distance $Y = 600$ a.u. The estimated interaction times obtained with this assumption for the several switching times, t_s, are presented in Table 1. As can be seen, these times are also of the same order of magnitude as those estimated based on our proposed method.

Finally, the presented comparative studies allow us to conclude that the entropic methods we propose estimate the interaction times range in a way consistent with that provided by other methods.

Previously, we examined the influence of changing the barrier height on the interaction time as a function of the switching time. However, we also expect that the interaction time depends on the barrier width while maintaining the same characteristics of the sampling state of the considered system. The results of these calculations are presented in Fig. 6. For a fixed value of the switching time, we determined the interaction time as a function of the Gaussian barrier width, w^2, based upon the time-dependent Wigner–Shannon entropy and the Wigner–Rényi one-half entropy. In both cases, we observe that an increase in the barrier width causes an increase in the interaction time, but the interaction times differ in numerical values. The interaction time determined with the help of the Wigner–Rényi one-half entropy is greater than its counterpart obtained using the Wigner–Shannon entropy. These results are consistent with conclusions resulting from the analysis Fig. 3, i.e. the symplectically invariant measure based on the Wigner–Rényi one-half entropy remains more sensitive on nonsymplectic WDF deformation due to its interaction with a barrier. Ipso facto forms the best estimation of the interaction time using entropic measures.

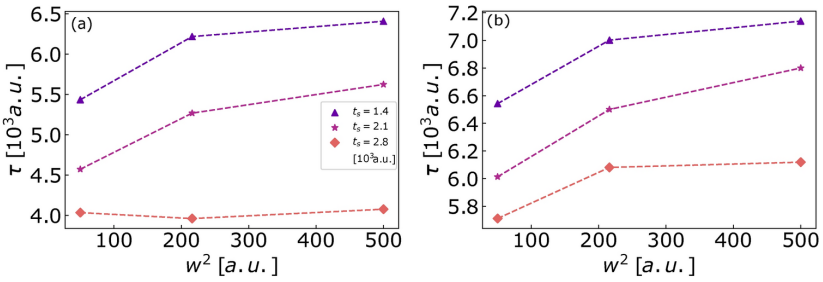

Fig. 6. Interaction time τ as a function of potential width w^2 for different switch times t_s, based upon (**a**) Wigner–Shannon entropy, (**b**) Wigner–Rényi one-half entropy.

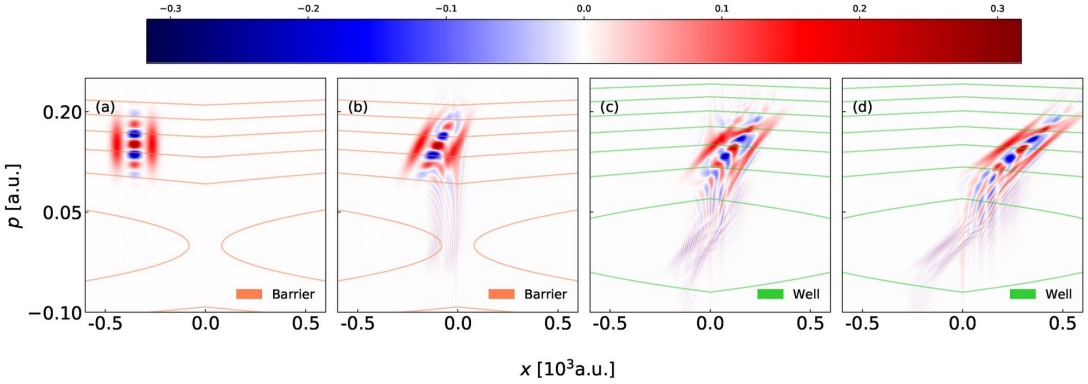

Fig. 7. The phase-space snapshot of the SC-WDF with a single potential change at $t_s = 2.1 \times 10^3$a.u. shown in snapshots taken at (**a**) $t = 0.0 \times 10^3$a.u., (**b**) 1.9×10^3a.u., (c) 3.6×10^3a.u. and (d) 5.0×10^3a.u. The red and green lines stand for the isolines of Hamiltonian for barrier and well forms of potential energy, respectively.

Barrier-well switching

In the following case, we consider a second setup in which the amplitude of the Gaussian potential changes sign once, which means that the Gaussian barrier becomes the Gaussian well. For this purpose, we assume that the time-dependent part of the potential term, $\Sigma(t)$, has the following form,

$$\Sigma(t) = 1 - 2\theta(t - t_s), \tag{37}$$

where $\theta(\cdot)$ is the Heaviside step and t_s is the switching time. As in the previous case, we determine the time evolution of the WDF by the numerical solution of the Moyal equation based on the discussed algorithm. The example snapshots of the WDF during its time evolution in the phase space are shown in Fig. 7 for $t_s = 2.1 \times 10^3$ a.u..

Qualitatively, the initial dynamics of the WDF, before approaching the interaction zone, resembles a free evolution, as can be seen in Fig. 7a. Any changes inflicted in the shape of the WDF directly result from shearing transformation, leading to the symplectic deformation of this function. Then, the freely evolving WDF enters the interaction zone, where it begins interacting with the potential barrier, as seen in Fig. 7b. In this case, all three elements of the time evolution can be highlighted: free movement of the highly energetic parts of the WDF, scattering and tunnelling of the intermediate and low energetic parts of the WDF. These last two processes are responsible for destroying the symplectic deformation of the WDF resulting from the free evolution of this state in the phase space.

During interaction, the Gaussian barrier is suddenly switched to the Gaussian well, forming a state that on one hand evolves with slight disturbance, and on the other is submitted partially to the bounding within potential well, as visible in Fig. 7c. Finally, we observe the trichotomy of the WDF in the form of transmitted, reflected and trapped parts. The overall form of the WDF deformation strongly depends on its trapped part, see Fig. 7d, sparking our interest due to its role in the interaction with the potential. To gain better understanding

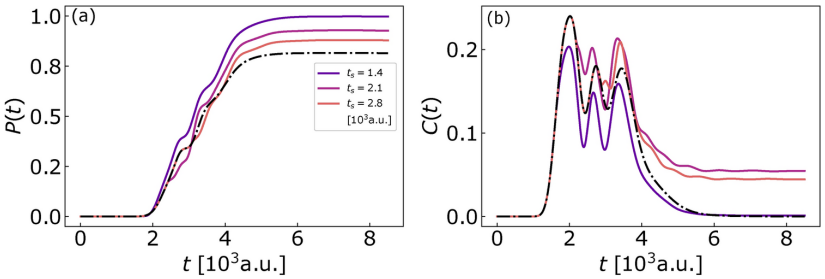

Fig. 8. (**a**) Dynamical transmission P, and (**b**) dynamical capture C coefficients as functions of time t, in the case of barrier-to-well switching. Different colors stand for the different potential switching times t_s and the black dash-dotted line corresponds to the case of time-independent potential barrier.

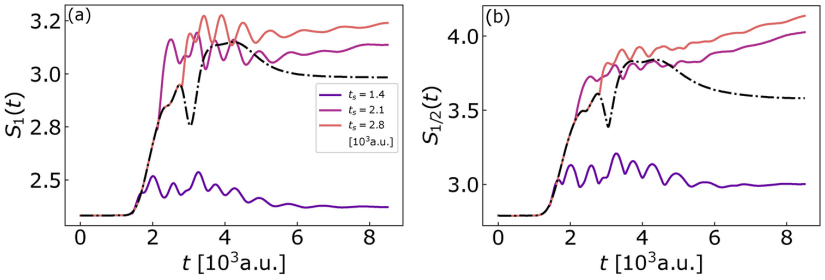

Fig. 9. (**a**) The Wigner–Shannon entropy and (**b**) the Wigner–Rényi one-half entropy of the WDF state against time. Different colors stand for different potential change time t_s and the black dash-dotted line corresponds to the case of time-independent potential barrier.

in this matter, we support these findings by calculating the dynamical transmission and capture coefficients as a time function for different switching time values. The results of these calculations are shown in Fig. 8.

The observed changes in the dynamical transmission coefficient [cf. Fig. 8a] allow us to conclude that the switching time influences the passage rate through the interaction zone. In particular, if the switch between the barrier and the well occurs when the state is inside the region of the interaction zone, then the dynamical transmission coefficient is lower. A natural implication would be that some amounts of the WDF are trapped in the created well. This statement can be supported by the dynamical capture coefficient, displayed in Fig. 8b. The non-zero values assigned to the dynamics of the WDF for $t > 6 \times 10^3$ a.u. suggest that there are indeed parts of the WDF bounded within potential well. The scenario is more complicated when the potential barrier changes to the potential well at the moment when the WDF is in the interaction zone. Namely, the nonsymplectic deformation of the WDF due to the interaction of the state with the Gaussian barrier results in the appearance of low-momentum tail of the WDF, which is sensitive to the presence of the potential well. Consequently, partial trapping of the WDF within potential well reduces the dynamical transmission coefficient through the interaction zone. As a result, the further time evolution of the WDF cannot be described as a free motion, and thus it is a limitation for determining the interaction time based on the method we proposed.

Namely, WDF can be divided in two parts: one part trapped within potential well that is subjected to non-metaplectic transformations, and other freely evolving deformed state. The contribution of the former to the general picture of the evolution invalidates method proposed in Proposition 1, as a proper method for determining the interaction time in this scenario. To finalize this counter-exemplary analysis, we calculated the Wigner–Shannon entropy and the Wigner–Rényi one-half entropy as functions of time. These results are presented in Fig. 9a, b, respectively. Let us note that both these dynamical quantities do not stabilize over time during the performed simulations. This lack of long-time stability, in terms of constant, non-varying value of the symplectically invariant measure, is strictly connected to the reminder of the WDF trapped within potential well, deeming our method unsatisfactory in presented case. In this subsection, we presented an example of the time-dependent potential in which the method of determining the interaction time based on the symplectic covariance of the WDF fails. Consequently, this time is not defined correctly, although the Wigner–Shannon entropy and the Wigner–Rényi one-half entropy can be calculated. It is clear that despite the apparent stabilization of some of these curves, an attempt to determine the interaction time on this basis is challenging. Therefore, the example of the time-dependent potential presented here can be regarded rather as a counterexample, thus showing the limitations of the method mentioned above.

Concluding remarks

We have presented the idea of the symplectic covariance of the Wigner distribution function in an application to the problem of determining the interaction time of the quantum state, represented by the Wigner distribution function, with the potential in the form of an absolutely integrable function. The interaction time has been defined as the traversal time of this state through the interaction zone determined by the range of a sufficient decaying potential. To estimate this time, we used time-dependent entropic measures in the form of the Wigner–Rényi one-half entropy and the Wigner–Shannon entropy. We have examined this issue in the case of scattering of the Schrödinger cat state on the time-dependent Gaussian potential. For this purpose, we have determined the time evolution of the state initially taken as the Schrödinger cat state, by numerically solving the Moyal equation using the Strang splitting algorithm adapted to the time-dependent potentials. We have performed simulations considering two models of the switching of the potential amplitude. One corresponds to a one-time change in the barrier height value, and the second corresponds to a one-time switch between the barrier and the well (in this case, the sign of the Gaussian potential is changed). Although the first case fully complies with the proposed method for determining the interaction time, the second clearly shows its limitations, making it a great counterexample of the proposed method. We have investigated both cases in detail by performing augmented dynamical transmission and capture coefficients calculations. The results obtained have allowed us to state that the choice of the instant of switching between the barrier and the well significantly influences the Wigner distribution dynamics in the interaction zone. This is because the switching time is responsible for the amount of the Wigner distribution function reflected by the potential barrier or trapped in the interaction zone by the Gaussian well, depending on the case analyzed. Changing the height of the amplitude of the potential before the interaction allows for greater transmission of the Wigner distribution function, whereas delaying this change results in an increase in the amount scattered. Regardless of the complexity of the quantum dynamics, we have obtained the interaction time as a function of the switching time according to our proposition. We have also extended our analysis by changing the potential width, resulting in an insight of how the change of the barrier parameters affects the interaction time. On the other hand, changing the potential barrier to potential well at the specific moment of the interaction of the considered bimodal state temporarily traps it in the interaction zone. This trait of the time evolution, namely the appearance of the low-momentum tails of the Wigner function trapped within a potential well, affects the symplectically invariant measures used to determine the interaction time. As a result, both measures do not stabilize over time, suggesting an ongoing interaction between the Wigner distribution function and the potential. Summarizing this discussion, based on the symplectic covariance of the Wigner distribution function and the concept of symplectic invariant quantities, we have shown that for the rapidly decaying potential barriers, the time-dependent entropic measures: Wigner–Rényi one-half entropy, and Shannon entropy are suitable dynamical quantities for estimating the interaction time with varying sensitivity. However, when the state becomes partially localized in the potential wells, the presented method indicates that the interaction time becomes infinite, thus not providing a quantitative answer to the problem posed. The proposed entropic method of estimating the interaction time can be realized upon the tomographical methods of reconstructing the Wigner distribution function[59–61] with ultrafast sampling. We believe this approach can be improved by deep machine learning, reducing the efforts needed to reconstruct the Wigner distribution function accurately[62].

One can use the entropic method in the case of states with finite lifetimes, such as resonances, but it requires great caution in interpreting the result and certainly longer simulation times. This thread will be developed in our forthcoming work.

Data availability

The datasets used and/or analysed in the current study are available from the corresponding author upon reasonable request.

Received: 8 February 2024; Accepted: 9 December 2024
Published online: 28 December 2024

References

1. Merzbacher, E. *Quantum Mechanics* (Wiley, New York, 1998).
2. Büttiker, M. & Landauer, R. Traversal time for tunneling. *Phys. Rev. Lett.* **49**, 1739. https://doi.org/10.1103/PhysRevLett.49.1739 (1982).
3. Landauer, R. & Martin, T. Barrier interaction time in tunneling. *Rev. Mod. Phys.* **66**, 217. https://doi.org/10.1103/RevModPhys.66.217 (1994).
4. Tannor, D. *Introduction to Quantum Mechanics: A Time-Dependent Perspective* (University Science Books, Sausalito, 2007).
5. Yafaev, D. R. *Mathematical Scattering Theory: Analytic Theory* (American Mathematical Society, Providence, 2010).
6. Hauge, E. H. & Støvneng, J. A. Tunneling times: A critical review. *Rev. Mod. Phys.* **61**, 917. https://doi.org/10.1103/RevModPhys.61.917 (1989).
7. Sokolovski, D. & Akhmatskaya, E. No time at the end of the tunnel. *Commun. Phys.* **1**, 47. https://doi.org/10.1038/s42005-018-0049-9 (2018).
8. Shafir, D. et al. Resolving the time when an electron exits a tunnelling barrier. *Nature* **485**, 343. https://doi.org/10.1038/nature11025 (2012).
9. Ramos, R., Spierings, D., Racicot, I. & Steinberg, A. M. Measurement of the time spent by a tunnelling atom within the barrier region. *Nature* **583**, 529. https://doi.org/10.1038/s41586-020-2490-7 (2020).
10. Spierings, D. C. & Steinberg, A. M. Measuring the time tunneling particles spend in the barrier. In *Optical, Opto-Atomic, and Entanglement-Enhanced Precision Metrology II* (eds Shahriar, S. M. & Scheuer, J.) (SPIE, 2020). https://doi.org/10.1117/12.2552583.
11. Rivlin, T., Pollak, E. & Dumont, R. S. Comparison of a direct measure of barrier crossing times with indirect measures such as the Larmor time. *New J. Phys.* **23**, 063044. https://doi.org/10.1088/1367-2630/ac047b (2021).

12. Yeh, L. & Kim, Y. S. Correspondence between the classical and quantum canonical transformation groups from an operator formulation of the Wigner function. *Found. Phys.* **24**, 873. https://doi.org/10.1007/BF02067652 (1994).
13. Bonet-Luz, E. & Tronci, C. Hamiltonian approach to Ehrenfest expectation values and Gaussian quantum states. *Proc. R. Soc. A Math. Phys.* **472**, 20150777. https://doi.org/10.1098/rspa.2015.0777 (2016).
14. Dias, N. C. & Prata, J. N. Quantum mappings acting by coordinate transformations on Wigner distributions. *Rev. Mat. Iberoam.* **35**, 317. https://doi.org/10.4171/rmi/1056 (2019).
15. Groenewold, H. J. On the principles of elementary quantum mechanics. *Physica* **12**, 405. https://doi.org/10.1016/S0031-8914(46)80059-4 (1946).
16. Moyal, J. E. Quantum mechanics as a statistical theory. *Proc. Camb. Philos. Soc.* **45**, 99. https://doi.org/10.1017/S0305004100000487 (1949).
17. Baker, G. A. Formulation of quantum mechanics based on the quasi-probability distribution induced on phase space. *Phys. Rev.* **109**, 2198. https://doi.org/10.1103/PhysRev.109.2198 (1958).
18. Bayen, F., Flato, M., Fronsdal, C., Lichnerowicz, A. & Sternheimer, D. Quantum mechanics as a deformation of classical mechanics. *Lett. Math. Phys.* **1**, 521. https://doi.org/10.1007/BF00399745 (1977).
19. Schleich, W. P. *Quantum Optics in Phase Space* (Wiley, New York, 2001).
20. Błaszak, M. & Domański, Z. Phase space quantum mechanics. *Ann. Phys.* **327**, 167. https://doi.org/10.1016/j.aop.2011.09.006 (2012).
21. Bordemann, M. Deformation quantization: A survey. *J. Phys. Conf. Ser.* **103**, 012002. https://doi.org/10.1088/1742-6596/103/1/012002 (2008).
22. Curtright, T. L., Fairlie, D. B. & Zachos, C. K. *A Concise Treatise on Quantum Mechanics in Phase Space* (World Scientific Publishing Co. Pte. Ltd., Singapore, 2014).
23. Wigner, E. On the quantum correction for thermodynamic equilibrium. *Phys. Rev.* **40**, 749. https://doi.org/10.1103/PhysRev.40.749 (1932).
24. de Gosson, M. *The Wigner Transform* (World Scientific Publishing Europe Ltd., Singapore, 2017).
25. Chruściński, D. & Młodawski, K. Wigner function and Schrödinger equation in phase-space representation. *Phys. Rev. A* **71**, 052104. https://doi.org/10.1103/PhysRevA.71.052104 (2005).
26. Kalka, M., Spisak, B. J., Woźniak, D., Wołoszyn, M. & Kołaczek, D. Dynamical entropic measure of nonclassicality of phase-dependent family of schrödinger cat states. *Sci. Rep.* **13**, 16266. https://doi.org/10.1038/s41598-023-43421-2 (2023).
27. Cordero, E., de Gosson, M., Dörfler, M. & Nicola, F. On the symplectic covariance and interferences of time-frequency distributions. *SIAM J. Math. Anal.* **50**, 2178. https://doi.org/10.1137/16M1104615 (2018).
28. Cordero, E., Nicola, F. & Rodino, L. Integral representations for the class of generalized metaplectic operators. *J. Fourier Anal. Appl.* **21**, 694. https://doi.org/10.1007/s00041-014-9384-8 (2015).
29. de Gosson, M. *Symplectic Geometry and Quantum Mechanics* (Birkhäuser, Basel, 2006).
30. de Gosson, M. *Symplectic Methods in Harmonic Analysis and in Mathematical Physics* (Birkhäuser, Basel, 2011).
31. de Gosson, M. A. *Born-Jordan Quantization* (Springer, Basel, 2016).
32. Pazy, A. *Semigroups of Linear Operators and Applications to Partial Differential Equations* (Springer, New York, 1983).
33. Büyükaşık, A. Ş. & Çayiç, Z. Exactly solvable Hermite, Laguerre, and Jacobi type quantum parametric oscillators. *J. Math. Phys.* **57**, 122107. https://doi.org/10.1063/1.4972293 (2016).
34. Littlejohn, R. G. The semiclassical evolution of wave packets. *Phys. Rep.* **138**, 193. https://doi.org/10.1016/0370-1573(86)90103-1 (1986).
35. Hörmander, L. Symplectic classification of quadratic forms, and general Mehler formulas. *Math. Z.* **219**, 413. https://doi.org/10.1007/BF02572374 (1995).
36. Schleich, W., Pernigo, M. & Kien, F. L. Nonclassical state from two pseudoclassical states. *Phys. Rev. A* **44**, 2172. https://doi.org/10.1103/PhysRevA.44.2172 (1991).
37. Gerry, C. C. & Knight, P. L. Quantum superpositions and Schrödinger cat states in quantum optics. *Am. J. Phys.* **65**, 964. https://doi.org/10.1119/1.18698 (1997).
38. Ourjoumtsev, A., Jeong, H., Tualle-Brouri, R. & Grangier, P. Generation of optical 'Schrödinger cats' from photon number states. *Nature* **448**, 784. https://doi.org/10.1038/nature06054 (2007).
39. Ozorio de Almeida, A. M. Entanglement in phase space. In *Entanglement and Decoherence: Foundations and Modern Trends* Vol. 157 (eds Buchleitner, A. et al.) (Springer, Berlin, 2008). https://doi.org/10.1007/978-3-540-88169-8.
40. Walschaers, M. Non-gaussian quantum states and where to find them. *PRX Quantum* **2**, 030204. https://doi.org/10.1103/PRXQuantum.2.030204 (2021).
41. Kira, M., Koch, S. W., Smith, R. P., Hunter, A. E. & Cundiff, S. T. Quantum spectroscopy with Schrödinger-Cat States. *Nat. Phys.* **7**, 799. https://doi.org/10.1038/nphys2091 (2011).
42. Wright, J. C. Schrödinger cat state spectroscopy—A new frontier for analytical chemistry. *Anal. Chem.* **92**, 8638. https://doi.org/10.1063/1.5019221 (2020).
43. Garbaczewski, P. Differential entropy and time. *Entropy* **7**, 253. https://doi.org/10.3390/e7040253 (2005).
44. Bialynicki-Birula, I. & Rudnicki, Ł. *Entropic Uncertainty Relations in Quantum Physics* Vol. 1 (Springer, Netherlands, Dordrecht, 2011).
45. Dias, N. C., de Gosson, M. A. & Prata, J. N. A refinement of the Robertson–Schrödinger uncertainty principle and a Hirschman–Shannon inequality for Wigner distributions. *Fourier Anal. Appl.* **25**, 210. https://doi.org/10.1007/s00041-018-9602-x (2019).
46. Tatarskiĭ, V. I. The Wigner representation of quantum mechanics. *Sov. Phys. Usp.* **26**, 311. https://doi.org/10.1070/PU1983v026n04ABEH004345 (1983).
47. Kołaczek, D., Spisak, B. J. & Wołoszyn, M. Phase-space studies of backscattering diffraction of defective Schrödinger cat states. *Sci. Rep.* **11**, 11619. https://doi.org/10.1038/s41598-021-90738-x (2021).
48. Sadeghi, P., Khademi, S. & Nasiri, S. Nonclassicality indicator for the real phase-space distribution functions. *Phys. Rev. A* **82**, 012102. https://doi.org/10.1103/PhysRevA.82.012102 (2010).
49. Kenfack, A. Comment on "nonclassicality indicator for the real phase-space distribution functions". *Phys. Rev. A* **93**, 036101. https://doi.org/10.1103/PhysRevA.93.036101 (2016).
50. Khademi, S., Sadeghi, P. & Nasiri, S. Reply to "Comment on 'Nonclassicality indicator for the real phase-space distribution functions' ". *Phys. Rev. A* **93**, 036102. https://doi.org/10.1103/PhysRevA.93.036102 (2016).
51. Strang, G. On the construction and comparison of difference schemes. *SIAM J. Numer. Anal.* **5**, 506. https://doi.org/10.1137/0705041 (1968).
52. Cabrera, R., Bondar, D. I., Jacobs, K. & Rabitz, H. A. Efficient method to generate time evolution of the Wigner function for open quantum systems. *Phys. Rev. A* **92**, 042122. https://doi.org/10.1103/PhysRevA.92.042122 (2015).
53. MacNamara, S. & Strang, G. Operator splitting. In *Splitting Methods in Communication, Imaging, Science, and Engineering* Vol. 95 (eds Glowinski, R. et al.) (Springer, Cham, 2016). https://doi.org/10.1007/978-3-319-41589-5.
54. Kołaczek, D., Spisak, B. J. & Wołoszyn, M. The phase space approach to time evolution of quantum states in confined systems: The spectral split-operator method. *Int. J. Appl. Math. Comput. Sci.* **29**, 439. https://doi.org/10.2478/amcs-2019-0032 (2019).
55. Jensen, K. L., Lebowitz, J. L., Riga, J. M., Shiffler, D. A. & Seviour, R. Wigner wave packets: Transmission, reflection, and tunneling. *Phys. Rev. B* **103**, 155427. https://doi.org/10.1103/PhysRevB.103.155427 (2021).

56. Dragoman, D. Wigner distribution function expression for the tunnelling time in quantum resonant structures. *Opt. Quantum Electron.* **29**, 79. https://doi.org/10.1023/a:1018581417180 (1997).
57. Pollak, E. Transition path time distribution, tunneling times, friction, and uncertainty. *Phys. Rev. Lett.* **118**, 70401. https://doi.org/10.1103/PhysRevLett.118.070401 (2017).
58. Dumont, R. S., Rivlin, T. & Pollak, E. The relativistic tunneling flight time may be superluminal, but it does not imply superluminal signaling. *New J. Phys.* **22**, 93060. https://doi.org/10.1088/1367-2630/abb515 (2020).
59. Lutterbach, L. G. & Davidovich, L. Method for direct measurement of the wigner function in cavity QED and ion traps. *Phys. Rev. Lett.* **78**, 2547. https://doi.org/10.1103/PhysRevLett.78.2547 (1997).
60. Flühmann, C. & Home, J. P. Direct characteristic-function tomography of quantum states of the trapped-ion motional oscillator. *Phys. Rev. Lett.* **125**, 043602. https://doi.org/10.1103/PhysRevLett.125.043602 (2020).
61. Winkelmann, F.-R. et al. Direct measurement of the Wigner function of atoms in an optical trap. *J. Phys. B At. Mol. Opt. Phys.* **55**, 194004. https://doi.org/10.1088/1361-6455/ac8bb8 (2022).
62. Chen, H.-B. et al. Unveiling the nonclassicality within quasi-distribution representations through deep learning. *Quantum Sci. Technol.* **10**, 015029. https://doi.org/10.1088/2058-9565/ad8ef0 (2024).

Acknowledgements
We are grateful to Marta Wleklińska and Piotr Pigoń from AGH University of Krakow for critical discussions. The research project is supported by the program 'Initiative for Excellence - Research University' for the AGH University of Krakow.

Author contributions
D.W. is the leader of the project, developed its framework, and carried out the calculations. The rest of the Authors, M.K., D.K., M.W., and B.J.S., contributed to the discussion and analysis of the results. Finally, all Authors participated in writing the manuscript and reviewed it.

Declarations

Competing interests
The authors declare no competing interests.

Additional information
Supplementary Information The online version contains supplementary material available at https://doi.org/10.1038/s41598-024-82744-6.

Correspondence and requests for materials should be addressed to B.J.S.

Reprints and permissions information is available at www.nature.com/reprints.

Publisher's note Springer Nature remains neutral with regard to jurisdictional claims in published maps and institutional affiliations.

- The article: **Interaction time of Schrödinger cat states with a periodically driven quantum system: Symplectic covariance approach [186]**
  According to APS Physical Review Journals policy: *Yes, the author has the right to use the article or a portion of the article in a thesis or dissertation without requesting permission from APS, provided the bibliographic citation and the APS copyright credit line are given on the appropriate pages.*[2]

[2]Question "As the author of an APS-published article, may I include my article or a portion of my article in my thesis or dissertation?" in: https://journals.aps.org/copyrightFAQ.html#thesis¸

PHYSICAL REVIEW A **110**, 022416 (2024)

Interaction time of Schrödinger cat states with a periodically driven quantum system: Symplectic covariance approach

D. Woźniak, B. J. Spisak,* M. Kalka, M. Wołoszyn, M. Wleklińska, and P. Pigoń
AGH University of Krakow, Faculty of Physics and Applied Computer Science, and aleja A. Mickiewicza 30, 30-059 Krakow, Poland

D. Kołaczek
Department of Applied Mathematics, University of Agriculture in Kraków, ulica Balicka 253c, 30–198 Kraków, Poland

(Received 27 March 2024; accepted 16 July 2024; published 12 August 2024)

The symplectic invariance property of the Wigner-Rényi entropies family is used to estimate the interaction time for the propagating Schrödinger cat state that interacts with the periodically changing potential. With the help of this property, the hierarchy of the interaction times is specified for the quantum dynamics of the periodically driven system. It is also demonstrated that the lower and upper bounds of the interaction time are determined by the Wigner-Rényi entropies corresponding to increasing Rényi index values, respectively. The interpretation of the presented results is supported by calculations of the dynamical transmission and capture coefficients, which give a clear insight into the scattering of the non-Gaussian state on the periodically changing potential, which switches between the Gaussian potential barrier and the well.

DOI: 10.1103/PhysRevA.110.022416

I. INTRODUCTION

Physical systems interacting with an explicitly time-dependent periodic external force are referred to as periodically driven systems [1]. In recent times, a notable surge in research efforts dedicated to unraveling the intricate dynamics exhibited by such systems has been witnessed. The widespread applications of the periodic driving include the ratchet effect, both quantum [2,3] and classical [4,5], laser interactions [6], Bose condensation [7], and, even further, such systems are employed in the studies of topological insulators [8,9], time crystals [10], or periodically driven optical lattices [11]. Various formulations of quantum theory can be utilized to describe the dynamics of periodically driven quantum systems, helping to highlight different features of their behavior [1,12]. Here, we explore the dynamics of periodically driven quantum systems within the phase-space framework in which the state of the system is represented by the Wigner distribution function (WDF). Using this approach, it is possible not only to gain deeper insights into the behavior of the system in the domain of conjugated variables (e.g., momentum and position), but also to acquire correspondence with the classical dynamics [13]. The approach based on the concept of the WDF has found a wide range of applications, from quantum optics [14,15] and quantum information [16–18], through quantum chemistry [19–21] and biology [22,23], to Bose-Einstein condensates [24–27] or quantum Brownian motion [28–30]. It has recently also been applied in the study of periodically driven systems [31]. Notably, the WDF can take negative values in some regions of the phase space. This property prevents the interpretation of the WDF as a proper probability distribution function on the phase space. Due to this distinctive property, the WDF is also used to detect and study the nonclassicality of quantum states [32]. Another characteristic that distinguishes the WDF and provides additional insight into the considered quantum system is the symplectic covariance [33–37]. Not only does the area occupied by the WDF in the phase space remain unchanged under symplectic transformations (shear, rotation, or scaling), but there are also WDF-dependent functions whose integrals over the phase space remain constant when the time evolution of the WDF is given by symplectic transformations (e.g., motion in the free space). Such integrals can be used to define the so-called symplectically invariant measures, which can be used to detect the state interaction with the potential barrier in the scattering experiments. From many symplectically invariant measures, it is worth distinguishing phase-space entropic measures. They are particularly relevant if one looks at the phase-space formulation of quantum theory as a statistical theory in which entropic quantities play a key role in describing the physical system. Among many formulations of phase-space entropies based on the WDF [38,39] and other phase-space distributions [40], we would like to focus on the Wigner-Rényi entropy [39,41]. This measure, depending on the Rényi parameter, allows the determination of phase-space analogues of well-established entropic measures in statistical theory (e.g., Shannon entropy, collisional entropy, maximum entropy) and, furthermore, for a one-half Rényi index, it can be interpreted as a measure of nonclassicality of the state [41]. As we previously showed, the symplectic covariance of a dynamical measure can be successfully employed to determine the interaction time of a quantum state, with the potential barrier given by the absolutely integrable function.

*Contact author: bjs@agh.edu.pl

This approach provides a new perspective on the decades-old and often confusing problem of establishing the barrier crossing time [42]. Over the years, many different theories have been developed, which have given plenty of opportunities to determine how long it takes to pass through the barrier. Therefore, in this work, we would like not only to determine another interaction time, but also to prove that the interaction time obtained from symplectically invariant measures allows us to indicate an upper and lower limit on such interaction time.

In this paper, by employing entropic measures, we show how to apply a symplectic covariance approach to estimating interaction time within a periodically driven system. Including entropic measures when calculating interaction time in a periodically driven system is beneficial as they offer insights into the intricate relationship dynamics, facilitating a deeper comprehension of system behavior and temporal interactions. Owing to that, we were able to bound the interaction time and show that the lowest barrier crossing times can be achieved by using the Wigner-Rényi entropy with one-half Rényi index.

The paper is organized as follows. Section II consists of the theoretical background in a nutshell and a description of the used numerical algorithm. In Sec. III, we present the results and their discussion. Section IV contains a summary and conclusions. Finally, the paper ends with appendices that contain a detailed derivation of the presented algorithm and a proof of the monotonicity property of the Wigner-Rényi entropies for continuous probability distribution functions.

II. THEORETICAL FRAMEWORK

A. Phase-space dynamics and symplectic invariance

In the phase-space representation of quanta, any isolated quantum-mechanical system is characterized by the Weyl symbol of the Hamiltonian [43,44]. In particular, this symbol for the one-particle system in one dimension has a form consistent with its classical counterpart, i.e., this is a real function of the position and the momentum defined on the two-dimensional phase space generated by these two canonically conjugated variables and can be written in the form $H(x,p)=p^2/(2m)+U(x)$, where m is the mass, p is the momentum, x is the position, and $U(x)$ is the potential energy. It is important to remember that the momentum and the position occurring in this formula are the Weyl symbols corresponding to these quantities. However, this form of the Hamiltonian is insufficient for the description of time-dependent systems presented in Sec. I. Motivated by this deficiency, we generalize the Hamiltonian mentioned above to the time-dependent form. For this purpose, we assume that the new one-particle Hamiltonian explicitly depends on the time through the potential part, denoted by $W(x,t)$. Furthermore, we assume its separable form, namely, $W(x,t)=U(x)\Sigma(t)$, where $U(x)$ is the spatial part, and the function $\Sigma(t)$ is the temporal part of this term. Taking into account these assumptions, we can characterize the time-dependent system under consideration by the Weyl symbol of the effective Hamiltonian in the form

$$H(x,p,t)=\frac{p^2}{2m}+U(x)\Sigma(t). \tag{1}$$

The specification of the functions $U(x)$ and $\Sigma(t)$ is given later in this work.

Within the phase-space representation, the WDF can express the state of this time-dependent system. This real and normalized function can take negative values in some regions of the phase space for some states. In fact, this property disqualifies the intuitive interpretation of the WDF as a proper probability distribution function on the phase space despite having well-defined marginals. On the other hand, this property is often used to indicate the quantumness of the system state represented by the WDF [32]. In the case when the system is in a pure state, the corresponding WDF is given by the formula [45]

$$\varrho(x,p,t)=\frac{1}{2\pi\hbar}\int_{\mathbb{R}} dX\ \psi^*\left(x+\frac{X}{2},t\right)\psi\left(x-\frac{X}{2},t\right)e^{-\frac{i}{\hbar}pX}, \tag{2}$$

where, for each time instant, $t\in\mathbb{R}:\psi(\cdot,t)\in L^2(\mathbb{R},dx)$ is the time-dependent Schrödinger wave function and the asterisk symbol denotes the complex conjugate. The time evolution of the WDF is determined by the solution of the Cauchy problem for the Moyal equation,

$$\begin{aligned}\partial_t\varrho(x,p,t)&=-i\hat{\mathcal{L}}_M(t)\varrho(x,p,t),\quad t>0\\ \varrho(x,p,0)&=\varrho_0(x,p),\end{aligned} \tag{3}$$

where $\varrho_0(x,p)$ represents the initial condition and $\hat{\mathcal{L}}_M(t)$ is the Moyal operator defined by the formula

$$\begin{aligned}-i\hat{\mathcal{L}}_M(t):=-\frac{p}{m}\partial_x+\frac{1}{i\hbar}\Sigma(t)\Bigg[U\left(x+\frac{i\hbar}{2}\partial_p\right)\\ -U\left(x-\frac{i\hbar}{2}\partial_p\right)\Bigg].\end{aligned} \tag{4}$$

Alternatively, the expression in the square bracket of the second term in the right-hand side of the Moyal operator (4) can be written in a differential form, namely,

$$\begin{aligned}\hat{\mathcal{L}}_M(t)=i\left\{-\frac{p}{m}\partial_x+\Sigma(t)[\partial_x U(x)]\partial_p\right\}\\ +i\sum_{r=1}^{\infty}\frac{(-1)^r\Sigma(t)}{(2r+1)!}\left(\frac{\hbar}{2}\right)^{2r}\partial_x^{2r+1}U(x)\partial_p^{2r+1}.\end{aligned} \tag{5}$$

Owing to this, the physical interpretation of the operator (5) seems to be more transparent. Namely, the first term in the right-hand side of this expression corresponds to the Liouville operator [46]. This operator generates the classical dynamics of the WDF in the phase space, i.e., its center of mass moves along the classical trajectory resulting from the solution of the Hamilton equations. In turn, the second term, i.e., a series called a Moyal expansion, represents the operator related to quantum effects. This term describes the perturbations of the classical dynamics of the WDF by systematically considering increasingly high-order terms in the Moyal expansion. This is why the full quantum dynamics of the WDF emerges from the Moyal equation. Let us note that this approach allows one to look at quantum dynamics as the deformation of the classical one, and the Planck constant measures this deformation. One more thing that results from this approach is worth noting. Namely, the Moyal equation reduces to the mere Liouville equation for polynomial potentials of the order less than or

equal to 2. This result leads to the important conclusion that the classical and quantum dynamics of the WDF are precisely the same for this class of potentials. In this case, the time dependence of the wave function, appearing in Eq. (2) by definition, is determined by the metaplectic time-evolution operator [47], and the corresponding time evolution of the WDF is given by point transformation, represented by the appropriate symplectic matrix $\mathbf{S}_t$. This property is known as a symplectic covariance of WDF [34]. Using this property, one might notice that all integrals of the form

$$I(t) = \int_{\mathbb{R}^2} dxdp\, f[\varrho(x,p,t)], \tag{6}$$

defined for any function $f : [-1/(\pi\hbar), 1/(\pi\hbar)] \to \mathbb{R}$ such that the composition $(x, p) \mapsto (f \circ \varrho)(x, p, t)$ is integrable on $\mathbb{R}^2$ for every $t \geqslant 0$, are invariant with respect to such transformations, namely,

$$\begin{aligned} I(t) &= \int_{\mathbb{R}^2} dxdp\, f\{\varrho_0[\mathbf{S}(t)(x\ p)^T]\} \\ &= \int_{\mathbb{R}^2} dxdp\, f[\varrho_0(x,p)] = I(0), \end{aligned} \tag{7}$$

where for point transformations given by symplectic matrices, the Jacobian determinant is equal to 1. For any f defined by the conditions above, we say that $I(t)$ is an invariant measure. It is worth mentioning that in the context of the time evolution of the quantum systems, the maximal covariance group of the WDF consists solely of symplectic transformations [36]. From the point of view of this work, two particularly interesting cases of symplectic covariance arise from the evolution of the WDF in potentials of the zeroth and second order. Physically, they correspond to the cases of free-particle and harmonic-oscillator potentials. The Moyal equation for the harmonic oscillator, $U(x) = m\omega^2x^2/2$, where ω is the angular frequency, has the form

$$\partial_t\varrho(x,p,t) + \frac{p}{m}\partial_x\varrho(x,p,t) - m\omega x\partial_p\varrho(x,p,t) = 0. \tag{8}$$

For the given initial condition $\varrho_0(x, p)$, the solution of Eq. (8) is

$$\begin{aligned} \varrho(x,p,t) = \varrho_0\Big[& x\cos(\omega t) - \frac{p}{m\omega}\sin(\omega t),\, p\cos(\omega t) \\ & + xm\omega\sin(\omega t)\Big]. \end{aligned} \tag{9}$$

This motion is the elliptical rotation in the phase space and, consequently, we conclude that the values of the WDF are preserved along the classical trajectory. Based on this result, we can also find the solution of the free-space Moyal equation by calculating the limit of Eq. (9) for $\omega \to 0$. The obtained result is the following:

$$\varrho(x,p,t) = \varrho_0\Big(x - \frac{p}{m}t, p\Big). \tag{10}$$

In this case, the motion of the WDF is given by the shearing transformation. The meaning of the solutions given by Eq. (9) and Eq. (10) is crucial for our studies, as they both fulfill the previously mentioned invariance condition given by Eq. (6). This expresses the fact that the value of the integral of any function f composed with rotated or sheared WDF does not change with respect to the integral of f composed with the initial condition. This property is crucial for our further studies of the interaction time based on the symplectically invariant measures. Let us now focus on the previously defined Cauchy problem for the Moyal equation given by Eq. (3). Its formal solution can be written in the form

$$\varrho(x,p,t) = \hat{\mathcal{U}}(t,0)\varrho_0(x,p), \tag{11}$$

where $\hat{\mathcal{U}}(t,0) \equiv \hat{\mathcal{U}}(t)$ is the time-evolution operator whose form is given by the time-ordered exponential operator,

$$\hat{\mathcal{U}}(t,0) = \hat{\mathcal{T}}\exp\Big[-i\int_0^t dt'\,\hat{\mathcal{L}}_M(t')\Big], \tag{12}$$

wherein $\hat{\mathcal{T}}$ stands for the time ordering [48,49]. Therefore, the WDF at time $t + \Delta t$, where Δt is a finite time increment, can be expressed by the formula

$$\varrho(x,p,t+\Delta t) = \hat{\mathcal{T}}\exp\Big[-i\int_t^{t+\Delta t} dt'\,\hat{\mathcal{L}}_M(t')\Big]\varrho_0(x,p,t). \tag{13}$$

On the other hand, using the results of Suzuki [50], any time-ordered exponential operator can be expressed by the ordinary exponential operator in the form

$$\hat{\mathcal{T}}\exp\Big[-i\int_0^t dt'\,\hat{\mathcal{L}}_M(t')\Big] = \exp\{[\hat{\mathcal{L}}_M(t) + \hat{D}]\Delta t\}, \tag{14}$$

where the operator $\exp(\hat{D}\Delta t)$, defined by the formula

$$\hat{F}(t)\exp(\hat{D}\Delta t)\hat{G}(t) = \hat{F}(t+\Delta t)\hat{G}(t), \tag{15}$$

is called the left-time shift operator and formally is expressed by the differential operator, i.e., $\hat{D} = \overleftarrow{\partial_t}$, where the arrow indicates in which direction the derivative acts. Owing to this, combining Eqs. (13) and (14), we obtain the expression for the WDF at the instant time $t + \Delta t$ in the following form:

$$\varrho(x,p,t+\Delta t) = \exp\{[\hat{\mathcal{L}}_M(t) + \hat{D}]\Delta t\}\varrho(x,p,t). \tag{16}$$

The expression obtained in this way has a convenient form for applying the symmetric Strang splitting formula for the exponential operator [51–53]. Taking into account the separable form of the time-dependent potential, $W(x,t) = U(x)\Sigma(t)$, and taking advantage of the fact that each operator is unitarily equivalent to some multiplication operator owing to the adequate Fourier transform allows us to convert Eq. (16) into the following formula:

$$\begin{aligned} \varrho(x,p,t+\Delta t) \approx\ & \mathcal{F}^{-1}_{1,\lambda\to x}\exp\Big(-\frac{i\Delta t}{2m}\lambda p\Big)\mathcal{F}_{1,x\to\lambda} \\ & \times\mathcal{F}^{-1}_{2,y\to p}\exp\Big\{i\Delta t\,\Sigma\Big(t+\frac{\Delta t}{2}\Big)\Big[U\Big(x+\frac{y}{2}\Big) \\ & -U\Big(x-\frac{y}{2}\Big)\Big]\Big\}\mathcal{F}_{2,p\to y} \\ & \times\mathcal{F}^{-1}_{1,\lambda\to x}\exp\Big(-\frac{i\Delta t}{2m}\lambda p\Big)\mathcal{F}_{1,x\to\lambda}\varrho(x,p,t), \end{aligned} \tag{17}$$

where the symbol $\mathcal{F}_{a\to\alpha}$ denotes the ordinary Fourier transform and $\mathcal{F}^{-1}_{\alpha\to a}$ corresponds to the inverse Fourier transform, while a and α are a pair of the canonically conjugate variables. The physical meanings of such pairs (a, α) are directly related

to the phase-space variables. The appropriate definitions and the derivation of the formula given by Eq. (17) can be found in Appendix A. The presented scheme can be further simplified if one considers the temporal part $\Sigma(t)$ of the potential $W(x,t)$ to be piecewise constant at some intervals $[t_k, t_{k+1})$ with an amplitude A_k, namely, dividing the whole simulation time into the intervals given by

$$[0, t_{\max}) = \bigcup_{k=0}^{N} [t_k, t_{k+1}). \tag{18}$$

In this way, one obtains the numerical algorithm for a single step of the time evolution of the WDF, expressed by the formula

$$\varrho(x,p,t_{k_{j+1}}) \approx \mathcal{F}^{-1}_{1,\lambda\to x} \exp\left(-\frac{i\Delta t}{2m}\lambda p\right)\mathcal{F}_{1,x\to\lambda}\mathcal{F}^{-1}_{2,y\to p} \exp\left\{iA_k\Delta t\left[U\left(x+\frac{y}{2}\right)-U\left(x-\frac{y}{2}\right)\right]\right\}$$
$$\times\mathcal{F}_{2,p\to y}\mathcal{F}^{-1}_{1,\lambda\to x} \exp\left(-\frac{i\Delta t}{2m}\lambda p\right)\mathcal{F}_{1,x\to\lambda}\varrho(x,p,t_{k_j}), \tag{19}$$

where the subindex k_j stands for iteration within the interval $[t_k, t_{k+1})$ in which $\Sigma(t) = A_k$.

B. Entropic measures

A handy concept to describe quantum states in the phase space constitutes the Wigner-Rényi entropy because it provides information on the complexity of these states [39,41,54,55]. In particular, it enables one to describe the extension or shape of the state, which the WDF represents in the phase space. The sign problem of the WDF is not so severe in the case of pure states because the WDF corresponding to these states is interpreted as the probability density amplitude in the phase space according to the arguments presented in Ref. [56]. Hence, the squared modulus of the normalized WDF in the sense of the norm $L^2(\mathbb{R}^2)$, i.e., $\widetilde{\varrho}(x,p,t) = \varrho(x,p,t)/||\varrho(\cdot,\cdot,t)||_{L^2(\mathbb{R}^2)}$, is the proper probability density in the phase space [56], where $||\varrho(\cdot,\cdot,t)||_{L^2(\mathbb{R}^2)} = (2\pi\hbar)^{-1/2}$. The Wigner-Rényi entropy corresponding to the probability density, $|\widetilde{\varrho}(x,p,t)|^2$, in the phase space for the Rényi index α, where $0 < \alpha < \infty$ and $\alpha \neq 1$, is defined as follows:

$$S_\alpha(t) = \frac{1}{1-\alpha}\ln\left\{(2\pi\hbar)^{\alpha-1}\int_{\mathbb{R}^2} dxdp\,[|\widetilde{\varrho}(x,p,t)|^2]^\alpha\right\}, \tag{20}$$

whereby, between the Wigner-Rényi entropies corresponding to different Rényi indexes α and α', there is the inequality $S_\alpha(t) > S_{\alpha'}(t)$ for $\alpha < \alpha'$ and a fixed time t, as demonstrated in Appendix B. The attractive property of the Wigner-Rényi entropy is their relation to the Hartley entropy [57], the Wigner-Rényi's one-half [41], the Shannon entropy [39], the collision entropy [38], and the min-entropy [58] for the Rényi index, which equal $\alpha = 0, 1/2, 1, 2, \infty$, respectively. Let us note that the Wigner-Rényi entropies for different Rényi indexes can be regarded as examples of the symplectically invariant measures, by Eqs. (6) and (7). This observation plays a crucial role in the presented research. Here we focus our attention on only four of the previously mentioned entropies, defined up to a constant $\ln(1/2\pi\hbar)$, namely, the Wigner-Rényi's one-half entropy, which is given by the formula

$$S_{1/2}(t) = 2\ln\left[\int_{\mathbb{R}^2} dxdp\,|\widetilde{\varrho}(x,p,t)|\right], \tag{21}$$

the Shannon entropy which is given by the formula

$$S_1(t) = \lim_{\alpha\to 1} S_\alpha(t) = -2\int_{\mathbb{R}^2} dxdp \times |\widetilde{\varrho}(x,p,t)|^2 \ln[|\widetilde{\varrho}(x,p,t)|^2], \tag{22}$$

the collision entropy which is given by the formula

$$S_2(t) = -\ln\int_{\mathbb{R}^2} dxdp\,|\widetilde{\varrho}(x,p,t)|^4, \tag{23}$$

and last but not least, the min-max entropy,

$$S_\infty(t) = \lim_{\alpha\to+\infty}\frac{1}{1-\alpha}\ln\left\{\int_{\mathbb{R}^2} dxdp\,[|\widetilde{\varrho}(x,p,t)|^2]^\alpha\right\} = -\ln\left[\max_{(x,p)\in\mathbb{R}^2}|\widetilde{\varrho}(x,p,t)|^2\right]. \tag{24}$$

All of them have precise physical meanings. The Wigner-Rényi's one-half entropy is related to the area occupied by the negative part of the WDF in the phase space [41], and the Shannon entropy is associated with a deformation of the area occupied by the WDF in phase space caused by the quantum correlations of momentum position, which simultaneously influence the shape of this function. In turn, collision entropy is related to the inverse participation ratio in the phase space [59]. Last but not least, the min-max entropy is related to the maximum of the probability density over the phase space. The symplectic invariance of Rényi entropic measures is the essential property in defining the interaction time τ between the quantum state represented by the function $\varrho(x,p,t)$ and the potential $W(x,t)$. First of all, notice that at any given time t during the interaction with the absolutely integrable barrier-well potential, it cannot be approximated with good precision by a single polynomial of the order of, at most, 2 in the whole subset of $\mathbb{R}$, where the marginal distribution of the considered quantum state in the position space,

$$n(x,t) = \int_{\mathbb{R}} dp\varrho(x,p,t), \tag{25}$$

is noticeably nonzero. Hence, during the interaction with the potential, the time evolution of the WDF is nonsymplectic. Consequently, we expect that the Rényi entropy will be nonconstant during that time. However, away from the potential

center, the motion of the WDF can be regarded as a free propagation. As we have previously shown, this kind of evolution acts as a shearing transformation of the WDF [see Eq. (10)], leaving symplectically invariant measures constant, as implied by Eq. (7). Hence, during free propagation of the WDF, the Renyi entropy is constant. The beginning of the interaction t_i can be understood as an instance when WDF starts to interact with the potential and, consequently, a first visible change in the symplectically invariant measure occurs. Complementary to that, t_f is the time associated with the end of the interaction, when the WDF evolves freely, which results in stabilization of the symplectically invariant measure. Both instances are measured indirectly. They require a measuring device with given precision ε to detect the first and last changes in the evolution of the symplectically invariant measure. We have encapsulated our physical reasoning within the following definition:

Definition 1. For a fixed Rényi index $\alpha > 0$, the interaction time τ between the state represented by the Wigner distribution function and potential energy belonging to the class of absolutely integrable functions, based upon Wigner-Rényi entropic measure, can be defined as

$$\begin{aligned}\tau &= \min\{t \in \mathbb{R}_+ : |S_\alpha(t) - S_\alpha(\infty)| > \varepsilon(M-m)\} \\ &\quad -\max\{t \in \mathbb{R}_+ : |S_\alpha(t) - S_\alpha(0)| > \varepsilon(M-m)\} \\ &= t_f - t_i, \end{aligned} \tag{26}$$

where $S_\alpha(t)$ is a Wigner-Rényi entropy with Rényi index α, $S_\alpha(0)$ is the value of the entropy at the beginning of the evolution, $S_\alpha(\infty)$ is the value at the end of the evolution, $M = \max_{t\in\mathbb{R}_+} S_\alpha(t)$ is the maximum of the Wigner-Rényi entropic measure, $m = \min_{t\in\mathbb{R}_+} S_\alpha(t)$ is its minimum, and $0 < \varepsilon \ll 1$ is a dimensionless threshold parameter that can be understood as the precision of the measuring device.

The infinity that is present in the definition is treated as a time that is long enough so that the evolution after the interaction is that of a free particle, as usually taken in scattering theory. In the case of the numerical experiment, this is the time of the simulation. Ideally, $S_\alpha(0)$, $S_\alpha(\infty)$ should be known *a priori* so that a threshold comparison could be made on the go rather than after the experiment.

III. RESULTS AND DISCUSSION

The quantitative description of the quantum state scattering requires specification of the potential term of the system Hamiltonian, which represents the scatterer. We model this scatterer using a time-dependent finite-range potential with a periodically changing amplitude. For this purpose, we use a locally integrable function which allows us to determine the effective interaction region and the interaction time according to Definition 1. The results of all numerical calculations are presented in atomic units (a.u.), i.e., $e = \hbar = m = 1$.

In the presented study, we assume that the potential term $W(x,t) = U(x)\Sigma(t)$ of the Weyl symbol of the effective Hamiltonian (1) consists of the spatial term

$$U(x) = U_0 \exp\left[-\frac{(x-x_B)^2}{2w^2}\right], \tag{27}$$

representing a scattering center of strength $U_0 = 0.008$ a.u. localized at $x_B = 0$ a.u. and with width given by $w^2 = 50$ a.u., and the time-dependent term

$$\Sigma(t) = \theta(t_b - t) + \mathrm{sgn}\left[\sin\frac{2\pi(t-t_b)}{T}\right]\theta(t-t_b) \tag{28}$$

responsible for oscillations between the barrier regime and the well regime. These oscillations start after the delay time $t_b = 140$ a.u., and their rate is given by the period T which is a parameter of the model. Therefore, the choice of this parameter remains critical for studying the dynamics of the quantum state during its interaction with the time-varying obstacle represented by the periodic potential in the form given by Eqs. (27) and (28). Our proposition of determining the reasonable value of T is partially based on a measure of the similarity of two states resulting from the Hilbert-Schmidt distance definition [60], which can be expressed in terms of the WDF as follows:

$$\begin{aligned} d_{\varrho,\varrho_0}(t) &= \left\{2\pi\hbar\int_{\mathbb{R}^2} dxdp\left[\varrho(x,p,t) - \varrho_0\left(x-\frac{p}{m}t,p\right)\right]^2\right\}^{1/2} \\ &= \sqrt{2}[1 - c_{\varrho,\varrho_0}(t)]^{1/2}, \end{aligned} \tag{29}$$

where the dynamic overlap measure $c_{\varrho,\varrho_0}(t)$ is expressed by the formula

$$c_{\varrho,\varrho_0}(t) = 2\pi\hbar\int_{\mathbb{R}^2} dxdp\,\varrho(x,p,t)\varrho_0\left(x-\frac{p}{m}t,p\right), \tag{30}$$

in which $\varrho_0(x - pt/m, p)$ corresponds to the free-space dynamics of the WDF. In turn, the time dependence of the function $\varrho(x,p,t)$ results from the numerical solution of the Cauchy problem (3) for the Moyal equation with a fixed period T and with the initial condition given by the coherent superposition of two well-separated Gaussians,

$$\begin{aligned}\varrho_0(x,p) &= A_1^2\frac{(1-\beta)}{\pi\hbar}\exp\left[-\frac{(x-x_1)^2}{2\delta_x^2} - \frac{2\delta_x^2(p-p_0)^2}{\hbar^2}\right] \\ &\quad + A_1^2\frac{\beta}{\pi\hbar}\exp\left[-\frac{(x-x_2)^2}{2\delta_x^2} - \frac{2\delta_x^2(p-p_0)^2}{\hbar^2}\right] \\ &\quad + 2A_1^2\frac{\sqrt{\beta(1-\beta)}}{\pi\hbar}\cos\left[\vartheta + \frac{p-p_0}{\hbar}(x_1-x_2)\right] \\ &\quad \times\exp\left[-\frac{\left(x-\frac{x_1+x_2}{2}\right)^2}{2\delta_x^2} - \frac{2\delta_x^2(p-p_0)^2}{\hbar^2}\right], \end{aligned} \tag{31}$$

where the normalization factor A_1 has the form

$$A_1 = \left[1 + 2\sqrt{\beta(1-\beta)}\exp\left(-\frac{(x_1-x_2)^2}{8\delta_x^2}\right)\right]^{-\frac{1}{2}}. \tag{32}$$

The set of parameters defining this bimodal WDF is taken in the same form as in our previous work [61] for the quality parameter $\Gamma = 1$, namely, $\beta = 0.5$, $\vartheta = 0$, $\delta_x^2 = 500$ a.u., $x_1 = -300$ a.u., $x_2 = -500$ a.u., and $p_0 = 0.15$ a.u. In fact, the WDF given by Eq. (31) is the phase-space representation of the Schrödinger cat state [62]. Based on the solution of the Cauchy problem mentioned above with the initial condition in the form given by Eq. (31), we can determine the dynamic overlap measure, $c_{\varrho,\varrho_0}(t)$ because we also know the free-space

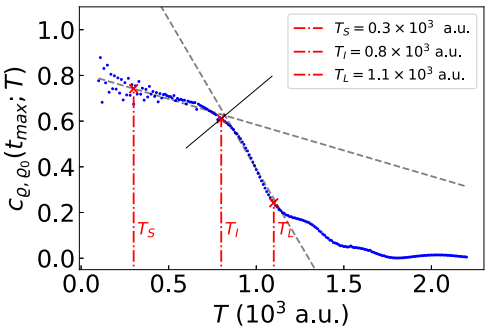

FIG. 1. Long-time dynamic overlap measure as a function of period T. The continuous gray line is the bisector of the angle between two gray dashed lines, which approximate the behavior at a short period interval and intermediate period interval. Red crosses stand for representatives which abscissas were taken for further analysis.

propagation form of the WDF, $\varrho_0(x - pt/m, p)$, with the same initial condition. However, let us note that this specified quantity parametrically depends on T, i.e., $c_{\varrho,\varrho_0}(t) = c_{\varrho,\varrho_0}(t; T)$. To determine the values of the potential period, we calculate the dynamic overlap measure, $c_{\varrho,\varrho_0}(t; T)$, as a function of the period T, for a fixed value of $t = t_{\max}$. Specifically, at a fixed time $t_{\max} = 8.5 \times 10^3$ a.u., corresponding to the maximum of the simulation time, this measure assesses the degree to which the propagating WDF deviates from the free-space propagation after interaction with the potential $W(x, t)$ within the prescribed potential period T, as presented in Fig. 1.

The disparities in the evolution of the quantum state in different configurations of the system are clearly visible: as T tends to zero, a substantial overlap (exceeding 80%) emerges between the free-propagating WDF and that confined within the rapidly oscillating potential T. The trend was followed by a predominant decrease in the measure, approaching nearly zero for T exceeding 1.7×10^3 a.u., indicating that the states are fundamentally distinct. The red line in the figure demarcates the characteristic period timescales T_S, T_L and the transitional timescale T_I. We refer to these scales as short (S), intermediate (I), and long (L). As a first step, we

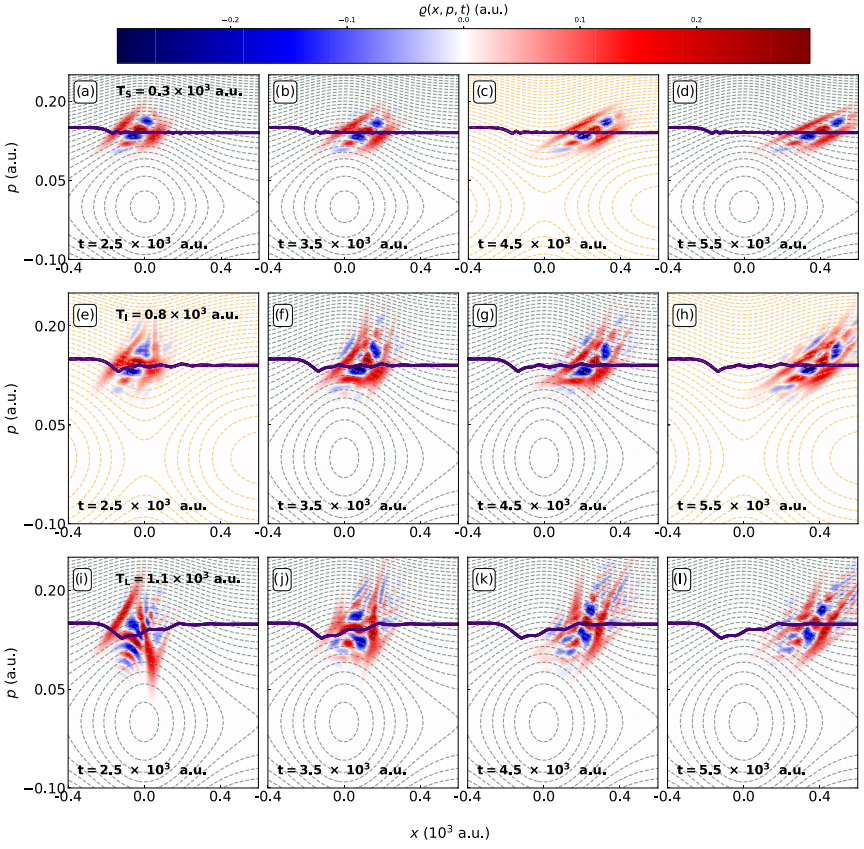

FIG. 2. The phase-space snapshots of the WDF taken at $t = 2.5 \times 10^3$ a.u., 3.5×10^3 a.u., 4.5×10^3 a.u., and 5.5×10^3 a.u. (columns) for different potential periods $T \in \{T_S, T_I, T_L\}$ (rows). The dashed lines stand for the phase-space portrait of the Weyl symbol of the Hamiltonian, whereas the solid purple line is the quantum trajectory of the WDF.

investigate the influence of the potential periods $\{T_S, T_I, T_L\}$ on the dynamics of the WDF. The results of the calculation are presented in Fig. 2 where the phase-space snapshots and quantum trajectories are displayed.

Undoubtedly, the dynamics of WDF depends on the period T of the modulator $\Sigma(t;T)$. With an increasing period, the time of interaction with the fixed state of the potential $U(x)$ increases. The rapid oscillating barrier ($T = T_S$), presented in Figs. 2(a)–2(d), almost does not disturb the evolution. The general influence of the potential can be noticed in the quantum trajectory, namely, a cusp associated with a diminished value of the average momentum. This effect is more visible in the next cases where periodic changes of the character are not as frequent. In addition to reducing the momentum of the WDF, its shape is also mutilated. By leveraging our understanding of the dynamics of the WDF, we determine the time-dependent Wigner-Rényi's entropies, $S_{1/2}(t)$, $S_1(t)$, $S_2(t)$, $S_\infty(t)$, which are examples of the symplectically invariant quantities. Furthermore, through these functions, we can estimate the interaction time, drawing on the insights highlighted in Definition 1. The results of the calculations are presented in Fig. 3 for different potential periods T. According to Fig. 3, all Wigner-Rényi α entropies, for $\alpha \in \{1/2, 1, 2, \infty\}$, exhibit three distinct regions of evolution. Namely, they are constant for the initial evolution of the WDF, then they start rapidly evolving in a nonmonotone manner, suggesting the ongoing interaction, finalized by yet again constant value. It is worth mentioning that for fixed α, the $S_\alpha(t)$ attains higher values in a long-time evolution for increasing values of the potential period T: $S_\alpha(t_{\max}; T_S) < S_\alpha(t_{\max}; T_I) < S_\alpha(t_{\max}; T_L)$. For a fixed T, the evolution of the Wigner-Rényi entropies of various orders, namely, $S_{1/2}(t)$, $S_1(t)$, $S_2(t)$, and $S_\infty(t)$, exhibit a consistent ordering such that $S_\infty(t)$ serves as the lower bound, while $S_{1/2}(t)$ is the upper bound, with $S_1(t)$ and $S_2(t)$ positioned in between, namely, $S_{1/2}(t) > S_1(t) > S_2(t) > S_\infty(t)$. Regardless of the value of the modulator period T, the long-time behavior of all these measures is approximately constant, rendering Definition 1 a valid method to determine the interaction time between the WDF and the potential $W(x,t)$. The estimated interaction times for $\varepsilon = 0.01$ are shown in Fig. 4. Generally, the interaction time as a function of T exhibits a decreasing trend as T increases. For $T \ll 1 \times 10^3$ a.u., the character of the evolution is similar to that of free motion due to rapid oscillations of the barrier, resulting in mutual cancellation of the effects characteristic to the interaction with potential barrier and well. Moreover, for $T > 0.5 \times 10^3$ a.u., the interaction time $\tau(T)$ resembles a reverse ordering in comparison to the Wigner-Rényi entropies in Fig. 3. Namely, the interaction time τ based on the Wigner-Rényi one-half entropy $S_{1/2}(t)$ yields a lower bound for the family of interaction times. We leverage two physical measures, i.e., dynamical capture and transmission coefficients, to validate the reliability of our proposition. These measures are not symplectically invariant, but their straightforward physical interpretation helps to assess whether our results align with the expected patterns, as shown in Figs. 3 and 4. The simplicity in their interpretation makes them valuable tools; in particular, they can serve as complementary measures to estimate the interaction time of the considered model. The dynamical capture coefficient,

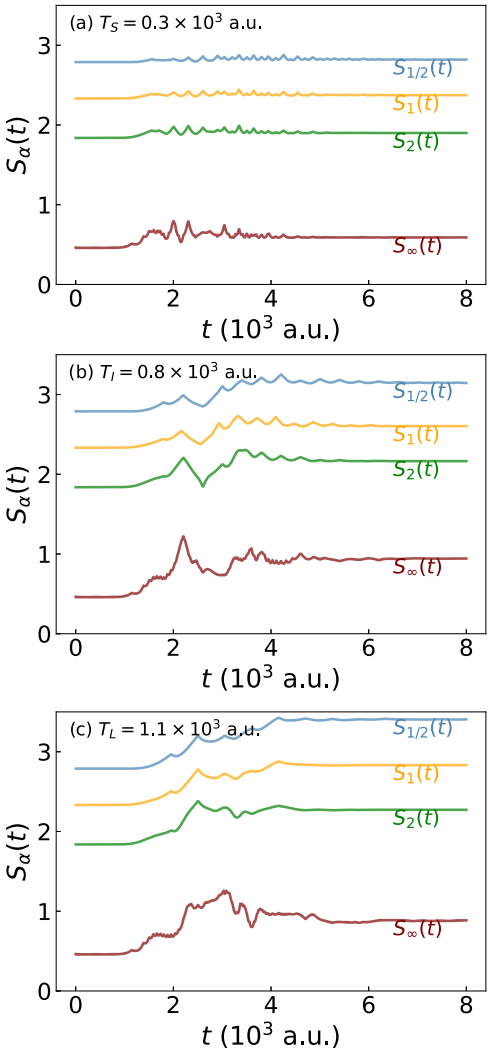

FIG. 3. The comparison between different entropic measures for $\alpha \in \{1/2, 1, 2, \infty\}$ for different potential periods (a) short, (b) intermediate, and (c) long.

defined as

$$C(t) = \int_{\mathbb{R}} \int_{L} dx dp\, \varrho(x, p, t), \tag{33}$$

where L is an interval containing the maximum of considered potential, quantifies the amount of the WDF within the potential $U(x)$. Complementary dynamical transmission coefficient

$$P(t) = \int_{\mathbb{R}} \int_{x_P}^{\infty} dx dp\, \varrho(x, p, t) \tag{34}$$

measures the amount of transmitted WDF. These coefficients satisfy the limit condition $\lim_{t\to+\infty}[R(t) + C(t) + P(t)] = 1$, where $R(t)$ is the dynamical reflection coefficient. The traits

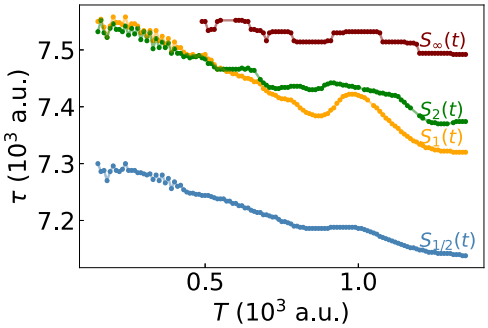

FIG. 4. The interaction time τ based upon different entropic measures $S_\alpha(t)$ for $\alpha \in \{1/2, 1, 2, \infty\}$. The results for $S_\infty(t)$ when $T < 0.5 \times 10^3$ a.u. were dropped as our method could not provide results smaller than the simulation time.

of the evolution of the WDF are captured in Figs. 5(a) and 5(b). The dynamical capture coefficient $C(t)$ quantifies the localization of WDF around the peak value of the Gaussian potential, while the dynamical transmission coefficient $P(t)$ provides the amount of the WDF that traversed a specific region of the space, distant from the potential. In the presented case, $C(t)$ starts to vary after the period of stagnation (where none of the WDF is currently interacting with the potential for

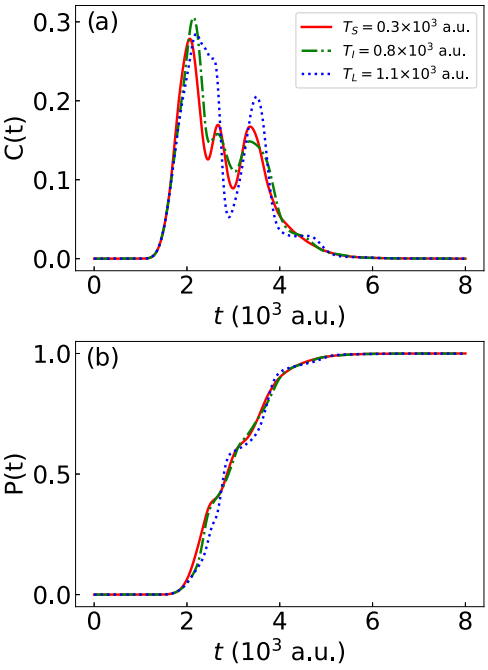

FIG. 5. (a) Dynamical capture C and (b) dynamical transmission P coefficients as functions of time t. The colored curves represent different periods T of potential $U(x;T)$: short T_S, intermediate T_I, and long T_L.

$t < t_1$). This interaction is followed by another time interval where $C(t) = 0$ for $t > t_2$. Generally, one could approach the problem of estimating the interaction time between the WDF and the potential purely on the basis of the distance between consecutive intervals where $C(t) = 0$, namely, $t_2 - t_1$. However, this approach does not align with the interaction time proposed in Definition 1, as it relies on the WDF's presence within a specific spatial interval, rather than the character of the evolution. In this context, the free evolution of the state serves as a natural indicator of the end of the interaction between the WDF and the potential. Crucially, the WDF exits the interaction zone in all presented cases of T [Fig. 5(a)]. This implies that irrespective of the interaction's nature, no WDF accumulates near the potential maximum. However, it does not necessarily imply that the WDF is no longer interacting. In particular, the hypothetical interaction time based on the dynamical capture coefficient results in a single value for all possible variations of the parameter T [as seen in Fig. 5(b)], which is in contradiction to the result presented in Fig. 4.

IV. CONCLUSIONS AND DISCUSSION

We have used the symplectic invariance property of the time-dependent family of the Wigner-Rényi entropies of the order of one-half, 1, 2, and ∞ to estimate the interaction time between a periodically driven system and a quantum state. The presented results have been achieved from the numerical solution of the Moyal equation with the initial condition in the form of the Schrödinger cat state for the driven system with the model of the time-dependent potential term in the separable form. Based on analyzing a dynamic overlap measure in the long-time regime, we selected three distinct potential periods, i.e., short, intermediate, and long, to represent different evolution traits of the considered state. Numerical analysis has revealed a descending order of the entropies, with the one-half Wigner-Rényi entropy as the upper limit and the Wigner-Rényi min-max entropy as the lower limit, which analytical calculations have supported. Furthermore, adequate entropy exhibited a higher long-term value with an increasing potential period for a fixed value of the Rényi index. The considered entropies demonstrate a nearly constant behavior, both at the initiation and finalization of the simulation, facilitating the estimation of the interaction time, as outlined by our Definition. By calculating the difference between two distinct time instances that mark the beginning and end of the interaction, we estimated the duration of the interaction between the state and the potential. Interestingly, the interaction time exhibited reverse ordering compared to the entropies, with one-half Wigner-Rényi entropy now serving as a lower bound. In addition, we have observed that as the intensity of the oscillations equivalently increased, the potential period was lowered and the strength of the interaction between the state and the potential increased, resulting in a longer exposure of the state to the deformations provided by the barrier.

ACKNOWLEDGMENT

The research project is supported by the program "Initiative for Excellence – Research University" for the AGH University of Krakow.

APPENDIX A: ALGORITHM FOR SOLVING MOYAL EQUATION WITH TIME-DEPENDENT POTENTIALS

Here, we will derive the formula used for calculating the Wigner distribution function (WDF) for the time-dependent potential. According to Eq. (4), the Moyal operator can be written symbolically as $-i\mathcal{L}_M(t)$. The formal solution, for an initial condition in the form $\varrho_0(x,p)$, is given by

$$\varrho(x,p,t) = \mathcal{T} e^{-i\int_0^t ds\, \hat{\mathcal{L}}_M(s)} \varrho_0(x,p), \tag{A1}$$

where $\mathcal{T}$ is Dysons' time-ordering operator. The exponential present in the above equation is crucial for describing the time evolution at any time instance $t+\Delta t$, for some time interval $\Delta t > 0$. In this case, it can be substituted by the following relation [50]:

$$\mathcal{T} e^{-i\int_t^{t+\Delta} ds\, \hat{\mathcal{L}}_M(s)} = \exp\{\Delta t[-i\hat{\mathcal{L}}_M(t) + \hat{D}]\}, \tag{A2}$$

where the operator $\hat{D}$ was defined in Eq. (15). This gives the equivalent expression for calculating the WDF at an instance $t+\Delta t$,

$$\begin{aligned}\varrho(x,p,t+\Delta t) &= \mathcal{T} e^{-i\int_t^{t+\Delta} \hat{\mathcal{L}}_M(s) ds} \varrho(x,p,t) \\ &= e^{\Delta t(-i\hat{\mathcal{L}}_M(t)+\hat{D})} \varrho(x,p,t).\end{aligned} \tag{A3}$$

Substituting the form of the operator $-i\hat{\mathcal{L}}_M(t)$ into the expression above yields

$$\varrho(x,p,t+\Delta t) = e^{\Delta t(\hat{T}+\hat{U}(t)+\hat{D})} \varrho(x,p,t), \tag{A4}$$

where $\hat{T}$ is a kinetic energy operator,

$$\hat{T} = -\frac{p}{m}\partial_x, \tag{A5}$$

and, complementary to that, $\hat{U}(t)$ is the time-dependent potential energy operator,

$$\hat{U}(t) = \frac{1}{i\hbar}\Sigma(t)\left[U\left(x+\frac{i\hbar}{2}\partial_p\right) - U\left(x-\frac{i\hbar}{2}\partial_p\right)\right]. \tag{A6}$$

For further manipulations, one must agree upon an approximation of the exponential expression or, in other words, splitting of the exponential. One of such methods is the Strang approximation [51] of the second order, for the operators $\hat{T}+\hat{D}$, and $\hat{U}(t)$, according to which

$$\varrho(x,p,t+\Delta t) \approx e^{\frac{\Delta t}{2}(\hat{T}+\hat{D})} e^{\Delta t\hat{U}(t)} e^{\frac{\Delta t}{2}(\hat{T}+\hat{D})} \varrho(x,p,t). \tag{A7}$$

Furthermore, per [50], the operators $\hat{T}$ and $\hat{D}$ commute, resulting in

$$\varrho(x,p,t+\Delta t) \approx e^{\frac{\Delta t}{2}\hat{T}} e^{\Delta t\hat{U}(t+\Delta t/2)} e^{\frac{\Delta t}{2}\hat{T}} \varrho(x,p,t). \tag{A8}$$

To omit the difficulties related to the evaluation of the exponential differential operator and to perform numerical calculations, we introduce the following Fourier transforms:

$$\mathcal{F}_{1,x\to\lambda}\varrho(x,p,t) = \frac{1}{\sqrt{2\pi\hbar}}\int_{\mathbb{R}} dx\, e^{-\frac{i}{\hbar}\lambda x}\varrho(x,p,t), \tag{A9}$$

$$\mathcal{F}^{-1}_{1,\lambda\to x}\varrho(\lambda,p,t) = \frac{1}{\sqrt{2\pi\hbar}}\int_{\mathbb{R}} d\lambda\, e^{\frac{i}{\hbar}\lambda x}\varrho(\lambda,p,t), \tag{A10}$$

$$\mathcal{F}_{2,p\to y}\varrho(x,p,t) = \frac{1}{\sqrt{2\pi\hbar}}\int_{\mathbb{R}} dp\, e^{-\frac{i}{\hbar}py}\varrho(x,p,t), \tag{A11}$$

$$\mathcal{F}^{-1}_{2,y\to p}\varrho(x,y,t) = \frac{1}{\sqrt{2\pi\hbar}}\int_{\mathbb{R}} dy\, e^{\frac{i}{\hbar}py}\varrho(x,y,t)dy, \tag{A12}$$

and we use the unitary equivalence between the derivative and multiplicative operators. As a result, the following algorithm for numerical calculation of the time evolution of the WDF in time-dependent potentials arises:

$$\begin{aligned}\varrho(x,p,t_0+\Delta t) \approx \mathcal{F}^{-1}_{1,\lambda\to x}\exp\left(-\frac{i\Delta t}{2m}\lambda p\right)\mathcal{F}_{1,x\to\lambda}\mathcal{F}^{-1}_{2,y\to p}\exp\left\{i\Delta t\,\Sigma\left(t_0+\frac{\Delta t}{2}\right)\left[U\left(x+\frac{y}{2}\right)-U\left(x-\frac{y}{2}\right)\right]\right\}\mathcal{F}_{2,p\to y}\mathcal{F}^{-1}_{1,\lambda\to x} \\ \times\exp\left(-\frac{i\Delta t}{2m}\lambda p\right)\mathcal{F}_{1,x\to\lambda}\varrho(x,p,t_0).\end{aligned} \tag{A13}$$

APPENDIX B: MONOTONE DECREASE OF WIGNER-RÉNYI ENTROPIES

Let $f(x,p,t) = \tilde{\varrho}^2(x,p,t)$ be a probability distribution function over a phase space generated by (x,p) variables for all t. We will show that the Wigner-Rényi entropy of the order $\alpha \geqslant 0$ satisfies the following inequality:

$$S_\alpha(t) \leqslant S_\beta(t), \quad \alpha \geqslant \beta. \tag{B1}$$

To see this, first, we calculate the derivative of $S_\alpha(t)$ with respect to the parameter α. This gives

$$\partial_\alpha S_\alpha(t) = \frac{1}{(1-\alpha)^2}\ln\left[\int_{\mathbb{R}^2} dxdp\, f^\alpha(x,p,t)\right] + \frac{1}{1-\alpha}\left[\int_{\mathbb{R}^2} dxdp\, f^\alpha(x,p,t)\right]^{-1}\int_{\mathbb{R}^2} dxdp\, f^\alpha(x,p,t)\ln f(x,p,t). \tag{B2}$$

Now, introducing new quantities: the αth power of the phase-space α-norm of $f(x,p,t)$,

$$N_\alpha(t) := \int_{\mathbb{R}^2} dxdp\, f^\alpha(x,p,t), \tag{B3}$$

and the normalized probability distribution,

$$q_\alpha(x,p,t) := \frac{1}{N_\alpha(t)} f^\alpha(x,p,t), \tag{B4}$$

where

$$\int_{\mathbb{R}^2} dxdp\, q_\alpha(x,p,t) = 1, \tag{B5}$$

one may rewrite

$$\partial_\alpha S_\alpha(t) = \frac{1}{(1-\alpha)^2}\ln N_\alpha(t) - \frac{1}{(1-\alpha)^2}\int_{\mathbb{R}^2} dxdp\, q_\alpha(x,p,t)\ln f^{\alpha-1}(x,p,t). \tag{B6}$$

Performing some manipulation regarding the logarithmic expression, we get

$$\ln f^{\alpha-1}(x,p,t) = \ln\left[\frac{f^\alpha(x,p,t)}{N(t)}\frac{N_\alpha(t)}{f(x,p,t)}\right] = \ln\left[q_\alpha(x,p,t)\frac{N_\alpha(t)}{f(x,p,t)}\right] = \ln\left[\frac{q_\alpha(x,p,t)}{f(x,p,t)}\right] + \ln N(t). \tag{B7}$$

This yields the following expression:

$$\partial_\alpha S_\alpha(t) = \frac{1}{(1-\alpha)^2}\ln N_\alpha(t) - \frac{1}{(1-\alpha)^2}\int_{\mathbb{R}^2} dxdp\, q_\alpha(x,p,t)\ln\frac{q_\alpha(x,p,t)}{f(x,p,t)} - \frac{\ln N_\alpha(t)}{(1-\alpha)^2}, \tag{B8}$$

equal to

$$\partial_\alpha S_\alpha(t) = -\frac{1}{(1-\alpha)^2}\int_{\mathbb{R}^2} dxdp\, q_\alpha(x,p,t)\ln\frac{q_\alpha(x,p,t)}{f(x,p,t)} = -\frac{1}{(1-\alpha)^2}\int_{\mathbb{R}^2} dxdp\, q_\alpha(x,p,t)\ln\frac{q_\alpha(x,p,t)}{\tilde{\varrho}^2(x,p,t)}, \tag{B9}$$

which is a relative entropy [Kullback-Leiber divergence $D_{KL}(q_\alpha,\tilde{\varrho}^2)$] of the probability distribution functions $q_\alpha(x,p,t)$ and $\tilde{\varrho}^2(x,p,t)$ that is non-negative [63],

$$D_{KL}(q_\alpha,\tilde{\varrho}^2) \geqslant 0 \Rightarrow \partial_\alpha S_\alpha(t) \leqslant 0, \tag{B10}$$

and thus $S_\alpha(t) \leqslant S_\beta(t),\ \alpha \geqslant \beta$. This property holds for any positive function $f \in L^1(\mathbb{R}^2, dxdp) \cap L^\alpha(\mathbb{R}^2, dxdp)$.

[1] T. Dittrich, P. Hänggi, G.-L. Ingold, B. Kramer, G. Schön, and W. Zwerger, *Quantum Transport and Dissipation* (Wiley-Vch, Weinheim, 1998), Vol. 3.

[2] A. Kenfack, J. Gong, and A. K. Pattanayak, Phys. Rev. Lett. **100**, 044104 (2008).

[3] C. Grossert, M. Leder, S. Denisov, P. Hänggi, and M. Weitz, Nat. Commun. **7**, 10440 (2016).

[4] P. Hänggi and F. Marchesoni, Rev. Mod. Phys. **81**, 387 (2009).

[5] P. Olbrich, J. Karch, E. L. Ivchenko, J. Kamann, B. März, M. Fehrenbacher, D. Weiss, and S. D. Ganichev, Phys. Rev. B **83**, 165320 (2011).

[6] H. R. Reiss, Phys. Rev. Lett. **25**, 1149 (1970).

[7] J. C. Bronski, L. D. Carr, B. Deconinck, J. N. Kutz, and K. Promislow, Phys. Rev. E **63**, 036612 (2001).

[8] T. Wang, N. F. Q. Yuan, and L. Fu, Phys. Rev. X **11**, 021024 (2021).

[9] M. Khazali, Quantum **6**, 664 (2022).

[10] K. Sacha and J. Zakrzewski, Rep. Prog. Phys. **81**, 016401 (2018).

[11] M. Holthaus, J. Phys. B: At. Mol. Opt. Phys. **49**, 013001 (2016).

[12] S. Blanes, F. Casas, J. A. Oteo, and J. Ros, Phys. Rep. **470**, 151 (2009).

[13] J. Weinbub and D. K. Ferry, Appl. Phys. Rev. **5**, 041104 (2018).

[14] W. P. Schleich, *Quantum Optics in Phase Space* (Wiley, New York, 2001).

[15] M. A. Alonso, Adv. Opt. Photon. **3**, 272 (2011).

[16] U. Chabaud, P.-E. Emeriau, and F. Grosshans, Quantum **5**, 471 (2021).

[17] R. Raussendorf, C. Okay, M. Zurel, and P. Feldmann, Quantum **7**, 979 (2023).

[18] L. Kocia and P. Love, Quantum **5**, 494 (2021).

[19] T. J. H. Hele, M. J. Willatt, A. Muolo, and S. C. Althorpe, J. Chem. Phys. **142**, 134103 (2015).

[20] W. Xie, W. Domcke, S. C. Farantos, and S. Y. Grebenshchikov, J. Chem. Phys. **144**, 104105 (2016).

[21] A. Montoya-Castillo and D. R. Reichman, J. Chem. Phys. **146**, 024107 (2017).

[22] L. Slocombe, M. Sacchi, and J. Al-Khalili, Commun. Phys. **5**, 109 (2022).

[23] H. Warman, L. Slocombe, and M. Sacchi, RSC Adv. **13**, 13384 (2023).

[24] B. Opanchuk and P. D. Drummond, J. Math. Phys. **54**, 042107 (2013).

[25] K. Kirkpatrick, A. E. Mirasola, and C. Prescod-Weinstein, Phys. Rev. D **102**, 103012 (2020).

[26] J. Su, H. Lyu, and Y. Zhang, Phys. Lett. A **443**, 128218 (2022).

[27] J. Bera, B. Halder, S. Ghosh, R.-K. Lee, and U. Roy, Phys. Lett. A **453**, 128484 (2022).

[28] P. Massignan, A. Lampo, J. Wehr, and M. Lewenstein, Phys. Rev. A **91**, 033627 (2015).

[29] S. Lally, N. Werren, J. Al-Khalili, and A. Rocco, Phys. Rev. A **105**, 012209 (2022).

[30] A. A. Valido, J. Stat. Mech. (2022) 073103.

[31] M. A. Prado Reynoso, P. C. López Vázquez, and T. Gorin, Phys. Rev. A **95**, 022118 (2017).

[32] A. Kenfack and K. Życzkowski, J. Opt. B: Quantum Semiclass. Opt. **6**, 396 (2004).
[33] E. Cordero, M. de Gosson, M. Dörfler, and F. Nicola, SIAM J. Math. Anal. **50**, 2178 (2018).
[34] M. de Gosson, *Symplectic Geometry and Quantum Mechanics* (Birkhäuser, Basel, 2006).
[35] A. J. Dragt and S. Habib, How Wigner functions transform under symplectic maps, Quantum aspects of beam physics, in *Proceedings, Advanced ICFA Beam Dynamics Workshop, Monterey, USA, January 4-9, 1998*, edited by P. Chen (World Scientific, Singapore, 1998), pp. 651.
[36] N. C. Dias, M. A. de Gosson, and J. N. Prata, Proc. Amer. Math. Soc. **142**, 3183 (2014).
[37] E. Bonet-Luz and C. Tronci, Proc. R. Soc. A: Math. Phys. Eng. Sci. **472**, 20150777 (2016).
[38] G. Manfredi and M. R. Feix, Phys. Rev. E **62**, 4665 (2000).
[39] N. C. Dias, M. A. de Gosson, and J. N. Prata, J. Fourier Anal. Appl. **25**, 210 (2019).
[40] R. Hanel and S. Thurner, Europhys. Lett. **96**, 50003 (2011).
[41] M. Kalka, B. J. Spisak, D. Woźniak, M. Wołoszyn, and D. Kołaczek, Sci. Rep. **13**, 16266 (2023).
[42] E. H. Hauge and J. A. Støvneng, Rev. Mod. Phys. **61**, 917 (1989).
[43] M. Błaszak and Z. Domański, Ann. Phys. **327**, 167 (2012).
[44] H. Weyl, Z. Phys. **46**, 1 (1927).
[45] E. Wigner, Phys. Rev. **40**, 749 (1932).
[46] M. E. Tuckerman, J. Alejandre, R. López-Rendón, A. Jochim, and G. J. Martyna, J. Phys. A **39**, 5629 (2006).
[47] R. G. Littlejohn, Phys. Rep. **138**, 193 (1986).
[48] F. J. Dyson, Phys. Rev. **75**, 486 (1949).
[49] K. Mizuta and K. Fujii, Quantum **7**, 962 (2023).
[50] M. Suzuki, Proc. Jpn. Acad. Ser. B **69**, 161 (1993).
[51] G. Strang, SIAM J. Numer. Anal. **5**, 506 (1968).
[52] D. Kołaczek, B. J. Spisak, and M. Wołoszyn, Int. J. Appl. Math. Comp. **29**, 439 (2019).
[53] R. Cabrera, D. I. Bondar, K. Jacobs, and H. A. Rabitz, Phys. Rev. A **92**, 042122 (2015).
[54] Z. Van Herstraeten and N. J. Cerf, Phys. Rev. A **104**, 042211 (2021).
[55] N. C. Dias and J. N. Prata, Ann. Henri Poincaré **24**, 2341 (2023).
[56] D. Chruściński and K. Młodawski, Phys. Rev. A **71**, 052104 (2005).
[57] A. E. Bernardini and O. Bertolami, J. Phys.: Conf. Ser. **1275**, 012032 (2019).
[58] S. H. Lie, S. Choi, and H. Jeong, Phys. Rev. A **103**, 042421 (2021).
[59] A. Wobst, G.-L. Ingold, P. Hänggi, and D. Weinmann, Eur. Phys. J. B **27**, 11 (2002).
[60] V. V. Dodonov, O. V. Man'ko, V. I. Man'ko, and A. Wünsche, J. Mod. Opt. **47**, 633 (2000).
[61] D. Kołaczek, B. J. Spisak, and M. Wołoszyn, Sci. Rep. **11**, 11619 (2021).
[62] A. M. Ozorio de Almeida, in *Entanglement and Decoherence: Foundations and Modern Trends*, edited by A. Buchleitner, C. Viviescas, and M. Tiersch (Springer, Berlin, 2008), pp. 157.
[63] S. Kullback and R. A. Leibler, Ann. Math. Statist. **22**, 79 (1951).

Bibliography

[1] A. Aghamohammadi, A. H. Fatollahi, M. Khorrami, and A. Shariati. Entropy as a measure of diffusion. *Phys. Lett. A*, 377(28-30):1677–1681, October 2013.

[2] F. Albarelli, M. G. Genoni, M. G. A. Paris, and A. Ferraro. Resource theory of quantum non-Gaussianity and Wigner negativity. *Phys. Rev. A*, 98(5), November 2018.

[3] V. V. Albert and L. Jiang. Symmetries and conserved quantities in Lindblad master equations. *Phys. Rev. A*, 89(2), February 2014.

[4] S. T. Ali, N. M. Atakishiyev, S. M. Chumakov, and K. B. Wolf. The Wigner function for general Lie groups and the wavelet transform. *Ann. Henri Poincare*, 1(4):685–714, September 2000.

[5] A. Arnold, I. M. Gamba, M. P. Gualdani, S. Mischler, C. Mouhot, and C. Sparber. The Wigner-Fokker-Planck equation: Stationary states and large-time behavior, 2010.

[6] V. I. Arnold. *Mathematical methods of classical mechanics*. Graduate texts in mathematics. Springer, New York, NY, December 2010.

[7] G. A. Baker. Formulation of quantum mechanics based on the quasi-probability distribution induced on phase space. *Phys. Rev.*, 109:2198–2206, Mar 1958.

[8] L. Barreira and C. Valls. *Dynamical Systems*. Universitext. Springer, London, England, 2013 edition, December 2012.

[9] I. Bengtsson and K. Zyczkowski. *Geometry of quantum states*. Cambridge University Press, Cambridge, England, May 2006.

[10] Y. M Berezansky, Z. G. Sheftel, and F. G. Us. *Functional Analysis*. Operator Theory: Advances and Applications. Springer, Basel, Switzerland, October 2011.

[11] F. A. Berezin and M. Shubin. *The Schrödinger equation*. Mathematics and its Applications. Springer, Dordrecht, Netherlands, 1991 edition, December 2012.

[12] J. Bernier. Exact splitting methods for semigroups generated by inhomogeneous quadratic differential operators. *Found. Comut. Math.*, 21(5):1401–1439, 2021.

[13] F. Bezrukov and D. Levkov. Dynamical tunneling of bound systems through a potential barrier: Complex way to the top. *J. Exp. Theor. Phys.*, 98(4):820–836, April 2004.

[14] R. Bhatia and P. Rosenthal. How and why to solve the operator equation AX-XB=Y. *Bull. Lond. Math. Soc.*, 29(1):1–21, January 1997.

[15] I. Białynicki-Birula, M. Cieplak, and J. Kamiński. *Teoria kwantów: mechanika falowa*. Wydaw. Naukowe PWN, 2001.

[16] M. Sh. Birman and M. Z. Solomjak. *Spectral theory of self-adjoint operators in Hilbert space*. Mathematics and its Applications. Springer, Dordrecht, Netherlands, 1987 edition, May 1987.

[17] M. Błaszak and Z. Domański. Phase space quantum mechanics. *Ann. Phys. (N. Y.)*, 327(2):167–211, February 2012.

[18] M. Błaszak and Z. Domański. Quantum trajectories. *Phys. Lett. A*, 376(47-48):3593–3598, November 2012.

[19] M. Błaszak and Z. Domański. Canonical quantization of classical mechanics in curvilinear coordinates. invariant quantization procedure. *Ann. Phys. (N. Y.)*, 339:89–108, December 2013.

[20] F. Bloch. Dynamical theory of nuclear induction. II. *Phys. Rev.*, 102(1):104–135, April 1956.

[21] D. I. Bondar, R. Cabrera, D. V. Zhdanov, and H. A. Rabitz. Wigner phase-space distribution as a wave function. *Phys. Rev. A*, 88(5), November 2013.

[22] D. Borthwick. *Introduction to partial differential equations*. Universitext. Springer International Publishing, Cham, Switzerland, 1 edition, January 2017.

[23] H.-P. Breuer, E.-M. Laine, J. Piilo, and B. Vacchini. Colloquium: Non-Markovian dynamics in open quantum systems. *Rev. Mod. Phys.*, 88:021002, Apr 2016.

[24] H.-P. Breuer and F. Petruccione. *The Theory of Open Quantum Systems*. Oxford University Press, 2002.

[25] H.-P. Breuer and F. Petruccione. Concepts and methods in the theory of open quantum systems. In *Irreversible Quantum Dynamics*, Lecture notes in physics, pages 65–79. Springer Berlin Heidelberg, Berlin, Heidelberg, 2003.

[26] C. Brif and A. Mann. Phase-space formulation of quantum mechanics and quantum-state reconstruction for physical systems with lie-group symmetries. *Phys. Rev. A*, 59:971–987, Feb 1999.

[27] O. Brodier, K. Mallick, and A. M. Ozorio de Almeida. Semiclassical work and quantum work identities in Weyl representation. *J. Phys. A Math. Theor.*, 53(32):325001, August 2020.

[28] B. Cahen. Schrödinger model and Stratonovich-Weyl correspondence for Heisenberg motion groups, 2016. Available at: `https://www.openstarts.units.it/entities/publication/f63d3c31-f06e-4c04-b1b0-275d3ecc922a/details`.

[29] W. B. Case. Wigner functions and Weyl transforms for pedestrians. *Am. J. Phys.*, 76(10):937–946, October 2008.

[30] G. Casella and R. Berger. *Statistical inference*. Chapman and Hall/CRC, Boca Raton, April 2024.

[31] S. Chaturvedi and F. Shibata. Time-convolutionless projection operator formalism for elimination of fast variables. Applications to Brownian motion. *Z Phys. B*, 35(3):297–308, September 1979.

[32] A. Chaves, D. R. da Costa, G. O. de Sousa, J. M. Pereira, and G. A. Farias. Energy shift and conduction-to-valence band transition mediated by a time-dependent potential barrier in graphene. *Phys. Rev. B Condens. Matter Mater. Phys.*, 92(12), September 2015.

[33] S. A. Chin. Symplectic integrators from composite operator factorizations. *Phys. Lett. A*, 226(6):344–348, March 1997.

[34] M. L. Chiofalo, M. Artoni, and G. C. L. Rocca. Atom resonant tunnelling through a moving barrier. *New J. Phys.*, 5:78–78, June 2003.

[35] M.-D. Choi. Completely positive linear maps on complex matrices. *Linear Algebra Appl.*, 10(3):285–290, June 1975.

[36] S. H. H. Chowdhury and S. T. Ali. The symmetry groups of noncommutative quantum mechanics and coherent state quantization. *J. Math. Phys.*, 54(3):032101, March 2013.

[37] D. Chruściński. Wigner function for damped systems. arXiv:math-ph/0209008, 2002.

[38] D. Chruściński and K. Młodawski. Wigner function and Schrödinger equation in phase-space representation. *Phys. Rev. A*, 71(5), May 2005.

[39] D. Chruściński and S. Pascazio. A brief history of the GKLS equation. *Open Syst. Inf. Dyn.*, 24(03):1740001, September 2017.

[40] A. Cianchi and V. Maz'ya. Friedrichs type inequalities in arbitrary domains, 2020.

[41] F. M. Cucchietti, D. A. R. Dalvit, J. P. Paz, and W. H. Zurek. Decoherence and the Loschmidt echo. *Phys. Rev. Lett.*, 91(21):210403, November 2003.

[42] L. T. Curtright, B. D. Fairlie, and K. C. Zachos. *A Concise Treatise on Quantum Mechanics in Phase Space*. World Scientific Publishing, 2016.

[43] T. L. Curtright and C. K. Zachos. Quantum mechanics in phase space. *Asia Pac. Phys. Newsl.*, 01(01):37–46, May 2012.

[44] Kolaczek D. *Dynamika stanów kwantowych w przestrzeni fazowej'*. PhD thesis, AGH Akademia Górniczo-Hutnicza, 2022.

[45] E. B. Davies. Markovian master equations. *Commun. Math. Phys.*, 39(2):91–110, June 1974.

[46] E. B. Davies. *Linear operators and their spectra*. Cambridge studies in advanced mathematics. Cambridge University Press, Cambridge, England, January 2010.

[47] M. A. de Gosson. *Symplectic Geometry and Quantum Mechanics*. Advances in Partial Differential Equations. Birkhauser Verlag AG, Basel, Switzerland, 2006 edition, December 2006.

[48] M. A. de Gosson. *Symplectic methods in harmonic analysis and in mathematical physics*. Pseudo-Differential Operators. Birkhauser Verlag AG, Basel, Switzerland, July 2011.

[49] M. A. de Gosson. Quantum blobs. *Found. Phys.*, 43(4):440–457, 2013.

[50] M. A. De Gosson. *The Wigner transform*. Advanced Textbooks In Mathematics. World Scientific Europe, London, England, May 2017.

[51] M. A. de Gosson and C. de Gosson. On the Wigner distribution of the reduced density matrix, 2022.

[52] S. Descombes and M. Thalhammer. An exact local error representation of exponential operator splitting methods for evolutionary problems and applications to linear Schrödinger equations in the semi-classical regime. *BIT*, 50(4):729–749, December 2010.

[53] N. C. Dias, M. A. de Gosson, and J. N. Prata. A refinement of the Robertson-Schrödinger uncertainty principle and a Hirschman-Shannon inequality for wigner distributions. *J. Fourier Anal. Appl.*, 25(1):210, 2019.

[54] P. Dirac. *The principles of quantum mechanics*. International Series of Monographs on Physics. Clarendon Press, Oxford, England, 4 edition, January 1981.

[55] R. S. Dumont and T. L. Marchioro II. Tunneling-time probability distribution. *Phys. Rev. A*, 47(1):85–97, January 1993.

[56] L. Dupays and J.-C. Pain. Closed forms of the Zassenhaus formula. *J. Phys. A Math. Theor.*, 56:255202, March 2023.

[57] F. J. Dyson. The S matrix in quantum electrodynamics. *Phys. Rev.*, 75(11):1736, June 1949.

[58] F. J. Dyson. The dynamics of a disordered linear chain. *Phys. Rev.*, 92(6):1331–1338, December 1953.

[59] K.-J. Engel and R. Nagel. *One-parameter semigroups for linear evolution equations*. Graduate Texts in Mathematics. Springer, New York, NY, 2000 edition, October 1999.

[60] L. C. Evans. *Partial Differential Equations*. Graduate studies in mathematics. American Mathematical Society, Providence, RI, 2 edition, March 2010.

[61] D. B. Fairlie. Moyal brackets, star products and the generalised Wigner function. *Chaos Soliton Fract*, 10(2):365–371, 1999.

[62] M. Fano. Description of states in quantum mechanics by density matrix and opertaor techniques. *Rev. Mod. Phys.*, 29:74, 1957.

[63] J. Fischer and H.-P. Breuer. Correlated projection operator approach to non-Markovian dynamics in spin baths. *Phys. Rev. A*, 76(5), November 2007.

[64] G. B. Folland. *Harmonic Analysis in Phase Space.* Annals of Mathematics Studies. Princeton University Press, Princeton, NJ, January 1989.

[65] M. Frigo and S. G. Johnson. The design and implementation of FFTW3. *Proceedings of the IEEE*, 93(2):216–231, 2005. Special issue on "Program Generation, Optimization, and Platform Adaptation".

[66] M. Gadella, M. A. Martin, L. M. Nieto, and M. A. del Olmo. The Stratonovich–Weyl correspondence for one-dimensional kinematical groups. *J. Math. Phys.*, 32(5):1182–1192, May 1991.

[67] B. Gardas, J. Dziarmaga, W. H. Zurek, and M. Zwolak. Defects in quantum computers. *Sci. Rep.*, 8(1), March 2018.

[68] C. W. Gardiner and P. Zoller. *Quantum noise*. Springer Series in Synergetics. Springer, Berlin, Germany, 3 edition, August 2004.

[69] K.-S. Giannopoulou. Construction of an approximate solution of the Wigner equation by uniformization of WKB functions. arXiv:1706.03111, 2017.

[70] K.-S. Giannopoulou and G. N. Makrakis. An approximate series solution of the semiclassical Wigner equation. arXiv:1705.06754, 2017.

[71] C. Gneiting, T. Fischer, and K. Hornberger. Quantum phase-space representation for curved configuration spaces. *Phys. Rev. A*, 88(6), December 2013.

[72] V. Gorini, A. Kossakowski, and E. C. G. Sudarshan. Completely positive dynamical semigroups of *N*-level systems. *J. Math. Phys.*, 17(5):821–825, May 1976.

[73] A. Goussev, R. A. Jalabert, H. M. Pastawski, and D. Wisniacki. Loschmidt echo. *Scholarpedia J.*, 7(8):11687, 2012.

[74] M. Grabowski and R.S. Ingarden. *Mechanika kwantowa: ujęcie w przestrzeni Hilberta*. Państwowe Wydawnictwo Naukowe. Oddział, 1989.

[75] I.S. Gradshteyn and I. M. Ryzhik. *Table of integrals, series, and products*. Academic Press, San Diego, CA, 8 edition, September 2014.

[76] H. J. Groenewold. On the principles of elementary quantum mechanics. *Physica*, 12:405 – 460, October 1946.

[77] J. Guillod. On the asymptotic stability of steady flows with nonzero flux in two-dimensional exterior domains. *Commun. Math. Phys.*, 352(1):201–214, May 2017.

[78] J. A. Gyamfi. Fundamentals of quantum mechanics in Liouville space. *Eur. J. Phys.*, 41(6):063002, November 2020.

[79] D. T. Haar. Theory and applications of the density matrix. *Rep. Prog. Phys.*, 24(1):304–362, January 1961.

[80] B. C. Hall. *Quantum Theory for Mathematicians*. Graduate texts in mathematics. Springer, New York, NY, 2013 edition, June 2013.

[81] B. C. Hall. *Lie groups, Lie algebras, and representations*. Graduate texts in mathematics. Springer International Publishing, Cham, Switzerland, 2 edition, May 2015.

[82] P. Hästö and J. Ok. Regularity theory for non-autonomous partial differential equations without Uhlenbeck structure. *Arch. Ration. Mech. Anal.*, 245(3):1401–1436, September 2022.

[83] J. V. Herod and R. W. McKelvey. A Hille-Yosida theory for evolutions. *Isr. J. Math.*, 36(1):13–40, March 1980.

[84] B. J. Hiley. On the relationship between the Wigner-Moyal and Bohm approaches to quantum mechanics: A step to a more general theory? *Found. Phys.*, 40(4):356–367, April 2010.

[85] B. J. Hiley. On the relationship between the Wigner–Moyal approach and the quantum operator algebra of von neumann. *J. Comput. Electron.*, 14(4):869–878, December 2015.

[86] B. J. Hiley. The Moyal-Dirac controversy revisited. *J. Proc. R. Soc. N. S. W.*, 154(2):139–160, December 2021.

[87] E. Hille. *Functional analysis and semi-groups*. Read Books, Alcester, England, November 2008.

[88] A. C. Hirshfeld and P. Henselder. Deformation quantization in the teaching of quantum mechanics. *Am. J. Phys.*, 70(5):537–547, May 2002.

[89] M. Holthaus. Floquet engineering with quasienergy bands of periodically driven optical lattices. *J. Phys. B At. Mol. Opt. Phys.*, 49(1):013001, January 2016.

[90] R. A Horn and C. R. Johnson. *Matrix Analysis*. Cambridge University Press, Cambridge, England, June 2012.

[91] R. L. Hudson. When is the Wigner quasi-probability density non-negative? *Rep. Math. Phys.*, 6(2):249–252, October 1974.

[92] J. Hussain, M. Nouman, F. Saif, and J. Akram. PT-symmetric potential impact on the scattering of a Bose-Einstein condensate from a gaussian obstacle. *Physica B Condens. Matter*, 587(412152):412152, June 2020.

[93] R. S. Ingarden and A. Kossakowski. On the connection of nonequilibrium information thermodynamics with non-hamiltonian quantum mechanics of open systems. *Ann. Phys. (N. Y.)*, 89(2):451–485, February 1975.

[94] A. Isar, A. Sandulescu, and W. Scheid. Phase space representation for open quantum systems within the Lindblad theory. *Int. J. Mod. Phys. B*, 10(22):2767–2779, October 1996.

[95] A. Isar, A. Sandulescu, H. Scutaru, E. Stefanescu, and W. Scheid. Open quantum systems. *Int. J. Mod. Phys. E*, 03(02):635–714, June 1994.

[96] A. P. Jauho, N. S. Wingreen, and Y. Meir. Time-dependent transport in interacting and noninteracting resonant-tunneling systems. *Phys. Rev. B Condens. Matter*, 50(8):5528–5544, August 1994.

[97] M. Kalka, B. J. Spisak, D. Woźniak, M. Wołoszyn, and D. Kołaczek. Dynamical entropic measure of nonclassicality of phase-dependent family of Schrödinger cat states. *Sci. Rep.*, 13(1):16266, September 2023.

[98] T. Kato. Integration of the equation of evolution in a Banach space. *J. Math. Soc. Jpn*, 5(2), July 1953.

[99] T. Kato. *Perturbation theory for linear operators*. Classics in mathematics. Springer, Berlin, Germany, 2 edition, February 1995.

[100] T. Kato and H. Tanabe. On the abstract evolution equation. *Osaka Math. J.*, 14(1):107 – 133, 1962.

[101] A. Kenfack and K. Życzkowski. Negativity of the Wigner function as an indicator of non-classicality. *J. Opt. B Quantum Semiclassical Opt.*, 6(10):396–404, October 2004.

[102] Y. L. Klimontovich. Dissipative equations for many-particle distribution functions. *Soviet Physics Uspekhi*, 26(4):366, apr 1983.

[103] D. Kołaczek, B. J. Spisak, and M. Wołoszyn. Phase-space studies of backscattering diffraction of defective Schrödinger cat states. *Sci. Rep.*, 11(1):11619, June 2021.

[104] M. Kontsevich. Operads and motives in deformation quantization. *Lett. Math. Phys.*, 48(1):35–72, 1999.

[105] A. Kossakowski. On quantum statistical mechanics of non-hamiltonian systems. *Rep. Math. Phys.*, 3(4):247–274, 1972.

[106] B. Kramer and A. MacKinnon. Localization: theory and experiment. *Rep. Prog. Phys.*, 56(12):1469–1564, December 1993.

[107] K. Kraus. General state changes in quantum theory. *Ann. Phys. (N. Y.)*, 64(2):311–335, June 1971.

[108] C. S. Kubrusly. Trace-class and nuclear operators. *Concr. Oper.*, 9(1):53–69, January 2022.

[109] A. Lampo, S. H. Lim, J. Wehr, P. Massignan, and M. Lewenstein. Lindblad model of quantum Brownian motion. *Phys. Rev. A*, 94:042123, October 2016.

[110] D. P. Landau and K. Binder. *A guide to Monte Carlo simulations in statistical physics*. Cambridge University Press, Cambridge, England, 4 edition, November 2014.

[111] Y. L. Lin and O. C. O. Dahlsten. Necessity of negative Wigner function for tunneling. *Phys. Rev. A*, 102(6), December 2020.

[112] G. Lindblad. On the generators of quantum dynamical semigroups. *Commun. Math. Phys.*, 48(2):119–130, June 1976.

[113] J. D. Logan. *Applied partial differential equations*. Undergraduate texts in mathematics. Springer International Publishing, Cham, Switzerland, 3 edition, December 2014.

[114] W. Magnus. On the exponential solution of differential equations for a linear operator. *Commun. Pure Appl. Math.*, 7(4):649–673, November 1954.

[115] G. D. Mahan. *Many-particle physics*. Physics of Solids and Liquids. Springer, New York, NY, December 2010.

[116] H. Mäkelä and M. Möttönen. Effects of the rotating-wave and secular approximations on non-Markovianity. *Phys. Rev. A*, 88(5), November 2013.

[117] A. Mandilara, E. Karpov, and N. J. Cerf. Extending Hudson's theorem to mixed quantum states. *Phys. Rev. A*, 79(6), June 2009.

[118] G. Manfredi and M. R. Feix. Entropy and wigner functions. *Phys. Rev. E Stat. Phys. Plasmas Fluids Relat. Interdiscip. Topics*, 62(4):4665–4674, October 2000.

[119] S. Maniscalco, J. Piilo, F. Intravaia, F. Petruccione, and A. Messina. Lindblad- and non-Lindblad-type dynamics of a quantum Brownian particle. *Phys. Rev. A*, 70(3), September 2004.

[120] P. Manju, K. S. Hardman, M. A. Sooriyabandara, P.B. Wigley, J. D. Close, N. P. Robins, M. R. Hush, and S. S. Szigeti. Quantum tunneling dynamics of an interacting Bose-Einstein condensate through a Gaussian barrier. *Phys. Rev. A*, 98(5), November 2018.

[121] M. Măntoiu and M. Ruzhansky. Pseudo-differential operators, Wigner transform and Weyl systems on type I locally compact groups. *Doc. Math.*, 22:1539–1592, 2017.

[122] D. Manzano. A short introduction to the Lindblad master equation. *AIP Adv.*, 10(2):025106, February 2020.

[123] H. Marcinkowska. *Dystrybucje, przestrzenie Sobolewa, równania różniczkowe*. Biblioteka Matematyczna. Wydawnictwo Naukowe PWN, 1993.

[124] J. E. Marsden and T. S. Ratiu. *Introduction to mechanics and symmetry*. Texts in applied mathematics. Springer, New York, NY, December 2010.

[125] J. Maruskin. *Dynamical systems and geometric mechanics*. De Gruyter Studies in Mathematical Physics. de Gruyter, 2 edition, August 2018.

[126] J. E. Moyal. Quantum mechanics as a statistical theory. *Math. Proc. Camb. Philos. Soc.*, 45(1):99–124, January 1949.

[127] S. Nakajima. On quantum theory of transport phenomena. *Prog. Theor. Phys.*, 20(6):948–959, December 1958.

[128] M. A. Nielsen and I. L. Chuang. *Quantum Computation and Quantum Information*. Cambridge University Press, Cambridge, England, June 2012.

[129] D. Nigro. On the uniqueness of the steady-state solution of the Lindblad–Gorini–Kossakowski–Sudarshan equation. *J. Stat. Mech.*, 2019(4):043202, April 2019.

[130] P. J. Olver. Evolution equations possessing infinitely many symmetries. *J. Math. Phys.*, 18(6):1212–1215, June 1977.

[131] P. J. Olver. *Introduction to partial differential equations*. Undergraduate texts in mathematics. Springer International Publishing, Cham, Switzerland, 1 edition, November 2013.

[132] R. E. E. Omer, E. B. M. Bashier, and A. I. Arbab. Numerical solutions of a system of ODEs based on Lie-Trotter and Strang operator-splitting methods. *Univers. J. Comput. Math.*, 5(2):20–24, April 2017.

[133] A. Pazy. *Semigroups of linear operators and applications to partial differential equations*. Applied mathematical sciences. Springer, New York, NY, 1983 edition, December 2012.

[134] G. K. Pedersen. *Analysis now*. Graduate texts in mathematics. Springer, New York, NY, 1989 edition, December 2012.

[135] A. Peres. Stability of quantum motion in chaotic and regular systems. *Phys. Rev. A Gen. Phys.*, 30(4):1610–1615, October 1984.

[136] A. Peres. *Quantum Theory*. Fundamental Theories of Physics. Plenum Publishing Corporation, May 2014.

[137] A. G. Redfield. On the theory of relaxation processes. *IBM J. Res. Dev.*, 1(1):19–31, January 1957.

[138] M. Reed and B. Simon. *Methods of modern mathematical physics: Functional Analysis: Volume 1*. Academic Press, San Diego, CA, July 1972.

[139] M. Reed and B. Simon. *Methods of modern mathematical physics:Fourier Analysis, Self-Adjointness: Volume 2*. Academic Press, San Diego, CA, November 1975.

[140] K. Rektorys. *Variational Methods in Mathematics, Science and Engineering*. Springer, Dordrecht, Netherlands, January 2012.

[141] M. Renardy and R. C. Rogers. *An introduction to partial differential equations*. Texts in Applied Mathematics. Springer, New York, NY, 2 edition, January 2004.

[142] H. Risken. *The Fokker-Planck equation*. Springer series in synergetics. Springer, Berlin, Germany, 2 edition, September 1996.

[143] A. Rivas and S. Huelga. *Open Quantum Systems*. SpringerBriefs in physics. Springer, Berlin, Germany, 2012 edition, September 2011.

[144] A. Royer. Wigner function as the expectation value of a parity operator. *Phys. Rev. A Gen. Phys.*, 15(2):449–450, February 1977.

[145] A. Royer. Combining projection superoperators and cumulant expansions in open quantum dynamics with initial correlations and fluctuating Hamiltonians and environments. *Phys. Lett. A*, 315(5):335–351, September 2003.

[146] W. Rudin. *Functional Analysis*. McGraw-Hill, New York, NY, December 1973.

[147] R. P. Rundle and M. J. Everitt. Overview of the phase space formulation of quantum mechanics with application to quantum technologies. *Adv. Quantum Technol.*, 4(6):2100016, June 2021.

[148] P. Sadeghi, S. Khademi, and A. H. Darooneh. Tsallis entropy in phase-space quantum mechanics. *Phys. Rev. A*, 86(1), July 2012.

[149] J. J. Sakurai and J. Napolitano. *Modern quantum mechanics*. Cambridge University Press, Cambridge, England, 3 edition, September 2020.

[150] H. Sambe. Steady states and quasienergies of a quantum-mechanical system in an oscillating field. *Phys. Rev. A Gen. Phys.*, 7(6):2203–2213, June 1973.

[151] J. F. Schipper. Wigner Quantum Density Function in the Classical Limit. Development of a Three-Dimensional WKBJ-Type Solution. *Phys. Rev.*, 184:1283–1302, August 1969.

[152] K. Schmüdgen. *Unbounded self-adjoint operators on Hilbert space*. Graduate texts in mathematics. Springer, Dordrecht, Netherlands, 2012 edition, July 2012.

[153] L. Schwartz. *Mathematics for the physical sciences*. Dover Books on Mathematics. Dover Publications, Mineola, NY, April 2008.

[154] A. Shaji and E. C. G. Sudarshan. Who's afraid of not completely positive maps? *Phys. Lett. A*, 341(1-4):48–54, June 2005.

[155] F. Shibata and N. Hashitsume. Statistical mechanical theory of non-equilibrium systems. *Progr. Theoret. Phys. Suppl.*, 64:83–99, February 1978.

[156] F. Shibata, Y. Takahashi, and N. Hashitsume. A generalized stochastic Liouville equation. Non-Markovian versus memoryless master equations. *J. Stat. Phys.*, 17(4):171–187, October 1977.

[157] K. Siudzińska and D. Chruściński. Quantum evolution with a large number of negative decoherence rates. *J. Phys. A Math. Theor.*, 53(37):375305, September 2020.

[158] C. Sparber, J. A. Carrillo, P. A. Markowich, and J. Dolbeault. On the long-time behavior of the quantum Fokker-Planck equation. *Mon. Hefte Math.*, 141(3):237–257, March 2004.

[159] B. J. Spisak, M. Wołoszyn, and D. Szydłowski. Dynamical localisation of conduction electrons in one-dimensional disordered systems. *J. Comput. Electron.*, 14(4):916–921, December 2015.

[160] A. D. Stone, M. Y. Azbel, and P. A. Lee. Localization and quantum-mechanical resonant tunneling in the presence of a time-dependent potential. *Phys. Rev. B Condens. Matter*, 31(4):1707–1714, February 1985.

[161] I. Strandberg, G. Johansson, and Quijandría F. Wigner negativity in the steady-state output of a Kerr parametric oscillator. *Phys. Rev. Res.*, 3(2), April 2021.

[162] G. Strang. On the construction and comparison of difference schemes. *SIAM J. Numer. Anal.*, 5(3):506–517, September 1968.

[163] R. L. Stratonovich. On distributions in representation space. *Soviet Physics JETP-USSR*, 4(6):891, 1957.

[164] D. F. Styer, Miranda S. Balkin, K. M. Becker, M. R. Burns, C. E. Dudley, S. T. Forth, J. S. Gaumer, M. A. Kramer, D. C. Oertel, L. H. Park, M. T. Rinkoski, C. T. Smith, and T. D. Wotherspoon. Nine formulations of quantum mechanics. *Am. J. Phys.*, 70(3):288–297, March 2002.

[165] M. Suzuki. Decomposition formulas of exponential operators and Lie exponentials with some applications to quantum mechanics and statistical physics. *J. Math. Phys.*, 26(4):601–612, 1985.

[166] M. Suzuki. General theory of fractal path integrals with applications to many-body theories and statistical physics. *J. Math. Phys.*, 32(2):400–407, February 1991.

[167] M. Suzuki. General decomposition theory of ordered exponentials. *P. Jpn. Acad. B-Phys.*, 69(7):161–166, 1993.

[168] W. Thirring. *A course in mathematical physics 1*. Springer, Vienna, Austria, 1 edition, July 1983.

[169] W. Thirring. *A course in mathematical physics 3*. Springer, Vienna, Austria, 1 edition, February 1991.

[170] T. Tilma, M. J. Everitt, J. H. Samson, W. J. Munro, and K. Nemoto. Wigner functions for arbitrary quantum systems. *Phys. Rev. Lett.*, 117:180401, Oct 2016.

[171] K. Tosio. Abstract evolution equations of parabolic type in Banach and Hilbert spaces. *Nagoya Math. J.*, 19:93–125, October 1961.

[172] Z. Van Herstraeten and N. J. Cerf. Quantum Wigner entropy. *Phys. Rev. A*, 104:042211, 2021.

[173] I. Varga and J. Pipek. Rényi entropies characterizing the shape and the extension of the phase space representation of quantum wave functions in disordered systems. *Phys. Rev. E Stat. Nonlin. Soft Matter Phys.*, 68(2 Pt 2):026202, August 2003.

[174] J. C. Varilly. The Stratanovich-Weyl correspondence: a general approach to Wigner functions, 1989. Available at: `https://www.kerwa.ucr.ac.cr/items/149614ec-732e-4356-b7c4-1422416444fa`.

[175] J. C. Várilly and J. Gracia-Bondía. The Moyal representation for spin. *Ann. Phys. (N. Y.)*, 190(1):107–148, February 1989.

[176] J. von Neumann. Die eindeutigkeit der Schrödingerschen operatoren. *Math. Ann.*, 104(1):570–578, December 1931.

[177] J. Von Neumann. *Mathematical foundations of quantum mechanics*. Princeton Landmarks in Mathematics and Physics. Princeton University Press, Princeton, NJ, October 1996.

[178] R. K. Wangsness and F. Bloch. The dynamical theory of nuclear induction. *Phys. Rev.*, 89(4):728–739, February 1953.

[179] S. Weinberg. *The quantum theory of fields: Foundations volume 1*. Cambridge University Press, Cambridge, England, May 2013.

[180] J. Weinbub and D. K. Ferry. Recent advances in Wigner function approaches. *Appl. Phys. Rev.*, 5(4):041104, December 2018.

[181] H. Weyl. Quantenmechanik und gruppentheorie. *Z. Phys.*, 46:1–46, Nov 1927.

[182] E. Wigner. On the quantum correction for thermodynamic equilibrium. *Phys. Rev.*, 40:749–759, June 1932.

[183] K. B. Wolf. The Heisenberg–Weyl ring in quantum mechanics. In *Group Theory and its Applications*, pages 189–247. Elsevier, 1975.

[184] M. Wołoszyn, B. J. Spisak, J. Adamowski, and P. Wójcik. Magnetoresistance anomalies resulting from Stark resonances in semiconductor nanowires with a constriction. *J. Phys. Condens. Matter*, 26(32):325301, August 2014.

[185] D. Woźniak, M. Kalka, D. Kołaczek, M. Wołoszyn, and B. J. Spisak. Wignerian symplectic covariance approach to the interaction-time problem. *Sci. Rep.*, 14(1):31294, December 2024.

[186] D. Woźniak, B. J. Spisak, M. Kalka, M. Wołoszyn, M. Wleklińska, P. Pigoń, and D. Kołaczek. Interaction time of Schrödinger cat states with a periodically driven quantum system: Symplectic covariance approach. *Phys. Rev. A*, 110(2), August 2024.

[187] B. Yan, L. Cincio, and W. H. Zurek. Information scrambling and loschmidt echo. *Phys. Rev. Lett.*, 124(16), April 2020.

[188] H. Yoshida. Uniqueness of steady states of Gorini-Kossakowski-Sudarshan-Lindblad equations: A simple proof. *Phys. Rev. A*, 109(2), February 2024.

[189] W. H. Zurek. Decoherence, chaos, quantum-classical correspondence, and the algorithmic arrow of time. *Phys. Scr.*, 1998(T76):186, January 1998.

[190] W. H. Zurek. Decoherence and the transition from quantum to classical –REVISITED. arXiv:quant-ph/0306072, 2003.

[191] W. H. Zurek. Decoherence, einselection, and the quantum origins of the classical. *Rev. Mod. Phys.*, 75(3):715–775, May 2003.

[192] W. H. Zurek and J. P. Paz. Decoherence, chaos, and the second law. *Phys. Rev. Lett.*, 72(16):2508–2511, April 1994.

[193] R. Zwanzig. Ensemble method in the theory of irreversibility. *J. Chem. Phys.*, 33(5):1338–1341, November 1960.